

Durham E-Theses

*Mechanistic studies of aromatic substitutions with
aniline and phenoxide nucleophiles.*

Robotham, Ian A.

How to cite:

Robotham, Ian A. (1997) *Mechanistic studies of aromatic substitutions with aniline and phenoxide nucleophiles.*, Durham theses, Durham University. Available at Durham E-Theses Online:
<http://etheses.dur.ac.uk/5063/>

Use policy

The full-text may be used and/or reproduced, and given to third parties in any format or medium, without prior permission or charge, for personal research or study, educational, or not-for-profit purposes provided that:

- a full bibliographic reference is made to the original source
- a [link](#) is made to the metadata record in Durham E-Theses
- the full-text is not changed in any way

The full-text must not be sold in any format or medium without the formal permission of the copyright holders.

Please consult the [full Durham E-Theses policy](#) for further details.

**MECHANISTIC STUDIES OF AROMATIC
SUBSTITUTIONS WITH ANILINE
AND PHENOXIDE NUCLEOPHILES.**

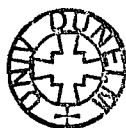
by

Ian A. Robotham, B. Sc. (Dunelm)

Van Mildert College.

The copyright of this thesis rests
with the author. No quotation
from it should be published
without the written consent of the
author and information derived
from it should be acknowledged.

A thesis submitted for the degree of Doctor of Philosophy in the
Department of Chemistry, University of Durham
1997.



19 FEB 1998

MECHANISTIC STUDIES OF AROMATIC SUBSTITUTIONS WITH ANILINE AND PHENOXIDE NUCLEOPHILES.

by Ian A. Robotham

A thesis submitted for the degree of Doctor of Philosophy in the
Department of Chemistry, University of Durham, 1997.

ABSTRACT

Kinetic studies are reported of the reactions of 1,3,5-trinitrobenzene with aniline in dimethyl sulfoxide (DMSO). In the presence of buffers containing 1,4-diazabicyclo(2.2.2)octane, (Dabco), and its acid salt, DabcoH^+ , the anilide σ -adduct is formed. The reaction of ethyl 2,4,6-trinitrophenyl ether with aniline in DMSO containing Dabco occurs in two stages. The first gives a σ -adduct intermediate on the substitution pathway, which has been identified spectroscopically. The second yields 2,4,6-trinitrodiphenylamine, the substitution product. Kinetic studies show that proton transfer is rate-limiting both in the formation of the intermediate and in its subsequent acid-catalysed decomposition. Phenoxide is a considerably better leaving group than ethoxide and the substitution reactions of phenyl 2,4,6-trinitrophenyl ethers and phenyl 2,4-dinitronaphthyl ether with aniline in DMSO occur without the accumulation of intermediates. The kinetics indicate both uncatalysed and base catalysed pathways.

Values have been determined for the pK_a in DMSO of several ammonium ions derived from amines which have previously been widely used as nucleophiles in nucleophilic aromatic substitution reactions; values are also given for four polynitrodiphenylamines used as indicators.

Second order rate constants (k_s) are presented for the reaction of substituted phenyl 2,4,6-trinitrophenyl ethers with a series of phenolate ions having pK_a values both higher and lower than that of the respective leaving groups in aqueous solution. The rate constants for the reverse reaction (k_{-s}) have also been measured. The Brønsted diagram formed when plotting $\log k_s$ versus pK_a shows a change in slope when $\Delta\text{pK}_a = 0$ (ΔpK_a being the difference in pK_a values of the leaving group and nucleophile). This is consistent with a two step process involving a discrete σ -adduct intermediate. From the measured β values effective charges have been determined and the overall effective charge map constructed.

Kinetic studies have been made for the reactions of substituted phenyl 2,4,6-trinitrophenyl ethers with substituted phenolate ions in 74% DMSO-water (v/v). Two reactions are observed. The evidence suggests that the more rapid involves formation of a 1,1 σ -adduct between the substrate and the phenolate ions. The slower reaction is attributed to hydroxide attack at the 3-position of the substrate.

ACKNOWLEDGEMENTS

When I reflect back over my time in Durham there are many people who have made my time here very enjoyable and now I have a chance to say thank you.

Firstly I would like to thank my supervisor Dr. M. R. Crampton, for all his time, guidance, patience and most of all his friendship throughout the years. Talking about work or the great game of football was and always will be a pleasure, thank you. A colleague who has also been greatly appreciated is Mr. Colin "CG" Greenhalgh. Not only for his technical wizardry, which is second to none, but for being a great friend and excellent company.

I am grateful to my fellow Phys. Org. lab members, Andy, Si, Alex, Munro, Swifty, Kathryn, Gaynor, E, Lynsey, Pablo and McAninly, either past or present and close friends Archie, Sarah and Phil. A special mention as well goes to Jean and Hazel for their marriage counselling and advice, all I'll say is never!

In addition I would like to thank all the members of the Interchem 5-side football team, which I was lucky to be a part of, for their overwhelming lack of skill and especially the successful 96/97 cup winning team. Similarly I will always be treasured with the memories of Grad. Soc. A. F. C. past and present for all the entertainment both on and off the field.

Finally it leaves me to say thank you to my parents who have always encouraged and supported me throughout my studies and last but not least to Penny for tolerating me over the past few months yet always being there to share my troubles with and cheer me up, thank you.

DECLARATION

The material in this thesis is the result of research undertaken in the Department of Chemistry, University of Durham between October 1994 and October 1997. It is the original work of the author except where acknowledged by reference and has not been submitted for any other degree.

STATEMENT OF COPYRIGHT

The copyright of this thesis lies with the author. No quotations from it should be published without his prior written consent, and information derived from it should be acknowledged.

To my Mum & Dad

and in memory of my Grandparents.

CONTENTS

	Page
Chapter 1: Introduction.	1
1.1 Nucleophilic Aromatic Substitution.	2
1.2 Activated Aromatic Substitution Processes.	3
1.2.1 S _N Ar Substitutions.	3
1.2.2 S _N Ar ^H Substitutions.	5
1.2.3 Activated Nucleophilic Aromatic Photo Substitutions.	9
1.3 Nucleophilic Substitutions of Non-Activated Aromatic Substrates.	11
1.3.1 The Benzyne Mechanism.	11
1.3.2 Nucleophilic Substitutions on Aromatic Diazonium Compounds.	12
1.3.3 A Single Step Mechanism for S _N Ar.	13
1.3.4 Radical Mechanisms, S _{RN} 1 & S _{RN} 2.	18
1.3.5 S _{ON} 2 Mechanism.	21
1.4 The S _N Ar Substitutions.	22
1.4.1 Stability of the σ-Complexes.	23
1.4.2 Evidence for the Formation of σ-Complexes.	25
1.4.3 Leaving Group Ability.	26
1.4.4 Solvent Effects.	27
1.4.5 The Role of π-Complexes.	28
1.5 Nucleophilic Aromatic Substitutions with Amines.	31
1.5.1 Base Catalysis.	36
1.5.1.1 The Specific Base General Acid Catalysed Mechanism.	37
1.5.1.2 Rate Limiting Proton Transfer.	40
1.6 Reactions of Aromatic Amines & Alcohols.	44
1.6.1 Aromatic Amines.	44
1.6.2 Aromatic Alcohols.	50
1.7 References.	55
Chapter 2: Kinetic and Equilibrium Studies Involving the Reactions of Aniline with Electron Deficient Aromatic Substrates in Dimethyl Sulfoxide.	61
2.1 The Reactions of Aniline.	62
2.2 pK _a Values.	63

	Page	
2.3	Reactions of 1,3,5-Trinitrobenzene, 2.2.	64
	2.3.1 Experimental Procedure.	65
	2.3.2 Dependence on Aniline.	66
	2.3.3 Dependence on Dabco.	67
	2.3.4 Determination of the Equilibrium Constant, K_1K_{Dabco} , for σ -Adduct Formation using Absorbance Measurements.	68
	2.3.5 Kinetic Analysis.	69
	2.3.6 Carbon-Bonded σ -Adduct?	71
2.4	Reactions of Ethyl 2,4,6-Trinitrophenyl Ether, 2.5.	75
	2.4.1 ^1H NMR Studies.	77
	2.4.2 Formation of the σ -Complex, 2.7.	80
	2.4.2.1 Experimental Procedure.	80
	2.4.2.2 Dependence on Aniline.	81
	2.4.2.3 Dependence on Dabco.	82
	2.4.2.4 Determination of the Equilibrium Constant for σ -Adduct Formation using Absorbance Measurements.	83
	2.4.2.5 Kinetic Analysis of σ -Adduct Formation.	84
	2.4.3 Formation of the Substituted Product, 2.8.	86
	2.4.3.1 Kinetic Analysis.	86
2.5	Reactions of Phenyl 2,4,6-Trinitrophenyl Ethers, 2.10.	88
	2.5.1 Reactions of 2.10a-e with Aniline.	89
	2.5.2 Reactions of 2.10a-e with Aniline and Dabco.	91
	2.5.3 Kinetic Analysis.	92
	2.5.4 Interaction of 2.10 and Dabco.	92
2.6	Reactions of Phenyl 2,4-Dinitronaphthyl Ether, 2.13.	93
	2.6.1 Dependence on Aniline and Dabco Concentration.	93
2.7	Synthesis of Substrates.	95
	2.7.1 Preparation of the 4-Substituted Phenyl 2,4,6-Trinitrophenyl Ethers.	95
	2.7.2 NMR Data and Melting Points of the Substrates Synthesised.	96
2.8	Discussion and Comparisons.	98
	2.8.1 Reactions of 1,3,5-Trinitrobenzene, 2.2.	98
	2.8.2 Reactions of Ethyl 2,4,6-Trinitrophenyl Ether, 2.5.	100
	2.8.3 Reactions of Substituted Phenyl 2,4,6-Trinitrobenzenes, 2.10a-e.	102
	2.8.4 Reactions of Phenyl 2,4-Dinitronaphthyl Ether, 2.13.	103
2.9	References.	104

	Page
Chapter 3: Acidities of Various Substituted Ammonium Ions in Dimethyl Sulfoxide.	106
3.1 Introduction.	107
3.2 Spectroscopic Technique: Indicators.	109
3.3 Synthesis of Indicators and Amine Salts.	111
3.3.1 Synthesis of Indicators.	111
3.3.1.1 NMR Data and Melting Points of Indicators.	111
3.3.2 Synthesis of Amine Salts.	114
3.3.2.1 NMR Data for Amine Salts.	114
3.4 Experimental Procedure.	115
3.5 Results.	116
3.5.1 Indicator: 4',2,4,6-Tetranitrodiphenylamine.	118
3.5.2 Indicator: 2,4,6-Trinitrodiphenylamine.	118
3.5.3 Indicator: N-Phenyl-2,4-Dinitronaphthylamine.	119
3.5.4 Indicator: 2,4-Dinitrodiphenylamine.	121
3.6 Equilibrium Constants.	122
3.6.1 Determination of Equilibrium Constants.	122
3.6.2 Determination of pK_a Values.	124
3.7 Discussion.	125
3.7.1 Amine Basicities.	125
3.7.2 Indicator Acidities.	127
3.8 References.	128
Chapter 4: Stepwise versus Concerted Mechanism in the Reactions of Phenoxide Ions with Phenyl Picrates?	130
4.1 Conflicting Evidence.	131
4.2 Linear Free Energy Relationships.	133
4.2.1 Brønsted Equation.	133
4.3 Experimental Procedure.	135
4.3.1 Buffer Solutions.	136
4.3.2 Sampling Technique.	137
4.4 The Forward Process: Reactions of Substituted Phenyl 2,4,6-Trinitrophenyl Ethers.	139
4.4.1 4'-Nitrophenyl 2,4,6-trinitrophenyl Ether, 4.5.	140
4.4.2 3',4'-Dinitrophenyl 2,4,6-Trinitrophenyl Ether, 4.6.	142
4.4.3 3'-Nitrophenyl 2,4,6-Trinitrophenyl Ether, 4.7.	143

	Page
4.4.4 Forward Process: Brønsted Diagrams.	144
4.5 The Reverse Process: Dependence on Substrate Structure.	147
4.5.1 Phenol Nucleophile.	148
4.5.2 4-Chloro-Phenol Nucleophile.	149
4.5.3 Reverse Process: Brønsted Diagrams.	150
4.6 Kinetic Analysis.	151
4.6.1 Forward Process.	151
4.6.2 Reverse Process.	152
4.6.3 Brønsted β Values.	153
4.6.4 Effective Charge Map.	154
4.7 Reactions of Hydroxide with Substrates, 4.5 & 4.7.	156
4.7.1 Experimental Procedure.	157
4.7.2 Results and Kinetic Analysis.	157
4.8 Synthesis of Substrates.	159
4.8.1 NMR Data and Melting Points of Substrates Synthesised.	159
4.9 Discussion.	160
4.9.1 Global Equation and Brønsted Diagram.	160
4.9.2 Charge Distribution.	161
4.10 References.	163
Chapter 5: Kinetic Studies on the Reaction of Substituted Aryl 2,4,6-Trinitrophenyl Ethers with Various Phenols in DMSO / H₂O Mixtures. The Elusive Intermediate?	164
5.1 Kinetic and Equilibrium Studies.	165
5.2 Experimental Procedure.	166
5.2.1 Determination of pH.	167
5.3 Solvent Studies.	168
5.3.1 Observation of a Slow Reaction.	168
5.3.2 Observation of a Fast Reaction.	170
5.4 Reaction of 4'-Methoxy-Phenyl 2,4,6-Trinitrophenyl Ether with 4-Methoxy-Phenol.	172
5.4.1 Reactions of 5.2 with Sodium Hydroxide.	173
5.4.1.1 Kinetic Analysis.	175
5.4.2 The Fast Process: Reaction of 5.2 with 4-Methoxy-Phenolate.	176
5.4.2.1 Kinetic Analysis: Fast Process.	177
5.4.3 The Slow Process: Reaction of 5.2 with 4-Methoxy-Phenolate.	178

	Page
5.4.3.1 Constant Buffer Ratio.	178
5.4.3.2 Variation in Buffer Ratio, [MeO-PhOH : MeO-PhO ⁻].	178
5.4.4 Kinetic Analysis: Slow Process.	180
5.5 Reactions of Phenyl 2,4,6-Trinitrophenyl Ether with Phenol.	183
5.5.1 Reactions of 5.3 with Sodium Hydroxide.	184
5.5.1.1 Kinetic Analysis.	185
5.5.2 The Fast Process: Reaction of 5.3 with Phenolate.	186
5.5.2.1 Kinetic Analysis: Fast Process.	187
5.5.3 The Slow Process: Reaction of 5.3 with Phenolate.	188
5.5.3.1 Constant Buffer Ratio.	188
5.5.3.2 Various Buffer Ratio, [PhOH : PhO ⁻].	189
5.4.4 Kinetic Analysis: Slow Process.	190
5.6 Reactions of 1,3,5-Trinitrobenzene with Phenol.	192
5.6.1 Reactions with Sodium Hydroxide and Methoxide.	193
5.6.1.1 Kinetic Analysis.	194
5.6.2 The Fast Process: Reaction of 5.4 with Phenolate.	195
5.6.2.1 Kinetic Analysis: Fast Process.	195
5.6.3 The Slow Process: Reaction of 5.4 with Phenolate.	196
5.6.3.1 Constant Buffer Ratio.	196
5.6.3.2 Various Buffer Ratio, [PhOH : PhO ⁻].	196
5.6.4 Kinetic Analysis: Slow Process.	198
5.7 Reactions of Substrates 5.2, 5.3 & 5.4 with Borax Buffers.	201
5.8 Discussion and Summary.	202
5.8.1 The Slow Process: Attack by Hydroxide Ions.	202
5.8.2 Base Catalysis, k_{PhO^-} .	203
5.8.3 π -Complexes.	205
5.8.4 The Fast Process: Addition of Phenolate.	205
5.8.4.1 Carbon Bound σ -Adduct?	205
5.8.4.2 Formation of the 1,1 σ -Adduct.	206
5.9 References.	208
Chapter 6: Experimental Details	209
6.1 Measurement Techniques.	210
6.1.1 U.V./Vis. Spectrophotometry.	210

	Page
6.1.2 Stopped-Flow Spectrophotometry.	213
6.1.3 NMR Spectroscopy.	213
6.1.4 pH Measurements.	213
6.2 Materials.	214
6.2.1 Solvents.	214
6.2.2 Reagents.	214
6.3 Derivation of Rate Equations.	215
6.3.1 Attack at an Unsubstituted Ring Position.	215
6.3.2 Attack at a Substituted Ring Position.	218
6.3.3 Formation of the Substituted Product.	222
Appendix.	225
A.1 First Year Induction Course (October 1994).	226
A.2 Research Colloquia, Seminars and Lectures arranged by Durham University Chemistry Department 1994 - 1997.	227
A.3 Conferences Attended.	235

Chapter 1.

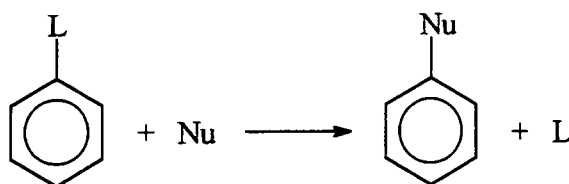
Introduction.

1.1 Nucleophilic Aromatic Substitution.

For many years the term "aromatic substitution" was largely confined to reactions involving electrophiles. Much effort was devoted to understanding the regioselectivity of substitution; to determine why, of the five nuclear hydrogen atoms in a monosubstituted benzene, sometimes one of the two meta to the substituent was replaced and at other times one of the three in the ortho- and para-positions. Another problem was to establish the identity of the effective electrophiles provided by the various chemicals used to effect the substitution.

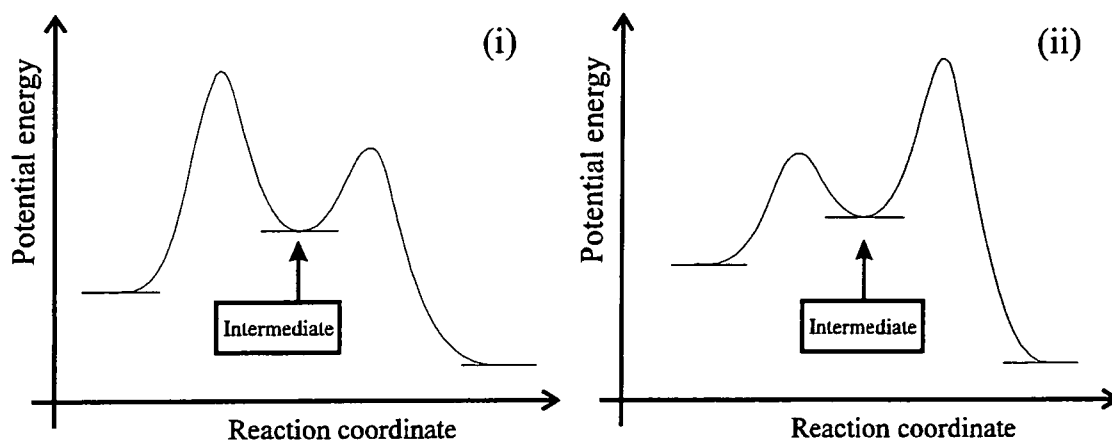
In nucleophilic aromatic substitution the analogous problems have only subordinate interest. Hydrogen is seldom displaced, due to the fact that the hydride ion (H^-) is a very poor leaving group.¹ The readily displaceable groups are those which can depart with the bonding electron pair as stable anions or molecules. There is usually only one displaceable group per molecule and so the directing effects of other substituents are not often considered. The effective form of the nucleophilic reagent is usually obvious.

A general nucleophilic aromatic substitution can be defined as a reaction in which an anionic or neutral nucleophile displaces a potential leaving group L at a ring position, equation 1.1. However, because of its π -electron system, it is obvious that a benzene ring is intrinsically reluctant to react with a nucleophile. Accordingly, the question follows of how such substitutions can actually proceed under relatively mild conditions.

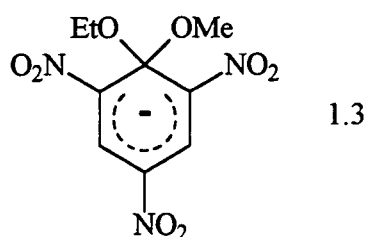


equation 1.1

Figure 1.1 Two possible representations for reactions involving an intermediate such as in equation 1.2.

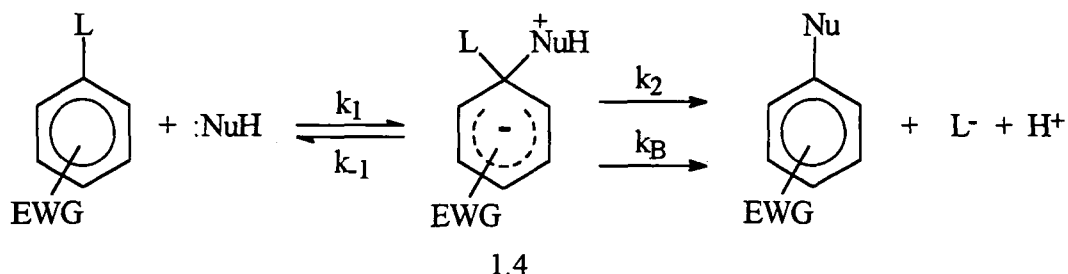


The mechanism is supported by significant analogies with other phenomena. This includes electrophilic aromatic substitution, for which the intermediate complex mechanism has been recognised on experimental grounds,⁴ and the formation of isolable addition complexes by the interaction of nucleophilic reagents with activated aromatic substrates. Foremost of these is complex 1.3, formed and isolated by the addition of methoxide ion to 2,4,6-trinitrophenetole. This initial work and assignment of the structure of 1.3 was carried out by Jackson⁵ and Meisenheimer⁶ at the turn of the century and resulted in a class of compounds designated Meisenheimer complexes. Probably the most convincing evidence is the recent successful and unambiguous NMR identification of the intermediates of the type 1.1 along some substitution pathways of nitroaromatics.^{7,8}



The stability of the σ -complexes is enhanced by the use of a protic / dipolar aprotic cosolvent system, i.e. H_2O -DMSO, ROH-DMSO. The use of DMSO as a cosolvent has made available a much wider range of adducts to be studied and hence provided more information on the mechanism of $\text{S}_{\text{N}}\text{Ar}$ reactions.⁹⁻¹⁵

In general, reactivity of S_NAr reactions is found to vary with nucleophile, leaving group and solvent. If the reaction involves a neutral nucleophile e.g. water, alcohols, amines, the mechanism can be represented by equation 1.3. The noticeable difference in this case is that the initially formed σ -adduct, 1.4, is zwitterionic and usually contains an acidic proton which can be removed by the nucleophile itself or an external base. Consequently conversion of the zwitterion to the products can either proceed via an uncatalysed pathway, k_2 , or a base catalysed pathway, k_B .



equation 1.3

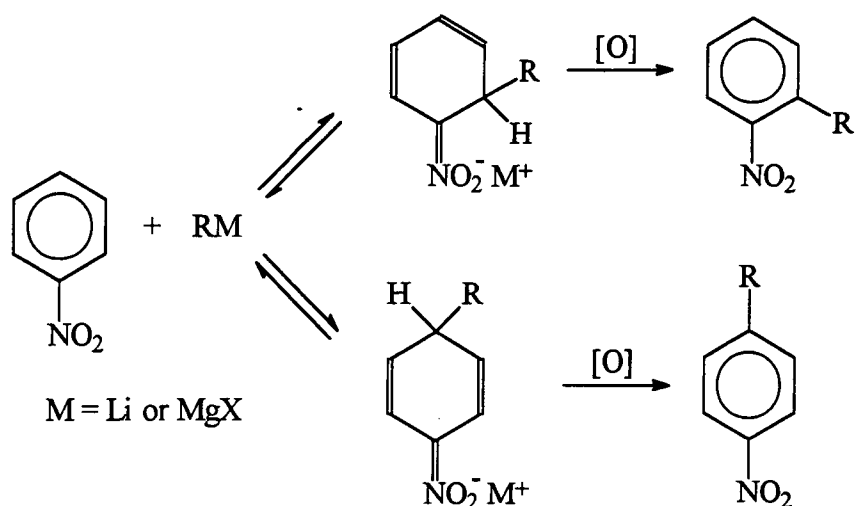
1.2.2 S_NAr^H Substitutions.

Nucleophilic substitutions of a hydrogen in an electron-deficient aromatic substrate via an S_NAr mechanism is not a common process. This is because the hydride ion has a low stability and hence is a very poor leaving group.^{2,9,10,17} The first examples of the displacement of hydrogen in the benzene ring by action of nucleophiles were reported in the literature about one hundred years ago, e.g. reaction of nitroaromatics with the hydroxide anion in the presence of air oxygen yields a mixture of ortho- and para-nitrophenols.¹⁸

These types of reactions which will be referred to as S_NAr^H processes, and are often of considerable interest for the functionalisation of nitroarene systems. As with general S_NAr reactions, they usually occur by addition of the nucleophile to form σ -complex type intermediates. These intermediates then decompose in various oxidation pathways formally achieving nucleophilic aromatic substitution of hydrogen in the aromatic ring.

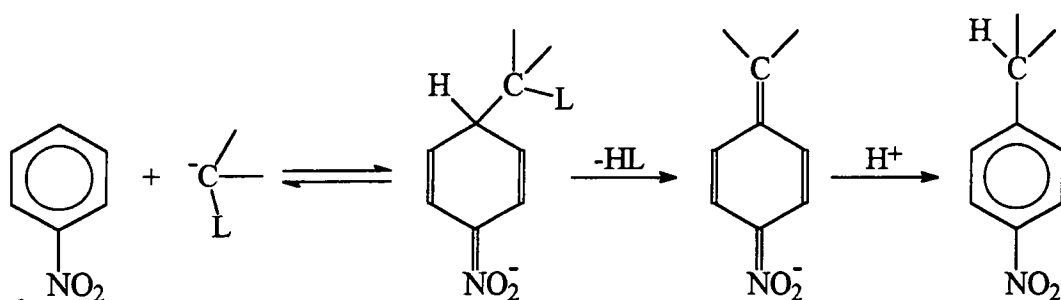
In this field, three main types of process may be distinguished. The first is where the rearomatization is undoubtedly the result of chemical oxidation of the σ -complex intermediate, scheme 1.1.

The oxidation process most often occurs "spontaneously" (i.e. without addition of an oxidising agent) as nitroarenes themselves can be reduced. But the presence of an oxidant (H_2O_2 , N-bromosuccinimide), can aid the completion of the process. Generally the reactions take place under basic conditions unless a readily protonated leaving group is not present.



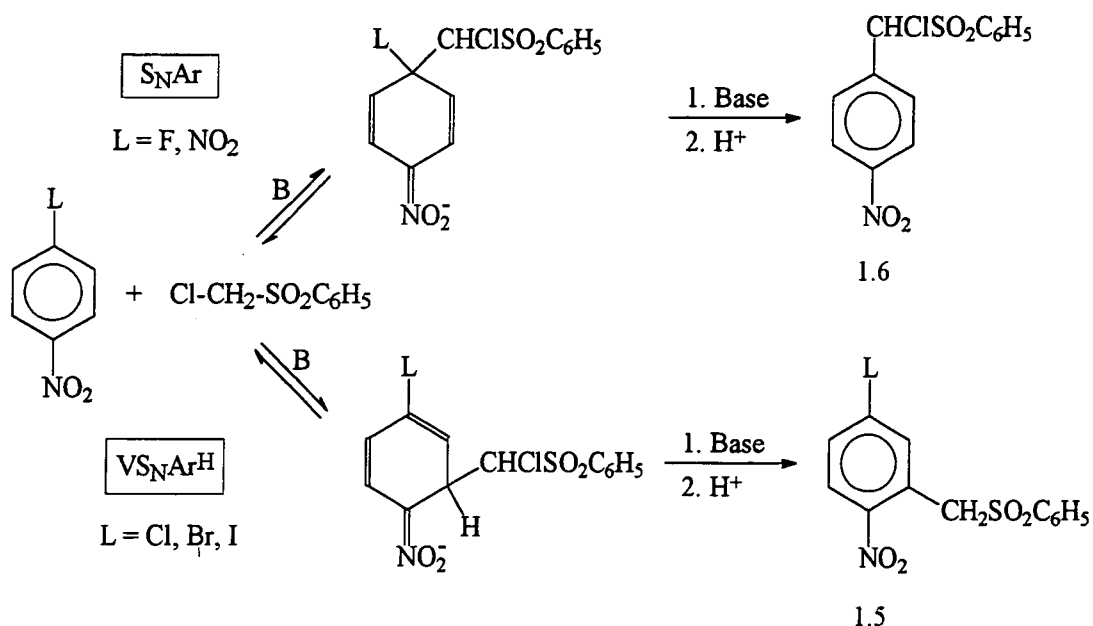
scheme 1.1

Vicarious Nucleophilic Aromatic Substitutions ($\text{VS}_{\text{N}}\text{Ar}^{\text{H}}$) is the name given to the second type of process, equation 1.4. The reactions have been developed by Makosza and co-workers over the past fourteen years. Their investigations found that carbanions containing leaving groups at the reaction centre promote the reaction with nitroarenes, substituting the hydrogen atom para- or ortho- to the nitro group.¹⁹ The hydrogen bonded to the sp^3 carbon of these adducts departs accompanied by the nucleofugal group in a base induced β -elimination step.



equation 1.4

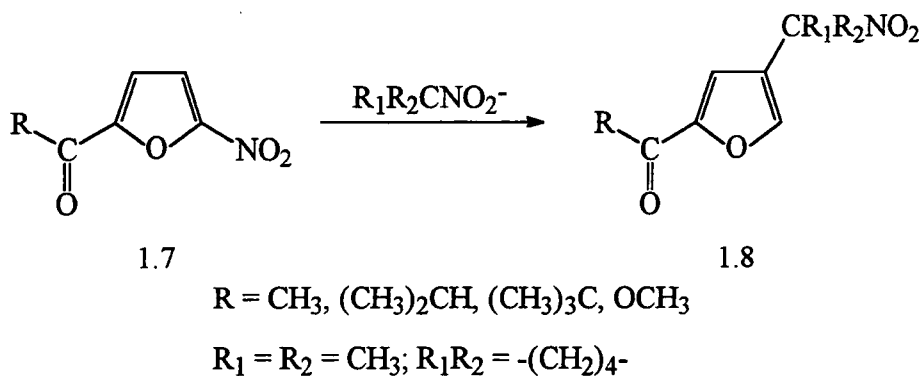
Since both S_NAr and VS_NAr^H reaction pathways involve the σ -complex intermediate, in appropriate systems the two pathways may compete.²⁰ Scheme 1.2 shows this behavior in the reaction of para-substituted nitrobenzenes with chloromethyl phenyl sulphone in the presence of a strong base (KOH, NaOH or *t*-BuOK) in DMSO.



scheme 1.2

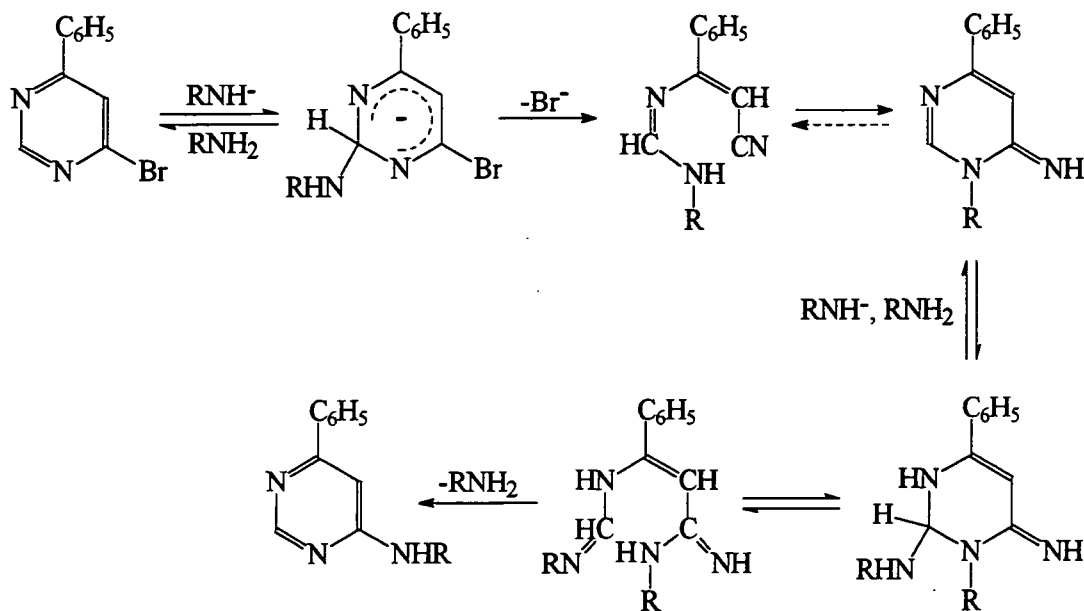
In the case of the 4-chloro, 4-bromo and 4-iodo substituent the product is exclusively the corresponding 3-halo-6-nitrobenzyl phenyl sulfone, 1.5. The S_NAr substitution product, α -chloro-4-nitrobenzyl phenyl sulfone 1.6, was not detected suggesting that the vicarious pathway proceeds at a much faster rate. Only when replacing the substituents with greater electron-withdrawing properties, e.g. F or NO_2 is the S_NAr process able to compete and both sulphones are produced. In this case addition of excess base would greatly favour hydrogen substitution.²¹

Equation 1.5 is an example of the third type of hydrogen substitution process. Such reactions are referred to as cine-substitutions when the incoming group enters α position adjacent to the leaving group. Tele-substitutions are when the incoming group is meta or para to the leaving group. Upon treatment of the 5-acyl or 5-alkoxycarbonyl-2-nitrofurans 1.7 with salts of secondary nitroalkanes such as 2-nitropropane and nitrocyclopentane, the cine-substitution products 1.8 are formed in yields of upto 90%.²²



equation 1.5

Within the area of $\text{S}_{\text{N}}\text{Ar}^{\text{H}}$ substitutions, the characteristic behaviour of aza-aromatic compounds is of importance. The inherent activation is provided by their ring nitrogen atoms, resulting in susceptibility to both $\text{S}_{\text{N}}\text{Ar}^{\text{H}}$ substitutions, and $\text{S}_{\text{N}}\text{Ar}$ if a suitable leaving group is present. The difference occurs in strongly basic media, in that initial addition of the nucleophile (AN) at an unsubstituted ring carbon may induce a multistep reaction sequence scheme 1.3, involving ring opening-reclosure of the heterocyclic moiety (RORC).^{23,24}

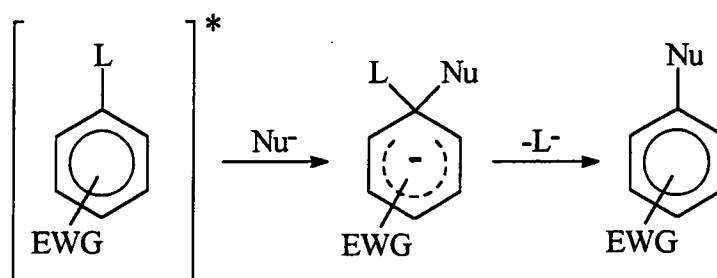


scheme 1.3

1.2.3 Activated Nucleophilic Aromatic Photo-Substitutions.

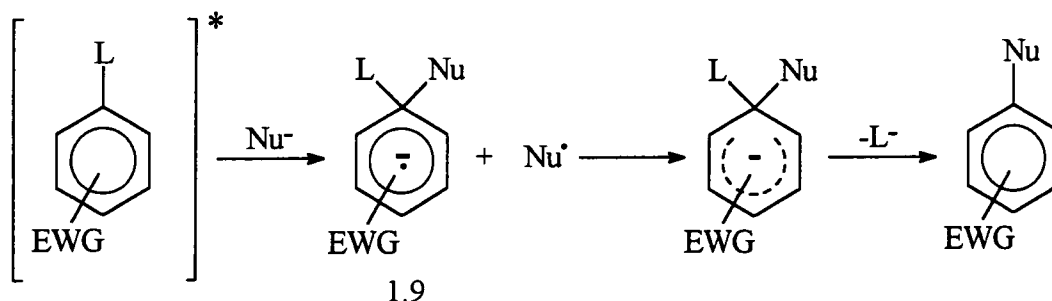
Substitutions of electron-deficient aromatics may be suitably induced by light irradiation with the elimination of either a leaving group or a hydrogen atom. Three main mechanisms have been identified so far, equations 1.6, 1.7, 1.8.

By far the most important mechanism for activated nucleophilic aromatic photosubstitutions is the S_N2Ar^* , equation 1.6.²⁵⁻²⁷ This pathway is typical for photosubstitutions involving meta activation by an NO_2 group as opposed to ortho or para directing effects observed so far.^{25,26} It involves the formation of an intermediate σ -complex through direct interaction between the excited nitroaromatic substrate and the nucleophile.



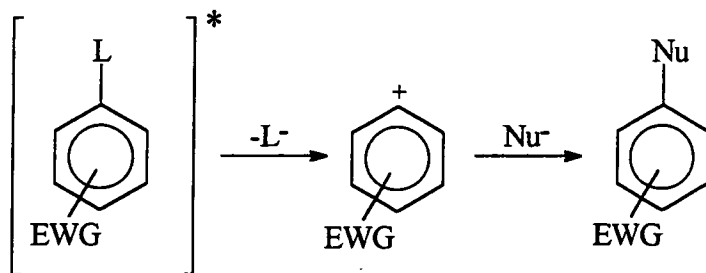
equation 1.6

The $S_N(Et)Ar^*$ mechanism shown in equation 1.7 was first proposed by Havinga and co-workers in 1969. This was later elaborated by Mutai and co-workers in photosubstitutions exhibiting ortho/para activation by the NO_2 group.²⁸ The mechanism involves an initial electron transfer from the nucleophile to the excited nitroaromatic substrate to form a radical anion intermediate 1.9, followed by coupling of the resulting radicals to give a σ -complex.



equation 1.7

Finally the unexpected unimolecular behaviour in photosubstitutions has been accounted for by the proposed S_N1Ar^* mechanism, equation 1.8.^{25,26}



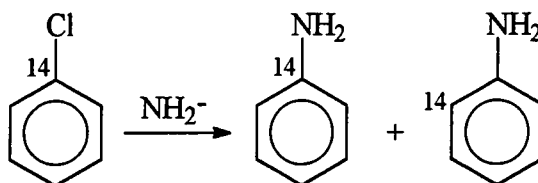
equation 1.8

1.3 Nucleophilic Substitutions of Non-Activated Aromatic Substrates.

In the absence of strongly electron-withdrawing groups, nucleophilic substitutions of unactivated or poorly activated aromatics cannot be promoted by initial covalent addition of the nucleophile to the ring. The processes contained within this criteria have been summarised below.

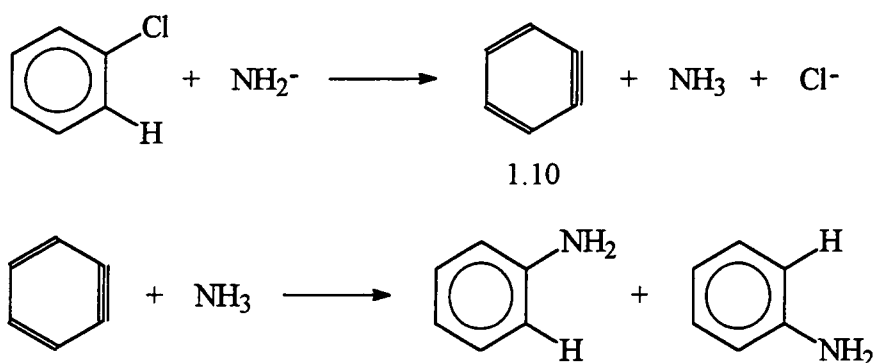
1.3.1 The Benzyne Mechanism.

The conversion of non-activated aryl halides with metallic amides yields arylamines. The S_NAr mechanism is thought not to apply here as there are no strong electron-withdrawing groups present. It was not until 1953 that Roberts postulated an elimination-addition mechanism involving a benzyne intermediate.²⁹⁻³¹ The preliminary evidence for the benzyne intermediate was obtained through ^{14}C -tracer studies of rearrangements with halobenzenes. The reaction of 1- ^{14}C -chlorobenzene with potassium amide produced roughly equal amounts of aniline, labelled in the 1- and 2-position as shown in equation 1.9.



equation 1.9

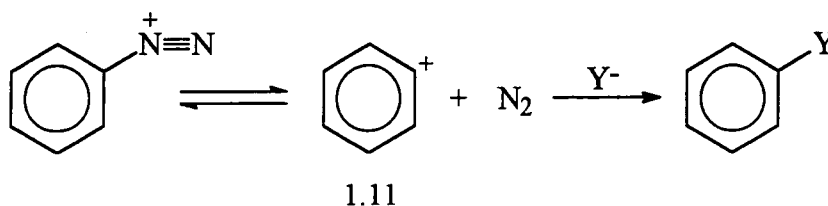
Experiments designed to determine the role of the hydrogen atom located ortho to the displaced halogen atom have been reported. Comparison of the rates of formation of the arylamine from bromobenzene and bromobenzene-2-d result in $k_H / k_D = 5.5$. Hence the proton is removed from the substrate in the rate-determining step.³⁰ In the case of fluorobenzene-2-d however no arylamine is formed, even though its deuterium is known to exchange with the solvent a million times faster than deuterobenzene.³² Evidently when the halogen is weakly electron-withdrawing but a good leaving group, hydrogen abstraction is the slow step; though, when the halogen is strongly electron-withdrawing but unreactive as a leaving group, its expulsion is the slow step. The proposed mechanism, scheme 1.4, shows the symmetrical benzyne 1.10 which can be attacked by ammonia at either of two positions, explaining why half of the labelled carbon is at the 2-position.



scheme 1.4

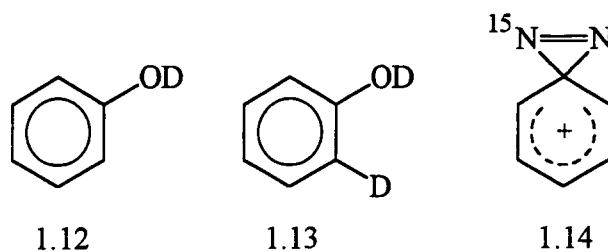
1.3.2 Nucleophilic Substitutions on Aromatic Diazonium Compounds.

A nucleophilic aromatic substitution mechanism, specific for substitution on aromatic diazonium compounds is shown in equation 1.10. There is good evidence to support the intermediacy of aryl cations, such as 1.11, when a leaving group as stable as N_2 is present.³³⁻³⁶

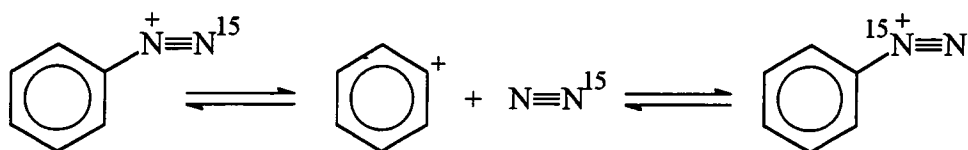


equation 1.10

D_2O reacts with the diazonium salt to give only the product 1.12, none of the product 1.13 is formed. This enables the exclusion of the benzyne mechanism discussed previously. Also there is no nucleophilic involvement of water in the rate determining step as D_2O and H_2O react at almost equal rates.³³



The thermal decomposition (dediazonation) of ^{15}N -labelled diazonium salt proceeds with a significant accompanying amount (*ca.* 8%) of isotopic rearrangement. When the reaction is conducted under 300 atm of unlabelled nitrogen, 2.5% of external nitrogen is incorporated into the residual diazonium ion at 70% dediazonation.³⁶ This is believed to be due to a dissociation, reassociation (equation 1.11) and not through a spirodiazirine cation intermediate 1.14.

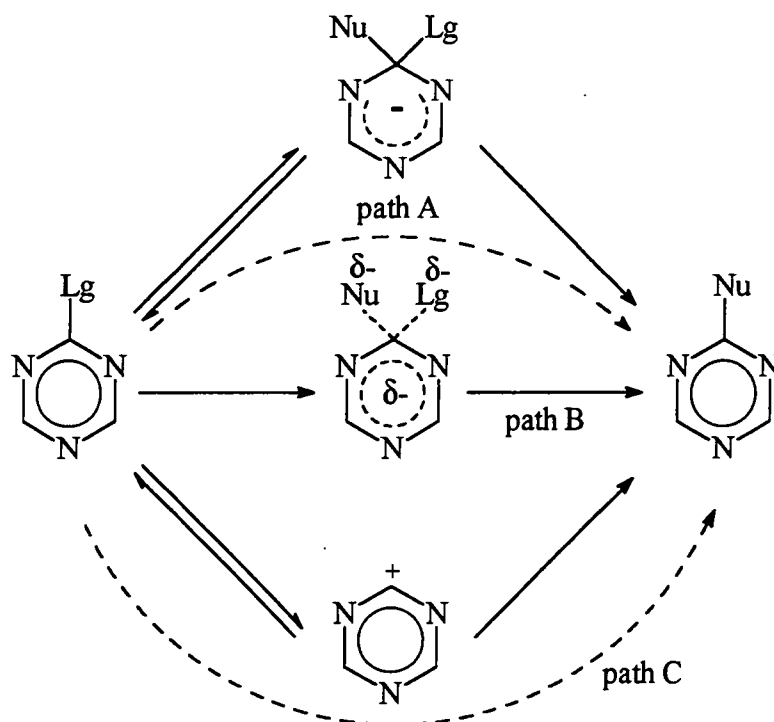


equation 1.11

1.3.3. A Single Step Mechanism for Nucleophilic Aromatic Substitutions.

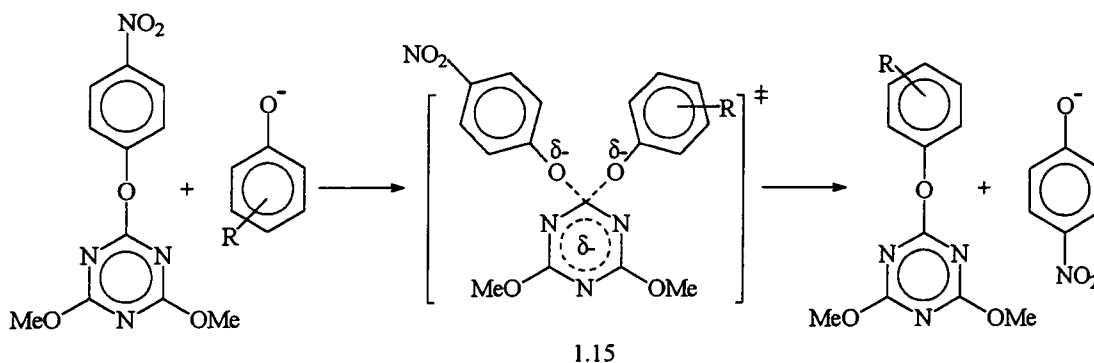
Nucleophilic substitution at a trigonal carbon often involves the formation of an intermediate with tetrahedral carbon which collapses to yield the transferred product. This mechanism has been challenged for reactions at a carbonyl centre where under certain conditions, the reaction operates through a single transition state.³⁷

Nucleophilic aromatic substitution is known where heterolytic mechanisms exist with two extremes of timing sequence for bond formation and bond fission, scheme 1.5.2,9,38 Evidence is found in the existence of aryne and carbocation intermediates for path C, scheme 1.5. Consequently it may be possible under favourable conditions (*i.e.* by suitable manipulation of the structures of solvent, nucleophile, leaving group and aromatic nucleus) to observe a concerted $S_{\text{N}}2$ type process, indicated by path B.



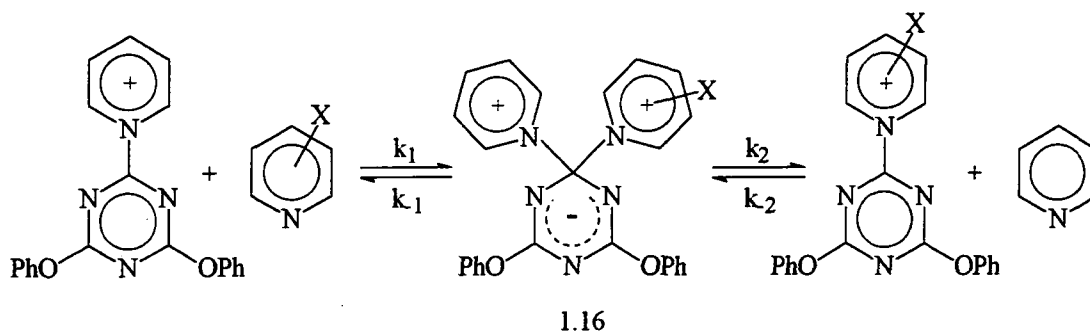
scheme 1.5

Recent work published by Williams indicates the displacements of 4-nitrophenolate ions from 2-(4-nitrophenoxy)-4,6-dimethoxy-1,3,5-triazine by substituted phenolate ions, equation 1.12 (using pK_a values both above and below that of the leaving group, 4-nitrophenol) in aqueous solution obeys a linear Brønsted type equation.^{39,40} The absence of curvature in the Brønsted free energy relationship formed by plotting the second-order rate constant for displacement, versus the pK_a of the attacking nucleophile, is considered good evidence that there is no change in the rate limiting step and hence a concerted single step mechanism applies.⁴¹ Here 1.15 is a transition state rather than a reaction intermediate.



equation 1.12

Similarities have not been seen in the analogous reaction, equation 1.13 of substituted pyridines with 1'-(4,6-diphenoxy-1,3,5-triazin-2-yl)pyridinium ion in aqueous solution.^{42,43} The Brønsted free energy plot consists of two intersecting linear correlations consistent with a two step mechanism involving a Meisenheimer like intermediate, 1.16.



equation 1.13

In the Brønsted equation, shown below equation 1.14, the coefficient β measures the susceptibility of rate constant, k_B , to change in base strength, K_B , of reacting bases. Values of β may be used to estimate bonding changes and changes in effective charge during the course of a reaction.

$$\log k_B = \beta \log K_B + \text{constant} \quad \text{equation 1.14}$$

In a stepwise reaction, such as 1.13, Brønsted exponents may be assigned to individual rate coefficients. Thus β_1 refers to the k_1 step, β_2 to the k_2 step, etc. The value of $\Delta\beta$ ($= \beta_2 - \beta_1$) corresponds to the difference in effective charge on a reacting atom in the transition states corresponding to the k_2 and k_1 steps. The observation that $\Delta\beta = 0$ (corresponding to a linear plot) indicates that the transition states have the same electronic charge (and by inference the same structure) and that there is no intermediate intervening between them.

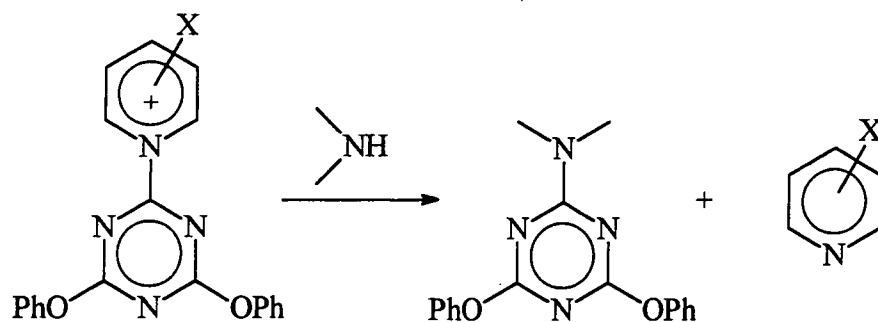
In the cases discussed above $\Delta\beta \leq 0.1$ for the transfer of the triazin-2-yl group between phenolate ions and implies a concerted ($A_N D_N$) reaction mechanism.^{39,40} Where as $\Delta\beta = 0.67$ for the displacement reactions between pyridines and triazin-2-ylpyridinium ions ($\Delta\beta = 0.63$ in the case of pyridinium chloride) implicating a two step mechanism ($A_N + D_N$).^{42,43}

The Hammett equation is another form of free energy relationship, equation 1.15. Here rate constants are correlated with the appropriate σ values for ring-substituents in the nucleophile.

$$\log \frac{k}{k_0} = \sigma\rho \quad \text{equation 1.15}$$

Williams in 1996 used this technique to study the dependence of rate constants for the reactions of morpholine and 4-dimethylaminopyridine with various 2-(substituted phenoxy)-4,6,-dimethoxy-1,3,5-triazines.⁴⁴ The results are consistent with a concerted (A_ND_N) mechanism for aminolysis of arlyoxytriazines. A value of $\Delta\beta$ could not be obtained since the reactions studied involve displacement of ligands by nucleophiles of different fundamental structure and it is not possible to compare effective charges for bond formation and bond fission because effective charge is defined by different ionisation equilibria in each case.⁴⁴ The way around this problem is to use Leffler "methodology".^{45,46} The Leffler α , which measures the extent of bond change relative to the total bond change provides evidence that the process is concerted.

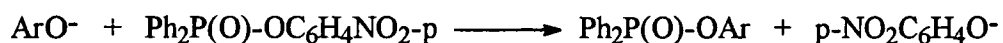
The latest study is that of the aminolysis (using primary and secondary amines) of N-(4,6-diphenoxy-1,3,5-triazin-2-yl) substituted pyridinium salts, equation 1.16 below.⁴⁷ Application of Leffler α values again provides information about the extent of coupling between the two bonding processes, as structures of both the nucleophile and leaving group are varied from reactions studied previously.⁴¹⁻⁴³ In the aminolysis of the triazinyl pyridinium salts the changes in bond fission and bond formation signalled by the polar substituent effects give Leffler α_{lg} and α_{nuc} values of 0.38 and 0.54, respectively, which indicate strong coupling between the bonding changes consistent with a concerted process for the displacement reaction. The adduct in the putative stepwise mechanism is considered too reactive to possess a significant barrier for it to exist as a discrete molecule. This contrasts with the Meisenheimer type intermediate observed in the pyridinolysis of triazin-2-ylpyridinium ion. It may also be important to note that the methylene dipyridinium salt (${}^+py-CH_2-py^+ 2Br^-$) is stable and has been isolated.⁴⁸



equation 1.16

Although Williams and co-workers have produced strong arguments that some S_NAr reactions involve a single step, the evidence may still be considered to be somewhat controversial. There are many examples of S_NAr reactions where the evidence for a two step mechanism is clear cut, so that to prove the absence of an intermediate in a shallow potential well is difficult. Doubts arise regarding the actual method used to distinguish between single step or two step mechanisms. When using the traditional method, the pK_a of the nucleophile is varied by altering the substituents on the nucleophile. However a novel method has been introduced where pK_a variations are imparted by a gradual variation of solvent composition while the identity of the nucleophile is retained.

This technique has been examined by Buncl for the reaction of phenoxides with *p*-nitrophenyl diphenylphosphinate in DMSO- H_2O media at $25^\circ C$, equation 1.17.⁴⁹ The traditional method provides a curved Brønsted plot that is believed to indicate a two step process, as opposed to the novel method which results in a set of individual non-overlapping straight lines implicating a single step process.



equation 1.17

This method has also been applied to the mechanism of sulfonyl transfer reactions, equation 1.18. In this case the new method indicates a stepwise process and contradicts the single step mechanism proposed by the traditional method.⁵⁰



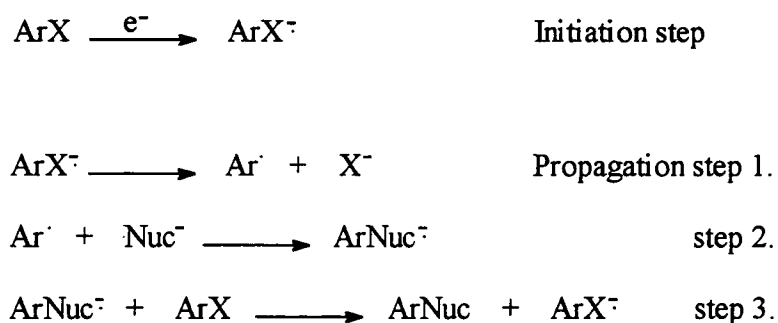
equation 1.18

The current situation is therefore somewhat confused. The novel method based on solvent variation is shown to be a good diagnostic tool and provide accurate information regarding transition state structures. But the traditional method must not yet be discredited until further studies and comparisons come to light.

1.3.4 Radical Mechanisms, $S_{RN}1$ & $S_{RN}2$.

Nucleophilic substitution reactions can occur through a chain process with radicals and radical anions as intermediates. There are two suggestions for the propagation steps, either fragmentation of the radical intermediate anion to give a radical ($Ar\cdot$) which then reacts with a nucleophile ($S_{RN}1$), or the single step reaction of a radical intermediate anion ($ArX^{\cdot-}$) with the nucleophile ($S_{RN}2$) to give the substituted product.

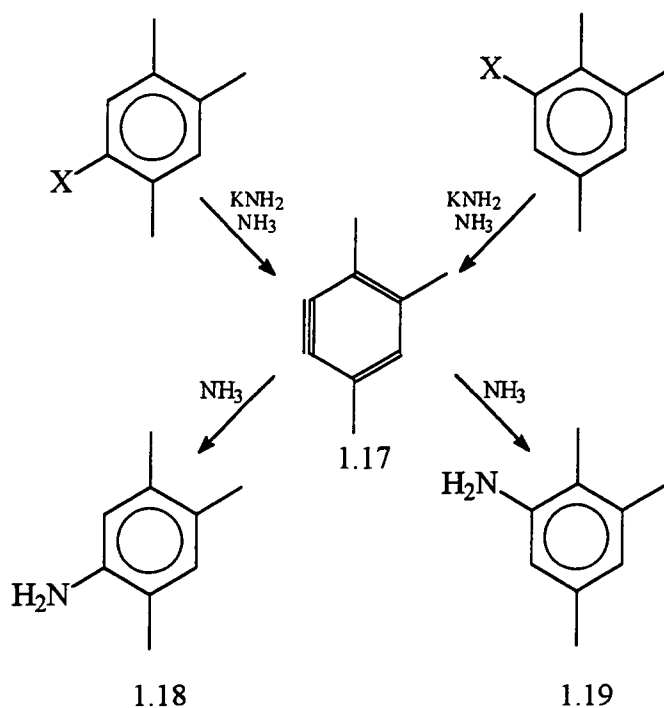
The $S_{RN}1$ mechanism, first proposed in 1970 by Bunnett,⁵¹ involves unimolecular cleavage of the radical anion ($ArX^{\cdot-}$) derived from the substrate. The mechanism can be seen as an example of a potentially general phenomenon, electron-transfer (or redox) catalysis, where a transformation which is not overall an oxidation or reduction is accelerated via a mechanism involving electron-transfer steps, scheme 1.6. It is useful to draw analogy with acid-base (proton transfer) catalysis, where a transformation which does not consume acid or base is accelerated via a mechanism involving proton transfer steps. Here the substrate is activated by oxidation or reduction and not protonation or deprotonation.



scheme 1.6

In the propagation cycle, fragmentation of the radical anion formed by electron transfer to the substrate gives a radical and the anion of the nucleofugal group, step 1. This radical couples with the nucleophile to give a radical anion of the product, step 2. The final step is electron transfer to the substrate, ArX, to continue the cycle, step 3.

It was the reactions of 5- and 6-halo-1,2,4-trimethylbenzenes with KNH_2 in liquid ammonia that first lead to the suggestion of a radical mechanism.⁵² According to the aryne mechanism the reactions should proceed via an intermediate 1.17 and form 5- and 6-amino-1,2,4-trimethylbenzenes (1.18 and 1.19 respectively) in roughly equivalent amounts. Neither the identity of the halogen nor its location (5- or 6-position) should drastically affect the product ratio, scheme 1.7.



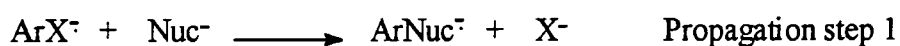
scheme 1.7

These expectations are only fulfilled in the case of bromo and chloro ($\text{X} = \text{Br}, \text{Cl}$) compounds. The products, 1.18 and 1.19, are produced in high yield with a product ratio 1.19:1.18 approximately equal to 1.5 for both 5- and 6-X reactants. However, for iodo ($\text{X} = \text{I}$) compounds, 5- and 6-X product ratios are 0.6 and 5.9 respectively. This result implies that retention of the original orientation is occurring overall and therefore a non-rearranging mechanism is present. The presence of a small amount of the rearranged isomer is evidence that the benzyne mechanism is also taking place but only in a minor role.

Further evidence is obtained when the iodo reaction takes place in the presence of a radical scavenger (e.g. tetraphenylhydrazine). In these cases the product ratio shifted closer to that of 1.5, the aryne ratio.

$S_{RN}1$ reactions have been found to be fairly general for aromatic compounds that are easily reduced. No special substituents are required on the aromatic ring; in fact, simple aryl halides undergo reaction as do aryl halides substituted with alkyl, aryl and alkoxy groups. The processes can be initiated in a variety of ways, photochemically, electrochemically from a cathode or sodium amalgam, or with solvated electrons in liquid ammonia. The leaving group does not have to be iodine. All of the halogens, except fluorine, have been used as leaving groups, as have $-SPh$, $+N(CH_3)_3$, and $-OP(OCH_2CH_3)_2$. There have been attempts to study the effect of substituents on rate constants using a variety of methods of measurement. Competitive experiments have measured the relative rates of electron transfer to an aromatic compound. A comparison of overall rate constants will also include initiation and termination steps. Many different agents have been employed as nucleophiles, e.g. ketone and ester enolate ions, thiolate ions (RS^-), and the amide ion (NH_2^-), harder bases such as alkoxides and aryloxides are not effective. The reaction of the nucleophile with the radical (step 2 in scheme 1.6) is presumed to be diffusion controlled as changing the nucleophile has only a small effect on the rate.⁵³ The observation that the nature of the leaving group does not affect the relative rate of nucleophilic attack provides good evidence that attack is occurring on the radical and not on the radical anion intermediate.

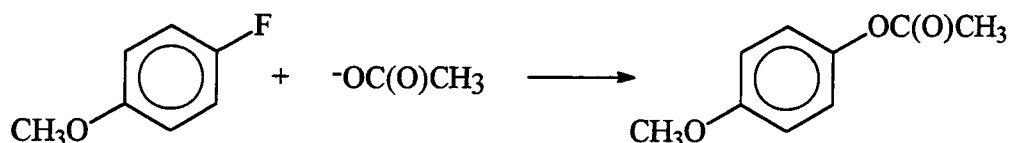
The $S_{RN}2$ mechanism is a bimolecular process which involves direct attack by the nucleophile on the radical anion, equation 1.19. Arguments against the general applicability of the $S_{RN}2$ mechanism include incompatibility with experimental observations or infringement of quantum-mechanical principles.⁵⁴ The $S_{RN}2$ mechanism is thought to operate for reactions involving relatively stable radical anions, which fragment slowly. Possible examples include the photo- or electro-stimulated reactions of pentafluoronitrobenzene with nucleophiles involving fluoride displacement⁵⁵ or the displacement of the nitro group in 4-nitrobenzophenone and 4-nitrobenzotrile.⁵⁶



equation 1.19

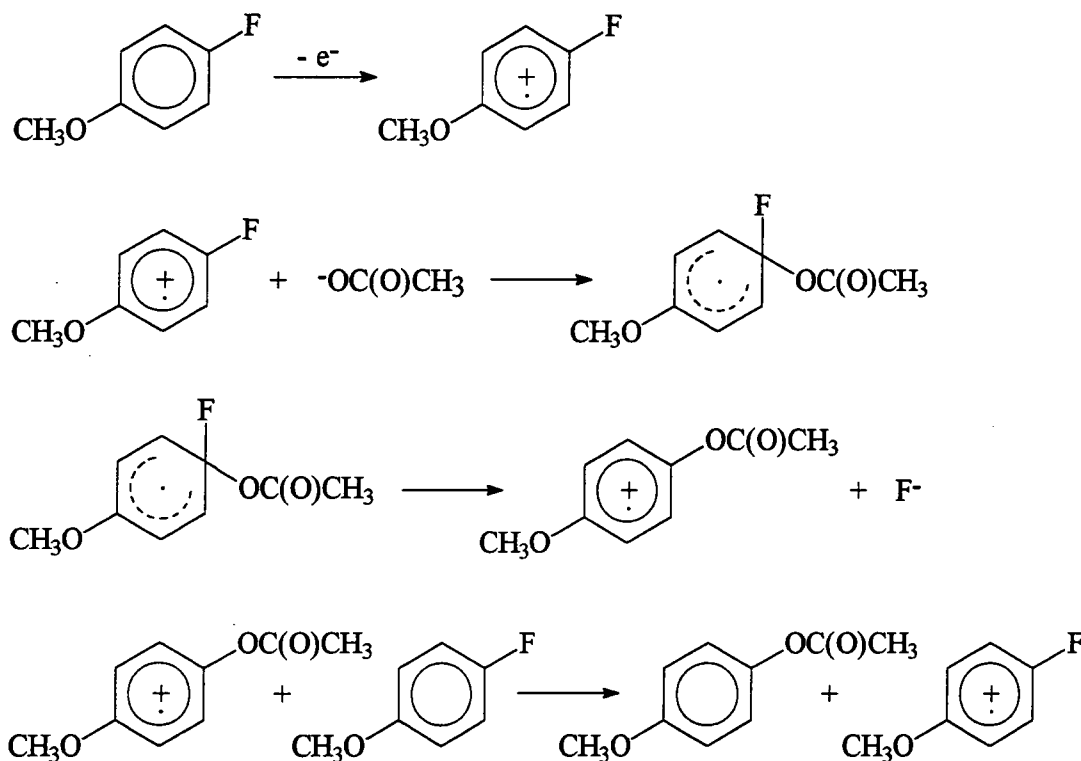
1.3.5 $S_{ON}2$ Mechanism.

Another illustration of an electron transfer chain process is the $S_{ON}2$ (oxidatively initiated nucleophilic substitution, bimolecular) mechanism. The reaction of p-fluoroanisole with ethanoate ion is an example shown below in equation 1.20.



equation 1.20

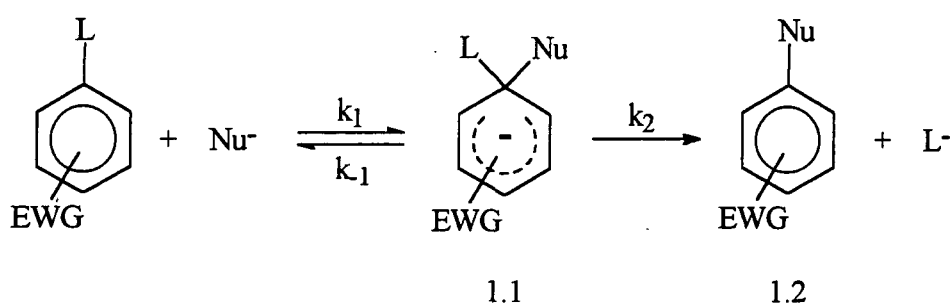
The reaction requires anodic initiation and its mechanism is shown in scheme 1.8. The number of possible starting materials that will react via this process is limited. Both the leaving group X^- and nucleophile must be difficult to oxidise, and the product must be less oxidizable than the starting material or else the last step is inhibited.



scheme 1.8

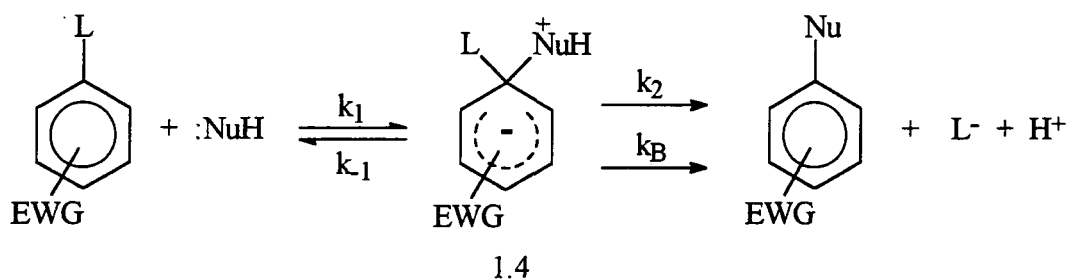
1.4 The S_NAr Substitutions.

The addition-elimination mechanism for S_NAr reactions was proposed in 1951 by Bunnett.^{2,3} The basic features involve firstly the addition of a nucleophile (Nu) to an aromatic electrophile to form a cyclohexadienyl anion commonly referred to as a Meisenheimer or σ-complex, 1.1, followed finally by the loss of a leaving group (L) to produce the overall substituted product, 1.2. Note that the carbon centre undergoing substitution becomes sp³ hybridised and the benzenoid resonance is broken until expulsion of the leaving group enables rearomatisation. Depending on the relative energies of the transition states either nucleophilic attack or elimination of the leaving group can be the rate limiting step. The mechanism postulated for the reaction of anionic nucleophiles can be viewed in equation 1.21.



equation 1.21

If the reaction involves a neutral nucleophile e.g. water, alcohols, amines, the initially formed σ-adduct, 1.4, is zwitterionic and usually contains an acidic proton which can be removed by an external base or in some instances the nucleophile itself. The outcome of this is that transformation of the zwitterion to the product can follow either an uncatalysed pathway, k₂, or a base catalysed pathway, k_B. The mechanism is represented below in equation 1.22.

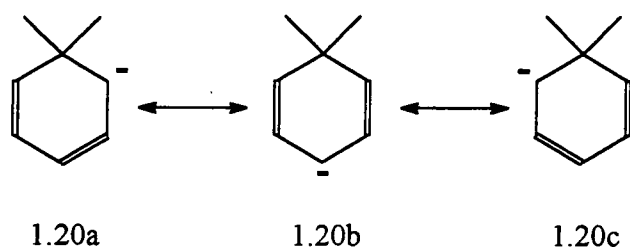


equation 1.22

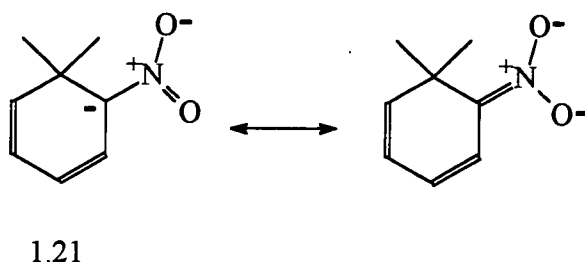
The next sections will discuss how various experimental and theoretical results have shown undoubtedly that the suggested reaction sequences, equations 1.21 and 1.22 are justified.

1.4.1 Stability of the σ -Complex.

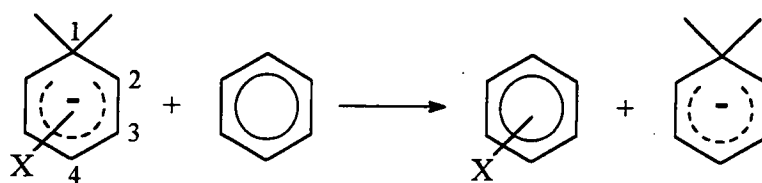
The S_NAr reaction of a nucleophile with an aromatic substrate which is not electron deficient does not appear very probable due to the repulsion between the π electron system and the approaching nucleophile. This is overcome primarily by the presence of electron withdrawing groups (EWG) such as NO_2 , which have the consequence of reducing the electron density of the benzenoid system. First consider the unsubstituted σ -complex and the three contributing resonance structures, 1.20a, b, c.



The distribution of negative charge at the ortho and para positions, possibly by the interaction of EWG groups at these positions, would lead to a significant stabilisation of the σ -complex, 1.21. Theoretical studies performed by Dewar calculate that formation of a σ -complex from benzene is associated with only 41.8 kJ/mol reduction in resonance energy.⁵⁷



The exchange reaction, equation 1.23, has allowed the comparison of stabilisation energies of mono-substituted σ -complexes relative to substituted benzenes.⁵⁸ The result of which can be viewed in table 1.1.



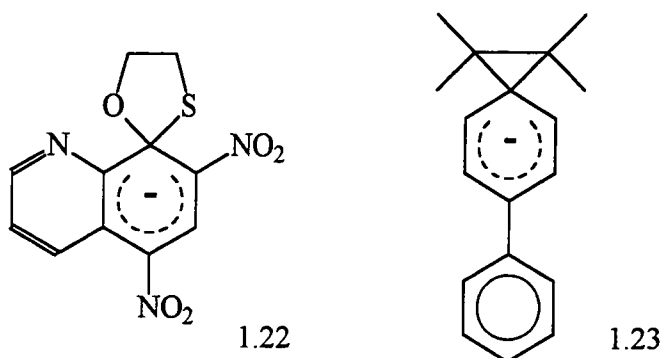
equation 1.23

A positive value denotes the greater stability of the substituted anion compared to the unsubstituted anion. It can be clearly noticed that the electron withdrawing nitro group provides the greatest amount of stabilisation in the order of position para > ortho >> meta.

Table 1.1 Stabilisation energies (kJ / mol) of mono-substituted σ -complexes.

Substituent	1	2	3	4
	H	0	0	0
CH ₃	-5.3	-5.7	-4.6	-3.5
CN	54.1	125.8	69.6	148.6
NO ₂	129.9	178.9	87.5	201.8
F	29	10.4	27.9	-6.6

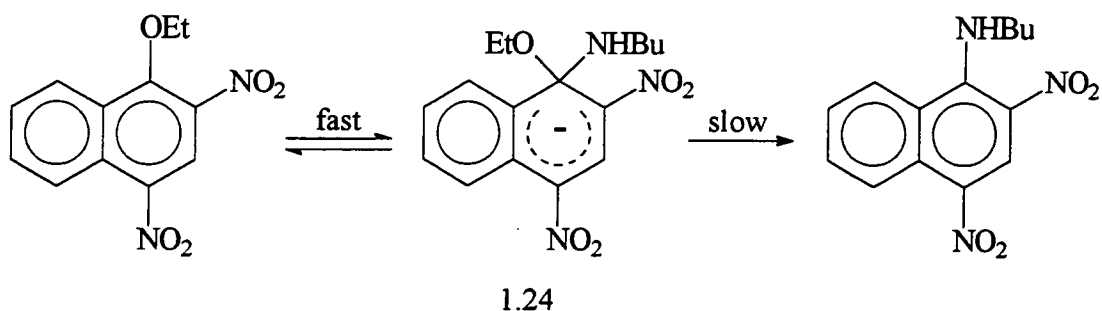
No definite evidence of a mono substituted nitrobenzene adduct has yet been reported,¹⁰ but the introduction of further nitro groups in the ortho and/or para position(s) improves stabilisation greatly.⁵⁻⁸ Benzoannulation augments the stability of a σ -complex, 1.22 as the delocalisation is able to take place over an extended aromatic system.⁵⁹⁻⁶⁰ Exocyclic phenyl rings have also been proven to be capable of dispersing negative charge. Spiro adduct, 1.23 has been identified by NMR studies and is formed by reacting biphenylchloroalkanes with alkali metals in THF.⁶¹



1.4.2 Evidence for the Formation of σ -Complexes.

Extensive NMR and UV/Visible spectroscopy studies have been completed on various S_NAr type processes.¹⁰ Initial attempts to identify intermediates on the substitution pathway were hampered by the relatively short lifetimes of the σ -adducts and the tendency for nucleophilic attack to occur at the 3-position and form the undesired 1,3-addition complexes.

The first reliable study was performed in 1970 by Bunnett and Orvik.⁶² It involved the reaction of 1-ethoxy-2,4-dinitronaphthalene with either *n*- or *t*-butylamine in DMSO, equation 1.24. The reaction takes place in two distinct stages, firstly the rapid formation of the proposed intermediate 1.24 followed by the gradual formation of the butylamino substituted product. The intermediate was monitored using UV/Vis spectroscopy and it was established that the rate of decomposition of 1.24 was equal to the rate of appearance of the substituted product. Fyfe later used a technique of low temperature flow NMR spectroscopy,^{7,8} which enables high resolution NMR spectra to be obtained in a flowing chemically reacting system. He was able to detect and characterise the species in equation 1.24. This provided conclusive evidence for the proposed 1,1 σ -adduct.



equation 1.24

The first report of the NMR spectrum of a σ -adduct was that of Crampton and Gold who in 1964 determined the 1H NMR spectra of methoxide adducts of 2,4,6-trinitroanisole and 1,3,5-trinitrobenzene.¹⁵ Since then this technique and the use of x-ray crystallography has proved invaluable in giving structural information on hundreds of adducts.

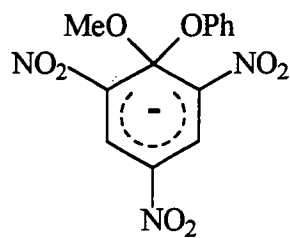
The solvent, DMSO, has proved extremely useful in studies of this kind as it shows good solvation properties for σ -adducts without interacting with them chemically. Like other dipolar-aprotic solvents such as dimethyl formamide and acetonitrile it is good at solvating the delocalised negative charge found in 1:1 σ -adducts.

1.4.3 Leaving Group Ability.

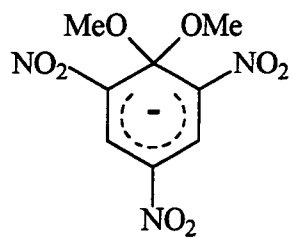
Many different aspects have to be considered in an attempt to understand the reactivity correlations within S_NAr processes. No one common factor can be identified and it is the understanding of several effects, that of the nucleophile, leaving group and solvent which is required to comprehend experimental observations. A brief view of the general trends which are regularly encountered will be discussed.

The halogens often act as leaving groups in nitro activated aromatic compounds. The order of reactivity $F > Cl \approx Br > I$ is commonly found and signifies that nucleophilic attack is rate limiting in the S_NAr process.^{2,9} The high reactivity of aromatic fluorides is due to three reasons. The strong polarisation of the $C^{\delta+}-F^{\delta-}$ bond compared to other carbon halogen bonds, the ability of fluorine's strong electron withdrawing effect when attached to an sp^3 carbon to stabilise σ -adducts (α or ipso effect) and finally the small polarisability of fluorine that lowers the repulsive interactions against an incoming "hard" nucleophile.^{2,9,63} When "soft" highly polarisable nucleophiles e.g. SCN^- react there is less distinction between repulsion effects and the reactivity order is very similar.^{9,10,64} Reversal of the order, i.e. $I > Br > Cl > F$ is accounted for when leaving group expulsion is rate limiting and dependent on carbon-halogen bond strengths.^{2,9,10}

Other recognised leaving groups are OCH_3 , OC_6H_5 , SO_2R , SOR , SR and $+NR_3$. Although no common reactivity trend can be produced as it results from the combination of many effects, an approximation can be made with regards to pK_a of the leaving group.² Uncatalysed phenoxide ion departure in aqueous solution from 1.25 is approximately 10^7 times faster than methoxide ion departure from 1.26 and the result indicates a high sensitivity of the leaving group ability to the pK_a of the leaving group.⁶⁵ On the other hand, there exist reports of much lower sensitivity and at present it is not known precisely what factors determine this.^{66,67} The amide group ($-NR_1R_2$) will not readily depart ($pK_a \approx 38$) until it is protonated⁶⁸ and the hydride ion which has been mentioned previously is a very poor leaving group ($pK_a \approx 36$).⁶⁹ Highly polarisable nucleophiles have been known to displace the nitro group due to its high polarity and also to favourable dispersion interaction in the ipso intermediate.⁶³



1.25



1.26

1.4.4 Solvent Effects.

It is important to note that the solvent is a factor which can profoundly affect the rate and equilibrium parameters for the formation and decomposition of σ -adducts.⁷⁰ Care must therefore be taken to use comparable parameters in evaluations of reactivities.

The primary effects of dipolar aprotic solvents (e.g. DMSO, DMF, chloroform) as opposed to protic solvents (e.g. water, alcohols) is to alter the solvation of the nucleophile and to enhance the stability of the 1:1 σ -adduct. The energy of small anions with a high charge density (e.g. F^- , OH^- , RO^- , SO_3^{2-}) and amines is greatly increased, unlike anions that are large and polarisable (e.g. PhO^- , PhS^-). The effect of dipolar aprotic solvents on the equilibrium constant for 1:1 σ -adduct formation, K_1 , reflects an increase in the rate of formation, k_1 , and a decrease in the rate of decomposition, k_{-1} .

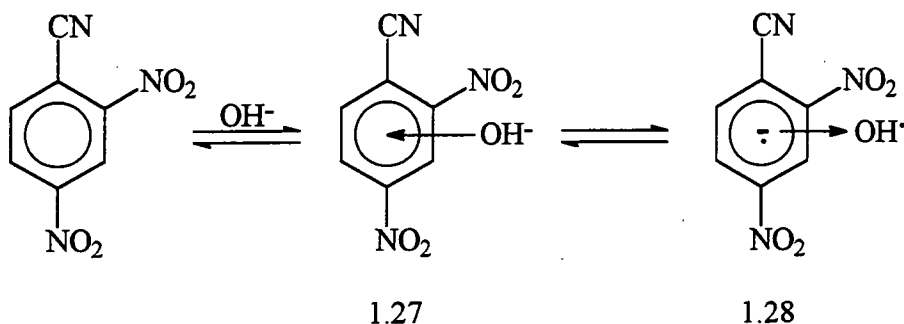
Small anions are very well solvated in protic media. The anion is visualised as being in the centre of a solvent cage which leads to its stabilisation and low reactivity. In general, transfer from a protic solvent like water to another protic solvent like methanol or ethanol does not markedly alter the k_1 , k_{-1} and K_1 reactivity sequences found for 1:1 σ -complexes.⁷¹ Ion pairing effects represent an additional factor to consider in some circumstances with alcohols.⁷²⁻⁷⁴ However the small anions with localised charge are desolvated in dipolar aprotic solvents which solvate by dipole-dipole interactions.

In contrast with that of 1:1 complexes, the stability of 1:2 complexes decreases on transfer from protic to dipolar aprotic solvents.⁷⁵ However this is consistent with the destabilisation of such anions which bear at least two relatively localised negative charges and are therefore poorly solvated by solvents like DMSO.

1.4.5 The Role of π -Complexes.

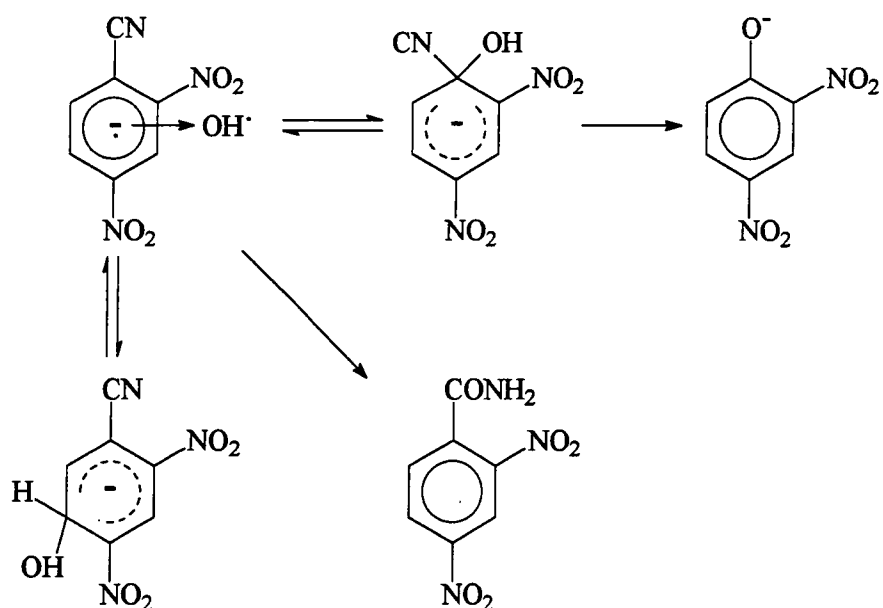
The intermediacy of σ -adducts in S_NAr substitutions is well established.^{9,10,38} The role of charge-transfer (CT) or π -complexes in such processes remains controversial. There is a developing view that single electron transfer may be the initial step in a wide range of chemical reactions. Strong evidence has already been supplied for the radical chain $S_{RN}1$ mechanism of aromatic substitution in apolar solvents.⁷⁶

Bunton and co-workers believe that the reaction of hydroxide with 2,4-dinitrobenzonitrile in water or water-DMSO solvent mixtures involves the formation of a charge-transfer complex, 1.28 of the radical anion of the substrate and the hydroxyl radical, which will collapse to give Meisenheimer complexes and eventually the final product, the benzoate ion.⁷⁷ A π or encounter complex, 1.27 of the substrate and the hydroxyl radical is presumed to form initially in a very rapid equilibrium, equation 1.25.

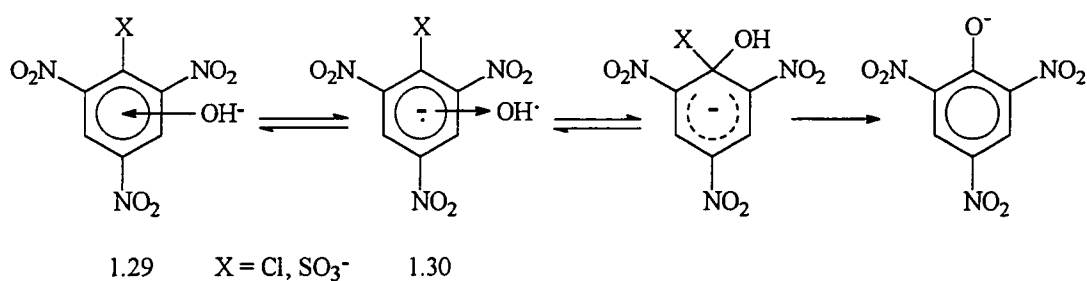


equation 1.25

The charge-transfer intermediate may return to reactants, collapse to form a new covalency, or dissociate into free radicals, especially in aprotic solvents. Electron withdrawing groups strongly stabilise these complexes and appear to be necessary for their observation in polar solvents. When the cyano substituent is present collapse can give various Meisenheimer complexes, nucleophilic addition to the cyano group or nucleophilic substitution on loss of the cyano group from the 1:1 σ -adduct, scheme 1.9. Physical evidence submitted for the postulated reaction scheme is the exchange of arene hydrogen and extensive broadening of ¹H NMR signals of the substrates during the reaction. There seems to be little doubt that low concentrations of radicals are produced during the reaction. However it is not certain that they are intermediates in the substitution pathway.

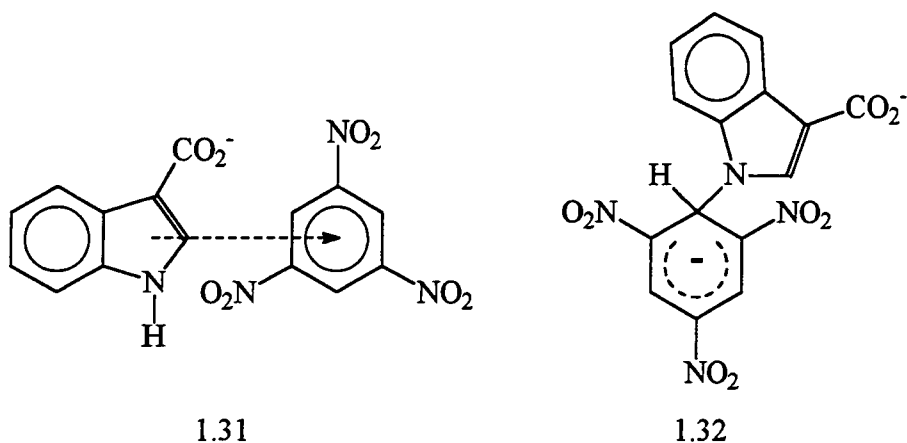


The reactions of hydroxide with 1,3,5-trinitrobenzene (TNB), 1-chloro-2,4,6-trinitrobenzene, 2,4,6-trinitrobenzenesulfonic acid and 1-chloro-2,4-dinitronaphthalene in water-DMSO solvent system have been investigated. Bunton suggests that the mechanism does not occur by a rate limiting, single step addition of hydroxide but involves a process similar to the one discussed previously, equation 1.25. Rapid formation of a π -complex, 1.29 of the substrate with hydroxide, followed by creation of a charge transfer complex, 1.30 of the arene anion and hydroxyl radicals by single electron transfer.⁷⁸ Rearrangement can occur to give the 1- or 3- σ -adducts, with the foremost undergoing elimination of the leaving group to effect the overall substituted product, equation 1.26.



The results however are not conclusive. The reactions have since been repeated under similar experimental conditions and the proposed intermediates, 1.29 and 1.30 were not detected.⁷⁹

Evidence has been given for the presence of π -complexes in substitution or σ -complex forming reaction processes. Buncl and Terrier have recently identified and isolated (as the sodium salt) what is believed to be the π -complex precursor, 1.31 in the reaction of TNB with indole 3-carboxylate.⁸⁰ Interestingly when 1.31 is placed in DMSO it rapidly gives rise to the TNB N-adduct, 1.32. There is also evidence that the carbon-bound TNB adduct may be produced after decarboxylation and also for an N- and C-bound diadduct.

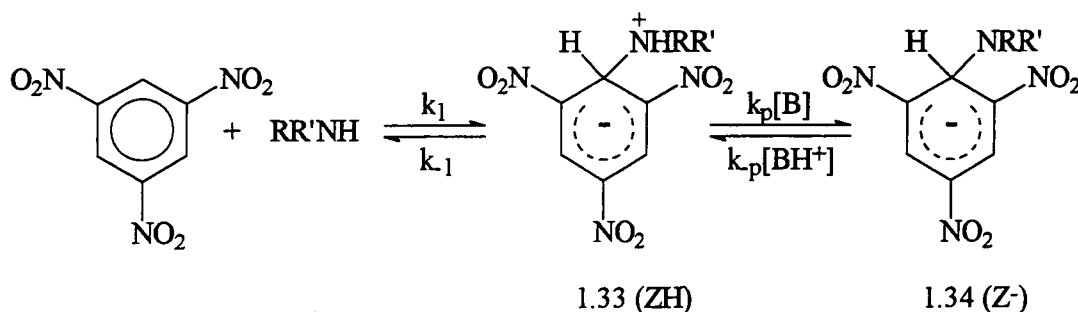


There is no doubt that reactions of aromatic nitro compounds with bases in non-polar solvents may yield π -complexes,^{81,82} but the authenticity of charge transfer complexes such as 1.28 and 1.30 is still uncertain.

1.5 Nucleophilic Aromatic Substitutions with Amines.

One of the main arguments for the S_NAr mechanism has come from studies of substitutions using amine nucleophiles. Many kinetic studies have been reported with both primary and secondary, aliphatic and aromatic amines. These have shown that changes in the nucleophile concentration or the addition of external agents may cause variation in rate constants for formation and / or decomposition of σ -adduct intermediates, and may change the nature of the rate determining step.^{10,62,83}

Due to the neutral character of amines, σ -adduct formation involves two steps. The reaction at an unsubstituted ring position of trinitrobenzene, depicted below in equation 1.27, involves firstly the addition of the amine to the aromatic substrate to form a zwitterion 1.33 (ZH), which then loses an alkylammonium proton to give the σ -adduct, 1.34 (Z^-). Further reaction of 1.34 is unfavourable. The rate constant k_p is assigned to the deprotonation of ZH by hydroxide or any general base (amine, Z^- , buffer base, solvent). Similarly k_{-p} refers to the reprotonation of Z^- by a proton or any general acid ($RR'NH_2^+$, ZH, solvent).



equation 1.27

Detailed studies of the mechanism have been completed for various systems in both DMSO and aqueous solvents.⁸⁴⁻⁸⁸ Each kinetic step has been scrutinised including the effect of the amine structure on both the nucleophilic addition and deprotonation steps. The proton transfer step for the reaction in DMSO may be rapid (2,2,2-trifluoroethylamine)⁸⁶, rate determining over the entire range of amine concentrations (piperidine)⁸⁵ or only at low amine concentrations (benzylamine, butylamine).⁸⁵ It is also important to note that the above results are solvent dependent. Thus in acetonitrile, the proton transfer is thought to be rate limiting in the reaction of TNB with 2,2,2-trifluoroethylamine.

Acetonitrile is much poorer than DMSO in solvating ionic species,⁸⁶ so that the zwitterion, ZH, will revert back to reactants very rapidly in acetonitrile. Hence $k_{-1}^{\text{CH}_3\text{CN}} \gg k_{-1}^{\text{DMSO}}$, accounting for $k_{-1} \gg k_p[\text{B}]$.

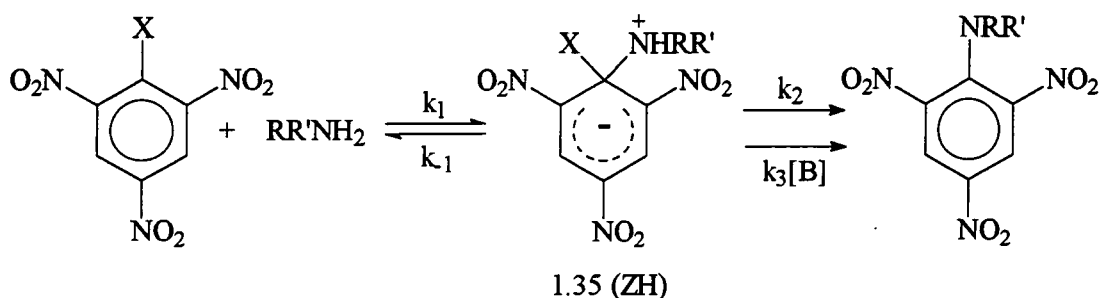
In σ -adduct forming reactions the rate constants for nucleophilic attack of amines generally follow the pattern often found in $S_{\text{N}}\text{Ar}$ substitution processes. The more basic secondary amines are more reactive than primary amines in all solvent systems studied, table 1.2. In particular cases stereoelectronic factors have to be considered, although commonly the effects are not as significant with attack at an unsubstituted carbon. Piperidine shows a lower reactivity than pyrrolidine even though their basicities are similar,⁸⁹ this may be a steric factor. Various results are shown below in table 1.2.^{84,85}

Table 1.2 Comparison of amines and solvent systems.

Amine	Solvent	$k_1 / \text{dm}^3 \text{ mol}^{-1} \text{ s}^{-1}$	k_{-1} / s^{-1}	$K_1 / \text{dm}^3 \text{ mol}^{-1}$	$\text{pK}_a(\text{water})^{90}$ ammonium ion
CH_3NH_2	10% dioxane- 90% water	160	1.5×10^5	1.1×10^{-3}	10.64
n-butylamine	"	123	1.5×10^5	8.2×10^{-4}	10.77
"	DMSO	4.5×10^4	2.3×10^4	2	10.77
$(\text{CH}_3)_2\text{NH}$	10% dioxane- 90% water	6.3×10^3	7.5×10^5	8×10^{-3}	10.73
pyrrolidine	"	8.1×10^3	1.5×10^6	5.8×10^{-3}	11.27
piperidine	"	3×10^3	2.1×10^6	1.4×10^{-3}	11.12

Interestingly the values for amine expulsion, k_{-1} , from the zwitterions ZH are all very high, i.e. $\geq 10^5 \text{ s}^{-1}$, and is the primary reason for rate limiting proton transfer, i.e. $k_{-1} \gg k_p[\text{B}]$. Another prominent factor is that the acidity of the zwitterionic complex is much greater than that of the parent $\text{RR}'\text{NH}_2^+$ ions, due to the electron withdrawing effect exerted by the trinitroaromatic moiety.⁹¹ The k_p step consequently represents a thermodynamically favoured proton transfer and one would expect the k_p values to be close to the diffusion controlled limit. Actual k_p values are found to be slightly lower *ca.* $10^7 \text{ dm}^3 \text{ mol}^{-1} \text{ s}^{-1}$, due to steric effects.⁸⁴ The variation in values of k_{-1} are indicative of steric strain present in the zwitterions ZH. This explains why amine expulsion occurs more readily with secondary as opposed to primary amines and is not totally dependent on their respective pK_a values.⁹²

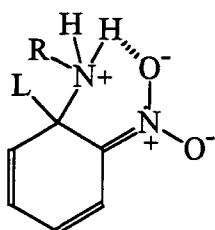
J. F. Bunnett first proposed the mechanism shown in equation 1.28 for the reaction of amines at a substituted ring position.² Nucleophilic addition to the aromatic substrate gives a zwitterionic intermediate 1.35 (ZH), which may be converted to the substituted product either directly, k_2 , or by base catalysis, $k_3[B]$. The acting base may be either the nucleophilic amine or another base specifically added to the reaction.^{10,83,92}



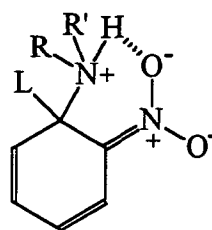
equation 1.28

The uncatalysed step commonly involves intramolecular proton transfer from nitrogen to the leaving group.^{7,83,92} The base catalysed step $k_3[B]$ may involve rate limiting proton transfer (RLPT) from the zwitterion ZH, or rapid interconversion of ZH into its deprotonated form, Z^- , followed by general acid catalysed leaving group departure (SBGA mechanism). The former usually applies in protic solvents, while in aprotic solvents the nature of the leaving group determines the reaction pathway. The occurrence and magnitude of base catalysis depends upon the ratio $k_2 + k_3[B] / k_{-1}$ which varies according to the identity of the amine, leaving group, base and solvent.^{17,92-95} Ordinarily base catalysis is favoured when $k_{-1} \gg k_2 + k_3[B]$ and this is often achieved in the presence of secondary amines, poor leaving groups and in non-polar solvents.⁹² The reactions of 1-chloro and 1-fluoro-2,4-dinitrobenzenes with aniline and 4-methylaniline in DMSO are not base catalysed. When the nucleophile is 2-methylaniline, the reaction of the fluoro compound is base catalysed whereas that of the chloro compound is not.⁹⁶ The results indicate that in certain cases, the incidence or absence of base catalysis in S_NAr reactions results from an interplay of steric and electronic factors as they affect the magnitude of the $k_2 + k_3[B] / k_{-1}$ ratio.

One explanation which has been given to explain why base catalysis is more significant with secondary than primary amine nucleophiles derives from the presence of an ortho NO₂ group.⁹⁷ It has been suggested that there may be stabilisation of zwitterionic intermediates by intramolecular hydrogen bonding between the amino proton and the ortho NO₂ group.⁹⁸



1.36



1.37

The reduction in k_{-1} values should be equivalent for both 1.36 and 1.37, the adducts for primary and secondary amines. Yet the influence on the value of k_2 should be greatly different. Structure 1.36 has a non hydrogen bonded proton that is easily transferred to the leaving group. Structure 1.37 has its only removable proton tightly bound through hydrogen bonding. This therefore will have the effect of decreasing the ratio $k_2 + k_3[B] / k_{-1}$ for secondary amines, with little effect on primary amines. However it should be noted that the ring carbon at the position of substitution is sp^3 hybridised so that the ammonium group will not be in the ring plane. Evidently hydrogen bonding as shown in 1.36 and 1.37 will be difficult, leading to competition with the surrounding solvent, e.g. DMSO which is known to be an excellent hydrogen bond acceptor. A change to non-polar solvents is likely to increase the value of k_{-1} due to the poor stabilisation of the zwitterion ZH.

The overall rate expression is given in equation 1.29. It is derived by applying the steady-state approximation to the reaction shown in equation 1.28, where k_A is the measured second order rate constant at a given base concentration.

$$\frac{\text{rate}}{[\text{ArX}][\text{RR}'\text{NH}]} = k_A = \frac{k_1 k_2 + k_1 k_3 [\text{B}]}{k_{-1} + k_2 + k_3 [\text{B}]} \quad \text{equation 1.29}$$

At least four possible circumstances can arise from equation 1.29

(i) $k_2 + k_3[B] \gg k_{-1}$

In this condition the formation of the intermediate is rate limiting and equation 1.29 simplifies to equation 1.30 and there is no contribution from base catalysis.

$$k_A = k_1 \quad \text{equation 1.30}$$

(ii) $k_{-1} \gg k_2 + k_3[B]$

This situation corresponds to the formation of 1.25, ZH, in a rapidly established pre-equilibrium with product formation being rate determining. The expression reduces to equation 1.31.

$$k_A = \frac{k_1 k_2 + k_1 k_3[B]}{k_{-1}} \quad \text{equation 1.31}$$

This predicts base catalysis with a linear dependence of k_A on base concentration.

(iii) $k_{-1} \gg k_2 + k_3[B]$ and $k_2 \gg k_3[B]$

Here, the rate determining step is the uncatalysed decomposition of the zwitterionic intermediate and no base catalysis is observed, equation 1.32.

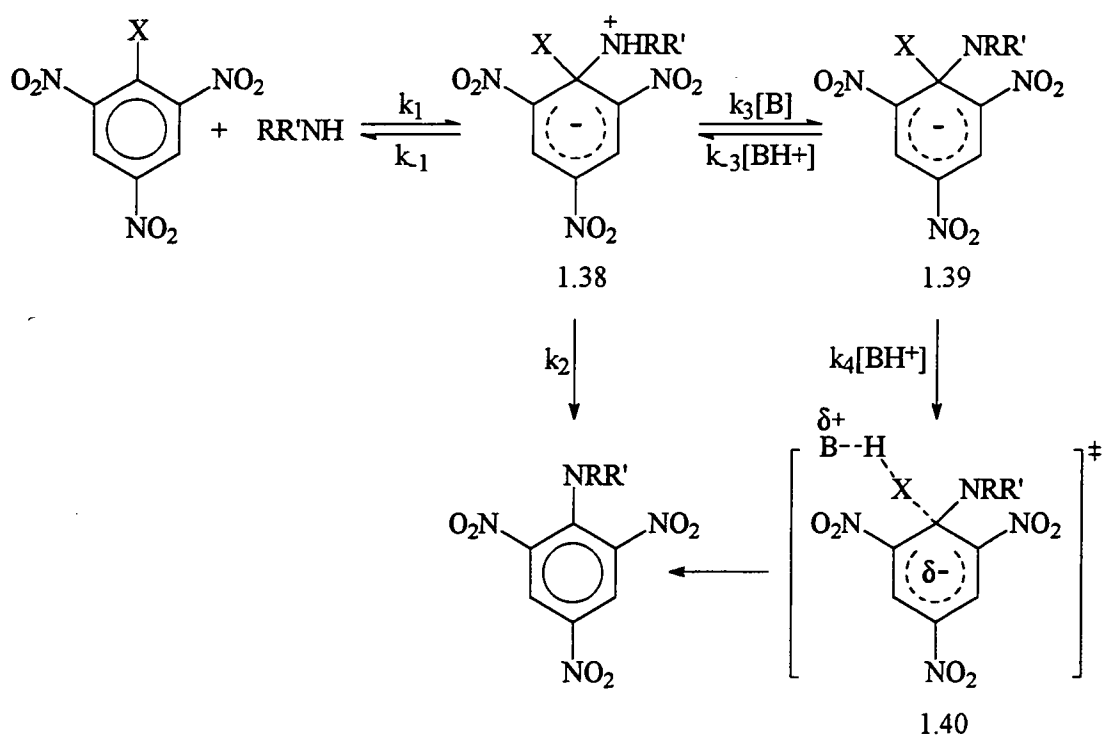
$$k_A = \frac{k_1 k_2}{k_{-1}} = K_1 k_2 \quad \text{equation 1.32}$$

(iv) $k_2 + k_3[B] \approx k_{-1}$

In this intermediate case, base catalysis may be observed at low base concentrations. The linear dependence on base concentration will eventually change to a plateau at high base concentrations, giving a characteristic curvilinear dependence.

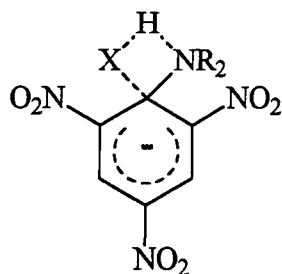
1.5.1 Base Catalysis.

Base catalysis is observed in a variety of S_NAr reactions. It provides good kinetic evidence for the two stage mechanism and a number of studies have been undertaken to improve our understanding of the phenomena. Both specific base/general acid leaving group departure (SB-GA) and rate limiting proton transfer (RLPT) mechanisms will be examined and examples supplied. However, firstly it is important to note that in some studies no base catalysis can occur and the reaction is believed to follow an uncatalysed (spontaneous) pathway, step k_2 , scheme 1.10 below.

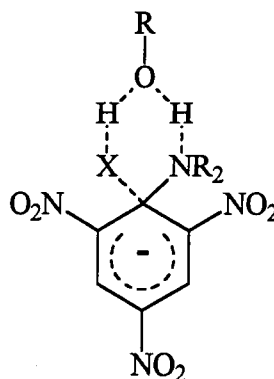


scheme 1.10

An interpretation of the spontaneous pathway in an aprotic solvent such as benzene is given by the transition state structure 1.41, depicting the intramolecular assistance of leaving group departure through hydrogen bonding with the amino proton.⁹⁹ A process similar to that of the catalysed pathway may also take place with a solvent molecule acting as a base. Reaction in a hydroxylic solvent would follow the mode shown in 1.42.



1.41



1.42

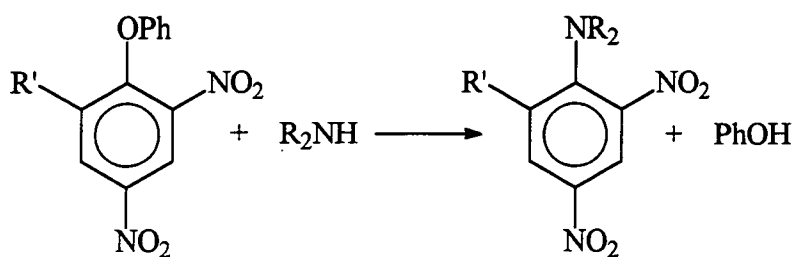
1.5.1.1 The Specific Base General Acid Catalysed Mechanism.

This mechanism involves the initially formed zwitterionic intermediate 1.38 ZH, undergoing a fast equilibrium proton transfer yielding the anionic σ -complex 1.39 Z⁻ followed by the rate determining removal of the leaving group catalysed by the general acid, BH⁺, via the shown transition state 1.40. The rate equation is equation 1.33, where k_4 is the rate coefficient for acid catalysed expulsion of the leaving group. The equilibrium constant that is present between the zwitterion ZH and the σ -complex Z⁻ is represented by K_3 .

$$k_A = \frac{k_1 k_2 + k_1 k_4 K_3 [B]}{k_{-1} + k_2 + k_4 K_3 [B]} \quad \text{equation 1.33}$$

The SB-GA mechanism was proposed in the 1960's and became generally accepted after Bunnett and Orvik,⁶² in 1970, presented direct evidence that in the reaction of 2,4-dinitro-1-naphthyl ether with n-butylamine in DMSO leaving group departure is in fact rate limiting and general acid catalysed, scheme 1.11. The process occurs in two distinct stages and U.V./Vis. spectra were recorded of the rapidly formed intermediate 1.43, followed by its slow decay to the identified product. Kinetic analysis indicated that formation of the intermediate is not base catalysed whereas transformation of 1.43 to 1.44 is first order in n-butylammonium ion but independent of amine concentration. The evidence is fully in accord with general acid catalysis of nucleofuge expulsion. The product will be present as the anion formed by loss of the amino proton, which is known to be relatively acidic in DMSO.

Bunnett and co-workers have also studied the reaction of 2,4-dinitrophenyl phenyl ether and 2,4-dinitro-6-methyl-phenyl phenyl ether with pyrrolidine and piperidine, equation 1.34, in a 60% dioxane / 40% water reaction medium.¹⁰⁰ Catalysis by NaOH was established and the transformation of the intermediate adduct to product was found to be an order of magnitude greater for pyrrolidine than piperidine. This reduced reactivity for the piperidino reaction was thought to indicate that leaving group expulsion was involved in the slow step of the reaction. This was taken as evidence for the SB-GA mechanism. However it is known⁸⁵ that rate constants for proton transfer from zwitterionic intermediates to base are also reduced when the nucleophile is changed from pyrrolidine to piperidine. Hence the evidence for the SB-GA mechanism here is not very strong.



R' = H, Me

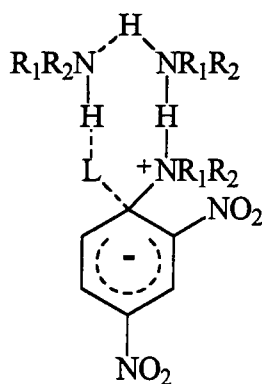
equation 1.34

Further reports have been published giving evidence for the SB-GA mechanism in other dipolar aprotic solvents, e.g. acetone or acetonitrile.^{104,105} Results for the reaction of 1-fluoro-2,4-dinitrobenzene with N-methylaniline in acetonitrile have been attributed to specific catalytic effects of added chloride ions.¹⁰⁶

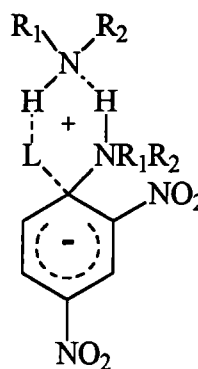
In non-polar aprotic solvents, such as benzene and toluene, different mechanisms have been proposed to allow for the inability of these solvents to stabilise ionic species. Two such possibilities, which may explain the high kinetic orders of amines often observed experimentally, are the dimer mechanism^{107,108} which involves the nucleophilic attack of the dimer of the amine to give a cyclic intermediate 1.45 and secondly a process involving single catalysing entities, 1.46 in a cyclic transition state.¹⁰⁹ Hirst has argued convincingly that in these non-polar solvents ammonium ions will be stabilised by association with amines to give homoconjugates, equation 1.35.



Catalysis, by the homoconjugates, of leaving group expulsion will give rise to a third-order dependence on the amine concentration.¹¹⁰



1.45

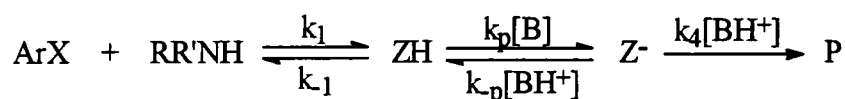


1.46

1.5.1.2 Rate Limiting Proton Transfer.

The process of rate limiting proton transfer (RLPT) involves formation of the zwitterionic intermediate ZH by nucleophilic attack of the amine, which then undergoes rate limiting base induced deprotonation followed by rapid uncatalysed or acid catalysed leaving group departure.

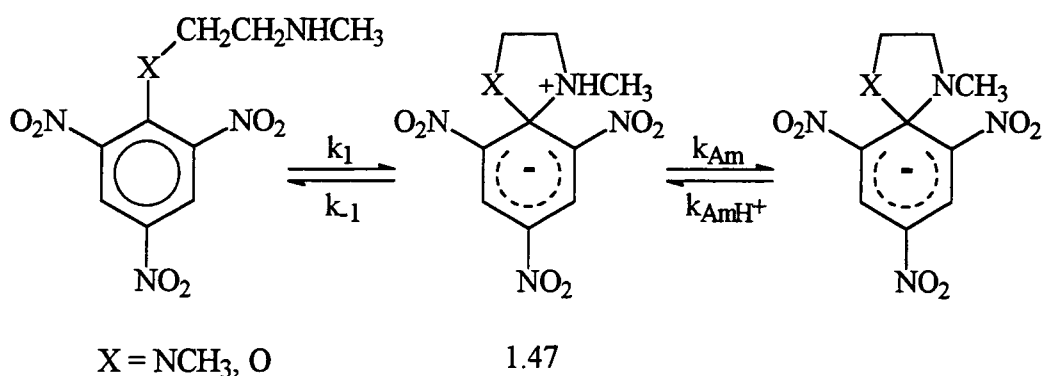
Bunnett and Randall in 1958 first proposed the mechanism,⁶⁴ although it was not readily acknowledged by the scientific community as proton transfers between "normal" (O, N) acids generally proceed at a rate which is close to diffusion controlled.¹¹¹ However, rate limiting diffusion controlled proton transfer steps have now been established and widely accepted.^{112,113} This can happen in a multi-step process where the species undergoing deprotonation are present in highly unfavourable equilibria or where reversion of this process is extremely rapid.⁹⁵ The general reaction process is expressed in equation 1.36, where k_p refers to the deprotonation of ZH by the base, k_{-p} refers to protonation of Z^- by an acid and k_4 relates to leaving group departure, either unassisted or catalysed by general acids.



equation 1.36

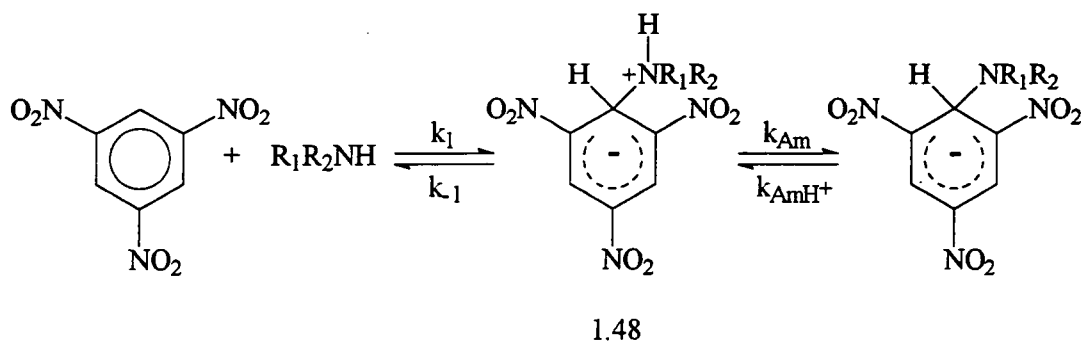
If the rate determining step is to be the deprotonation of ZH then $k_4 \gg k_p$ and $k_{-1} > k_p[B]$ must apply. Base catalysis will not be observed if only the first limit is satisfied.^{83,114,115}

Considerable evidence for the RLPT mechanism has been collected in cases of formation and decomposition of stable σ -adducts.^{84,85,88,89,116,117} Equations 1.37 and 1.38 below have revealed, using temperature jump techniques, that amine departure from zwitterionic complexes 1.47 and 1.48 is very rapid.



equation 1.37

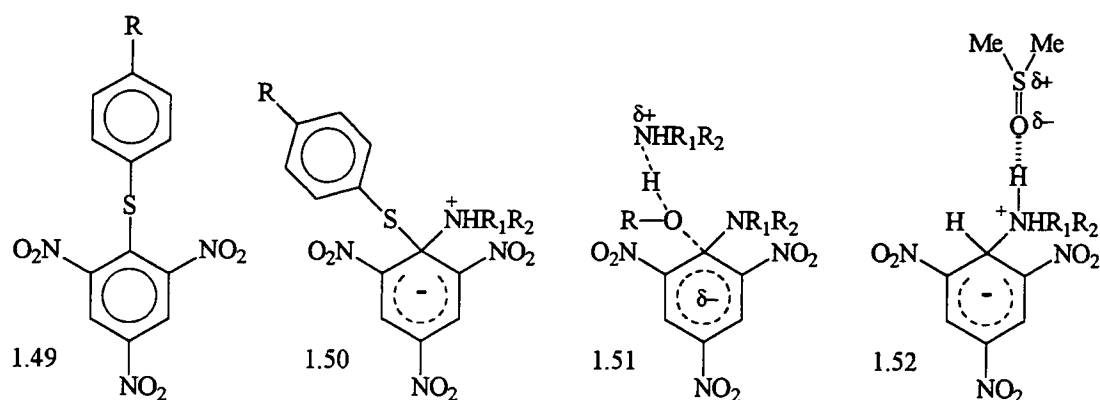
Deprotonation of 1.47 and 1.48 although thermodynamically favoured and essentially diffusion controlled, becomes rate limiting ($k_{-1} \gg k_p[B]$) or partially rate limiting ($k_{-1} > k_p[B]$) at low pH and low buffer concentrations where the concentrations of [B] will be small.^{83,114}



equation 1.38

Kinetic studies for the reaction of 1,3,5-trinitrobenzene with aliphatic amines in DMSO, equation 1.38, show that the proton transfer step may be rate limiting.^{85,118} For the reaction with *n*-butylamine the value of k_{Am} is *ca.* $10^7 \text{ dm}^3 \text{ mol}^{-1} \text{ s}^{-1}$. Values for the reaction of pyrrolidine and piperidine are 10^6 and $10^5 \text{ dm}^3 \text{ mol}^{-1} \text{ s}^{-1}$ respectively.

Bernasconi and co-workers have provided convincing evidence that in aqueous media base catalysis in the reactions of nitroaryl ethers with aliphatic amines is the result of rate limiting proton transfer.¹¹⁹ In DMSO the nature of the rate determining step depends on the amine and on the leaving group. The reactions of *n*-butylamine, pyrrolidine and piperidine with 4'-R-2,4,6-trinitrophenyl sulphides, 1.49, in DMSO result in rapid formation of anionic σ -adducts by attack at the unsubstituted 3-position. Attack at the 1-position of 1.49 and also of phenyl 2,4-dinitronaphthyl sulfide, and phenyl 2,6-dinitro-4-trifluoromethyl sulfide results in the displacement of the phenylthio group. The substitutions by *n*-butylamine show a first order dependence on the amine concentration, indicating that nucleophilic attack is rate determining, $k_{Am}[Am] \gg k_{-1}$. However, the substitutions by the secondary amines are subject to general base catalysis and the evidence suggests that this is the result of rate limiting deprotonation of the initially formed zwitterionic intermediates 1.50.¹²⁰ This is probably due to the lower values of k_{Am} expected for the reaction with the secondary amines resulting from steric hinderance to proton transfer. Values of k_{-1} for secondary amines are also likely to be higher due to steric strain in the zwitterions.



In substitutions of alkyl 2,4,6-trinitrophenyl ethers, which contain a poorer leaving group than the phenyl sulfides, general acid catalysed expulsion of the leaving group (SB-GA), with transition state 1.51, is rate determining. Comparison of rate constants for reaction with *n*-butylamine and with pyrrolidine indicates the greater steric requirement of the secondary amine.

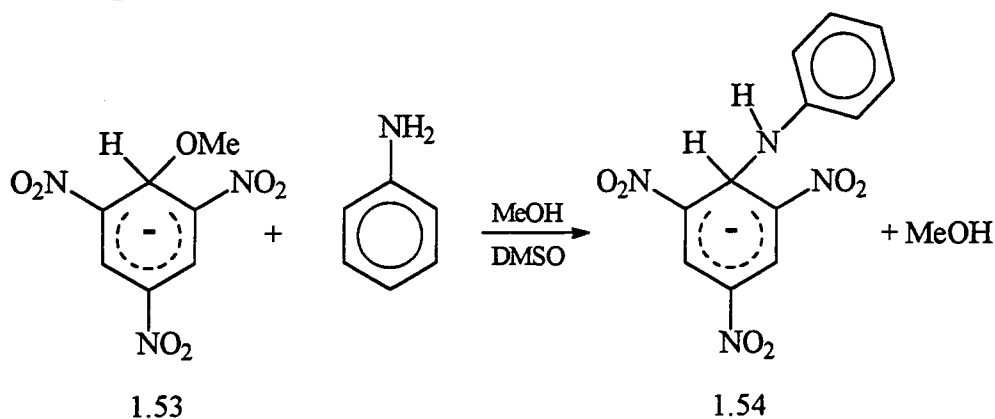
The corresponding amines have been studied with phenyl 2,4,6-trinitrophenyl ether in both DMSO and acetonitrile.^{121,122} Again base catalysis is observed and there is no evidence for the accumulation of intermediates on the reaction pathway, thus signifying rate limiting proton transfer. Results in DMSO indicate that values of the overall equilibrium constants for adduct formation are *ca.* 10^4 higher than in acetonitrile. A major factor here is probably the greater ability of DMSO than of acetonitrile to solvate charged species. Also the differences may reflect the greater relative stabilisation through hydrogen bonding interactions between DMSO and -NH^+ protons in ammonium ions and zwitterions. DMSO is known to be a strong hydrogen bond acceptor while acetonitrile shows weak hydrogen bonding properties.¹²³ To account for the lower values of k_{Am} and k_{AmH^+} observed in DMSO it is proposed that the transferrable proton in both the zwitterion and ammonium ion is bound strongly to DMSO, 1.52. In acetonitrile homoconjugation of substituted ammonium ions with free amine is an important factor.

1.6 Reactions of Aromatic Amines and Phenol.

1.6.1 Aromatic Amines.

Primary and secondary aliphatic amines react with electron deficient aromatic compounds to give 1:1 Meisenheimer or σ -complexes.¹⁰ In the presence of two or more equivalents of amine the complexes are observed as the ammonium salts.

Aromatic amines were thought to be insufficiently nucleophilic to react with electron deficient aromatics, other than by weak π interactions leading to charge-transfer complexes.¹²⁴ However in 1972, Buncl and Webb observed the formation of the σ -complex 1.54 between 1,3,5-trinitrobenzene (TNB) and aniline.¹²⁵ The complex 1.54 was produced indirectly by the reaction of aniline with the methoxide adduct 1.53 in DMSO and characterised by U.V./Vis. and ¹H NMR spectroscopy, equation 1.39 below. It was later shown that the same adduct could be produced by reaction of TNB with potassium anilide.



equation 1.39

The rationale for the lack of formation of σ -adducts with aromatic amines is presumed to be on the grounds of their very much weaker basicity in comparison with aliphatic amines. Table 1.3 shows a range of pK_a values for various ammonium ions in H_2O at 25°C.^{90,126}

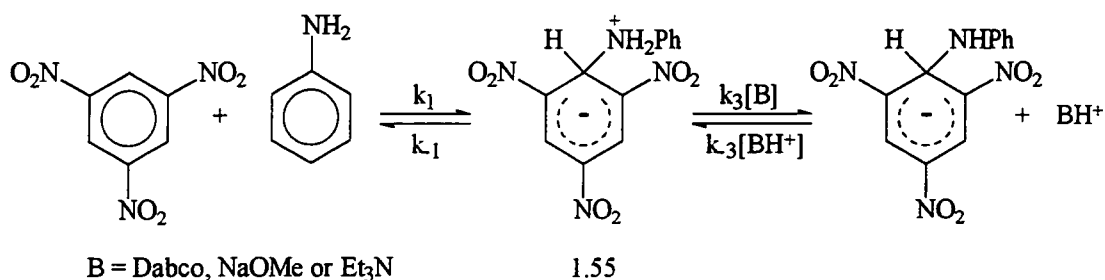
Table 1.3 pK_a values for various ammonium ions in H_2O at 25°C.

Amine	Aniline	N-methyl aniline	Benzylamine	Ethylamine	Diethylamine	Triethylamine
pK_a (water)	4.63	4.85	9.33	10.75	10.94	10.75

Arylamines are less basic than alkylamines because the nitrogen lone pair of electrons are delocalized by orbital overlap with the aromatic ring π electron system and are less available for bonding. In resonance terms, arylamines are stabilized relative to alkylamines because of the five contributing resonance structures that can be drawn. Resonance stabilization is lost on protonation, however, since only two resonance structures are possible for the arylammonium ion.

Buncel and co-workers have since obtained σ -complexes from secondary aromatic amines and from a series of ring substituted primary aromatic amines in the same way, by reaction with complex 1.53, and also by direct reaction with TNB in the presence of methoxide or tertiary amine bases.^{87,91,127,128}

A kinetic and equilibrium study of the reaction between TNB, aniline and 1,4-diazabicyclo-[2.2.2]-octane (Dabco) in DMSO solution, yielding the trinitrobenzene-anilide σ -complex has been performed⁸⁸, equation 1.40. The rate of the forward reaction is found to be first order with respect to TNB, PhNH₂ and Dabco, while the rate of the reverse reaction is first order with respect to TNB.NHPh⁻ and DabcoH⁺. The preferred reaction mechanism involves the pre-equilibrium formation of a zwitterionic complex 1.55, followed by its rate determining deprotonation by Dabco. The reaction thus provides a case in which proton transfer between two nitrogen atoms at a rate close to the diffusion limit constitutes the rate determining step for the overall reaction.



equation 1.40

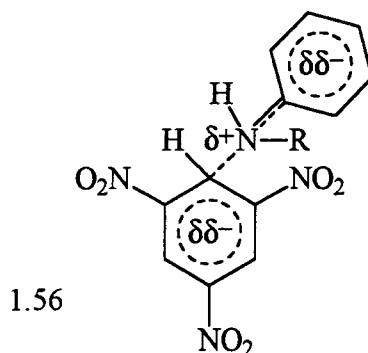
Aliphatic amines react with TNB in DMSO to form σ -adducts in the absence of added base. The failure to observe adducts from aniline in the absence of a strong base can be attributed to the much weaker basicity of the aromatic amine. This will be expected to result in a large reduction in the value of K_1 , the equilibrium constant for formation of the zwitterion. It is expected that the value of k_1 will be lower for aniline than for aliphatic amines and the value of k_{-1} will be higher.

The addition of Dabco (which is 10^4 times more basic than aniline) in the TNB / aniline reaction increases the equilibrium constant for deprotonation of the zwitterionic intermediate to the extent that now the overall reaction becomes feasible and formation of the σ -complex is observed.

The effect of tetraethylammonium chloride and perchlorate on the reaction of TNB with aniline and Dabco in DMSO has been investigated.¹²⁹ An increase in the overall equilibrium constant with increasing ionic strength is found. This is consistent with formation of ionic products from neutral reagents.^{130,131} In addition a specific effect of chloride ions was noted and was ascribed to the association of Cl^- with the conjugate acid of Dabco to yield the $\text{DabcoH}^+ \cdots \text{Cl}^-$ heteroconjugate complex.

A comparison has been made between aliphatic and aromatic nucleophiles with similar pK_a values in an attempt to determine whether basicity is the only major contributing reason for the differing results. Meisenheimer complex formation between TNB and the primary amines, aniline and 2,2,2-trifluoroethylamine (TFE) with $\text{pK}_a(\text{water})$ values 4.63 and 5.59, have been studied in both DMSO and acetonitrile.⁸⁶ The reaction with aniline is catalysed in both solvents by Dabco. With TFE catalysis by the TFE and Dabco is observed in acetonitrile, but not in DMSO.

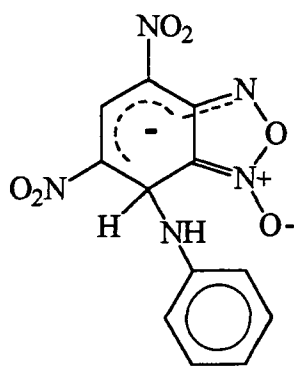
These results show that for the reaction with TFE the condition $k_3[\text{B}] \gg k_{-1}$ applies. This in turn implies that the value of k_{-1} is larger for the aniline reaction than for the reaction with TFE. It was suggested that this difference may result from stabilisation of the transition state for the decomposition of the adduct 1.55 to reactants for aromatic amines, by interaction of the partially liberated lone pair of electrons on the nitrogen atom with the aromatic ring of the amine as shown in 1.56.



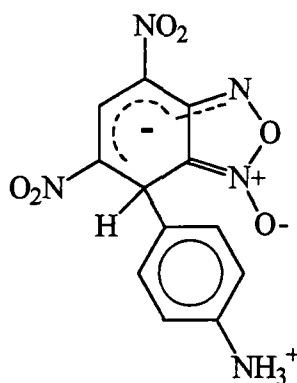
When the solvent is DMSO and the substrate is TNB, reactions with strongly basic aliphatic amines show base catalysis. Hence in these systems there is a change of mechanism from deprotonation of the zwitterionic adduct being rate limiting to its formation constituting the rate limiting step of the reaction, induced by a change of nucleophile. When base catalysis is observed the kinetic condition $k_{-1} \gg k_3[B]$ applies where the $k_3[B]$ term is actually the sum of all the catalytic rate constants for the deprotonation of the zwitterion by the basic species present in solution, including the solvent. The results outlined above can be understood if in DMSO the catalysed pathway when TFE is the nucleophile involves deprotonation of the zwitterion by solvent molecules. This pathway would not be favoured either in the poorly basic solvent acetonitrile, as there is *ca.* 10^7 fold difference in the basicities of DMSO and acetonitrile,¹³² or when the nucleophile (and consequently the catalyst base) is changed to more strongly basic amines.

σ -Complex formation between TNB and N-methylaniline ($pK_a(\text{water}) = 4.85$)⁹⁰ in the presence of Dabco has been studied in DMSO.¹¹⁷ The reaction is catalysed solely by Dabco in a linear fashion indicating rate limiting proton transfer. The rate constant for reversion of the zwitterion to reactants k_{-1} is an order of magnitude higher than in the case of aniline, reflecting the release of steric compression of the zwitterion on reversion to reactants. It was also concluded that reactions of N-methylaniline show a greater susceptibility to base catalysis than those of aniline owing to the difficulty in abstracting a proton from the zwitterion due to steric effects.

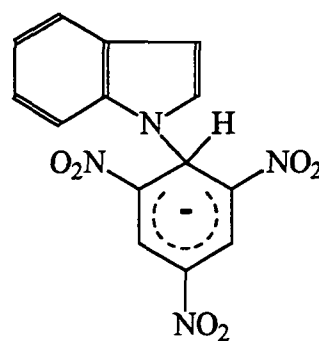
Drost in 1899 first treated 4,6-dinitrobenzofurazan 1-oxide with 1 molar equivalent of aniline in the absence of a catalyst and obtained a crystalline product which he thought to be 1.57, the nitrogen bonded adduct.¹³³ Later studies proved conclusively that the product was in fact 1.58 the carbon bonded adduct.¹³⁴



1.57



1.58



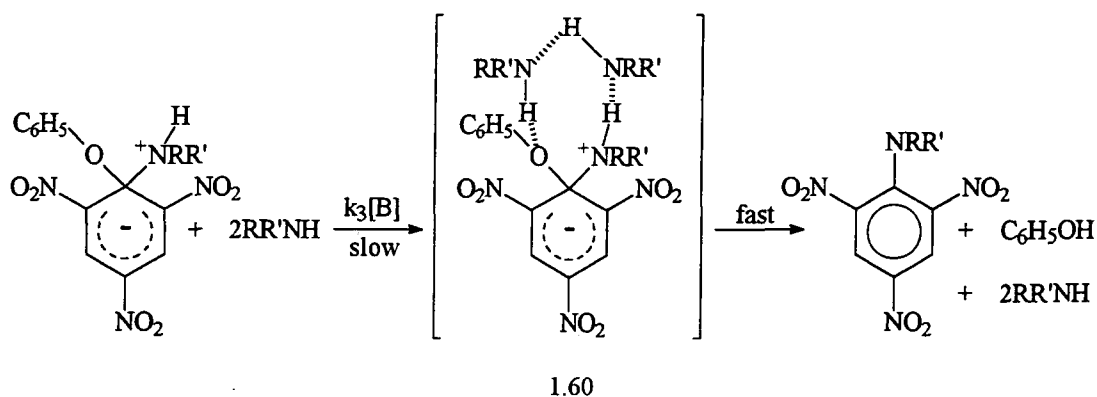
1.59

Stable Meisenheimer complexes formed from aniline, N-methylaniline and N,N-dimethylaniline with 4,6-dinitrobenzofurazan 1-oxide have been investigated.¹³⁵ The thermodynamic product is derived from reaction through the aromatic carbon para or, if the position is substituted, ortho to the amino group of the aromatic amine. In the presence of Dabco, aniline reacts with 4,6-dinitrobenzofurazan 1-oxide to give an unstable nitrogen bonded complex which is slowly converted into the carbon bonded complex. A similar effect has not been found in the reaction of aniline and TNB.

The interaction of indolide anions with nitroaromatics (e.g. TNB) to form σ -adducts can occur either at the C or N centres. Again the N-bonded adduct, 1.59, is formed through kinetic control while the C-bonded adduct forms as a result of thermodynamic control.¹³⁶ Interestingly decomposition of the N- and C-adducts of indolide anions with TNB is subject to specific acid catalysis in the former case and general acid catalysis in the latter typical of electrophilic aromatic substitutions (S_EAr).¹³⁷

There have been several studies of substitution reactions involving aniline derivatives as nucleophiles. When these substitutions take place in solvents of low dielectric constant then the presence of bases or other additives often gives rise to rate accelerations. A variety of explanations have been given for the origins of these effects, and some of these are summarised here. The reaction of 1-halogeno-2,4-dinitrobenzenes with p-anisidine in benzene are catalysed both by base and by tetra-n-butylammonium chloride. This was attributed to stabilisation by the additives of the transition state for the initial nucleophilic attack.¹³⁸ Banjoko and Otiono have shown that the reaction of 2,4,6-trinitrophenyl phenyl ether with aniline in methanol, acetonitrile, tetrahydrofuran, ethylacetate and benzene is base catalysed.¹³⁹ All gave a linear dependence in amine concentration, except benzene which gave a squared dependence, implicating two molecules of aniline contribute to the base catalysis of the rate limiting step, equation 1.41. The first molecule is accommodated for in the abstraction of the proton from the amine moiety and the second is predicted to be involved in the abstraction of the leaving group. Hydrogen bonding is thought to exist between the aniline hydrogens and the oxygen of the phenoxide ion, assisting leaving group departure. Further hydrogen bonding between these two bonded amine molecules then results in a cyclic transition state 1.60, followed by rapid decomposition into products.

When nucleophilic substitution reactions take place in solvents of low dielectric constant, the base catalysed decomposition of the intermediate may involve a cyclic transition state. The rationale behind the postulate is the need for electrophilic catalysis to assist the departure of poor leaving groups and the inability of such solvents to stabilise the ionic species required by the Bunnett type mechanism.

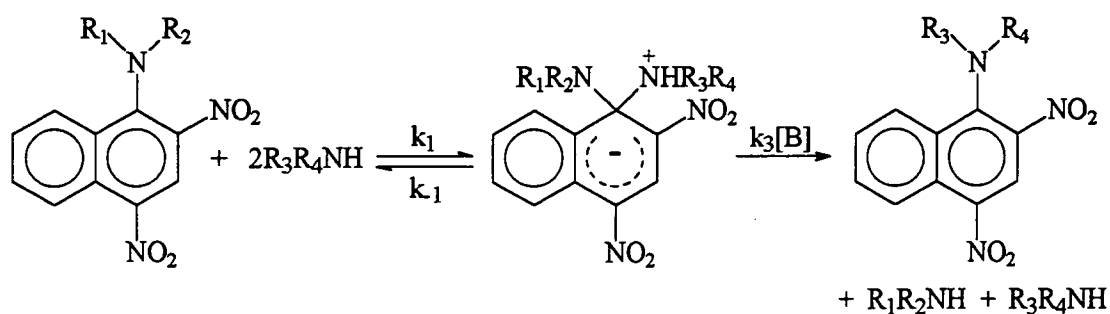


equation 1.41

Reaction of 2,4,6-trinitrochlorobenzene with aniline in methanol is not base catalysed owing to the good leaving group ability of the chloride ion.¹⁴⁰

Banjoko and Ezani have also observed the squared dependence on aniline when studying the reactions in benzene with 2,4,6-trinitrophenyl phenyl ether and derivatives containing various nitro substituents in the 2'-, 3'- and 4'-positions of the leaving group.¹⁴¹ With the exception of the 2', 6'-dinitro isomer, when the leaving group contains two nitro substituents, a linear relationship on aniline concentration is noted, i.e. the transition state for the decomposition of the intermediate to products only involves one molecule of aniline. This is easily understood as the introduction of a second nitro group will reduce the basicity of the oxygen atom in the σ -complex and decrease the population of the species hydrogen bonded to it and consequently the probability of attachment of a second aniline molecule. Hirst and co-workers have found a squared dependence evident in the reaction of N-methylaniline with the 4'-nitro derivative.¹⁴² Similar reactions of 2,4-dinitrophenyl phenyl ether and its 6-methyl derivative with aniline in benzene performed by Hirst were found to be too slow to be measured conveniently.¹⁴²

Although amines are not regarded as good leaving groups,⁹ kinetic studies have been reported on aromatic nucleophilic substitutions of 1-dialkylamino-2,4-dinitronaphthalenes with various amines¹⁴³ in DMSO, equation 1.42. The dialkylamino group (e.g. dimethyl-, diethyl-, and N-methylbutyl-amino, piperidino, and pyrrolidino) of 1-dialkylamino-2,4-dinitronaphthalenes is readily replaced by primary alkylamines in DMSO. However, substitution does not occur for secondary alkylamines except in the case of pyrrolidine. Aromatic primary amines (p-methoxy-, p-methyl-, and p-nitro-anilines and aniline) are found to be less reactive than aliphatic primary amines owing to their poor nucleophilicity and bulkiness. Benzylamine is more reactive than aromatic primary amines, but less reactive than primary amines. Results indicate that steric effects as well as the basicity of the attacking amines and corresponding amines to the amino group at C-1 are very important.



equation 1.42

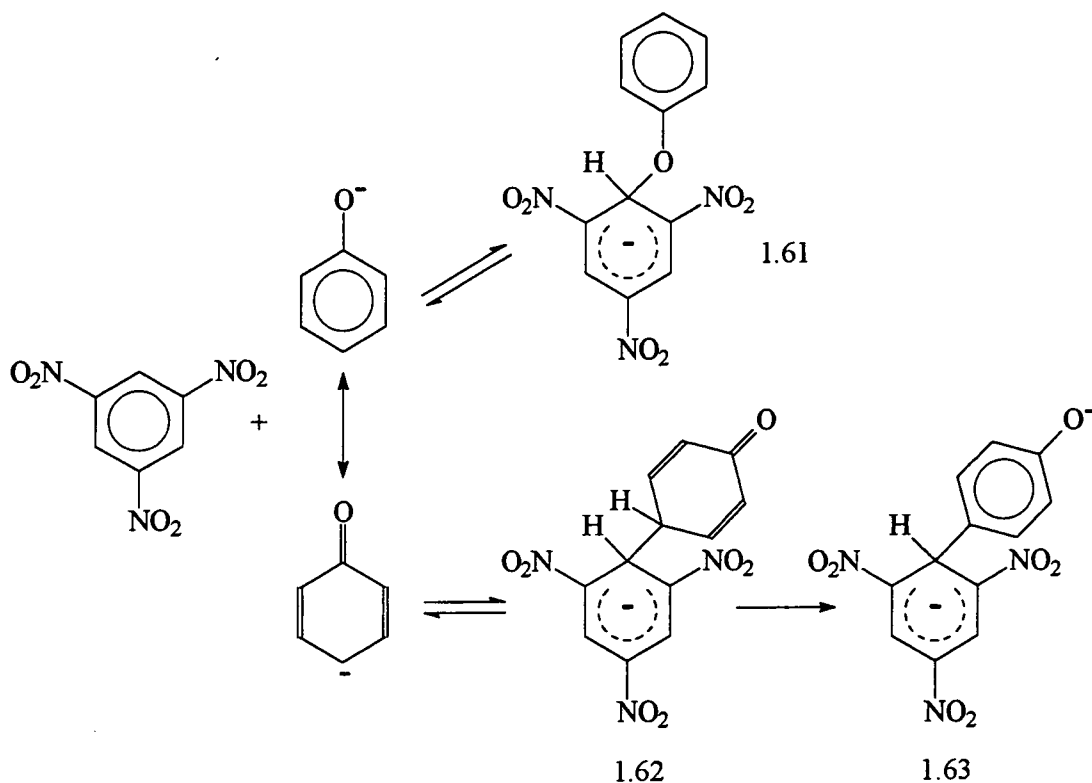
Rate constants have been determined for the displacement reactions of four picryl halides, 1,2,3,5-tetranitrobenzene, and 1,2,4-trinitrobenzene with aniline in ethanol.¹⁴⁴ The corresponding reactions of 1-halogen-2,4-dinitronaphthalenes, 2,4-dinitro-1-naphthyl toluene-p-sulphonate and 1-chloro-2,4,5-trinitronaphthalene have also been studied.¹⁴⁵

1.6.2 Phenols.

Phenoxide ions have the ability to act as either carbon or oxygen nucleophiles in σ -complex formation. Both aniline and indole also show ambident reactivity towards electron deficient aromatic and heteroaromatic compounds as discussed previously.

Carbon versus oxygen base additions have received considerable attention. 1,3,5-Trinitrobenzene (TNB) and more recently the highly electrophilic 4,6-dinitrobenzofuroxan (DNBF) and 4,6-dinitrobenzofurazan (DNBZ) have proved to be very suitable substrates for studying this behaviour.

Scheme 1.12 shows addition of the two different nucleophilic forms of phenoxide with TNB. It is important to note that the formation of the aryloxy complex 1.61 is reversible and occurs under kinetic control, while that of the C-bonded complex 1.63 is the thermodynamically stable species which is essentially irreversible due to the rearomatisation of the intermediate 1.62. C-Addition is found to occur at the ortho position for para-substituted phenoxides.¹⁴⁶ Complexes such as 1.63 are very stable but in acidic conditions may be protonated to give the nitronic acid forms.¹⁴⁷

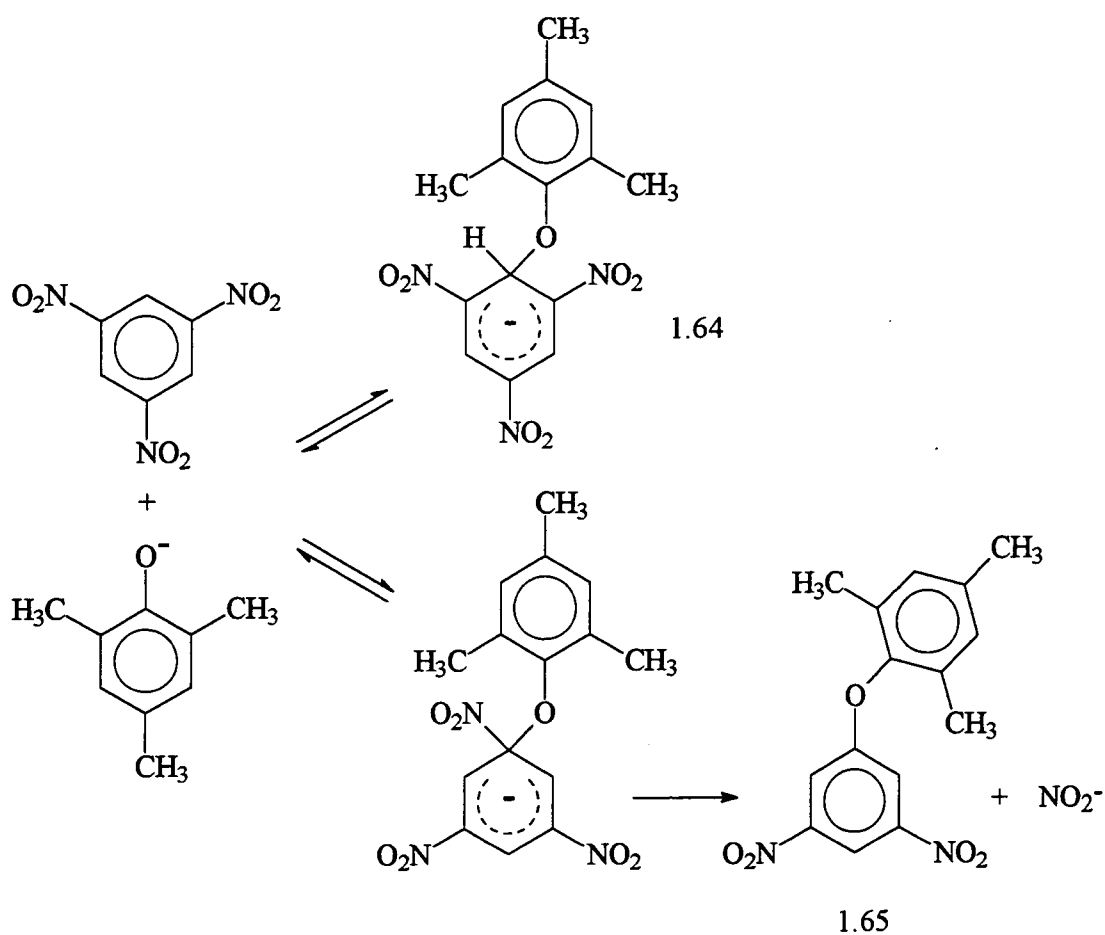


scheme 1.12

Various studies have been completed in which identification and characterisation of the oxygen bonded phenoxy adduct have proved elusive. The reaction of 2,4,6-trimethylphenoxide (mesitoxide, MesO⁻) ion with TNB was attempted by Buncl and co-workers, scheme 1.13, on the expectation that carbon-bonded adduct formation would be precluded and that oxygen-adduct formation would remain as the only alternative process.¹⁴⁸ The study showed, nevertheless, that a competing nitro group displacement took place readily in conjunction with σ -adduct formation and that the diaryl ether 1.65 was the only observed product.

Buncel and Manderville in 1993 provided for the first time definitive observation of both O- and C-bonded phenoxide σ -adducts establishing the formation of the former through kinetic control.¹⁴⁹ A novel reaction system (CD_3CN -glyme- d_{10}) was used which allowed the investigation of species formed at low temperatures (-40°C) as opposed to previous studies at ambient temperatures in d_6 -DMSO.

It is concluded from ^{13}C NMR parameters that σ -adducts 1.61 and 1.64 adopt a planar configuration in which conjugation of the p-type lone pair orbital of the oxygen with the aromatic π -electron system is maximized.¹⁴⁹

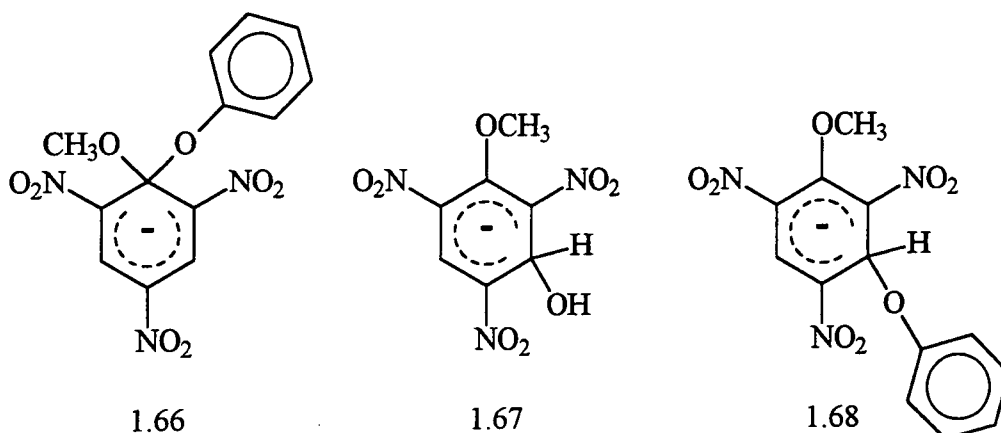


scheme 1.13

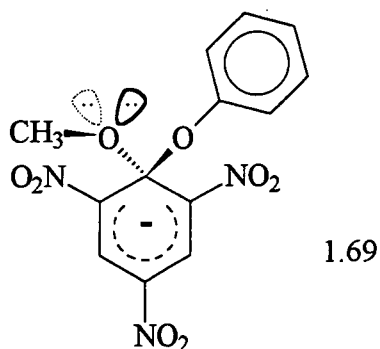
Bernasconi and Muller in 1978 carried out a stopped-flow / temperature jump study to investigate Meisenheimer complex formation between 2,4,6-trinitroanisole (TNA) and phenoxide ions in water / DMSO mixtures.⁶⁵ A transient complex with a life time of only a few seconds was identified and evidence indicates that the species is the 1-methoxy-1-phenoxy substituted σ -adduct 1.66, formed by the attack of the phenoxide ion through oxygen on the 1-position of TNA.

Slow reactions are involved consistent with hydroxide attack at the 3-position to give 1.67, and at the 1-position. The latter process ultimately leads to formation of the picrate ion. Kinetic results show a first order dependence on phenoxide concentration at a constant buffer ratio, which is in agreement with initial formation of 1.66. Arguments were provided showing that the initial transient complex is the 1:1 σ -adduct and not the alternative 1:3 σ -adduct, 1.68.

In further studies Buncel and co-workers investigated the reaction of TNA and phenoxide ions in both d_6 -DMSO at ambient temperatures and CD_3CN -glyme- d_{10} at $-40^\circ C$. They were able to identify the kinetically favoured initial formation of the 1,1 σ -adduct.¹⁵⁰ The 1,3 O-bonded σ -adduct is not observed at all. After a significant amount of time the 1,3 C-bonded σ -adduct is detected in the CD_3CN -glyme- d_{10} solvent system only. This reaction sequence is unexpected since previous studies involving the reaction of alkoxides indicate the general pattern to be formation of the kinetically preferred oxygen bonded 1,3 anionic σ -adduct which then isomerises to a more stable 1,1 adduct, classified as K3T1.^{10,74,121,151}



Recently reported is the reaction of the sterically hindered aryloxide nucleophile 2,4,6-trimethylphenoxide ion ($MesO^-$), which can only react as a oxygen nucleophile.¹⁵² Upon addition of TNA, NMR studies at $-40^\circ C$ show a kinetic preference for the 1,1 σ -adduct but the σ -adduct that appears from C-3 attack is thermodynamically more stable, K1T3 behaviour. This is in accord with results obtained for the phenoxide ion, showing a kinetic preference for C-1 attachment. The regioselectivity of attack was discussed in terms of stereoelectronic stabilisation of C-1 adducts through $n-\pi^*$ interaction of antiperiplanar lone pairs with the required C-O acceptor bonds, 1.69.



NMR Studies at low (-40°C) and ambient temperatures have been completed on the reaction of picryl chloride and picryl fluoride with a series of aryloxy nucleophiles (phenoxide, 2,4,6-trimethylphenoxide and 2,6-di-*t*-butylphenoxide) in which steric hinderance about the oxygen atom was gradually increased.¹⁵³ All exhibited a priority for C-1 attack over C-3 and clean $\text{S}_{\text{N}}\text{Ar}$ displacement of either halogen via the oxygen site for PhO^- and MesO^- or the para carbon site for 2,6-DTBP O^- gave the respective aryl picryl ether or picryl 2,6-di-*t*-butylphenol was observed. At no time were aryloxy oxygen σ -adducts detected by the NMR methods employed, indicating that nucleophilic attack was rate limiting and loss of halide was a fast process.

1.7 References.

1. M. Makosza, J. Golinski and J. Baran, *J. Org. Chem.*, 1984, **49**, 1488.
2. J. F. Bunnett and R. E. Zahler, *Chem. Rev.*, 1951, **49** 273.
3. J. F. Bunnett, *Q. Rev. Chem. Soc.*, 1958, **12**, 1.
4. L. Melander, *Arkiv Kemi*, 1950, **2**, 211.
5. C. J. Jackson and F. H. Gazzolo, *J. Am. Chem. Soc.*, 1900, **23**, 376.
6. J. Meisenheimer, *Justus Liebigs Ann. Chem.*, 1902, **323**, 205.
7. C. A. Fyfe, A. Koll, S. W. H. Damji, C. D. Malkiewich and P. A. Forte., *J. Chem. Soc. Chem. Commun.*, 1977, 335.
8. C. A. Fyfe, S. W. H. Damji and A. Koll, *J. Am. Chem. Soc.*, 1979, **101**, 951.
9. J. Miller, "Aromatic Nucleophilic Substitution", Elsevier, Amsterdam, 1968.
10. E. Bunce, M. R. Crampton, M. J. Strauss and F. Terrier, "Electron-Deficient Aromatic & Heteroaromatic - Base Interactions", Elsevier, New York, 1984.
11. M. R. Crampton, *Adv. Phys. Org. Chem.*, 1969, **7**, 211.
12. M. J. Strauss, *Acc. Chem. Res.*, 1978, **11**, 147.
13. R. Foster and C. A. Fyfe, *Rev. Pure. Appl. Chem.*, 1966, **16**, 61.
14. E. Bunce, A. R. Norris and K. E. Russell, *Q. Rev. Chem. Soc.*, 1968, **22**, 123.
15. M. R. Crampton and V. Gold, *J. Chem. Soc.*, 1964, 4293.
16. M. R. Crampton and V. Gold, *J. Chem. Soc. B*, 1966, 893.
17. J. F. Bunnett and C. F. Bernasconi, *J. Org. Chem.*, 1970, **35**, 70.
18. A. Wohl, *Chem. Ber.* 1899, **32**, 3486.
19. M. Makosza, *Pol. J. Chem.* 1992, **3**, 66.
20. M. Makosza and J. Winarski, *Acc. Chem. Res.*, 1987, **20**, 282.
21. M. Makosza and T. Glinka, *J. Org. Chem.*, 1983, **48**, 3860.
22. B. J. Barnes, P. J. Newcombe, R. K. Norris and K. J. Wilson, *J. Chem. Soc. Chem. Commun.*, 1985, 1408.
23. H. C. Van der Plas, *Acc. Chem. Res.* 1978, **11**, 462.
24. H. C. Van der Plas, M. Wozniak and H. J. W. Van den Hoak, *Adv. Heterocycl. Chem.* 1983, **33**, 96.
25. E. Havinga and J. L. Cornelisse, *Pure Appl. Chem.*, 1976, **47**, 1.
26. J. L. Cornelisse, G. P. de Gunst and E. Havinga, *Adv. Phys. Org. Chem.* 1975, **11**, 225.
27. J. L. Cornelisse, G. Lodder and E. Havinga, *Rev. Chem. Intermed.*, 1979, **2**, 231.

28. R. Nakagaki, M. Hiramatsu, K. Mutai and S. Nagakura, *Chem. Phys. Lett.*, 1985, **121**, 262.
29. J. D. Roberts, H. E. Simmons Jr., L. A. Carlsmith and C. W. Vaughan, *J. Am. Chem. Soc.*, 1953, **75**, 3290.
30. J. D. Roberts, D. A. Semenov, H. E. Simmons Jr. and L. A. Carlsmith, *J. Am. Chem. Soc.*, 1956, **78**, 601.
31. J. D. Roberts, C. W. Vaughan, L. A. Carlsmith and D. A. Semenov, *J. Am. Chem. Soc.*, 1956, **78**, 611.
32. G. E. Hall, R. Piccolini and J. D. Roberts, *J. Am. Chem. Soc.*, 1955, **77**, 4540.
33. C. G. Swain, J. E. Sheets and K. J. Harbison, *J. Am. Chem. Soc.*, 1975, **97**, 783.
34. C. G. Swain, J. E. Sheets, D. G. Gorenstein and K. G. Harbison, *J. Am. Chem. Soc.*, 1975, **97**, 791.
35. C. G. Swain, J. E. Sheets and K. J. Harbison, *J. Am. Chem. Soc.*, 1975, **97**, 796.
36. R. G. Bergstrom, R. G. M. Landells, G. W. Whal Jr. and H. Zollinger, *J. Am. Chem. Soc.*, 1976, **98**, 3301.
37. S. A. Ba-Saif, A. K. Luthra and A. Williams, *J. Am. Chem. Soc.*, 1987, **109**, 6362.
38. F. Terrier, "Nucleophilic Aromatic Displacement : Influence of the Nitro Group", VCH, Weinheim, 1991.
39. A. H. M. Renfrew, J. A. Taylor, J. M. J. Whitmore and A. Williams, *J. Chem. Soc. Perkin Trans. 2*, 1993, 1703.
40. A. H. M. Renfrew, D. Rettura, J. A. Taylor, J. M. J. Whitmore and A. Williams, *J. Am. Chem. Soc.*, 1995, **117**, 5484.
41. A. Williams, *Chem. Soc. Rev.*, 1994, 93.
42. N. R. Cullum, A. H. M. Renfrew, D. Rettura, J. A. Taylor, J. M. J. Whitmore and A. Williams, *J. Am. Chem. Soc.*, 1995, **117**, 9200.
43. A. H. M. Renfrew, J. A. Taylor, J. M. J. Whitmore and A. Williams, *J. Chem. Soc. Perkin Trans. 2*, 1994, 2383.
44. J. Shakes, C. Raymond, D. Rettura and A. Williams, *J. Chem. Soc. Perkin Trans. 2*, 1996, 1553.
45. A. Williams, *Adv. Phys. Org. Chem.*, 1992, **27**, 1.
46. A. Williams, *Acc. Chem. Res.*, 1984, **17**, 425.
47. N. R. Cullum, D. Rettura, J. M. J. Whitmore and A. Williams, *J. Chem. Soc. Perkin Trans. 2*, 1996, 1559.
48. F. Kröhnke, *Chem. Ber.*, 1950, **83**, 50.

49. E. Buncel, R. Tarkka and S. Hoz, *J. Chem. Soc. Chem. Commun.*, 1993, 109.
50. S. Hoz, P. Liu and E. Buncel, *J. Chem. Soc. Chem Commun.*, 1996, 95.
51. J. K. Rim and J. F. Bunnett, *J. Am. Chem. Soc.*, 1970, **92**, 448.
52. J. F. Bunnett, *J. Am. Chem. Soc.*, 1970, **92**, 7463.
53. C. Galli and J. F. Bunnett, *J. Am. Chem. Soc.*, 1981, **103**, 7140.
54. J. F. Bunnett, *Tetrahedron*, 1993, **49**, 4477.
55. J. Marquet, Z. Jiang, I. Gallardo, A. Batlle and E. Cayon, *Tetrahedron Lett.*, 1993, **34**, 2801.
56. D. B. Denney, D. Z. Denney and A. J. Perez, *Tetrahedron*, 1993, **49**, 4463.
57. M. J. Dewar, "The Electronic Theory of Organic Chemistry". Oxford University Press : London, 1949, p.77.
58. A. J. Birch, A. L. Hinde and L. Radom, *J. Am. Chem. Soc.*, 1980, **102**, 6430.
59. J. H. Fendler, W. L. Hinze and L. J. Liu, *J. Chem. Soc. Perkin Trans. 2*, 1975, 1768.
60. N. L. Khilkova, V. N. Knyazev, N. S. Patalakha and V. N. Drozd, *Izv. Timiryazevsk. Skh. Akad.*, 1991, 162; *Chem. Abs.*, 1991, **115**, 207888.
61. E. Grovenstein and P. C. Lu, *J. Am. Chem. Soc.*, 1982, **104**, 6681.
62. J. A. Orvik and J. F. Bunnett, *J. Am. Chem. Soc.*, 1970, **92**, 2417.
63. G. Bartoli and P. E. Todesco, *Acc. Chem. Res.*, 1977, **10**, 125.
64. J. F. Bunnett and J. J. Randall, *J. Am. Chem. Soc.*, 1958, **80**, 6020.
65. C. F. Bernasconi and M. C. Muller, *J. Am. Chem. Soc.*, 1978, **100**, 5530.
66. H. Al-Rawi and A. Williams, *J. Am. Chem. Soc.*, 1977, **99**, 2671.
67. P. J. Thomas and C. J. M. Stirling, *J. Chem. Soc. Chem. Commun.*, 1976, 829.
68. E. Buncel and B. C. Menon, *J. Organomet. Chem.*, 1977, **141**, 1.
69. E. Buncel and B. C. Menon, *J. Am. Chem. Soc.*, 1977, **99**, 4457.
70. F. Terrier, *Chem. Rev.*, 1982, **82**, 77.
71. C. F. Bernasconi and R. G. Bergstrom, *J. Org. Chem.*, 1971, **36**, 1325.
72. M. R. Crampton, *J. Chem. Soc. Perkin Trans. 2*, 1977, 1442.
73. M. R. Crampton, B. Gibson and F. W. Gilmore, *J. Chem. Soc. Perkin Trans. 2*, 1979, 91.
74. A. D. A. Alaruri and M. R. Crampton, *J. Chem. Res. (S)*, 1982, **2**, 60.
75. M. R. Crampton, *J. Chem. Soc. B*, 1967, 1341.
76. J. F. Bunnett, *Acc. Chem. Res.*, 1978, **11**, 413.
77. R. Bacaloglu, A. Blaskó, C. A. Bunton, F. Ortega and C. Zucco, *J. Am. Chem. Soc.*, 1992, **114**, 7708.

78. R. Bacaloglu, C. A. Bunton and F. Ortega, *J. Am. Chem. Soc.*, 1988, **110**, 3503.
79. M. R. Crampton, A. B. Davis, C. Greenhalgh and J. A. Stevens, *J. Chem. Soc. Perkin Trans. 2*, 1989, 675.
80. P. Sepulcri, R. Goumont, J. C. Hallé, E. Bunce and F. Terrier, *J. Chem. Soc. Chem. Commun.*, 1997, 789.
81. R. I. Cattana, J. O. Singh, J. D. Anunziata and J. J. Silber, *J. Chem. Soc. Perkin Trans. 2*, 1987, 79.
82. J. Hayami, S. Otani, F. Yamaguchi and Y. Nishikawa, *Chem. Lett.*, 1987, 739.
83. C. F. Bernasconi, *Acc. Chem. Res.*, 1978, **11**, 147.
84. C. F. Bernasconi, M. C. Muller and P. Schmid, *J. Org. Chem.*, 1979, **44**, 3189.
85. M. R. Crampton and B. Gibson, *J. Chem. Soc. Perkin Trans 2*, 1981, 533.
86. T. O. Bamkole, J. Hirst and J. Onyido, *J. Chem. Soc. Perkin Trans 2*, 1981, 1201.
87. E. Bunce, J. G. K. Webb and J. F. Wiltshire, *J. Am. Chem. Soc.*, 1977, **99** 4429.
88. E. Bunce and W. Eggimann, *J. Am. Chem. Soc.*, 1977, **99**, 5958.
89. S. Sekiguchi and J. F. Bunnett, *J. Am. Chem. Soc.*, 1981, **103**, 4871.
90. R. C. Weast and M. J. Astle, "CRC Handbook of Chemistry and Physics", 63rd. Edition, 1981, CRC Press Inc., Boca Raton, Florida, F-41.
91. E. Bunce and J. G. K. Webb, *Can. J. Chem.*, 1974, **52**, 630.
92. C. F. Bernasconi, *M. T. P. Int. Rev. Sci., Org. Chem., Ser. One*, 1973, **3**, 33.
93. L. Forlani and V. Tortelli, *J. Chem. Res. (S)*, 1982, **62**, 258.
94. R. I. Cattana, J. O. Singh, J. D. Anunziata and J. J. Silber, *J. Chem. Soc. Perkin Trans. 2*, 1987, 79.
95. H. Fujinuma, M. Hosokawa, T. Suzuki, M. Sato and S. Sekiguchi, *Bull. Chem. Soc. Jpn.*, 1989, **62**, 1969.
96. I. Onyido and J. Hirst, *J. Phys. Org. Chem.*, 1991, **4**, 367.
97. D. Ayediran, T. O. Bamkole, J. Hirst and I. Onyido, *J. Chem. Soc. Perkin Trans. 2*, 1977, 1580.
98. C. F. Bernasconi, *J. Phys. Chem.*, 1971, **75**, 3636.
99. A. J. Kirby and W. P. Jencks, *J. Am. Chem. Soc.*, 1965, **87**, 3217.
100. J. F. Bunnett, S. Sekiguchi and L. A. Smith, *J. Am. Chem. Soc.*, 1981, **103**, 4865.
101. J. F. Bunnett and A. V. Cartano, *J. Am. Chem. Soc.*, 1981, **103**, 4861.

102. Y. Hasegawa, *Bull. Chem. Soc. Jpn.*, 1983, **56**, 1314.
103. Y. Hasegawa, *J. Org. Chem.*, 1985, **50**, 649.
104. R. H. de Rossi and R. A. Rossi, *J. Org. Chem.*, 1974, **39**, 3486.
105. T. O. Bamkole, J. Hirst and J. Onyido, *J. Chem. Soc. Perkin Trans. 2*, 1982, 889.
106. T. O. Bamkole, J. Hirst and G. Hussain, *J. Chem. Soc. Perkin Trans. 2*, 1984, 681.
107. N. S. Nudelman and D. R. Palleros, *J. Org. Chem.*, 1983, **48**, 1607.
108. N. S. Nudelman and D. R. Palleros, *J. Org. Chem.*, 1983, **48**, 1613.
109. O. Banjoko and I. A. Bayeroju, *J. Chem. Soc. Perkin Trans. 2*, 1988, 1853.
110. J. Hirst, *J. Phys. Org. Chem.*, 1994, **6**, 78.
111. M. Eigen, *Angew. Chem., Int. Ed. Engl.*, 1964, **3**, 1.
112. W. P. Jencks, *Chem. Rev.*, 1972, **72**, 705.
113. R. E. Barnett, *Acc. Chem. Res.*, 1973, **6**, 41.
114. C. F. Bernasconi, *Chimia*, 1980, **34**, 1.
115. J. F. Bunnett and R. H. Gorst, *J. Am. Chem. Soc.*, 1965, **87**, 3879.
116. C. F. Bernasconi, C. L. Gehriger and R. H. de Rossi, *J. Am. Chem. Soc.*, 1976, **98**, 8451.
117. E. Bunzel, C. Innis and I. Onyido, *J. Org. Chem.*, 1986, **51**, 3680.
118. M. R. Crampton and C. Greenhalgh, *J. Chem. Soc. Perkin Trans. 2*, 1983, 1175.
119. C. F. Bernasconi, R. H. de Rossi and P. Schmid, *J. Am. Chem. Soc.*, 1977, **99**, 4090.
120. R. A. Chamberlin and M. R. Crampton, *J. Chem. Soc. Perkin Trans. 2*, 1994, 425.
121. R. A. Chamberlin and M. R. Crampton, *J. Chem. Soc. Perkin Trans. 2*, 1995, 1831.
122. M. R. Crampton and S. D. Lord, *J. Chem. Soc. Perkin Trans. 2*, 1997, 369.
123. M. J. Kamlet and R. W. Taft, *J. Am. Chem. Soc.*, 1976, **98**, 377.
124. R. Foster, "Organic Transfer Complexes", Academic Press, London, 1969.
125. E. Bunzel and J. G. K. Webb, *Can. J. Chem.*, 1972, **50**, 129.
126. J. McMurry, "Organic Chemistry", Brooks/Cole Publishing Company, Wadsworth, California, 1988.
127. E. Bunzel and H. W. Leung, *J. Chem. Soc. Chem. Commun.*, 1975, 19.
128. E. Bunzel, H. Jarrell, H. W. Leung and J. G. K. Webb, *J. Org. Chem.*, 1974, **39**, 272.
129. E. Bunzel and W. Eggimann, *J. Chem. Soc. Perkin Trans. 2*, 1978, 673.

130. J. H. Fendler, E. J. Fendler and M. V. Merritt, *J. Org. Chem.*, 1971, **36**, 2172.
131. M. R. Crampton and H. A. Khan, *J. Chem. Soc. Perkin Trans. 2*, 1972, (a) 1173, (b) 2286.
132. I. M. Kolthoff, M. K. Chantooni and S. Bhowmik, *J. Am. Chem. Soc.*, 1968, **90**, 23.
133. P. Drost, *Justus Liebigs Ann. Chem.*, 1899, **307**, 49.
134. R. J. Spear, W. P. Norris and R. W. Read, *Tetrahedron Lett.*, 1983, **24**, 1555.
135. R. W. Read, R. J. Spear and W. P. Norris, *Aust. J. Chem.*, 1984, **37**, 985.
136. J. C. Halle, F. Terrier, M. J. Pouet and M. P. Simonnin, *J. Chem. Res. (s)*, 1980, 360.
137. P. Sepulcri, R. Goumont, F. Terrier and E. Buncel, *J. Chem. Soc. Perkin Trans. 2*, 1996, 2241.
138. E. T. Akinyele, J. Hirst and I. Onyido, *J. Chem. Soc. Perkin Trans. 2*, 1988, 1859.
139. O. Banjoko and P. Otiono, *J. Chem. Soc. Perkin Trans. 2*, 1981, 399.
140. J. Hirst and K. U. Rahman, *J. Chem. Soc. Perkin Trans. 2*, 1973, 2119.
141. O. Banjoko and C. Ezani, *J. Chem. Soc. Perkin Trans. 2*, 1986, 531.
142. T. A. Emokpae, P. U. Uwakwe and J. Hirst, *J. Chem. Soc. Perkin Trans. 2*, 1991, 509.
143. S. Sekiguchi, T. Suzuki and M. Hosokawa, *J. Chem. Soc. Perkin Trans. 2*, 1989, 1783.
144. R. E. Parker and T. O. Read, *J. Chem. Soc.*, 1962, 9.
145. D. H. D. Elias and R. E. Parker, *J. Chem. Soc.*, 1962, 2616.
146. E. Buncel, A. Jonczyk and J. G. K. Webb, *Can. J. Chem.*, 1975, **53**, 3761.
147. E. Buncel and W. Eggimann, *Can. J. Chem.*, 1976, **54**, 2436.
148. E. Buncel, R. Y. Moir, A. R. Norris and A. P. Chatrousse, *Can. J. Chem.*, 1981, **59**, 2470.
149. E. Buncel and R. A. Manderville, *J. Phys. Org. Chem.*, 1993, **6**, 71.
150. E. Buncel, J. M. Dust, A. Jonezyk, R. A. Manderville and I. Onyido, *J. Am. Chem. Soc.*, 1992, **114**, 5610.
151. K. Servis, *J. Am. Chem. Soc.*, 1967, **89**, 1508.
152. R. A. Manderville and E. Buncel, *J. Am. Chem. Soc.*, 1993, **115**, 8985.
153. R. A. Manderville, J. M. Dust and E. Buncel, *J. Phys. Org. Chem.*, 1996, **9**, 515.

Chapter 2.

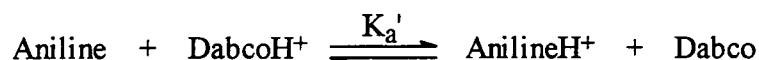
**Kinetic & Equilibrium Studies Involving the
Reactions of Aniline with Electron Deficient Aromatic
Substrates in Dimethyl Sulfoxide.**

The kinetics of the reactions of ethyl 2,4,6-trinitrophenylether, 2.5¹⁶ and some ring activated phenyl aryl ethers¹⁷ with aliphatic amines in DMSO have been previously examined. In agreement with the classic work of Bunnett and Orvik¹⁸ the results for 2.5 indicate that substitution involves the specific base general acid catalysis mechanism, SB-GA, in which leaving group expulsion is the overall rate limiting step. However, the observation of base catalysis in reactions of the phenyl aryl ethers was best explained in terms of rate limiting proton transfer from a zwitterionic intermediate to base.¹⁷ Previous studies of nucleophilic substitution using aniline as the nucleophile have shown that in reaction with methyl 2,4,6-trinitrophenyl ether there is a competition between attack at the ring carbon atom to give a diphenylamine derivative, and at the side chain carbon to give picric acid.¹⁹ Reactions of aniline with phenyl 2,4,6-trinitrophenyl ether yields the diphenylamine derivative and are subject to base catalysis in methanol, acetonitrile, THF, ethyl acetate and benzene.²⁰ However, there is little evidence for catalysis in DMSO.^{19,21}

This chapter describes the kinetics of the reactions of TNB, ethyl 2,4,6-trinitrophenyl ether, and of some ring activated phenyl aryl ethers with aniline in DMSO. The results show that in these reactions proton transfer may be the rate limiting step.

2.2 pK_a Values.

Kinetic and equilibrium measurements of the reaction with aniline were generally made in the presence of Dabco and Dabco hydrochloride. The pK_a values²² in DMSO of the protonated forms of the bases are aniline, 3.82 and Dabco, 9.06. Hence the value of the equilibrium constant K_a' for equation 2.2 is 5.8×10⁻⁶. Thus the concentrations of the reagents in the reaction mixture will be very similar to the stoichiometric concentrations; relatively little protonation of aniline will occur.



equation 2.2

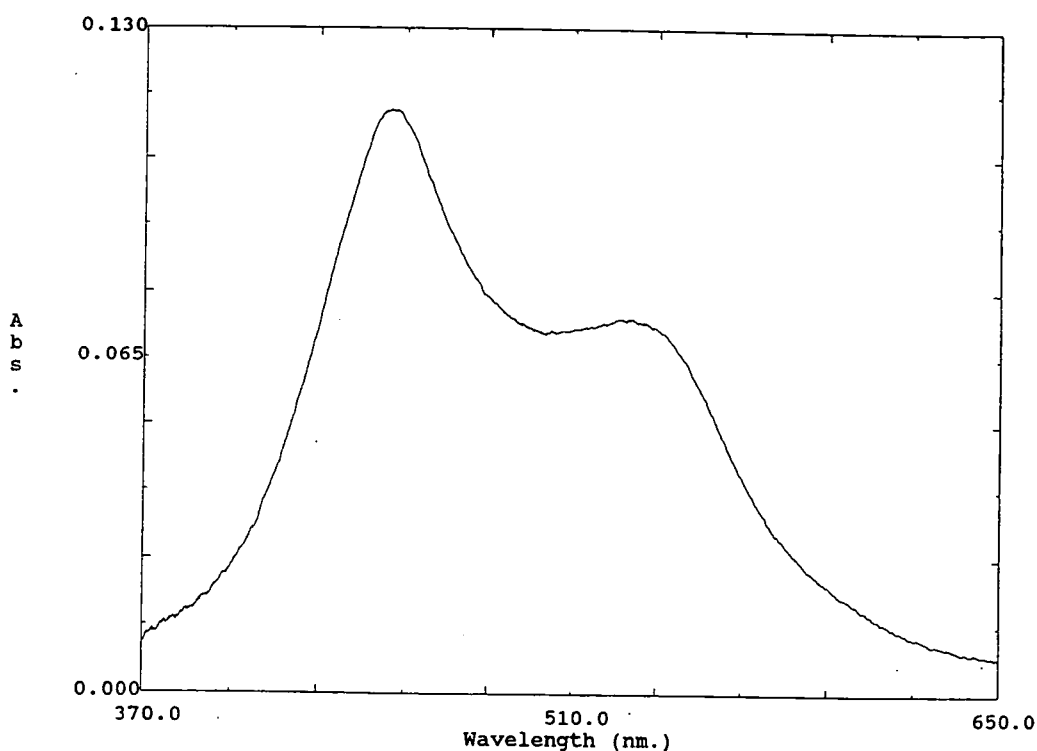
$$K_a' = \frac{K_a(\text{DabcoH}^+)}{K_a(\text{AnilineH}^+)} = 5.8 \times 10^{-6}$$

2.3 Reactions of 1,3,5-Trinitrobenzene, 2.2.

Previously Buncel and Eggimann¹⁰ have obtained kinetic data for the rapid reaction of TNB with aniline in the presence of Dabco, but without the addition of any acid salt, BH^+ . With the concentration of aniline and Dabco in large excess of the TNB concentration, the reaction shown in equation 2.1 leads to quite complex kinetics. This is because under these conditions the reaction is first order in the forward direction but second order in the reverse direction. Hence there is no straightforward dependence of concentration with time.¹⁵ In some cases the neutral salt, tetraethylammonium chloride, was present and it was found that the overall equilibrium constant increased in value with salt concentration. This is to be expected for a reaction in which ionic products are formed from neutral reagents.

In the present work the reactions of TNB have been studied in the presence of buffered solutions containing aniline, Dabco and $DabcoH^+$. This leads to simplified kinetics since the reactions of equation 2.1 are now first order in both forward and reverse directions. There is no reaction of TNB with aniline alone. U.V./Vis. spectra in the presence of Dabco and aniline show absorption maxima at 445nm and 530nm, figure 2.1. The spectrum is attributed to the anilide adduct 2.1.

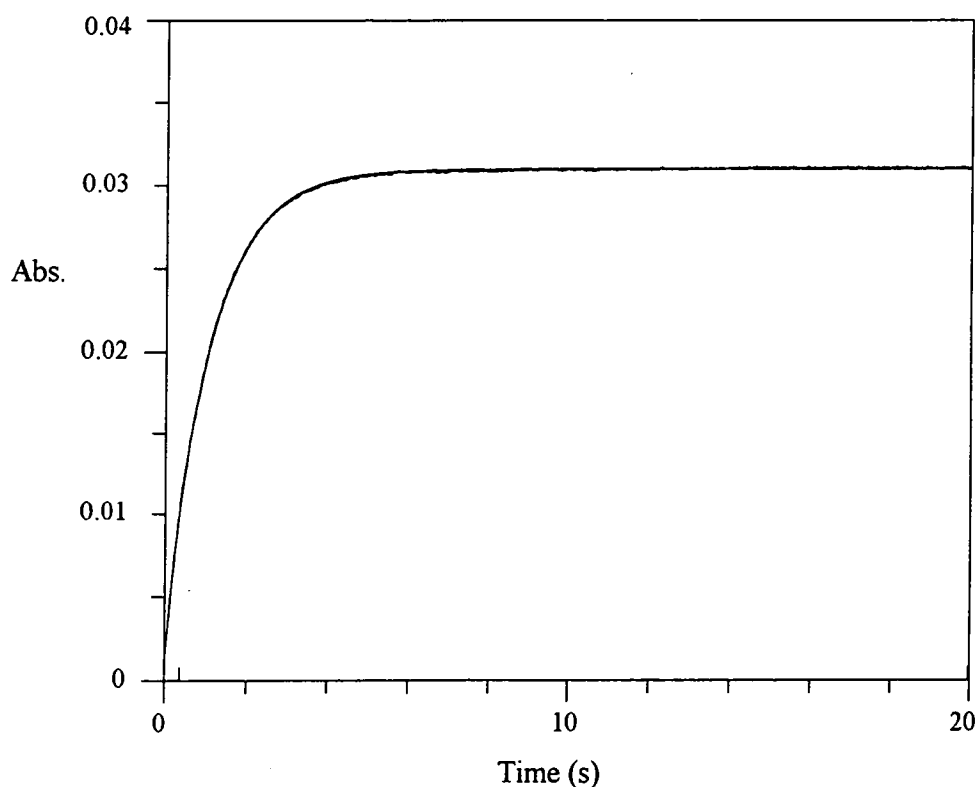
Figure 2.1 U.V./Vis. spectrum formed between TNB, 4×10^{-5} mol dm^{-3} , aniline 0.04 mol dm^{-3} , Dabco 0.1 mol dm^{-3} and $DabcoH^+$ 0.01 mol dm^{-3} .



2.3.1 Experimental Procedure.

Rate constants of reaction were determined by stopped-flow spectrophotometry at 25°C with aniline, Dabco and Dabco hydrochloride concentrations in large excess of TNB. A single solution containing the required concentrations of aniline, Dabco and Dabco hydrochloride was prepared, with the final addition of TNB occurring in the reaction cell of the stopped-flow. Dabco hydrochloride was prepared by the reaction of an equimolar solution of Dabco and hydrochloric acid. As the kinetic trace in figure 2.2 show, first order kinetics were observed providing rate constants, k_{fast} , with excellent correlation coefficients between 0.992 and 0.999. Measurements were made with two sets of conditions. Firstly the effect of varying the aniline concentration at constant Dabco concentration were examined followed by variation of Dabco concentration at constant aniline concentration. The $DabcoH^+$ concentration was kept constant, 0.01 mol dm^{-3} , throughout all the reactions to maintain constant ionic strength.

Figure 2.2 Kinetic trace for the reaction of TNB with aniline, Dabco and $DabcoH^+$ in DMSO at 25°C.



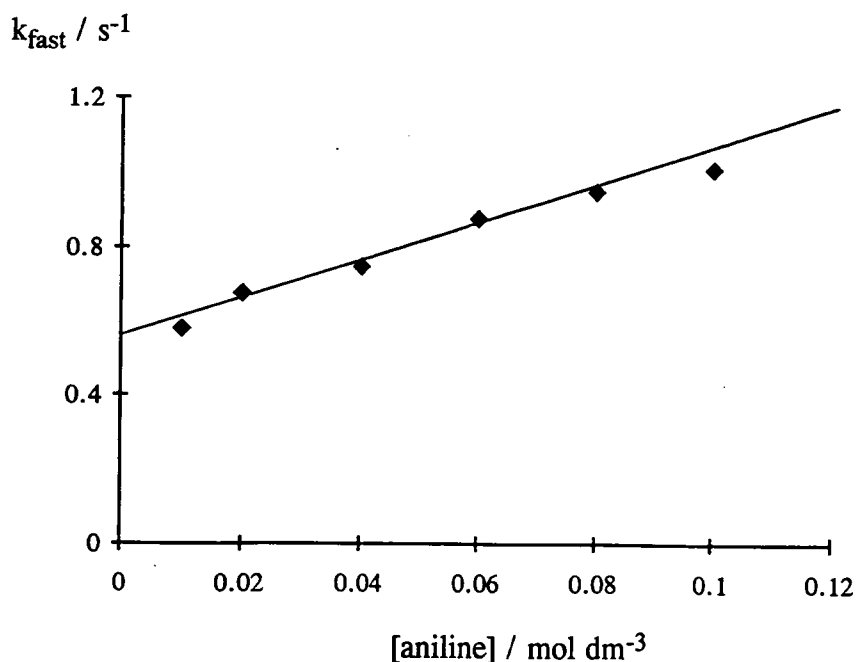
2.3.2 Dependence on Aniline.

Results shown below, table 2.1, were obtained at a wavelength $\lambda = 445\text{nm}$ for the reaction of TNB, $2 \times 10^{-5} \text{ mol dm}^{-3}$, Dabco 0.1 mol dm^{-3} , DabcoH⁺ 0.01 mol dm^{-3} , with various concentrations of aniline, (An), in DMSO at 25°C. Graphically the results are represented in figure 2.3, from which further kinetic information is obtained.

Table 2.1 Kinetic data for the formation of 2.1 from TNB, aniline, Dabco and DabcoH⁺ in DMSO at 25°C.

[An] / mol dm ⁻³	0.01	0.02	0.04	0.06	0.08	0.1
k _{fast} / s ⁻¹	0.58	0.68	0.75	0.88	0.95	1.01

Figure 2.3 Kinetic data for the formation of 2.1 from TNB, aniline, Dabco and DabcoH⁺ in DMSO at 25°C.



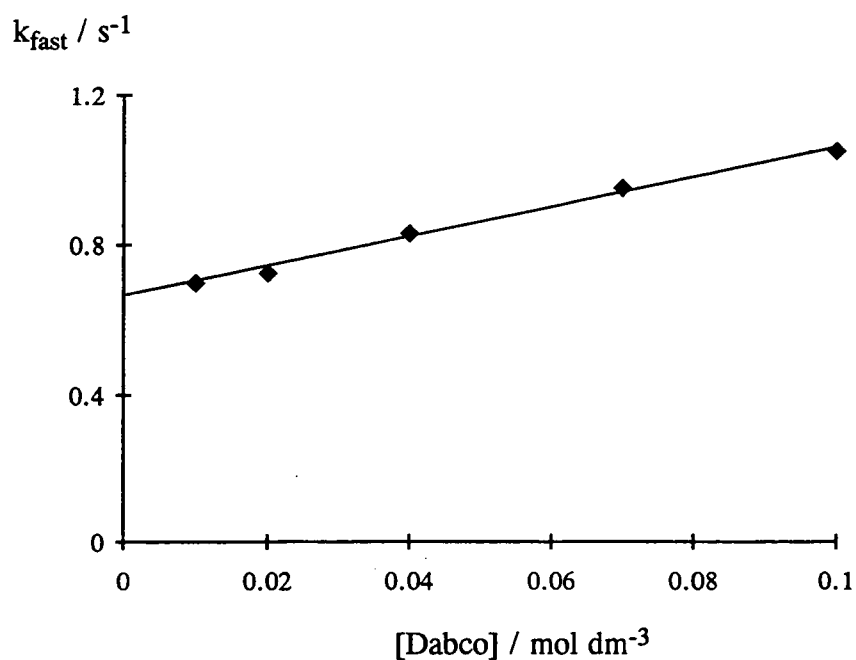
2.3.3 Dependence on Dabco.

Under the same experimental conditions Dabco concentration was varied keeping the concentration of TNB, $2 \times 10^{-5} \text{ mol dm}^{-3}$, aniline 0.1 mol dm^{-3} , and DabcoH^+ 0.01 mol dm^{-3} , constant in DMSO at 25°C . Results can be viewed in table 2.2 and graphically in figure 2.4.

Table 2.2 Kinetic data for the formation of 2.1 from TNB, aniline, Dabco and DabcoH^+ in DMSO at 25°C .

[Dabco] / mol dm^{-3}	0.01	0.02	0.04	0.07	0.10
$k_{\text{fast}} / \text{s}^{-1}$	0.70	0.72	0.83	0.95	1.04

Figure 2.4 Kinetic data for the formation of 2.1 from TNB, aniline, Dabco and DabcoH^+ in DMSO at 25°C .



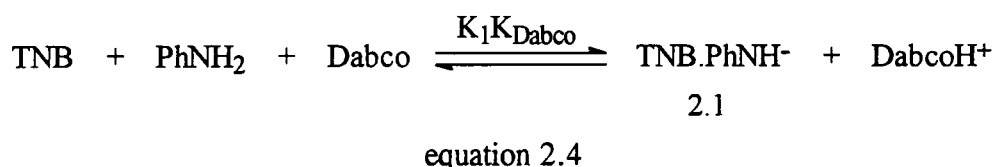
The plots shown in figures 2.3 and 2.4 are approximately linear with positive intercepts on the y-axis. Buncel and co-workers¹⁰ assumed that Dabco alone was active in the proton transfer step of equation 2.1, so that no reaction flux involved proton transfer to aniline. On this assumption they obtained the rate expression given in equation 2.3.

$$k_{\text{fast}} = K_1 k_{\text{Dabco}} [\text{An}] [\text{Dabco}] + k_{\text{DabcoH}^+} [\text{DabcoH}^+] \quad \text{equation 2.3}$$

On this basis the slope of figures 2.3 and 2.4 would allow the calculation of $K_1 k_{\text{Dabco}}$ while the intercepts should lead to values of k_{DabcoH^+} . In fact inspection of the figures indicates that the intercepts are different, so that a more detailed kinetic analysis is required. This analysis allowing for the participation of aniline in the proton transfer step is given later.

2.3.4 Determination of the Equilibrium Constant, $K_1 K_{\text{Dabco}}$, for σ -Adduct Formation using Absorbance Measurements.

Absorbance values, $\lambda = 445\text{nm}$, were taken at the completion of the reactions involving TNB $2 \times 10^{-5} \text{ mol dm}^{-3}$, aniline 0.1 mol dm^{-3} , and DabcoH⁺ 0.01 mol dm^{-3} , with varying concentrations of Dabco, described previously in table 2.2. Equation 2.4 defines an equilibrium constant $K_1 K_{\text{Dabco}}$ for the overall formation of the σ -adduct, 2.1, produced by the reaction of TNB with aniline in the presence of the base, Dabco. Application of equation 2.5 yields values of $K_1 K_{\text{Dabco}}$ and the results are presented in table 2.3. An absorbance value for the total conversion to the σ -adduct was not recorded, consequently a value of 0.11 was estimated.



$$K_1 K_{\text{Dabco}} = \frac{[2.1][\text{DabcoH}^+]}{[\text{TNB}][\text{An}][\text{Dabco}]} = \frac{(\text{Abs.})[\text{DabcoH}^+]}{(A_\infty - \text{Abs.})[\text{An}][\text{Dabco}]} \quad \text{equation 2.5}$$

Table 2.3 Absorbance and equilibrium data for the formation of 2.1 in DMSO containing various concentrations of Dabco at 25°C.
 $I = 0.01 \text{ mol dm}^{-3}$.

Dabco / mol dm ⁻³	0.01	0.02	0.04	0.07	0.10
10 ² Abs. (λ_{max} 445nm)	0.52	1.30	2.60	3.80	4.80
K_1K_{Dabco} / dm ³ mol ⁻¹	0.50 ^a	0.67	0.77	0.75	0.77

^a value of K_1K_{Dabco} not included in average.

A_∞ absorbance measurement for total conversion to 2.1, estimate = 0.11 for 2mm pathlength cell.

An average value of $K_1K_{\text{Dabco}} = 0.74 \pm 0.04 \text{ dm}^3 \text{ mol}^{-1}$ is found.

2.3.5 Kinetic Analysis.

The equilibrium constant, K_1K_{Dabco} , for the formation of 2.1 may also be defined in terms of the respective rate constants by equation 2.6. The absorbance values in table 2.3 lead to a value of K_1K_{Dabco} of $0.74 \pm 0.04 \text{ dm}^3 \text{ mol}^{-1}$. Alternatively the equilibrium constant may be defined in terms of the aniline concentration in equation 2.7. Use of equation 2.2 leads to equation 2.8. Since the value of K_a' is 5.8×10^{-6} , the value of K_1K_{An} will be many orders of magnitude lower than the value of K_1K_{Dabco} , explaining why adduct formation is not observed in the absence of Dabco.

$$K_1K_{\text{Dabco}} = \frac{[2.1]}{[\text{TNB}]} \cdot \frac{[\text{DabcoH}^+]}{[\text{An}][\text{Dabco}]} = \frac{k_1}{k_{-1}} \cdot \frac{k_{\text{Dabco}}}{k_{\text{DabcoH}^+}} \quad \text{equation 2.6}$$

$$K_1K_{\text{An}} = \frac{[2.1]}{[\text{TNB}]} \cdot \frac{[\text{AnH}^+]}{[\text{An}]^2} = \frac{k_1}{k_{-1}} \cdot \frac{k_{\text{An}}}{k_{\text{AnH}^+}} \quad \text{equation 2.7}$$

$$K_1K_{\text{An}} = K_1K_{\text{Dabco}} \cdot K_a' \quad \text{equation 2.8}$$

Nevertheless the kinetic results provide evidence that aniline is involved in the reaction flux of the proton transfer step as shown in the following analysis.

The variation of k_{fast} with values of the Dabco and aniline concentrations is compatible only with proton transfer being rate determining in the formation of 2.1. Using the condition $k_{-1} > k_{\text{B}}[\text{B}]$ and treating 2.3 as a steady state intermediate leads to the rate expression given in equation 2.9. Here k_{Dabco} and k_{An} represent k_{B} when the reaction involves Dabco and aniline respectively, while k_{DabcoH^+} and k_{AnH^+} represent k_{BH^+} for reactions with the appropriate conjugate acids. Since $K_{\text{An}} / K_{\text{Dabco}}$ has a constant value, equation 2.8, it is possible to reduce the number of variables in equation 2.9 to give equation 2.10.

$$k_{\text{fast}} = \frac{k_1}{k_{-1}} [\text{An}] (k_{\text{An}} [\text{An}] + k_{\text{Dabco}} [\text{Dabco}] + k_{\text{DabcoH}^+} [\text{DabcoH}^+] + k_{\text{AnH}^+} [\text{AnH}^+]) \quad \text{equation 2.9}$$

$$k_{\text{fast}} = K_1 k_{\text{Dabco}} [\text{An}] \left([\text{Dabco}] + \frac{k_{\text{An}}}{k_{\text{Dabco}}} [\text{An}] \right) + k_{\text{DabcoH}^+} [\text{DabcoH}^+] \left(1 + \frac{k_{\text{An}}}{k_{\text{Dabco}}} \frac{[\text{An}]}{[\text{Dabco}]} \right) \quad \text{equation 2.10}$$

Excellent agreement between the calculated and the observed values of k_{fast} was obtained with $K_1 k_{\text{Dabco}}$ $45 \pm 5 \text{ dm}^6 \text{ mol}^{-2} \text{ s}^{-1}$, k_{DabcoH^+} $56 \pm 2 \text{ dm}^3 \text{ mol}^{-1} \text{ s}^{-1}$ and $k_{\text{An}} / k_{\text{Dabco}}$ 0.015 ± 0.01 , table 2.4. The latter value indicates that aniline may compete, although poorly, with the much stronger base, Dabco in the proton transfer step, $2.3 \leftrightarrow 2.1$. This is discussed latter. Combination of the values of $K_1 k_{\text{Dabco}}$ and k_{DabcoH^+} leads to a value of $K_1 K_{\text{Dabco}}$ of $0.80 \text{ dm}^3 \text{ mol}^{-1}$ in acceptable agreement with that obtained independently from absorbance measurements at equilibrium. A computer correlation program was applied to a rearranged form of equation 2.10 to determine these final kinetic parameters.

Table 2.4 Kinetic data for the equilibration of TNB and 2.1 in DMSO at 25°C.

[An] / mol dm ⁻³	[Dabco] / mol dm ⁻³	[DabcoH ⁺] / mol dm ⁻³	k _{fast} / s ⁻¹	k _{calc} ^a / s ⁻¹
0.01	0.10	0.01	0.58	0.60
0.02	0.10	0.01	0.68	0.65
0.04	0.10	0.01	0.75	0.74
0.06	0.10	0.01	0.88	0.84
0.08	0.10	0.01	0.95	0.93
0.10	0.10	0.01	1.01	1.03
0.10	0.01	0.01	0.70	0.70
0.10	0.02	0.01	0.72	0.70
0.10	0.04	0.01	0.83	0.77
0.10	0.07	0.01	0.95	0.89
0.10	0.10	0.01	1.04	1.03

^a Calculated from equation 2.10 with $K_1 k_{\text{Dabco}} 45 \text{ dm}^6 \text{ mol}^{-2} \text{ s}^{-1}$, $k_{\text{DabcoH}^+} 56 \text{ dm}^3 \text{ mol}^{-1} \text{ s}^{-1}$ and $k_{\text{An}} / k_{\text{Dabco}} 0.015$.

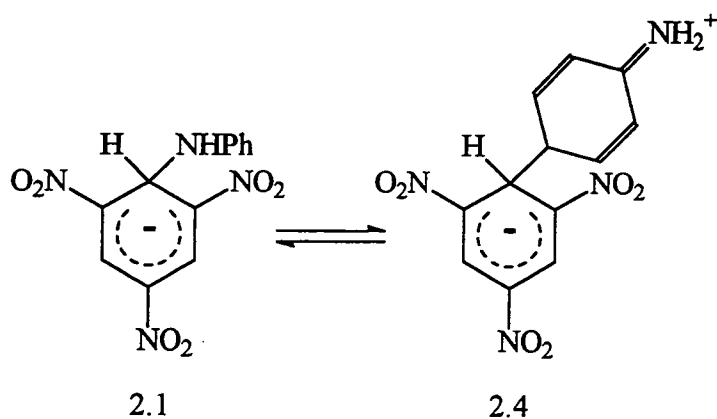
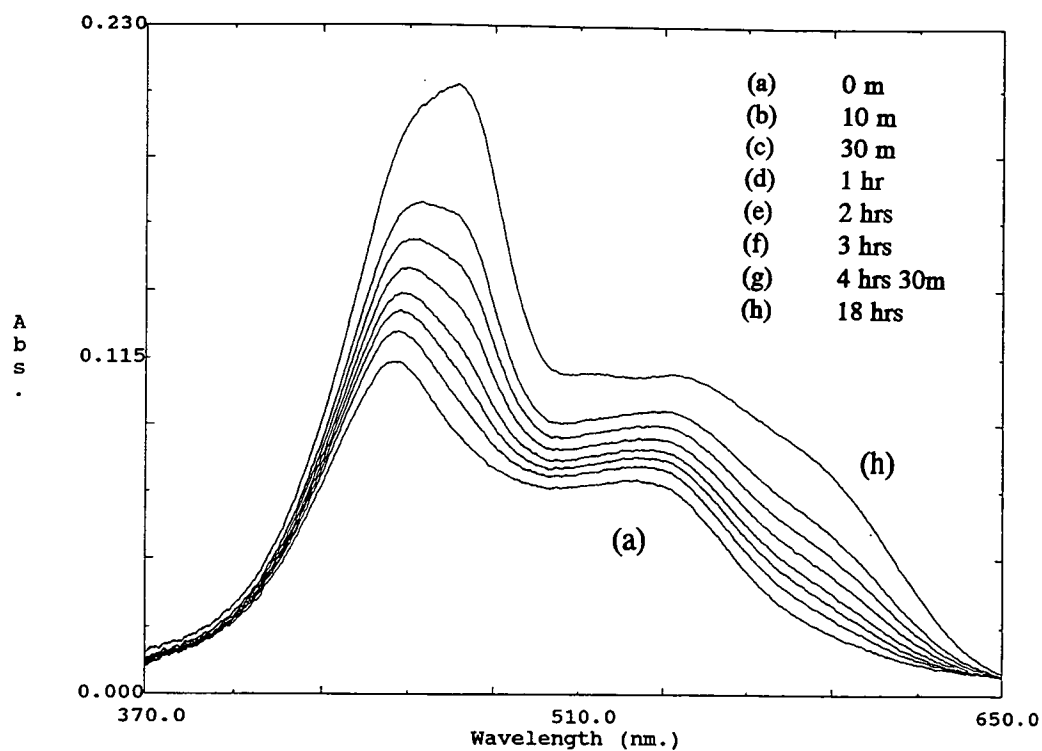
2.3.6 Carbon-Bonded σ -Adduct ?

Reactions mentioned previously in this section have a duration of approximately 40 seconds. U.V./Vis. spectra taken after this time showed a shift in wavelength from λ_{max} values 445, 530nm (σ -adduct 2.1) to λ_{max} values 465, 560nm over a time period of 5 hours. Figure 2.5 shows an example of the alteration in the U.V./Vis. spectrum that occurs. There is a possibility that the change may be due to the N-bonded σ -adduct undergoing an isomeric rearrangement, equation 2.11, to form the C-bonded σ -adduct, 2.4. Previous work has established this type of process in the aniline molecule, chapter 1, section 1.5.1 Aromatic Amines.

Preliminary kinetic studies completed provide no conclusive evidence for the proposed process. Values of k_{slow} were determined at $\lambda = 465\text{nm}$ with varying aniline concentration. A linear dependence is not observed, possibly indicating a complicated kinetic process whose rate limiting step is independent of aniline.

NMR studies have been completed in an attempt to observe the C-bonded σ -adduct. The ¹H NMR spectrum of TNB in *d*₆-DMSO shows a peak at δ/ppm 9.15 (ring hydrogens).

Figure 2.5 U.V./Vis. spectra for the reaction of TNB, 4×10^{-5} mol dm^{-3} , aniline 0.04 mol dm^{-3} , Dabco 0.1 mol dm^{-3} and DabcoH⁺ 0.01 mol dm^{-3} , taken at the time intervals indicated in DMSO at 25°C.

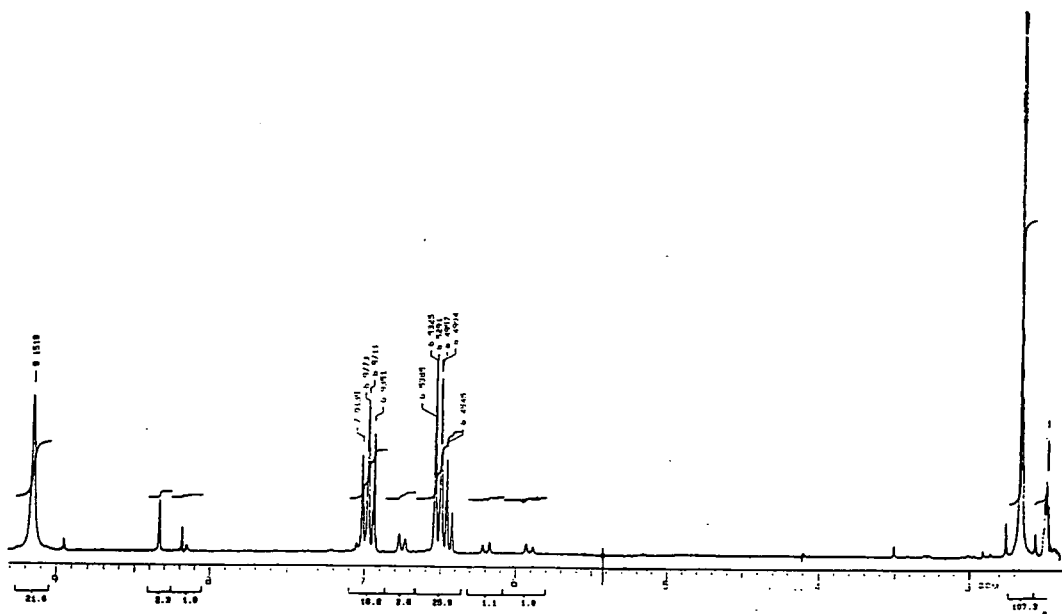


equation 2.11

In the presence of aniline (1 equiv.) and Dabco (1 equiv.) initial peaks are observed due to 2.1 at 8.33 (ring hydrogens) and 6.20 (d, $J = 9\text{Hz}$, sp^3H), figure 2.6. The anilide group of 2.1 shows a doublet at δ/ppm 5.90 (d, $J = 9\text{Hz}$, NH) attributed to the amino hydrogen. Peaks due to the ring hydrogens are covered by the unreacted spin coupled ring hydrogens of aniline at δ/ppm 6.97 (t), 6.50 (d) and 6.45 (t), $J = 8\text{Hz}$. Dabco gives a peak at δ/ppm 2.66 (s). Over a period of 70 hours no change in the ^1H NMR spectrum is noted, figure 2.7. To confirm that the signals in the spectrum were due to the N-bonded σ -adduct, D_2O was added to the sample. A single alteration occurred. The doublet attributed to the amino hydrogen, δ/ppm 5.9, was lost and the doublet at δ/ppm 6.15 collapsed to a singlet. This indicates the presence of the N-bonded σ -adduct only, figure 2.8.

The NMR study indicates that the nitrogen-bonded σ -adduct still predominates after 70 hours. The major difference between the U.V./Vis. and NMR experiments is in the concentrations of reagents. The TNB concentration is *ca.* 10^4 larger in the NMR experiments. It is possible that the changes noted in the U.V./Vis. spectra result from the presence of an impurity, present in only very low concentration.

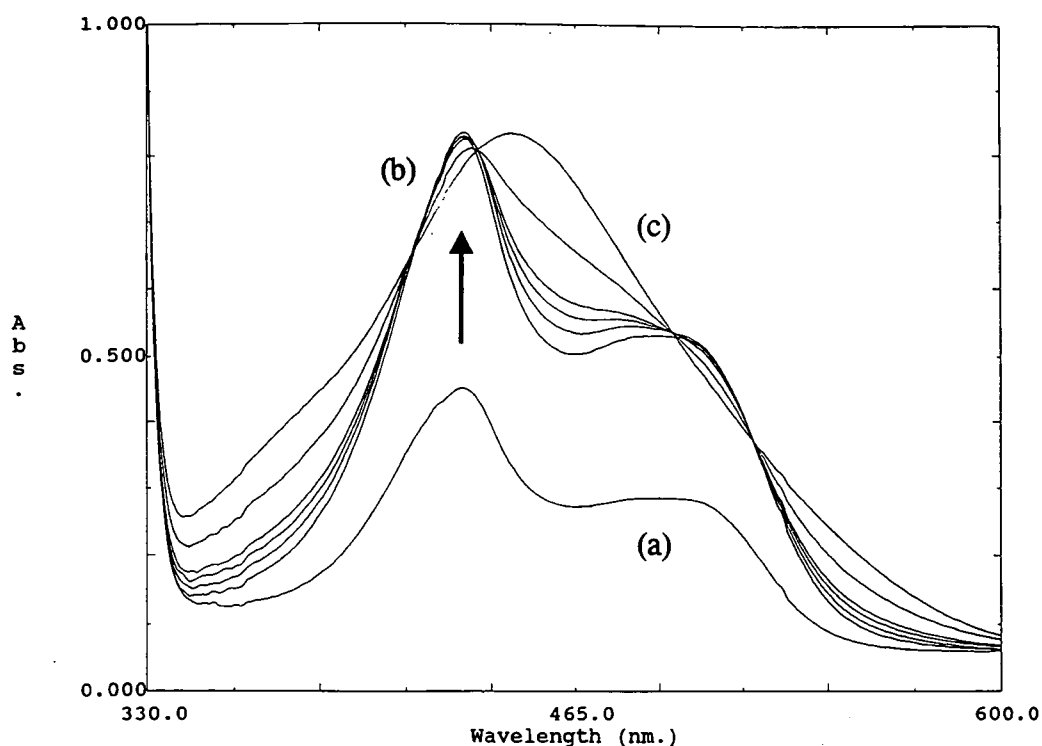
Figure 2.6 ^1H NMR for the reaction of TNB 0.1 mol dm^{-3} , aniline 0.1 mol dm^{-3} and Dabco 0.1 mol dm^{-3} in d_6 -DMSO after 5 mins.

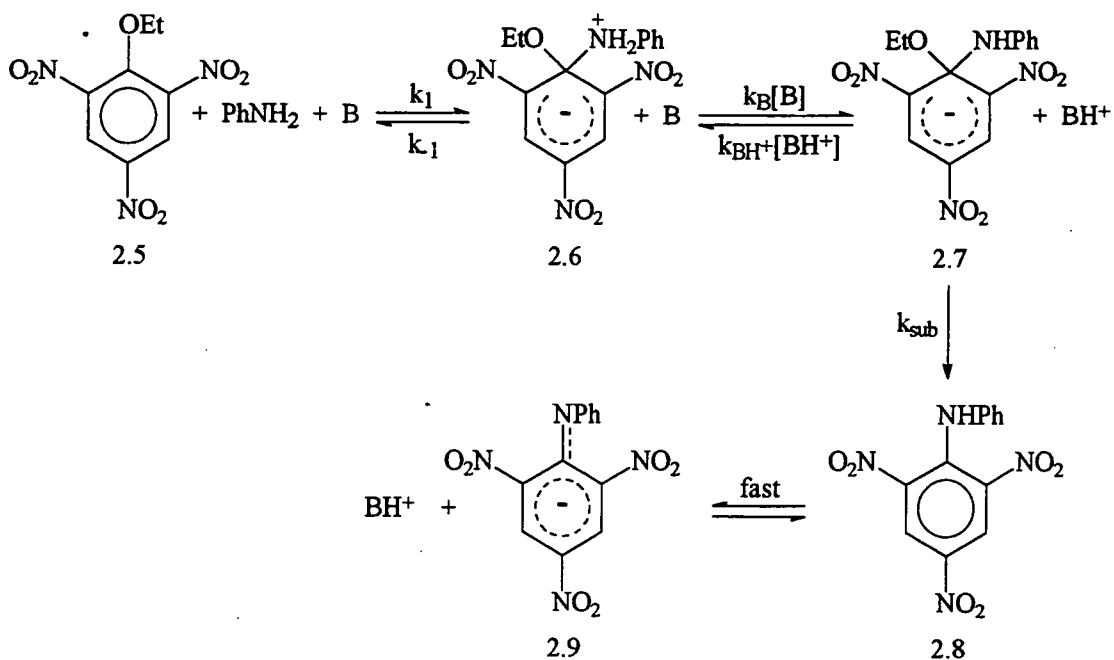


2.4 Reactions of Ethyl 2,4,6-Trinitrophenyl Ether, 2.5.

U.V./Vis. spectra of 2.5 in DMSO containing aniline (0.1 mol dm^{-3}) indicated no reaction during 90 minutes. When the reaction was repeated with the addition of Dabco and Dabco hydrochloride a biphasic reaction was observed. The spectra in figure 2.9 show that in the first stage a species with λ_{max} 430nm and 500nm is produced. The spectrum is typical of that for σ -adducts^{2,3} and ^1H NMR experiments confirm the formation of 2.7, the intermediate on the substitution pathway. A second, much slower reaction, gave a species with λ_{max} 445nm whose spectrum is identical to that of 2,4,6-trinitrodiphenylamine, 2.8, in the reaction medium. Since the pK_a value²² of 2.8 is 8.01, this species will be present largely in its deprotonated form, 2.9. Both spectra can be viewed in figure 2.10. Previous synthesis of 2.8 and the characterisation by both U.V./Vis. and ^1H NMR has confirmed the identification. The kinetic and equilibrium results can be interpreted in terms of scheme 2.1, in which the zwitterion, 2.6, is expected to be an intermediate present in low concentrations

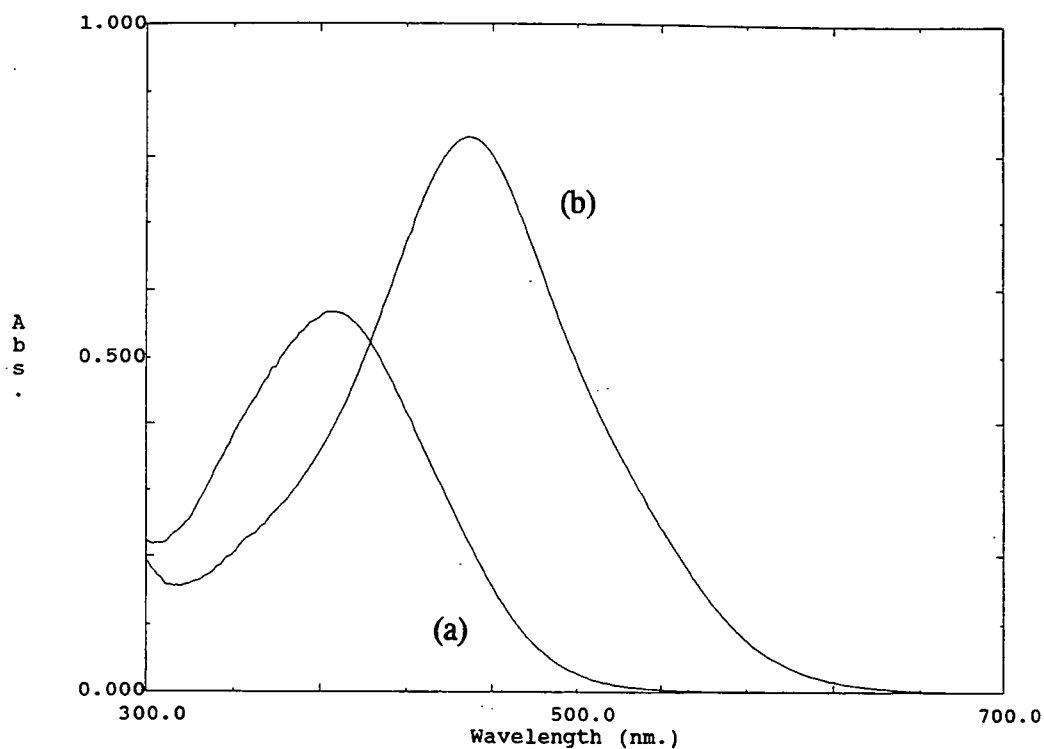
Figure 2.9 U.V./Vis. spectra of 2.5, $4 \times 10^{-5} \text{ mol dm}^{-3}$, in DMSO containing aniline 0.1 mol dm^{-3} , Dabco 0.05 mol dm^{-3} and Dabco hydrochloride 0.01 mol dm^{-3} taken after (a) 1 min, (b) 5 min, and (c) 3 hours.





scheme 2.1

Figure 2.10 U.V./Vis. spectra of (a) 2,4,6-trinitrodiphenylamine, 2.8, 4×10^{-5} mol dm^{-3} and (b) 2,4,6-trinitrodiphenylamine in the presence of excess base, 2.9.



2.4.1 ^1H NMR Studies.

The ^1H NMR. spectrum of 2.5 in d_6 -DMSO shows peaks at δ/ppm 9.09 (ring hydrogens), 4.26 (q, $J = 7\text{Hz}$, OCH_2) and 1.35 (t, CH_3). In the presence of aniline (0.1 mol dm^{-3}) and Dabco (0.1 mol dm^{-3}) peaks are observed due to 2.7 at 8.62 (ring hydrogens), 3.14 (q, $J = 7\text{Hz}$, OCH_2) and 1.08 (t, CH_3), figure 2.11. It is interesting^{4,5} that the anilide group of 2.7 shows a singlet at δ/ppm 5.98 attributed to the amino hydrogen together with spin-coupled, $J = 8\text{Hz}$, peaks due to ring hydrogens at δ/ppm 6.93 (t), 6.52 (t) and 6.35 (d). Over a period of 1 hour the peaks due to 2.7 decrease in intensity while peaks attributable to the substitution products, 2.8 and ethanol, increase in intensity, figure 2.12. A small peak at δ/ppm 8.58 is also observed indicating the formation of some picric acid. The ^1H NMR results support the U.V./Vis. spectra showing no evidence for nucleophilic attack of aniline at the 3-position in 2.5. Measurements with 2.5 (0.1 mol dm^{-3}) in d_6 -DMSO containing aniline (0.2 mol dm^{-3}), Dabco (0.25 mol dm^{-3}) and Dabco deuteriochloride (0.05 mol dm^{-3}) confirmed the previous assignments. At the higher aniline concentration conversion of reactants to products was faster. The buffered system Dabco / DabcoD⁺ suppressed the formation of picric acid.

Figure 2.11 ^1H NMR spectrum for the initial reaction products formed on addition of 2.5 to aniline and Dabco in d_6 -DMSO.

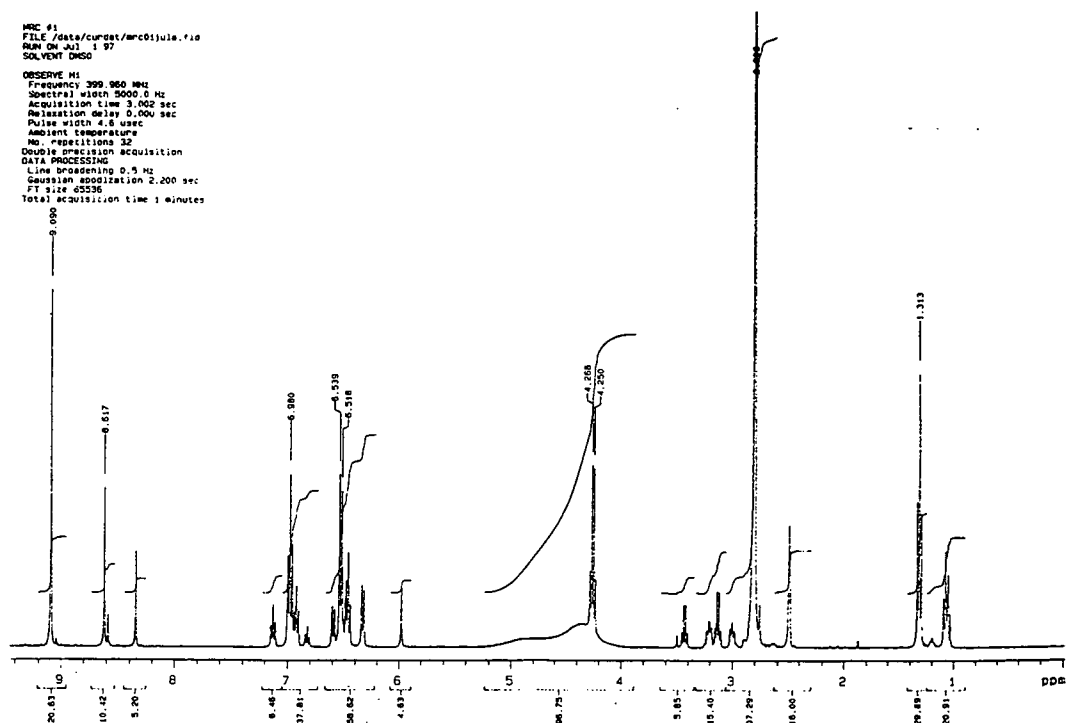


Figure 2.12 ^1H NMR spectrum for the reaction between 2.5, aniline and Dabco after 30 minutes in d_6 -DMSO.

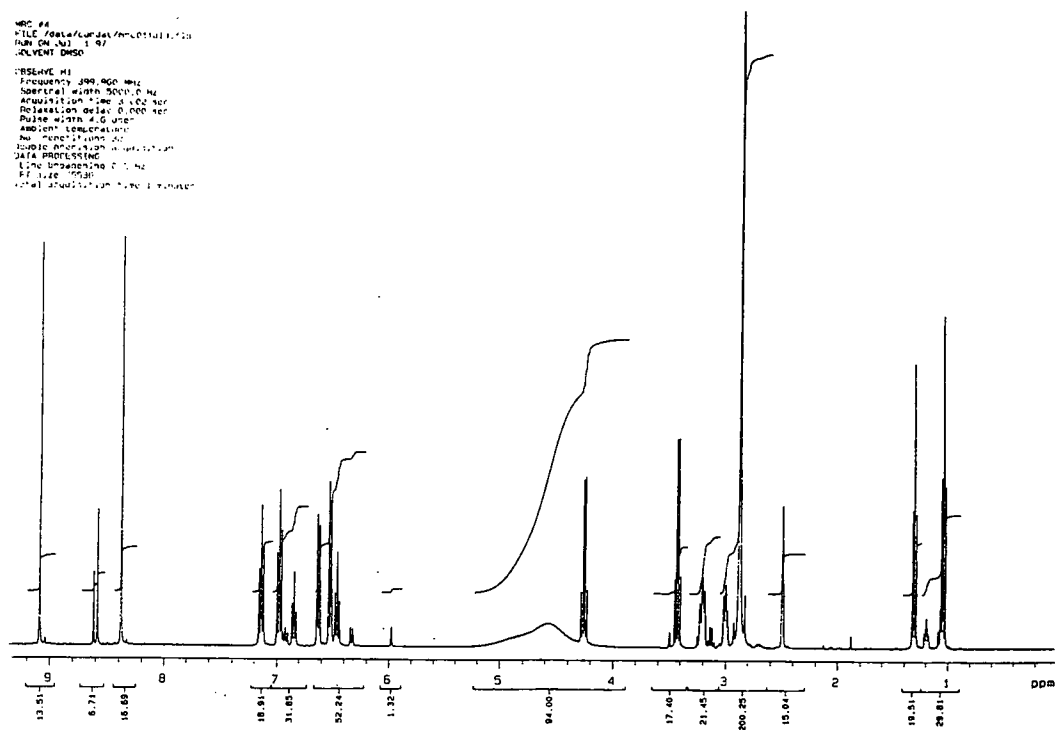


Figure 2.13 ^1H NMR spectrum for the reaction between 2.5, aniline and Dabco after 4 hours in d_6 -DMSO.

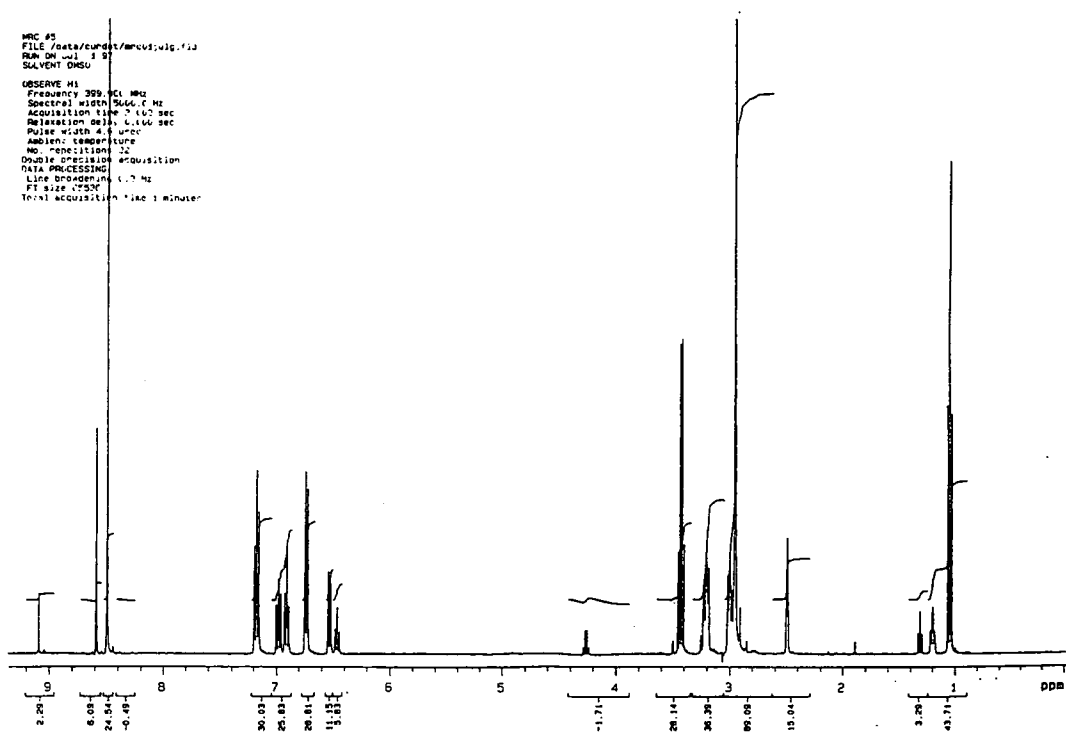
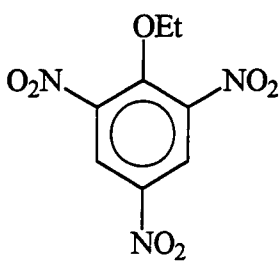
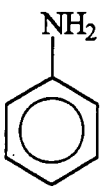
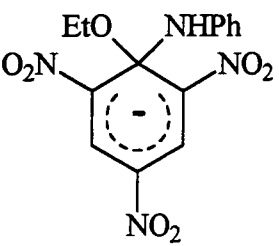
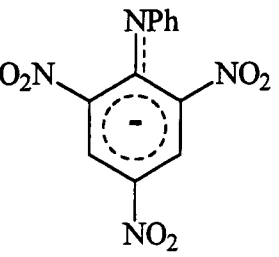


Table 2.5 Detailed summary of all ^1H NMR assignments.

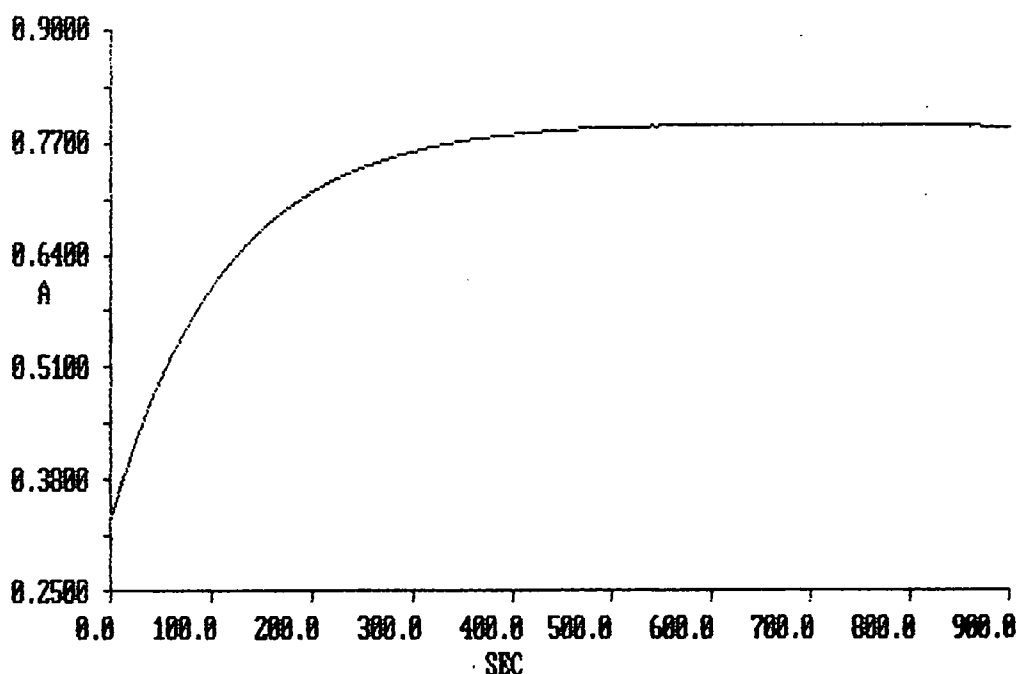
Structure	^1H NMR. signals / ppm in d_6 -DMSO
 <p>2.5</p>	9.09 (s, ring hydrogens) 4.26 (q, $J = 7\text{Hz}$, OCH_2) 1.31 (t, $J = 7\text{Hz}$, CH_3)
 <p>aniline</p>	6.48 (t, $J = 8\text{Hz}$, para CH) 6.55 (d, $J = 8\text{Hz}$, ortho CH) 7.00 (t, $J = 8\text{Hz}$, meta CH)
 <p>2.7</p>	8.62 (s, ring hydrogens) 5.98 (s, NH) 3.14 (q, $J = 7\text{Hz}$, OCH_2) 1.08 (t, $J = 7\text{Hz}$, CH_3) N-phenyl hydrogens, $J = 8\text{Hz}$ 6.93 (t, meta CH) 6.52 (t, para CH) 6.35 (d, ortho CH)
 <p>2.9</p>	8.34 (s, ring hydrogens) N-phenyl hydrogens, $J = 8\text{Hz}$ 7.13 (t, meta CH) 6.82 (t, para CH) 6.58 (d, ortho CH)
Liberated ethanol	3.42 (q, $J = 7\text{Hz}$, OCH_2) 1.05 (t, $J = 7\text{Hz}$, CH_3)

2.4.2 Formation of the σ -Complex, 2.7.

2.4.2.1 Experimental Procedure.

Rates of reaction for the formation of 2.7 were monitored at $\lambda = 430\text{nm}$ using a conventional spectrophotometer with aniline, Dabco and Dabco hydrochloride concentrations in large excess of 2.5. A 5ml solution containing the required concentrations of aniline, Dabco and DabcoH⁺ was prepared in DMSO and thermostatted at 25°C. After addition of 2.5, approximately 2ml of the solution was quickly transferred into a cuvette and placed in the spectrophotometer. As the kinetic trace in figure 2.14 shows, pseudo first order conditions were observed providing first order rate constants, k_{fast} , with excellent correlation coefficients between 0.992 and 0.999.

Figure 2.14 Kinetic trace for the formation of σ -complex 2.7.



U.V./Vis. measurements show that in the presence of Dabco a solution of 2.7 is very slowly converted to picric acid, λ_{max} 380nm. This reaction could be inhibited by the presence of Dabco hydrochloride. The latter observation indicates that picric acid formation is likely to be due to attack of hydroxide, formed from adventitious water in the solvent, equation 2.12, at the 1-position rather than attack by Dabco at the side chain ethyl group.

All quantitative measurements involving aniline were made in buffered solutions, Dabco with Dabco hydrochloride, to suppress picric acid formation.



Measurements were made with two sets of conditions. Firstly the variation with aniline at constant Dabco concentration was examined followed by variation with Dabco at constant aniline concentration. The Dabco hydrochloride concentration was kept constant throughout all the reactions to maintain constant ionic strength.

2.4.2.2 Dependence on Aniline.

Results shown in table 2.6, were obtained at a wavelength $\lambda = 430\text{nm}$ for the reaction of $2.5, 4 \times 10^{-5} \text{ mol dm}^{-3}$, Dabco 0.1 mol dm^{-3} , DabcoH^+ 0.01 mol dm^{-3} , with various concentrations of aniline, $[\text{An}]$, in DMSO at 25°C . Graphically the results are represented in figure 2.15, from which further kinetic information is obtained.

Figure 2.15 Kinetic data for the formation of 2.7 from 2.5, aniline, Dabco and Dabco hydrochloride in DMSO at 25°C .

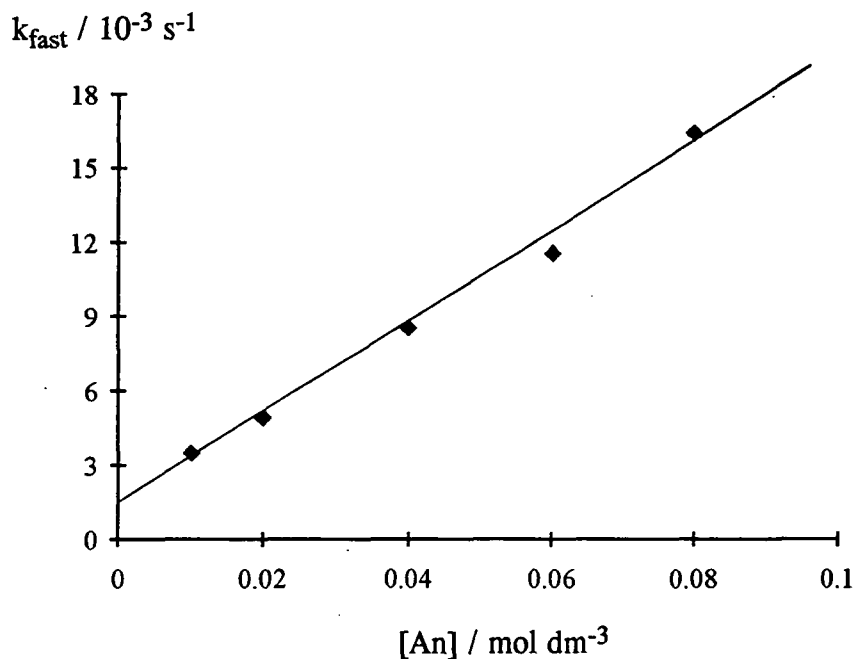


Table 2.6 Kinetic data for the formation of 2.7 from 2.5, aniline, Dabco and Dabco hydrochloride in DMSO at 25°C.

[An] / mol dm ⁻³	0.01	0.02	0.04	0.06	0.08
k _{fast} / 10 ⁻³ s ⁻¹	3.51	4.90	8.55	11.6	16.4

2.4.2.3 Dependence on Dabco.

Under the same experimental conditions Dabco concentration was varied keeping the concentration of 2.5, 4×10^{-5} mol dm⁻³, aniline 0.1 mol dm⁻³, and DabcoH⁺ 0.01 mol dm⁻³, constant in DMSO at 25°C. Results can be viewed in table 2.7 and graphically in figure 2.16.

Figure 2.16 Kinetic data for the formation of 2.7 from 2.5, aniline, Dabco and Dabco hydrochloride in DMSO at 25°C.

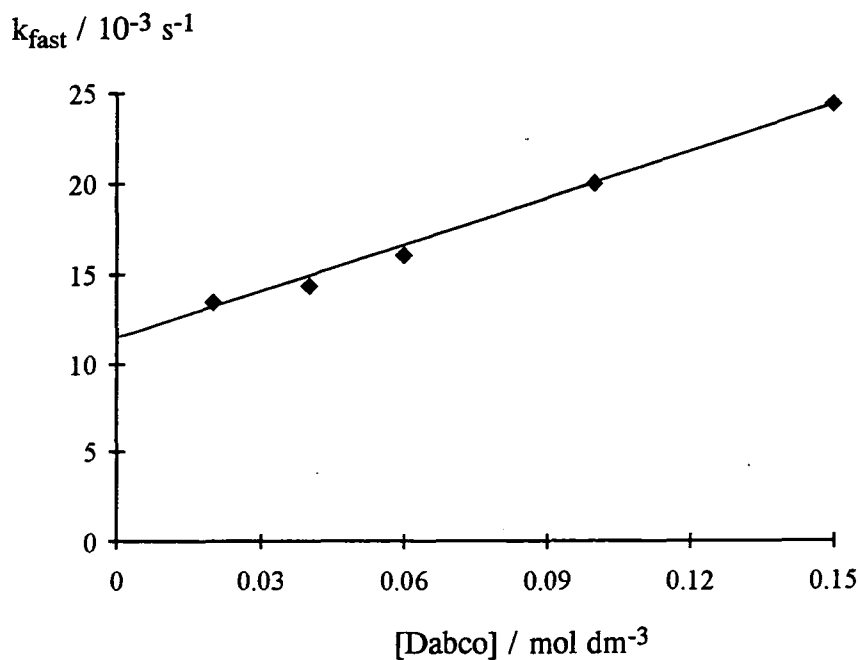


Table 2.7 Kinetic data for the formation of 2.7 from 2.5, aniline, Dabco and Dabco hydrochloride in DMSO at 25°C.

[Dabco] / mol dm ⁻³	0.02	0.04	0.06	0.10	0.15
k _{fast} / 10 ⁻³ s ⁻¹	13.5	14.4	16.1	20.0	24.4

Both sets of kinetic results can be interpreted in terms of scheme 2.1.

2.4.2.4 Determination of the Equilibrium Constant for σ -Adduct, 2.7, Formation using Absorbance Measurements.

Absorbance values, $\lambda = 430\text{nm}$, were taken at the completion of the reactions involving 2.5, $4 \times 10^{-5} \text{ mol dm}^{-3}$ and DabcoH⁺ 0.01 mol dm^{-3} , with varying concentrations of aniline and Dabco, described previously in table 2.6 and 2.7. Equation 2.13 defines an equilibrium constant, K_1K_{Dabco} , for the overall formation of the σ -adduct, 2.7, produced by the reaction of 2.5 with aniline in the presence of the base, Dabco. Application of equation 2.5 shown previously, can yield values of K_1K_{Dabco} and the results are presented in table 2.8.

An absorbance value for the total conversion, A_∞ , of 2.5 was 1.05.



equation 2.13

Table 2.8 Absorbance and equilibrium data for the formation of 2.7 in DMSO containing various concentrations of Dabco at 25°C.

$$I = 0.01 \text{ mol dm}^{-3}.$$

Dabco / mol dm ⁻³	0.02	0.04	0.06	0.10	0.10	0.10	0.10	0.10
[An] / mol dm ⁻³	0.10	0.10	0.10	0.10	0.01	0.02	0.04	0.06
Abs. (λ _{max} 430nm)	0.63	0.79	0.81	0.88	0.43	0.58	0.80	0.88
K ₁ K _{Dabco} / dm ³ mol ⁻¹	7.5	7.6	5.6	5.2 ^a	6.9	6.2	8.0	8.6

^a value of K₁K_{Dabco} not included in average.

An average value of K₁K_{Dabco} = 7.0 ± 1.0 dm³ mol⁻¹ is found.

2.4.2.5 Kinetic Analysis of σ-Adduct Formation.

Similar kinetic derivations can be used to those discussed earlier regarding the reactions of TNB. The equilibrium constant for the formation of 2.7 is defined in terms of the respective rate constants by equation 2.6 shown previously. The absorbance values in table 2.8 lead to a value of K₁K_{Dabco} of 7.0 ± 1.0 dm³ mol⁻¹. Alternatively the equilibrium constant may be defined in terms of the aniline concentration in equation 2.7. Use of equation 2.2 leads to equation 2.8 showing that the value of K₁K_{An} will be many orders of magnitude lower than the value of K₁K_{Dabco}, explaining why adduct formation is not observed in the absence of Dabco.

The variation of k_{fast} with values of the Dabco and aniline concentrations is compatible only with proton transfer being rate determining in the formation of 2.7. Using the condition k₋₁ > k_B[B] and treating 2.6 as a steady state intermediate leads to the rate expression given in equation 2.9. Again k_{Dabco} and k_{An} represent k_B when the reaction involves Dabco and aniline respectively, while k_{DabcoH}⁺ and k_{AnH}⁺ represent k_{BH}⁺ for reactions with the appropriate conjugate acids.

Since $K_{\text{An}} / K_{\text{Dabco}}$ has a constant value, equation 2.8, it is possible to reduce the number of variables in equation 2.9 to give equation 2.10. Excellent agreement between the calculated and the observed values of k_{fast} were obtained with $K_1 k_{\text{Dabco}}$ $1.17 \pm 0.1 \text{ dm}^6 \text{ mol}^{-2} \text{ s}^{-1}$, k_{DabcoH^+} $0.20 \pm 0.05 \text{ dm}^3 \text{ mol}^{-1} \text{ s}^{-1}$ and $k_{\text{An}} / k_{\text{Dabco}}$ 0.46 ± 0.1 , table 2.9. The latter value indicates that aniline competes effectively with the much stronger base Dabco in the proton transfer step, 2.6 \leftrightarrow 2.7. This is discussed later. It was not possible to obtain an acceptable fit between calculated and observed values of k_{fast} with lower values of the ratio $k_{\text{An}} / k_{\text{Dabco}}$. Combination of the values of $K_1 k_{\text{Dabco}}$ and k_{DabcoH^+} leads to a value of $K_1 K_{\text{Dabco}}$ of $5.9 \text{ dm}^3 \text{ mol}^{-1}$ in acceptable agreement with that obtained independently from absorbance measurements at equilibrium.

Table 2.9 Kinetic data for the equilibration of 2.5 and 2.7 in DMSO at 25°C.

[An] / mol dm ⁻³	[Dabco] / mol dm ⁻³	[DabcoH ⁺] / mol dm ⁻³	k_{fast} / 10 ⁻³ s ⁻¹	$k_{\text{calc}}^{\text{a}}$ / 10 ⁻³ s ⁻¹
0.10	0.02	0.01	13.5	14
0.10	0.04	0.01	14.4	14
0.10	0.06	0.01	16.1	16
0.10	0.10	0.01	18.6	20
0.10	0.15	0.01	24.4	24
0.01	0.10	0.01	3.51	3.5
0.02	0.10	0.01	4.90	4.9
0.04	0.10	0.01	8.55	8.5
0.06	0.10	0.01	11.6	12
0.08	0.10	0.01	16.4	16

^a Calculated from equation 2.10 with $K_1 k_{\text{Dabco}}$ $1.17 \pm 0.1 \text{ dm}^6 \text{ mol}^{-2} \text{ s}^{-1}$, k_{DabcoH^+} $0.20 \pm 0.05 \text{ dm}^3 \text{ mol}^{-1} \text{ s}^{-1}$ and $k_{\text{An}} / k_{\text{Dabco}}$ 0.46 ± 0.1 ,

2.4.3 Formation of the Substituted Product, 2.8.

The slow product forming reaction was measured at 445nm, corresponding to the deprotonated form, 2.9, of 2,4,6-trinitrodiphenylamine, figure 2.10. With concentrations of aniline, Dabco and Dabco hydrochloride in large excess of the concentration of 2.5, first order kinetics were observed. Dependencies of the first order rate constants, k_{slow} , with respect to aniline, Dabco and Dabco hydrochloride concentrations are reported in table 2.10.

2.4.3.1 Kinetic Analysis.

Making the assumption that during this stage of the reaction 2.6 and 2.7 are in rapid equilibrium leads to the rate expression of equation 2.14. Here $k_{\text{sub,DabcoH}^+}$ and $k_{\text{sub,AnH}^+}$ are respectively the rate constants for the substitution reactions involving protonated Dabco and aniline. Use of equation 2.2 results in equation 2.15. Analysis of the results using the known value for K_1K_{Dabco} of $7 \text{ dm}^3 \text{ mol}^{-1}$ shows that most of the reaction flux involves the protonated Dabco. Agreement between observed and calculated values of k_{slow} were optimised with values of $k_{\text{sub,DabcoH}^+}$ $0.06 \pm 0.01 \text{ dm}^3 \text{ mol}^{-1} \text{ s}^{-1}$ and $k_{\text{sub,AnH}^+} \cdot K_a'$ $0.005 \pm 0.002 \text{ dm}^3 \text{ mol}^{-1} \text{ s}^{-1}$. Using the known value of K_a' leads to a value for $k_{\text{sub,AnH}^+}$ of $860 \text{ dm}^3 \text{ mol}^{-1} \text{ s}^{-1}$.

$$k_{\text{slow}} = \left(k_{\text{sub,DabcoH}^+} [\text{DabcoH}^+] + k_{\text{sub,AnH}^+} [\text{AnH}^+] \right) \left(\frac{K_1 K_{\text{Dabco}} [\text{Dabco}] [\text{An}]}{K_1 K_{\text{Dabco}} [\text{Dabco}] [\text{An}] + [\text{DabcoH}^+]} \right) \quad \text{equation 2.14}$$

$$k_{\text{slow}} = \left(k_{\text{sub,DabcoH}^+} + k_{\text{sub,AnH}^+} \cdot K_a' \cdot \frac{[\text{An}]}{[\text{Dabco}]} \right) \left(\frac{K_1 K_{\text{Dabco}} [\text{Dabco}] [\text{An}] [\text{DabcoH}^+]}{K_1 K_{\text{Dabco}} [\text{Dabco}] [\text{An}] + [\text{DabcoH}^+]} \right) \quad \text{equation 2.15}$$

Table 2.10 Kinetic data for the formation of product 2.9 in DMSO at 25°C.

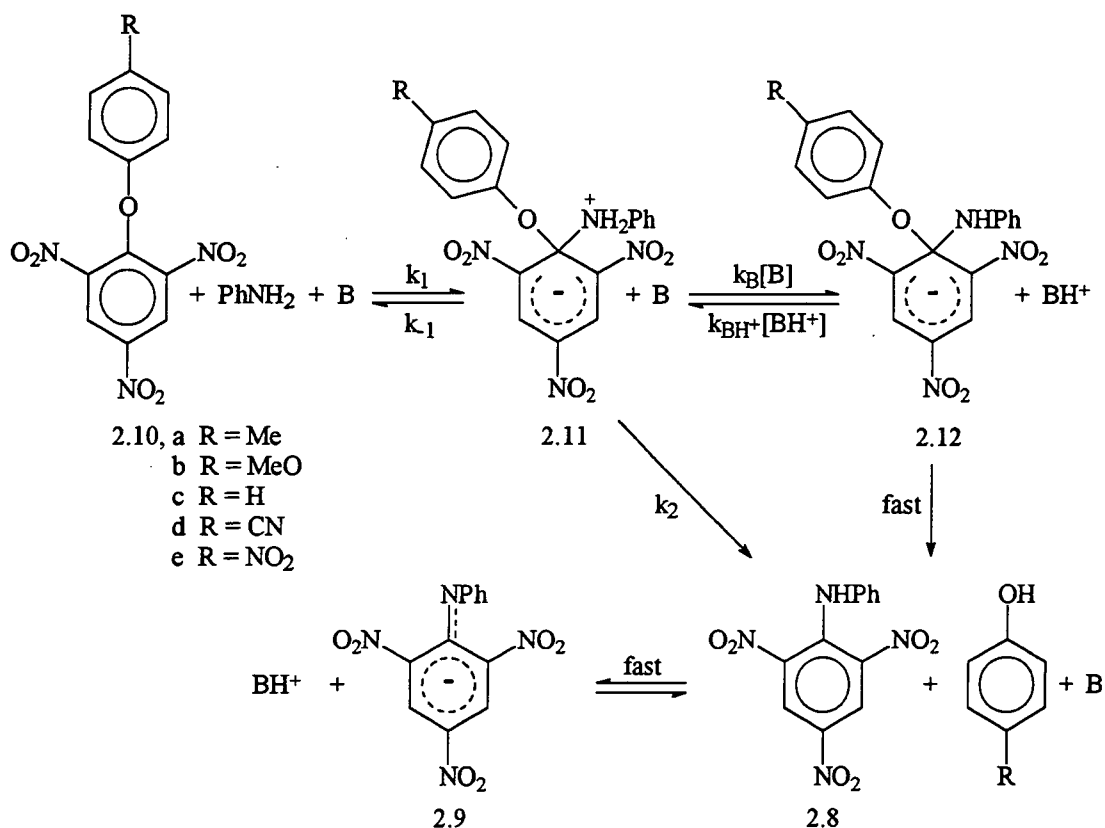
[An] / mol dm ⁻³	[Dabco] / mol dm ⁻³	[DabcoH ⁺] ^a / mol dm ⁻³	k _{slow} / 10 ⁻⁴ s ⁻¹	k _{calc} ^b / 10 ⁻⁴ s ⁻¹
0.10	0.02	0.01	3.40	3.5
0.10	0.04	0.01	4.26	4.5
0.10	0.06	0.01	5.06	5.1
0.10	0.10	0.01	5.45	5.7
0.10	0.15	0.01	5.93	6.1
0.01	0.10	0.01	4.70	4.5
0.02	0.10	0.01	5.18	5.0
0.04	0.10	0.01	5.50	5.3
0.06	0.10	0.01	5.58	5.5
0.08	0.10	0.01	5.77	5.6
0.05	0.05	0.003 ^a	1.82	1.7
0.05	0.05	0.005 ^a	2.60	2.5
0.05	0.05	0.007 ^a	3.40	3.3
0.05	0.05	0.010	4.30	4.1

^a Ionic strength maintained at 0.01 mol dm⁻³ using t-butylammonium chloride.

^b Calculated from equation 2.15 with $k_{\text{sub,DabcoH}^+} = 0.060 \text{ dm}^3 \text{ mol}^{-1} \text{ s}^{-1}$, $k_{\text{sub,AnH}^+} \cdot K_a' = 0.005 \text{ dm}^3 \text{ mol}^{-1} \text{ s}^{-1}$ and $K_1 K_{\text{Dabco}} = 7.0 \text{ dm}^3 \text{ mol}^{-1}$.

2.5 Reactions of Phenyl 2,4,6-Trinitrophenyl Ethers, 2.10.

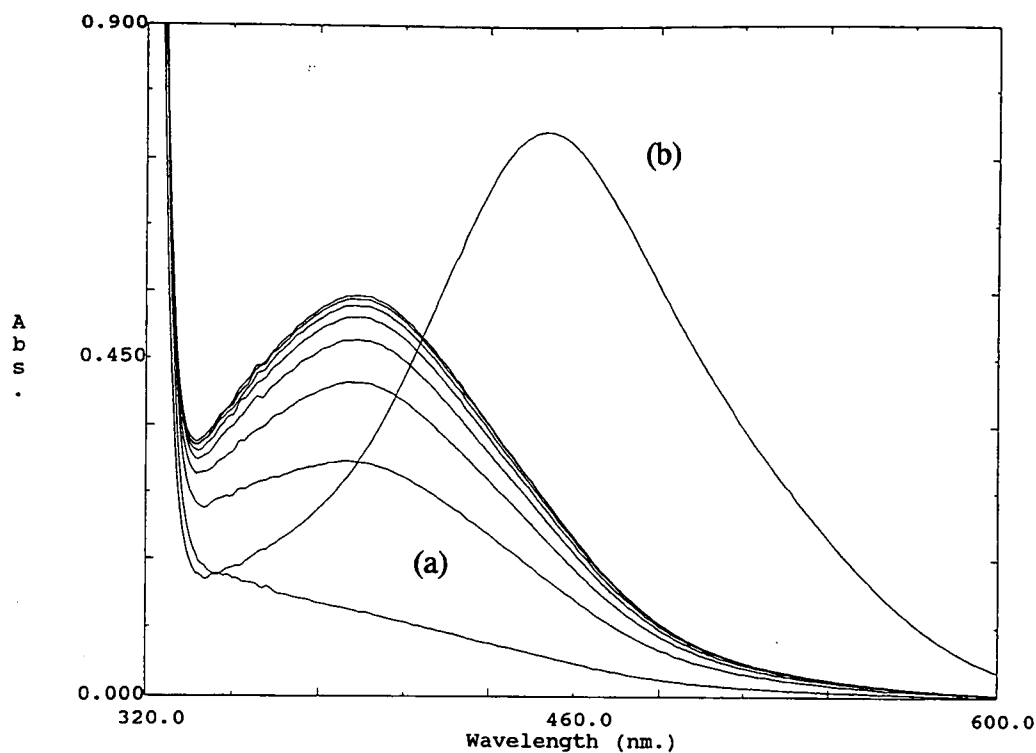
Reactions of 2.10a-e with aniline in DMSO proceeded without the observation of an intermediate. U.V./Vis. spectra, figure 2.17, and ^1H NMR spectra (in more concentrated solutions), at completion of the reactions were identical to that of 2.8, the expected substitution product, in the reaction medium. It is known^{17,23} that phenoxide is a considerably better leaving group than ethoxide, by a factor of *ca.* 10^6 . The failure to observe 2.12, the intermediate on the substitution pathway, may be attributed to its rapid decomposition by loss of phenoxide, scheme 2.2.



scheme 2.2

Kinetic measurements were made with aniline alone, unlike 2.2 and 2.5, and with solutions containing aniline, Dabco and Dabco hydrochloride at 25°C in DMSO. With these concentrations in large excess of the substrate concentration, 4×10^{-5} mol dm⁻³, first order kinetics were observed.

Figure 2.17 U.V./Vis. spectra (a) taken every 10 minutes for the reaction of 2.10a and aniline, (b) after addition of Dabco, 0.1 mol dm⁻³.



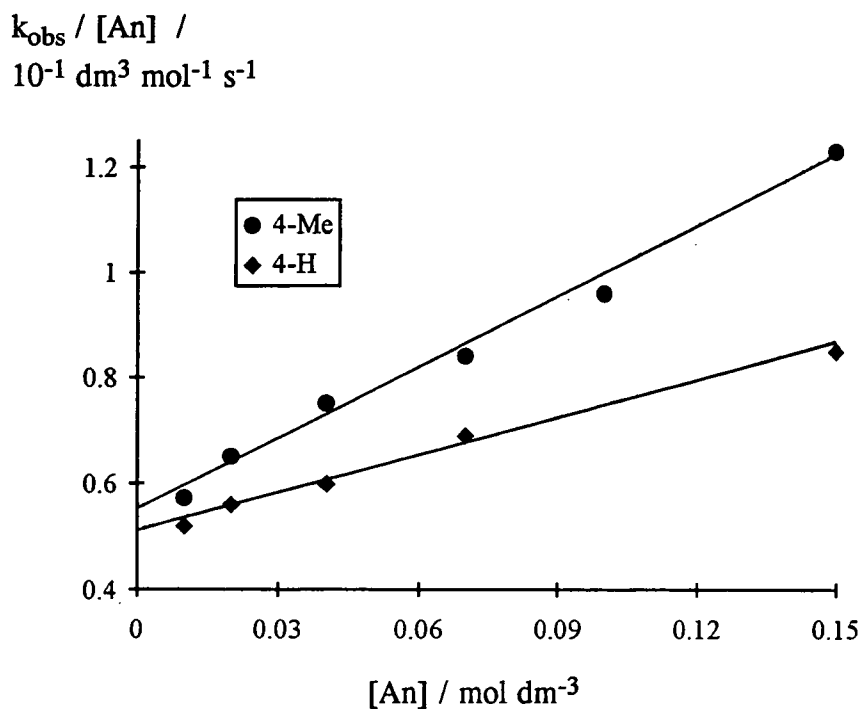
2.5.1 Reactions of 2.10a-e with Aniline.

Rates of reaction for the formation of 2.8 were monitored at $\lambda = 380\text{nm}$ using the same experimental technique and equipment as described in section 2.4.2.1. Data obtained with aniline alone are summarised in table 2.11. Plots of the second order rate constant, $k_{\text{obs}} / [\text{An}]$, versus aniline concentration were linear with positive intercepts. Figure 2.18 shows examples for 2.10a and 2.10c.

Table 2.11 Kinetic data for the formation of 2.8 from 2.10a-e with aniline in DMSO at 25°C.

[An] / mol dm ⁻³	$k_{\text{obs}} / [\text{An}] \text{ } 10^{-1} \text{ dm}^3 \text{ mol}^{-1} \text{ s}^{-1}$				
	R= Me	R= MeO	R= H	R= CN	R= NO ₂
0.01	0.57		0.52	2.2	-
0.02	0.65		0.56		-
0.03	-		-	2.3	-
0.04	-	1.0	0.60		-
0.05	-		-	2.5	-
0.06	-		-		3.6
0.07	0.84		0.69	2.4	-
0.08	-		-		3.6
0.10	0.96	1.2	-		3.7
0.15	1.23	1.3	0.85		4.1
0.20	-		-		4.5

Figure 2.18 Kinetic data for the formation of 2.8 from 2.10a and 2.10c with aniline in DMSO at 25°C.



2.5.2 Reactions of 2.10a-e with Aniline and Dabco.

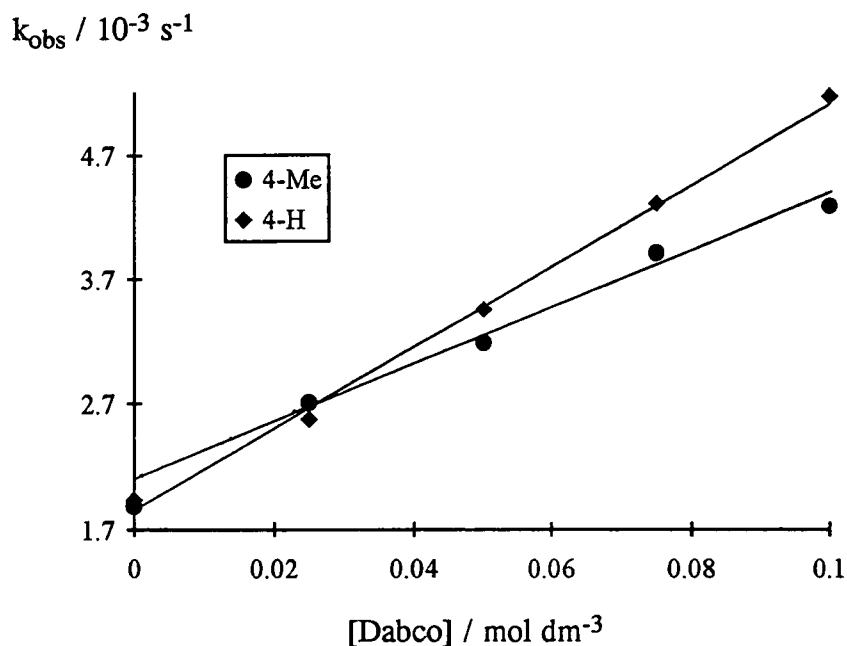
Rates of reaction for the formation of 2.9 were monitored at $\lambda = 450\text{nm}$ using the same experimental technique and equipment as described in section 2.4.2.1. Data obtained with aniline, Dabco and Dabco hydrochloride are summarised in table 2.12. At a constant aniline concentration, values of the first order rate constant, k_{obs} , increased linearly with Dabco concentration, as shown in figure 2.19.

Table 2.12 Kinetic data for the formation of 2.9 from 2.10 a-e, aniline 0.02 mol dm^{-3} , DabcoH^+ 0.05 mol dm^{-3} and various Dabco concentrations in DMSO at 25°C .

[Dabco] / mol dm^{-3}	$k_{\text{obs}} / 10^{-3} \text{ s}^{-1}$				
	R= Me	R= MeO	R= H	R= CN*	R= NO ₂
0	1.89	3.2	1.94	9.40	-
0.025	2.75	3.75	2.58	10.7	11.9
0.050	3.18	3.85	3.45	11.7	12.4
0.075	3.91	4.45	4.31	12.2	12.9
0.100	4.29	5.13	5.18	13.2	13.3

* Reactions performed with 0.03 mol dm^{-3} aniline.

Figure 2.19 Kinetic data for the formation of 2.9 from 2.10a and 2.10c with aniline, Dabco and DabcoH^+ in DMSO at 25°C .



2.5.3 Kinetic Analysis.

The information collected is interpreted in terms of the process shown in scheme 2.2. The assumption that 2.11 may be treated as a steady-state intermediate leads to the rate expression of equation 2.16, where k_{An} and k_{Dabco} represent k_B for the respected bases and k_2 represents uncatalysed intramolecular proton transfer. Ring substituents are expected to have a large influence on the value of k_2 . If the phenoxide ring contains electron withdrawing substituents, k_2 is likely to be more prominent. The results, which provide evidence for base catalysis, indicate that the condition $k_{-1} \gg k_2 + k_{An}[An] + k_{Dabco}[Dabco]$ applies so that equation 2.16 reduces to equation 2.17. Loss of the substituted phenoxide group from the σ -adduct 2.12 is believed to be rapid and not rate limiting. Values obtained for K_1k_2 , K_1k_{An} and K_1k_{Dabco} are summarised in table 2.13.

$$k_{obs} = \frac{k_1[An](k_2 + k_{An}[An] + k_{Dabco}[Dabco])}{k_{-1} + k_2 + k_{An}[An] + k_{Dabco}[Dabco]} \quad \text{equation 2.16}$$

$$k_{obs} = K_1[An](k_2 + k_{An}[An] + k_{Dabco}[Dabco]) \quad \text{equation 2.17}$$

Table 2.13 Summary of results for 2.10a-e.

Reactant	$K_1k_{An} /$ $dm^6 mol^{-2} s^{-1}$	$K_1k_{Dabco} /$ $dm^6 mol^{-2} s^{-1}$	$K_1k_2 /$ $dm^3 mol^{-1} s^{-1}$
2.10a	0.42	1.2	0.055
2.10b	0.27	1.0	0.090
2.10c	0.27	1.6	0.050
2.10d	0.35	1.3	0.220
2.10e	0.65	0.9	0.320

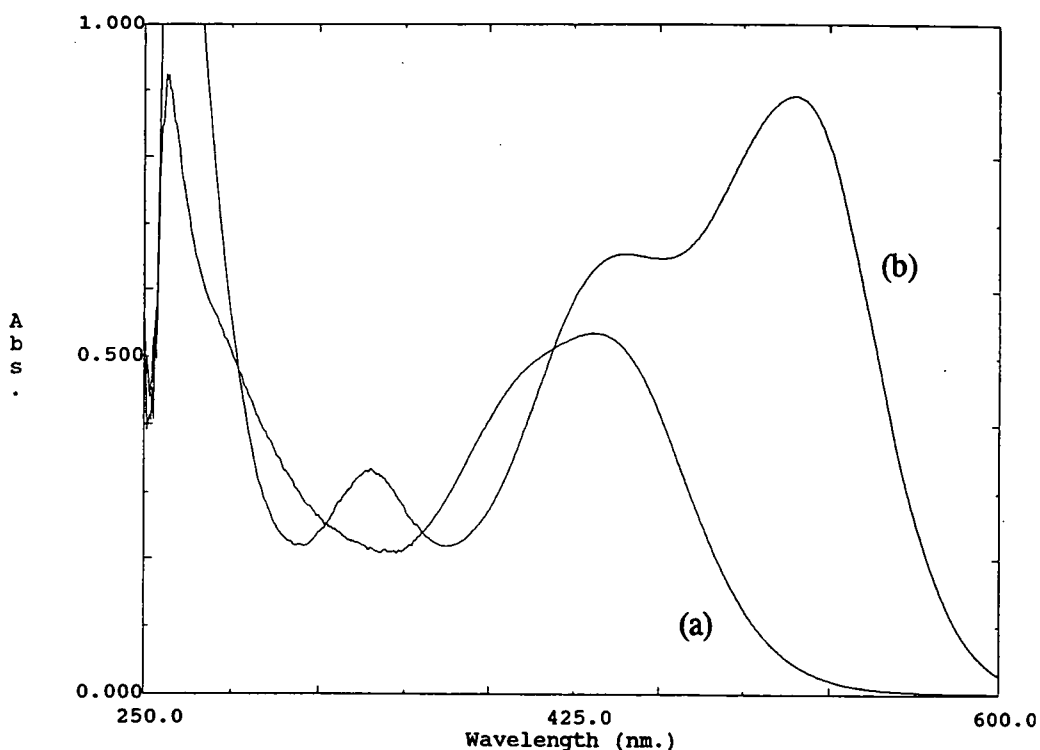
2.5.4 Interaction of 2.10 and Dabco.

It was noticed that 2.10 in the presence of Dabco would gradually form a species with λ_{max} 395nm. The cause could not be determined and 1H NMR studies were inconclusive. Rate constants of formation in the region of $10^{-5} s^{-1}$ were obtained which are significantly slower than that of the main aniline / Dabco reaction to be studied.

2.6 Reactions of Phenyl 2,4-Dinitronaphthyl Ether, 2.13.

U.V./Vis. and ^1H NMR studies showed that in the presence of aniline or aniline with Dabco, 2.13 (λ_{max} 290nm and 360nm) was smoothly converted into N-phenyl-2,4-dinitronaphthalene, 2.14, figure 2.20. Previous synthesis of 2.14 and characterisation by both U.V./Vis. and ^1H NMR had been carried out.

Figure 2.20 U.V./Vis. spectra of (a) 2.14, 4×10^{-5} mol dm^{-3} , (b) 2.14 in the presence of excess base.



2.6.1 Dependence on Aniline and Dabco Concentration.

Figure 2.21 shows the formation of 2.14 in the presence of aniline. Conditions resembling those discussed previously in section 2.4.2 were maintained. Kinetic measurements at 440nm showed a single first order process. Values of the rate constant, k_{obs} , are shown in table 2.14.

Data are interpreted in a manner similar to that described for 2.10, so that scheme 2.2 is applicable and equation 2.17 applies. Values calculated with K_1k_2 2.10×10^{-4} $\text{dm}^3 \text{mol}^{-1} \text{s}^{-1}$, K_1k_{An} 1.1×10^{-2} $\text{dm}^6 \text{mol}^{-2} \text{s}^{-1}$ and K_1k_{Dabco} 0.24 $\text{dm}^6 \text{mol}^{-2} \text{s}^{-1}$ give excellent agreement with values of k_{obs} .

Figure 2.21 Formation of the substituted product, 2.14.

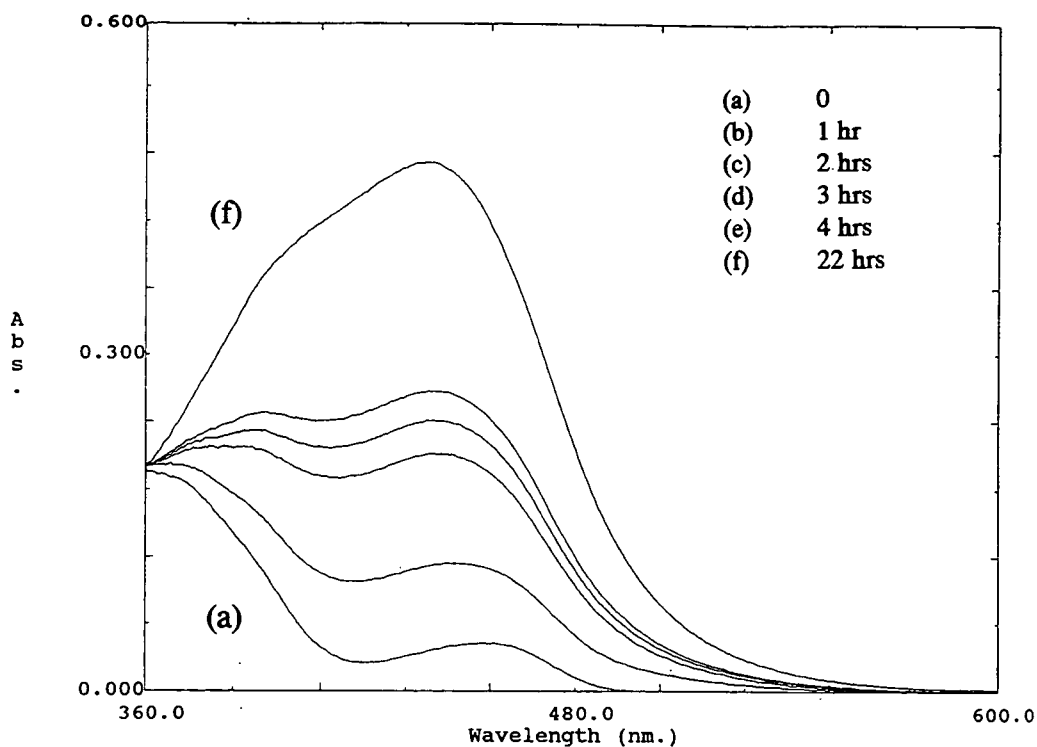


Table 2.14 Kinetic results for reaction of phenyl 2,4-dinitronaphthyl ether with aniline in DMSO at 25°C.

[An] / mol dm ⁻³	[Dabco] / mol dm ⁻³	k _{obs} / 10 ⁻⁵ s ⁻¹	k _{calc} ^a / 10 ⁻⁵ s ⁻¹
0.02	-	0.84	0.84
0.04	-	2.5	2.6
0.07	-	6.7	6.8
0.10	-	14	13
0.15	-	29	28
0.20	-	50	48
0.11	0.01	44	42
0.11	0.02	71	68
0.11	0.03	92	95
0.11	0.05	150	150
0.11	0.10	280	280

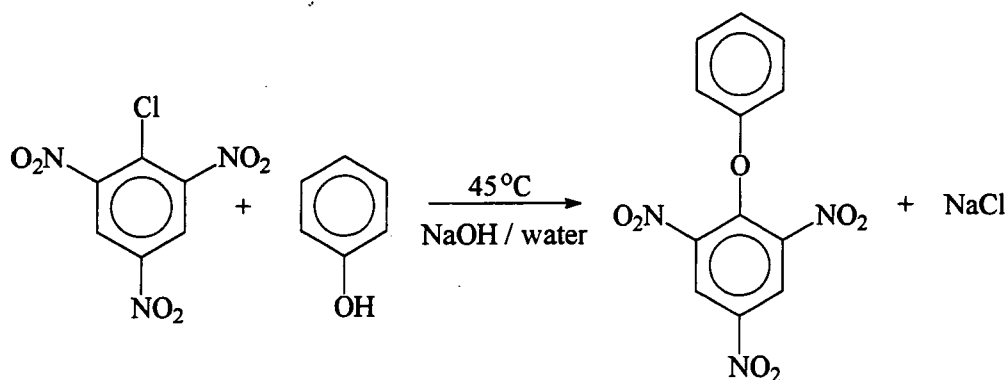
^a Calculated from equation 2.17 with K_1k_2 2.10×10^{-4} dm³ mol⁻¹ s⁻¹, K_1k_{An} 1.1×10^{-2} dm⁶ mol⁻² s⁻¹ and K_1k_{Dabco} 0.24 dm⁶ mol⁻² s⁻¹

2.7 Synthesis of Substrates.

Ethyl 2,4,6-trinitrophenyl ether,¹⁶ 2.5, phenyl 2,4,6-trinitrophenyl ether,¹⁷ 2.10c, and phenyl 2,4-dinitronaphthyl ether,¹⁷ 2.13, were available from previous work. The method used for the preparation of the 4-substituted phenyl 2,4,6-trinitrophenyl ethers 2.10a, b, d, e is discussed below in section 2.7.1. Synthesis of 2,4,6-trinitrodiphenylamine, 2.8, and N-phenyl-2,4-dinitronaphthylamine were available from previous work,²² chapter 3 pg. 111.

2.7.1 Preparation of the 4-Substituted Phenyl 2,4,6-Trinitrophenyl Ethers.

4-Substituted phenyl 2,4,6-trinitrophenyl ethers were prepared by the reaction of picryl chloride with the appropriate phenolate as shown in equation 2.18. The relevant phenol (0.013mol equiv) with sodium hydroxide (0.01mol, 0.4g) in water (15 ml) was stirred continuously for 15 minutes to give a colourless solution, after which picryl chloride (0.008mol, 2g) was added gradually over a 30 minute period. The solution was stirred and heated to a temperature of 45°C for 5 hours for all phenol derivatives and 8 hours for the less reactive 4-nitro and 4-cyano-phenols. Afterwards the solution was allowed to cool and a further 30 ml of water added. This dissolved any remaining sodium chloride or picric acid impurities. The precipitate produced was separated by filtration, washed with a small amount of ethanol and then dried *in vacuo* to produce a yellow powder. Depending on any other impurities still remaining, e.g. picryl chloride, a recrystallisation in ethanol is required.



equation 2.18

2.7.2 NMR Data and Melting Points of the Substrates Synthesised.

The melting points obtained are summarised in table 2.15 below.

Table 2.15 Melting point data for reactants.

Reactant	m.p. (T/°C)	Literature m.p. (T/°C)
2.10a	100	103 ²⁴
2.10b	148	145 ²⁴
2.10d	182	-
2.10e	163	157 ²⁵

¹H NMR data is summarised in table 2.16.

Table 2.16 ¹H NMR information for 2.10a-e in *d*₆-DMSO, 200MHz.

Substrate	¹ H NMR signals δ_{H} / ppm in <i>d</i> ₆ -DMSO.
2.10a	2.27 (3H, s, methyl) 6.93 (2H, d, J = 8.5Hz) and 7.17 (2H, d, J = 8.4Hz, phenyl ring). 9.22 (2H, s, nitro phenyl ring)
2.10b	3.73 (3H, s, methyl) 6.95 (4H, m, phenyl ring). 9.21 (2H, s, nitro phenyl ring)
2.10c	7.07 (2H, d, J = 7.7Hz), 7.18 (1H, t, J = 7.2Hz) and 7.38 (2H, t, J = 7.3Hz, phenyl ring). 9.25 (2H, s, nitro phenyl ring),
2.10d	7.30 (2H, d, J = 8.5Hz) and 7.92 (2H, d, J = 8.5Hz) phenyl ring. 9.30 (2H, s, nitro phenyl ring)
2.10e	7.35 (2H, d, J = 9.1Hz) and 8.30 (2H, d, J = 8.9Hz) phenyl ring. 9.32 (2H, s, nitro phenyl ring)

Examples of ^1H NMR spectra obtained are shown in figures 2.22 and 2.23. The bands at $\delta_{\text{H}}/\text{ppm}$ 2.49 and 3 - 4.5 are due to the solvent and adventitious water respectively. Impurity signals occur at $\delta_{\text{H}}/\text{ppm}$ 9.25 (picryl chloride) and 8.6 (picric acid).

Figure 2.22 ^1H NMR spectrum of 2.10a in d_6 -DMSO (200MHz).

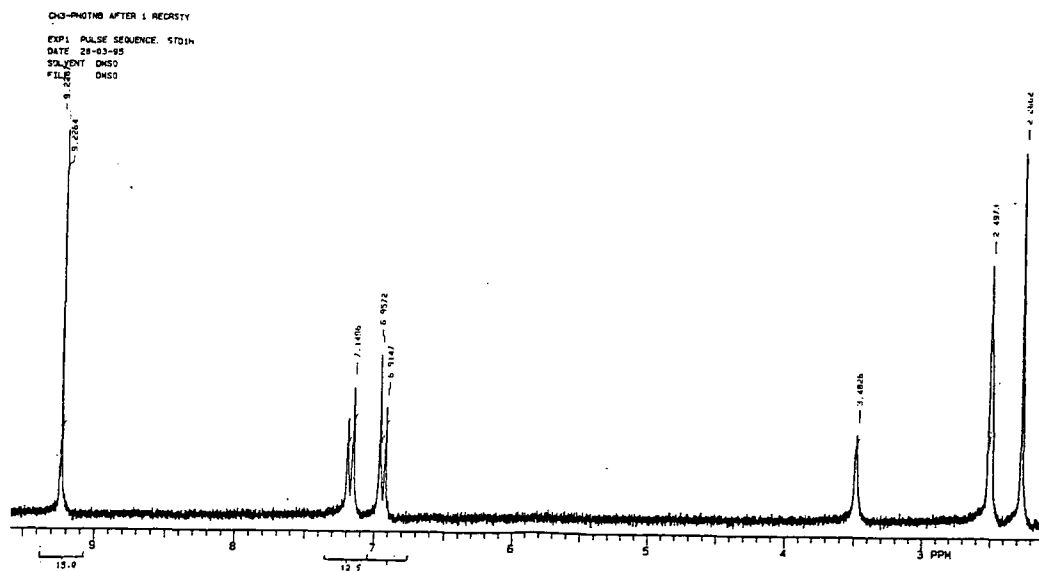
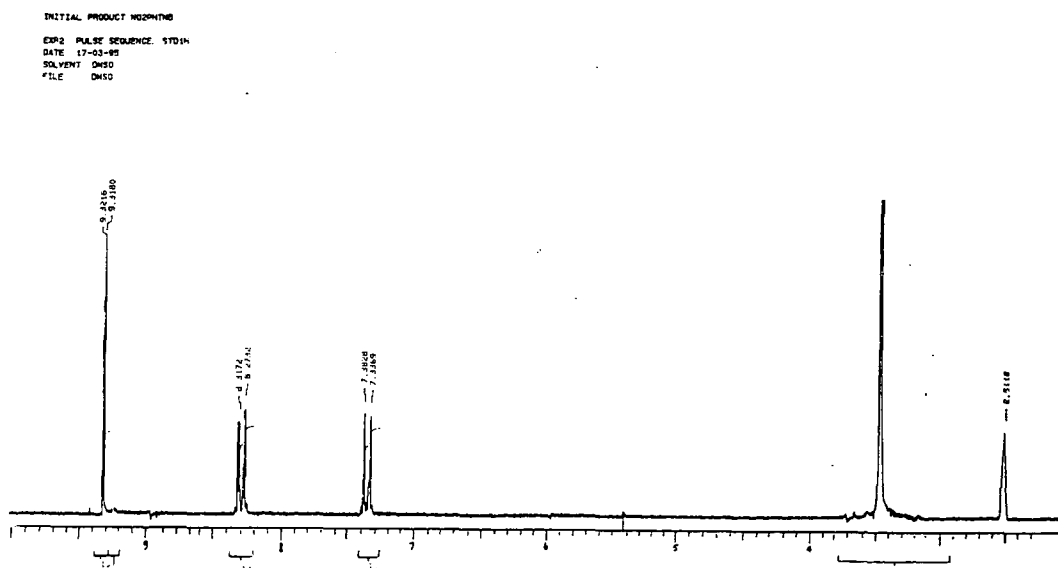


Figure 2.23 ^1H NMR spectrum of 2.10e in d_6 -DMSO (200MHz).



2.8 Discussion and Comparisons.

Data for reactions of 2.5, 2.10 and 2.13 are collected in table 2.17, where they are compared with values for the formation of 2.1 from TNB.

2.8.1 Reactions of 1,3,5-Trinitrobenzene, 2.2.

The results obtained for reaction with TNB are similar to those obtained by Buncel and Eggimann,¹² and again indicate that proton transfer is rate limiting. As discussed in section 2.8.2 the proton transfer from zwitterion to base is likely to be thermodynamically favoured, both when the transfer is to Dabco and to aniline. The present results differ from those of Buncel and Eggimann in that proton transfer to aniline has been detected. Nevertheless the $k_{\text{An}} / k_{\text{Dabco}}$ ratio of 0.015 indicates that Dabco is much more effective than aniline when the substrate is TNB. This may be a steric factor in that Dabco can approach the reaction centre more easily than aniline.

The $k_{\text{An}} / k_{\text{Dabco}}$ ratio of 0.46 observed with the ethyl ether, 2.5, is considerably higher. It is possible here that hydrogen bonding between the oxygen of the alkoxy group and anilino-hydrogen, as shown in 2.16, may facilitate proton transfer. Such hydrogen-bonding is not possible when the reaction involves TNB as indicated in 2.15.

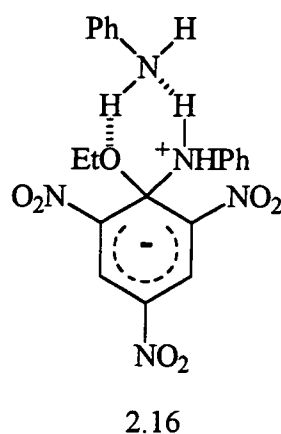
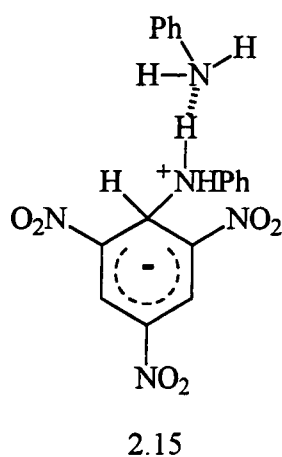


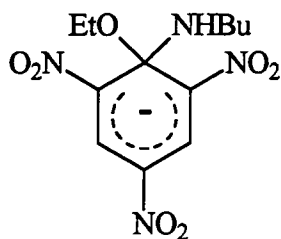
Table 2.17 Comparison of Data in DMSO at 25°C.

Reactant	$K_1 k_{An} /$ $\text{dm}^6 \text{ mol}^{-2} \text{ s}^{-1}$	$K_1 k_{Dabco} /$ $\text{dm}^6 \text{ mol}^{-2} \text{ s}^{-1}$	$K_1 k_2 /$ $\text{dm}^3 \text{ mol}^{-1} \text{ s}^{-1}$	$k_{Dabco} H^+ /$ $\text{dm}^3 \text{ mol}^{-1} \text{ s}^{-1}$	$K_1 K_{Dabco} /$ $\text{dm}^3 \text{ mol}^{-1}$	k_{An} / k_{Dabco}	k_{An} / k_2 $\text{dm}^3 \text{ mol}^{-1}$
2.2	0.68	45	-	56	0.77	0.015	-
2.2 ^a	-	26	-	74	0.35	-	-
2.5	0.54	1.17	-	0.2	7	0.46	-
2.10a	0.42	1.2	0.055	-	-	0.35	7.6
2.10b	0.27	1.0	0.090	-	-	0.27	3.0
2.10c	0.27	1.6	0.050	-	-	0.17	5.4
2.10d	0.35	1.3	0.220	-	-	0.27	1.6
2.10e	0.65	0.9	0.320	-	-	0.72	2.0
2.13	0.011	0.24	0.0002	-	-	0.045	55

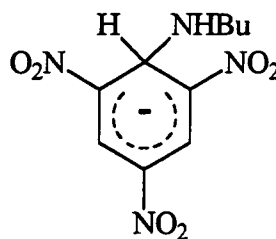
^a From ref. 12. Values quoted are in presence of tetraethylammonium chloride 0.01 mol dm^{-3} , to correspond with present data for reactant 2.2.

2.8.2 Reactions of Ethyl 2,4,6-Trinitrophenyl Ether, 2.5.

The value of K_1K_{Dabco} , the overall equilibrium constant for formation of the adduct 2.7 from 2.5, is *ca.* 10 times larger than that for formation of 2.1 by reaction at an unsubstituted ring position of TNB. The major effect is likely to be an increase in K_1 due to relief of steric strain present in the parent compound^{16,26} when the ethoxy group is twisted from the ring plane. The polar effect of the ethoxy group would be expected to result in an increase in the value of K_1 and may also give rise to a small increase in K_{Dabco} . For comparison¹⁶ the equilibrium constant for formation of 2.17 from 2.5 and *n*-butylamine has a value 50 times larger than that for the corresponding formation of 2.18.



2.17



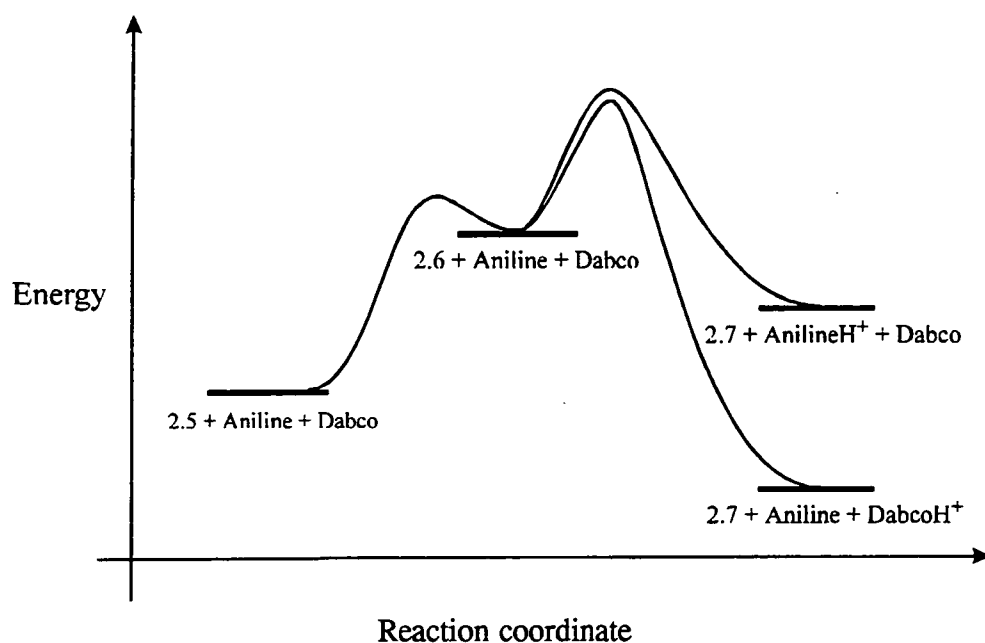
2.18

An adduct formed by attack of aniline at the unsubstituted 3-position of 2.5 has not been observed. This may be explained by the much lower thermodynamic stability expected for this adduct compared with its isomer 2.7 or with the adduct 2.1 formed from TNB. Attack at the 3-position of 2.5 will not relieve the steric strain present in the parent, and work with aliphatic amines¹⁶ suggests that the adduct so-formed would have a stability *ca.* 100 times lower than that of the adduct 2.1 from TNB.

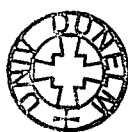
Buncel and co-workers^{10,11} have shown that in the formation of 2.1 from TNB and aniline the proton transfer step is rate limiting. Similarly in the formation of 2.7 the results described here indicate rate limiting proton transfer. From equations 2.2 and 2.8, $K_{\text{An}} / K_{\text{Dabco}}$ has the value 5.8×10^{-6} showing that the equilibrium constant for the proton transfer step is very much smaller when the reaction involves aniline than when the reaction involves Dabco. Nevertheless the ratio of 0.46 obtained for $k_{\text{An}} / k_{\text{Dabco}}$ shows that kinetically aniline may compete effectively with Dabco, a much stronger base, in the proton transfer step. This may seem surprising, however it should be remembered that the proton transfer step, $2.6 \leftrightarrow 2.7$, in scheme 2.1 will be thermodynamically favourable even when reaction involves aniline as B and the anilinium ion as BH^+ . Thus it is known^{5,27} that the trinitrocyclohexadienate group, even though negatively charged, is electron withdrawing relative to hydrogen.

Hence 2.6 will be more acidic than the anilinium ion. A possible reaction profile is shown below in figure 2.26, where both aniline and Dabco are in large excess of the concentration of 2.5. In the absence of Dabco, the energy of the products is higher than that of the reactants. Hence only a small amount of the adduct 2.7 is produced. However the presence of Dabco lowers the energy of the final state, so that large amounts of 2.7 form. Values of k_{An} and k_{Dabco} will be affected by steric factors rather than the relative basicities of the amines. It is likely that the proton to be transferred from 2.6 will be hydrogen bonded to a DMSO molecule in the solvent²⁸ and this together with steric hindrance to the approach of the reagents will reduce values of rate constants below the diffusion limit.

Figure 2.26 Reaction profile for (a) 2.5 and aniline, (b) 2.5, aniline and Dabco.



It is interesting to speculate on values of rate constants for the proton transfer step. It has previously been estimated^{15,16} that the presence of the trinitrocyclohexadienate ring in zwitterions such as 2.6 will acidify the adjacent ammonium protons by a factor of *ca.* 500, as indicated in equation 2.19. Use of equation 2.2 allows the comparison of the relative acidities of 2.6 and protonated Dabco as shown in equation 2.20. The ratio obtained corresponds to k_{Dabco} / k_{DabcoH^+} and since k_{DabcoH^+} has been found experimentally to be $0.2 \text{ dm}^3 \text{ mol}^{-1} \text{ s}^{-1}$ a value for k_{Dabco} of $1.7 \times 10^7 \text{ dm}^3 \text{ mol}^{-1} \text{ s}^{-1}$ is obtained. This allows the calculation of values for k_{An} $8 \times 10^6 \text{ dm}^3 \text{ mol}^{-1} \text{ s}^{-1}$ and K_1 $7 \times 10^{-8} \text{ dm}^3 \text{ mol}^{-1}$. Since the ratio given in equation 2.19 is not known precisely, the values calculated using it should be regarded only as estimates.



$$K_a(2.6) / K_a(\text{AnH}^+) \approx 500 \quad \text{equation 2.19}$$

$$K_a(2.6) / K_a(\text{DabcoH}^+) \approx 500 / 5.8 \times 10^{-6} \approx 8.6 \times 10^7 \quad \text{equation 2.20}$$

The data in table 2.17 indicate that values of rate constants for proton transfer are larger than in the formation of 2.1 from TNB, than in the formation of 2.7. Here reaction occurs at an unsubstituted ring position so that there is less steric congestion at the reaction centre. A calculation analogous to that given above leads here to a value for k_{Dabco} in excess of $10^9 \text{ dm}^3 \text{ mol}^{-1} \text{ s}^{-1}$.

The formation of 2.8 from 2.7 involves general acid catalysed expulsion of the ethoxy group. Values of the rate constants for the reaction with the anilinium ion, $860 \text{ dm}^3 \text{ mol}^{-1} \text{ s}^{-1}$, and DabcoH^+ , $0.06 \text{ dm}^3 \text{ mol}^{-1} \text{ s}^{-1}$, may be used in conjunction with equation 2.2 to calculate the Brønsted α value of 0.80.

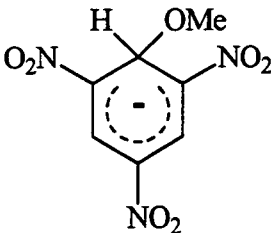
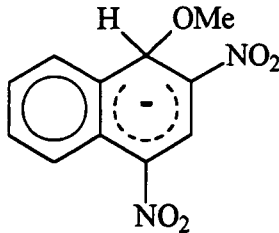
2.8.3 Reactions of Substituted Phenyl 2,4,6-Trinitrobenzenes, 2.10a-e.

Phenoxide is known to be a considerably better leaving group than ethoxide,^{17,23} and intermediates in the substitution reactions of the phenyl ethers 2.10a-e were not observed. The increases in the rate constant shown in figures 2.20 and 2.21 are interpreted as base catalysis. Previous work,^{19,21} at lower base concentrations, did not find evidence for base catalysis. The effects observed here are not particularly large. However, values calculated for $K_1 k_{\text{An}}$ and $K_1 k_{\text{Dabco}}$ for reaction of 2.10a-e are similar to those found for reaction of 2.5, where there is genuine base catalysis. These similarities are to be expected if proton transfer from the zwitterion, 2.11 or 2.6, to base is rate limiting. The presence of a phenoxy group at the 1-position, rather than an ethoxy group, is not expected to affect drastically the value of K_1 for formation of the zwitterion.²⁹ Nor will this change be expected to greatly affect the values of k_{An} or k_{Dabco} for the proton transfer step. A major difference between the phenyl ethers, 2.10 and the ethyl ether, 2.5, is that in the former case much of the reaction flux involves the direct uncatalysed decomposition of the zwitterions, 2.11, by the k_2 step. This step is likely to involve intramolecular proton transfer from nitrogen to oxygen coupled with carbon-oxygen bond cleavage. Leaving group expulsion is part of the rate limiting step here, so that reaction of the 4-nitrophenoxy, 2.10e, and 4-cyanophenoxy derivative, 2.10d, is 6 times faster than that of the phenoxy derivative, 2.10c, table 2.17.

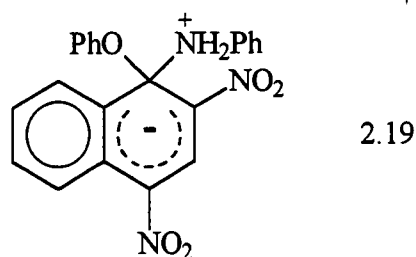
2.8.4 Reaction of Phenyl 2,4-Dinitronaphthyl Ether, 2.13.

Comparison of data for reaction of phenyl 2,4-dinitronaphthyl ether, 2.13, with that for phenyl 2,4,6-trinitrophenyl ether, 2.10c, shows decreases in K_1k_2 , K_1k_{An} and K_1k_{Dabco} by factors of 250, 24 and 7 respectively. These changes may be attributed^{2,3} to two main factors; the decrease in ring activation in 2.13 compared to 2.10c, and the reduction in steric crowding at the reaction centre in the zwitterionic intermediate 2.19 compared to that in the corresponding intermediate, 2.11c. The first factor will result in a decrease in the value of K_1 and hence in the value of K_1k_2 . The decrease in value of K_1 may be estimated at *ca.* 200 from data in table 2.18 which compares equilibrium constants for methoxide attack on TNB and 2,4-dinitronaphthalene.³⁰

Table 2.18 Data for the formation of respective σ -adducts.

$K / \text{dm}^3 \text{mol}^{-1}$	18	0.09
σ -Complex		

That the decreases observed for K_1k_{An} and K_1k_{Dabco} are smaller than that observed for K_1k_2 may be attributed to the second factor. A reduction in steric crowding in 2.19 compared to 2.11c may allow the easier approach of a base molecule to accept a proton from the zwitterionic intermediate. Hence values of k_{An} and k_{Dabco} may be larger in the 2,4-dinitronaphthyl system. The k_{An} / k_{Dabco} ratio is somewhat decreased in the dinitronaphthyl system and this may indicate that the situation is being approached where the reduction in the electron withdrawing ability of the ring system renders the proton transfer from 2.19 to aniline thermodynamically unfavourable.



2.9 References.

1. M. R. Crampton and V. Gold, *J. Chem. Soc. B*, 1967, 23.
2. E. Buncel, M. R. Crampton, M. J. Strauss and F. Terrier, "Electron-Deficient Aromatic & Heteroaromatic - Base Interactions", Elsevier, New York, 1984.
3. F. Terrier, "Nucleophilic Aromatic Displacement : Influence of the Nitro Group", VCH, Weinheim, 1991.
4. E. Buncel and J. G. K. Webb, *Can. J. Chem.*, 1972, **50**, 129.
5. E. Buncel and J. G. K. Webb, *Can. J. Chem.*, 1974, **52**, 630.
6. E. Buncel and J. G. K. Webb, *Tetrahedron Lett.*, 1976, 4417
7. E. Buncel, J. G. K. Webb and J. F. Wiltshire, *J. Am. Chem. Soc.*, 1977, **99** 4429.
8. E. Buncel and H. W. Leung, *J. Chem. Soc. Chem. Commun.*, 1975, 19.
9. T. O. Bamkole, J. Hirst and J. Onyido, *J. Chem. Soc. Perkin Trans 2*, 1981, 1201.
10. E. Buncel and W. Eggimann, *J. Am. Chem. Soc.*, 1977, **99**, 5958.
11. E. Buncel, W. Eggimann and H. W. Leung, *J. Chem. Soc. Chem. Commun.*, 1977, 55.
12. E. Buncel and W. Eggimann, *J. Chem. Soc. Perkin Trans. 2*, 1978, 673.
13. C. F. Bernasconi, M. C. Muller and P. Schmid, *J. Org. Chem.*, 1979, **44**, 3189.
14. C. F. Bernasconi, *Acc. Chem. Res.*, 1978, **11**, 147.
15. M. R. Crampton and B. Gibson, *J. Chem. Soc. Perkin Trans 2*, 1981, 533.
16. M. R. Crampton and P. J. Routledge, *J. Chem. Soc. Perkin Trans. 2*, 1984, 573.
17. R. A. Chamberlin and M. R. Crampton, *J. Chem. Soc. Perkin Trans. 2*, 1995, 1831.
18. J. A. Orvik and J. F. Bunnett, *J. Am. Chem. Soc.*, 1970, **92**, 2417.
19. J. Hirst, G. Hussain and I. Onyido, *J. Chem. Soc. Perkin Trans. 2*, 1986, 397.
20. O. Banjoko and P. Otiono, *J. Chem. Soc. Perkin Trans. 2*, 1981, 399.
21. T. A. Emokpae, P. U. Uwakwe and J. Hirst, *J. Chem. Soc. Perkin Trans. 2*, 1993, 125.
22. M. R. Crampton and I. A. Robotham, *J. Chem. Res. (S)*, 1997, 22.
23. C. F. Bernasconi and M. C. Muller, *J. Am. Chem. Soc.*, 1978, **100**, 5530.
24. I. G. Il'ina, S. V. Zabaznova, E. V. Ivanova and K. P. Butin, *Russ. J. Org. Chem.*, 1994, **30**, 2, 295.

25. C. Willgerodt and E. Huetlin, *Chem. Ber.*, 1884, **17**, 1766.
26. C. M. Gramaccioli, R. Destro and M. Simonetta, *Acta Cryst. Ser B*, 1968, **24**, 129.
27. M. R. Crampton, *J. Chem. Soc. B*, 1971, 2112.
28. M. R. Crampton and S. D. Lord, *J. Chem. Soc. Perkin Trans. 2*, 1997, 369.
29. R. Chamberlin, M. R. Crampton and R. L. Knight, *J. Chem. Res. (S)*, 1993, 444.
30. F. Terrier, *Chem. Rev.*, 1982, **82**, 77.

Chapter 3.

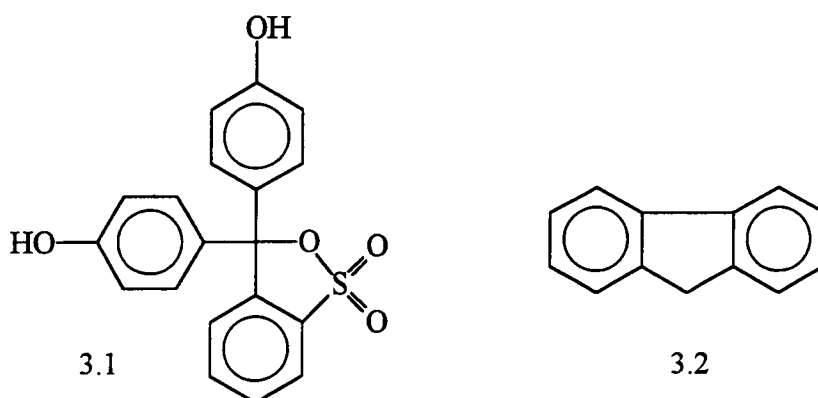
Acidities of Various Substituted Ammonium

Ions in Dimethyl Sulfoxide.

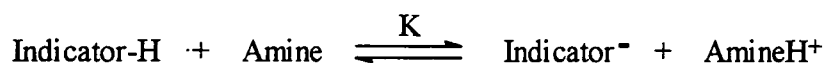
3.1 Introduction.

Dimethyl sulfoxide (DMSO) is a very useful solvent for studying nucleophilic aromatic substitution reactions and several kinetic and mechanistic studies involving reaction with amine nucleophiles have been reported.¹⁻⁸ In order to make comparisons of the amines a knowledge of their basicities in DMSO is very important. Surprisingly, pK_a values are not available for many ammonium ions derived from amines which have been used in substitution studies. These amines include piperidine, pyrrolidine, benzylamine and morpholine.

It was shown by Kolthoff and co-workers⁹ and by Ritchie and Uschold^{10,11} that potentiometric measurements using a glass electrode can be used to determine pK_a values in DMSO. Kolthoff has determined the dissociation constants in DMSO of various uncharged acids, monovalent cationic acids and some sulfonphthaleins, e.g. phenolsulfonphthalein (phenol red), 3.1, $pK_a(\text{DMSO})$ 13.7. Ritchie and Uschold measured values for a number of weak acids, including fluorene, 3.2, $pK_a(\text{DMSO})$ 20.5.



Previously a single acidity scale had been proposed to estimate the acidities of weak acids in DMSO.¹² However discrepancies undoubtedly arose from the fact that measurements in a variety of solvents were used in the establishment of the scale. A second contributing factor to the noted discordance is the complicating effect of ion pairing on some of the measurements which were made in solvents of extremely low dielectric constant.¹³ Extensive data in DMSO have been reported by Bordwell and his group^{14,15} using spectrophotometry with overlapping indicators which cover the range 0-32 pK_a units, equation 3.1.



equation 3.1

Dimethyl sulfoxide has many advantages for acidity measurements. It is readily available in a high scale of purity, non-toxic, stable to strong bases for a considerable length of time, an excellent solvent for most neutral organic compounds with reasonably good solvation properties for both anions and cations, and a very weak acid, table 3.1. Oxygen acids such as carboxylic acids, phenols, and alcohols have been found to be less acidic in DMSO than in water by many orders of magnitude. A major factor here is the reduced stabilisation of their anions because hydrogen bonding with the solvent is lacking.

DMSO is known to be a good hydrogen bond acceptor and is more effective at solvating cations and large delocalised anions unlike water and methanol etc. It also differs from other dipolar aprotic solvents (e.g. acetonitrile and dimethylformamide, DMF) in that its dielectric constant and polarisability (as measured by refractive index) are appreciably greater than those of the other solvents, table 3.1. Consequently it can be expected that electrostatic and dispersion effects will differ in DMSO from those of other solvents.

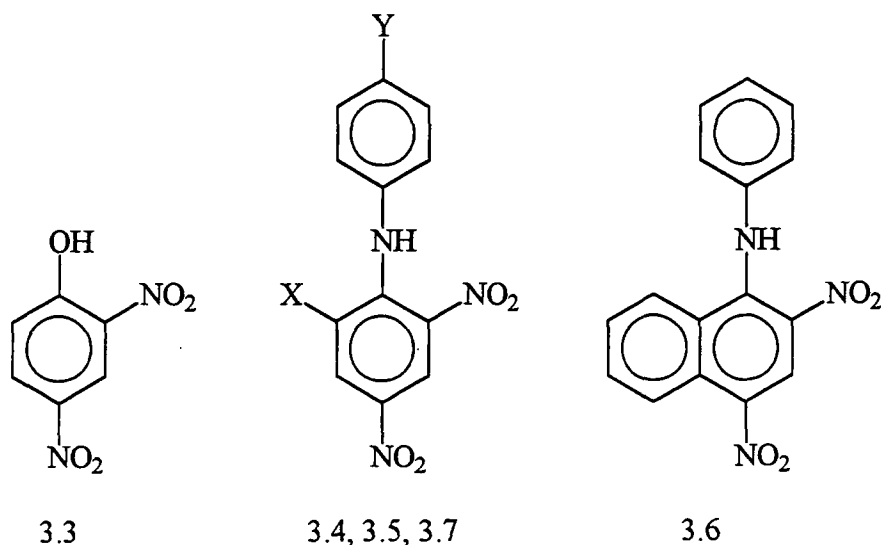
Table 3.1 Dielectric constants (D) and Autoprotolysis Constants (K_s) of some popular solvents at 25°C.¹⁶

Solvent	Water	DMSO	DMF	Acetonitrile	Ethanol	Dioxane
D	78.4	46.6	36.7	36.0	24.3	2.2
pK _s	14.0	ca.32	ca.21	28.5	19.1	-

3.2 Spectroscopic Technique: Indicators.

Results were obtained using the spectrophotometric method taking the indicator 2,4-dinitro-phenol, 3.3, to be the reference point. Its pK_a value is known to be 5.12 ± 0.04 in DMSO.¹⁴ The other indicators used were 4',2,4,6-tetranitrodiphenylamine, 3.4, 2,4,6-trinitrodiphenylamine, 3.5, N-phenyl-2,4-dinitronaphthylamine, 3.6, and 2,4-dinitrodiphenylamine 3.7; methods of preparation are given in section 3.3, pg. 111. The indicators were chosen to cover a range of acidities so that a scale could be built up to cover the basicities of all the desired amines.

It is known¹⁷ that the mode of ionisation of these indicators involves proton loss rather than base addition to give σ -adducts. All the indicators show a pronounced change in their U.V./Vis. spectrum on deprotonation. Figure 3.1 shows an example of the protonated and deprotonated U.V./Vis. spectra for indicator 3.6. Deprotonation was achieved using an excess of base. An instantaneous colour change is observed on addition of the base, e.g. orange to red in the example shown. Spectroscopic data for all indicators are summarised in table 3.2.



Substrate	3.4	3.5	3.7
X	NO ₂	NO ₂	H
Y	NO ₂	H	H

Figure 3.1 N-phenyl-2,4-dinitronaphthylamine 4×10^{-5} mol dm⁻³, with
 (a) no n-butylamine present, (b) 0.4 mol dm⁻³ n-butylamine in DMSO

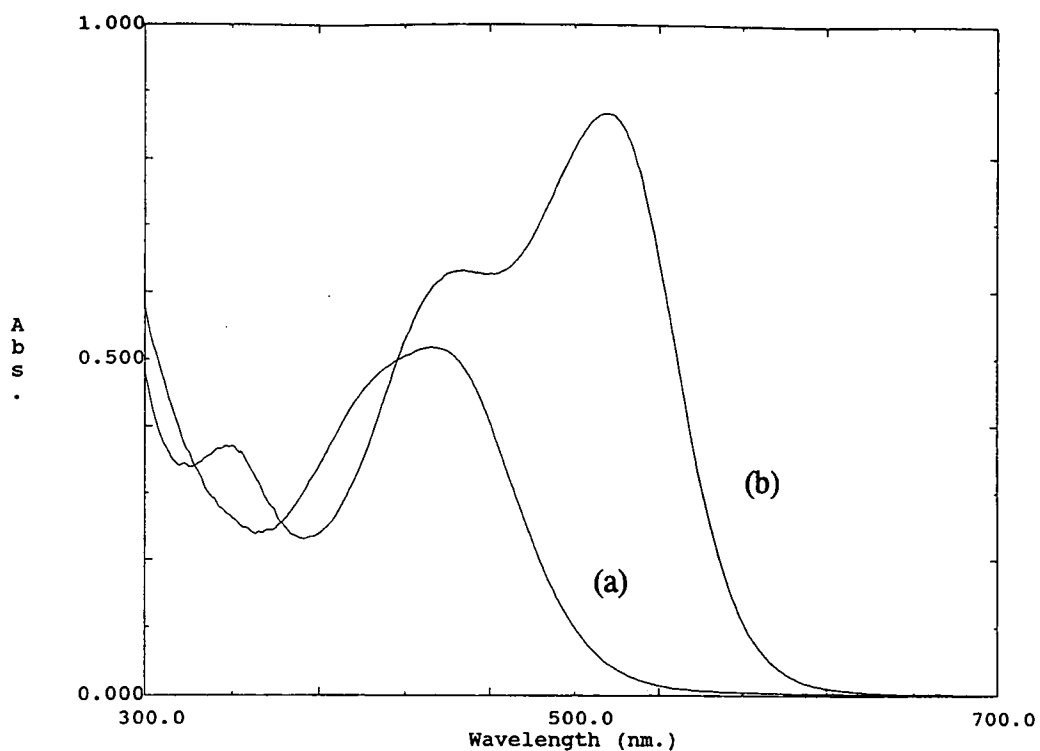


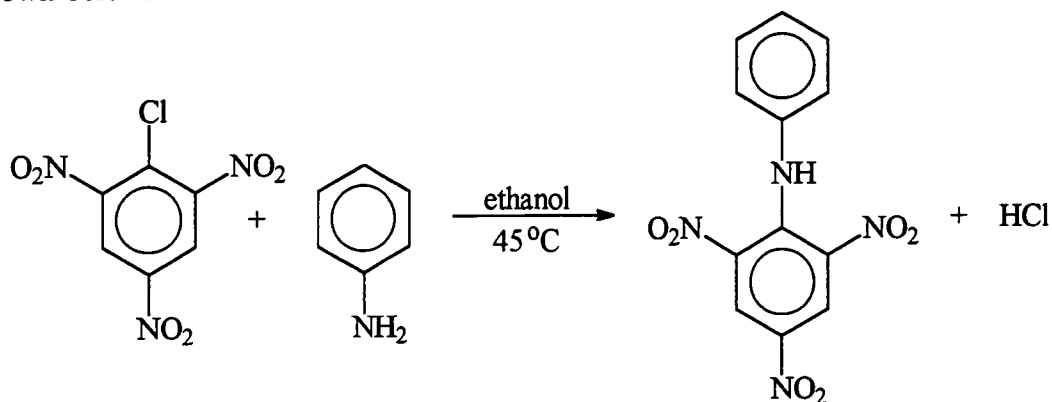
Table 3.2 Spectroscopic data for indicators.

Indicator	λ_{\max} /nm ($\log_{10} \epsilon$)	
	Deprotonated	Protonated
3.3	430 (4.31)	-
3.4	480 (4.53)	403 (4.32)
3.5	450 (4.37)	386 (4.15)
3.6	515 (4.35)	445 (4.11)
3.7	435 (4.29)	368 (4.25)

3.3 Synthesis of Indicators and Amine Salts.

3.3.1 Synthesis of Indicators.

These were prepared by the reaction of the appropriate chlorodinitro- or chlorotrinitro-aromatic compound (0.004mol) with aniline (0.012mol, 1.09ml) or, in the case of 3.4, 4-nitro-aniline (0.012mol, 1.66g) in ethanol (30 ml). The solution was stirred and heated to a temperature of 45°C for 5 hours for all aniline derivatives and for 12 hours for the less reactive 4-nitro-aniline. Afterwards the solution was allowed to cool and the precipitate produced was separated by filtration, washed with a small amount of ethanol and then dried *in vacuo* to produce bright orange powders (3.5 - 3.7) or a yellow powder (3.4). The equation for the synthesis of 3.5 is shown below.



equation 3.2

3.3.1.2 NMR Data and Melting Points of the Indicators.

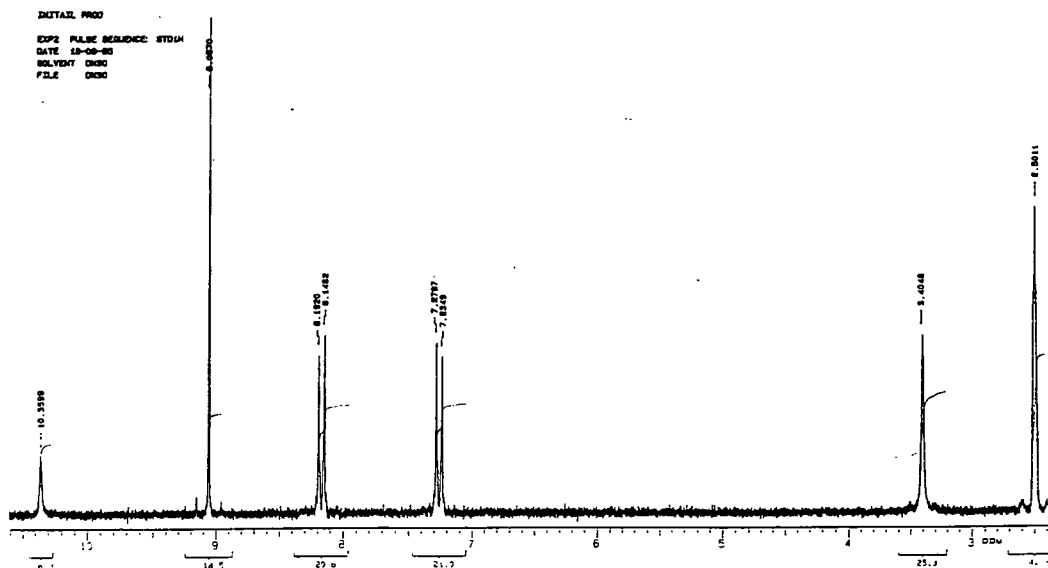
The melting points obtained are summarised in table 3.3 below.

Table 3.3 Melting point data for indicators.

Indicator	m.p. (T/°C)	Literature m.p. (T/°C)
3.3	208	213 ¹⁸
3.4	222	223 ¹⁹
3.5	183	178 ²⁰
3.6	180	180 ²¹
3.7	158	157 ²²

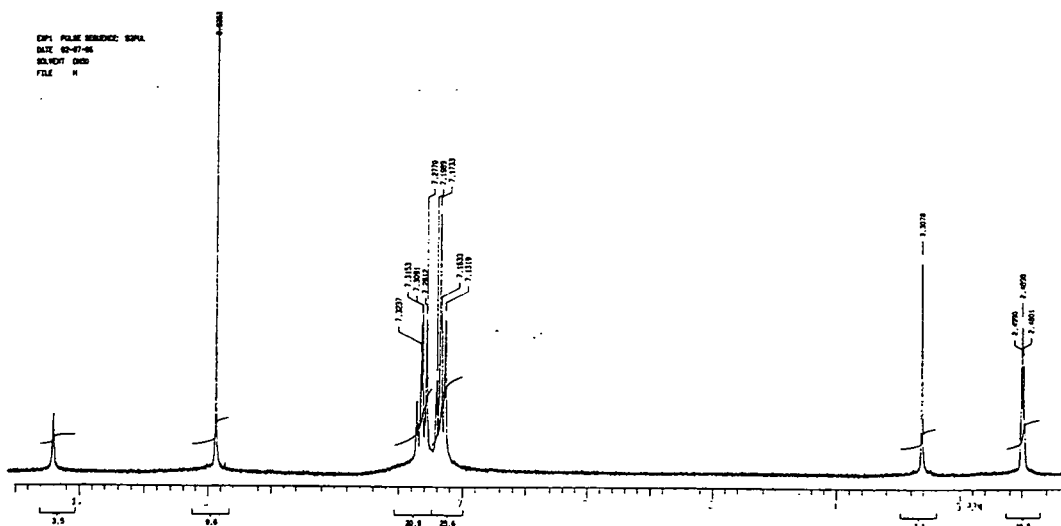
^1H NMR spectra were recorded at 200MHz in d_6 -DMSO. All spectra showed bands at $\delta_{\text{H}}/\text{ppm}$ 2.49 due to solvent and a band in the range $\delta_{\text{H}}/\text{ppm}$ 3 - 4.5 due to adventitious water. The ^1H NMR spectrum for 3.4 gave signals at $\delta_{\text{H}}/\text{ppm}$ 7.26 (2H, d, $J = 9\text{Hz}$, ring), 8.17 (2H, d, $J = 9\text{Hz}$, ring), 9.06 (2H, s, picryl ring) and 10.36 (1H, br s, NH), figure 3.2.

Figure 3.2 ^1H NMR spectrum of 4', 2,4,6-tetranitrodiphenylamine in d_6 -DMSO.



The ^1H NMR spectrum for 3.5 in d_6 -DMSO gave signals at $\delta_{\text{H}}/\text{ppm}$ 7.16 (2H, d, $J = 8\text{Hz}$, ring), 7.17 (1H, t, $J = 7\text{Hz}$, ring), 7.32 (2H, t, $J = 7\text{Hz}$, ring), 8.94 (2H, s, picryl ring) and 10.22 (1H, br s, NH), figure 3.3.

Figure 3.3 ^1H NMR spectrum of 2,4,6-trinitrodiphenylamine in d_6 -DMSO.



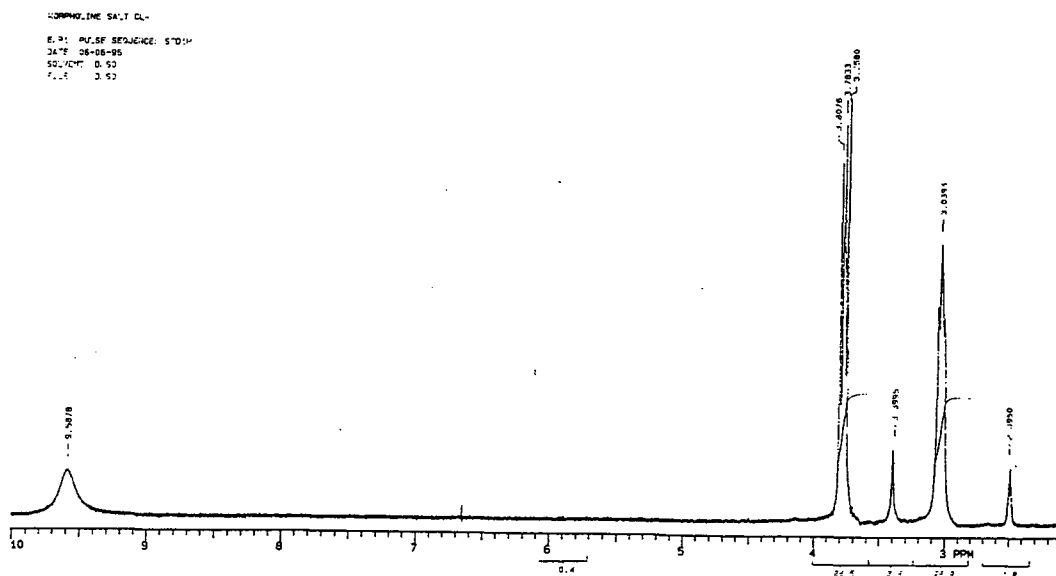
3.3.2 Synthesis of Amine Salts.

Morpholine and n-butylamine hydrochloride were synthesised using the following method. To 200ml diethyl ether was added morpholine (0.1mol, 8.7ml) or n-butylamine (0.1mol, 9.9ml) and the solution cooled to 0°C using an acetone-cardice bath. This was followed by the slow addition of hydrochloric acid (0.1mol) maintaining the temperature at 0°C. White crystals that precipitated out of solution were filtered, washed quickly with cold diethyl ether and dried *in vacuo*. The crystals were then stored under nitrogen due to both salts being very hygroscopic.

3.3.2.1 NMR Data for Amine Salts.

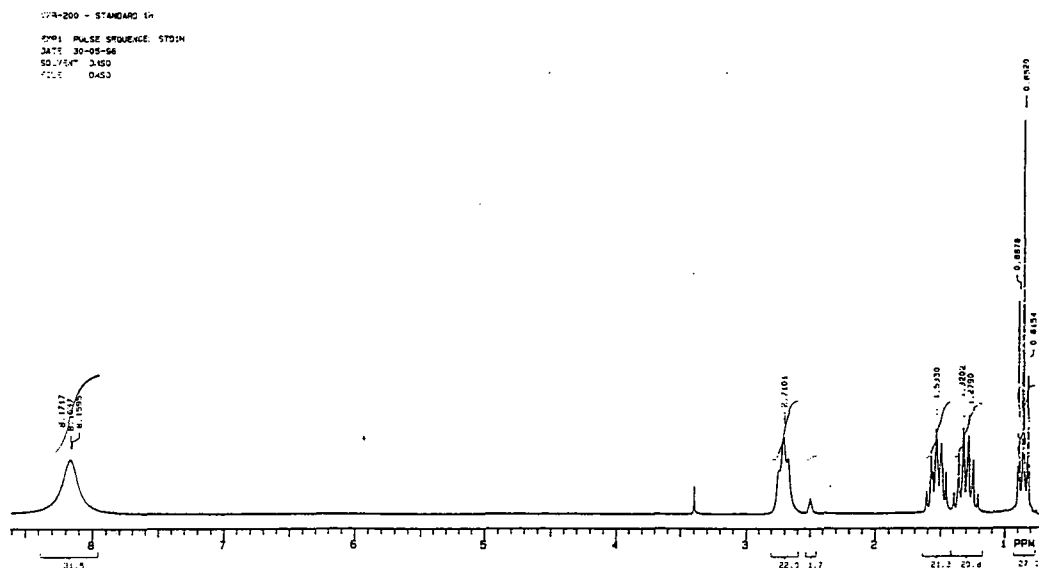
The ^1H NMR spectrum (200MHz) for morpholine hydrochloride in d_6 -DMSO gave signals at $\delta_{\text{H}}/\text{ppm}$, 3.04 (4H, m, $2\times\text{CH}_2$), 3.80 (4H, m, $2\times\text{CH}_2$) and 9.50 (2H, br s, NH_2), figure 3.6.

Figure 3.6 ^1H NMR spectrum of morpholine hydrochloride in d_6 -DMSO.



The ^1H NMR spectrum (200MHz) for n-butylamine hydrochloride in d_6 -DMSO gave signals at $\delta_{\text{H}}/\text{ppm}$, 0.85 (3H, t, $J = 7.2\text{Hz}$, CH_3), 1.32 (2H, sextet, $J = 8.24\text{Hz}$, CH_2) and 1.53 (2H, p, $J = 8.3\text{Hz}$, CH_2), 2.71 (2H, br t, CH_2), 8.17 (3H, br s, NH_3^+), figure 3.7.

Figure 3.7 ^1H NMR spectrum of n-butylamine hydrochloride in d_6 -DMSO.



3.4 Experimental Procedure.

In a typical experiment spectra were recorded with a constant concentration, $4 \times 10^{-5} \text{ mol dm}^{-3}$, of indicator in solutions buffered with various concentrations of amine and the corresponding amine salt. Usually measurements were made with a salt concentration of 0.01 mol dm^{-3} , if lower salt concentrations were used the ionic strength was maintained at $I = 0.01 \text{ mol dm}^{-3}$ with tetra-n-butylammonium chloride. Hydrochloride salts of imidazole, triethylamine, benzylamine and piperidine were available commercially. Since low concentrations of both morpholine and n-butylamine hydrochloride were required they were prepared in the laboratory, their synthesis can be viewed in section 3.3.2, pg.114. Those of aniline, Dabco (1,4-diazabicyclo[2.2.2]octane) and pyrrolidine were prepared in solution in DMSO by the reaction of equivalent quantities of amine and acid.

The required volumes of each amine and its salt were transferred to a 5ml volumetric flask and the indicator added. A colour change occurred instantaneously. The solution was then transferred into a cell and thermostatted at 25°C for 5 minutes after which the U.V./Vis. spectrum was obtained. An absorbance reading at the appropriate wavelength could then be obtained.

3.5 Results.

Absorbance measurements were taken at the λ_{\max} value for the deprotonated forms of the indicators with various concentrations of each suitable amine. Representative results for two indicators 3.3 and 3.6 in solutions containing aniline / anilineH⁺Cl⁻ and imidazole / imidazoleH⁺Cl⁻ respectively are shown in figure 3.8 & 3.9 and table 3.4 & 3.5. Spectra correspond to the conditions given in the tables.

Figure 3.8 U.V./Vis. spectra of 2,4-dinitrophenol, 4×10^{-5} mol dm⁻³, in DMSO containing various concentrations of aniline.

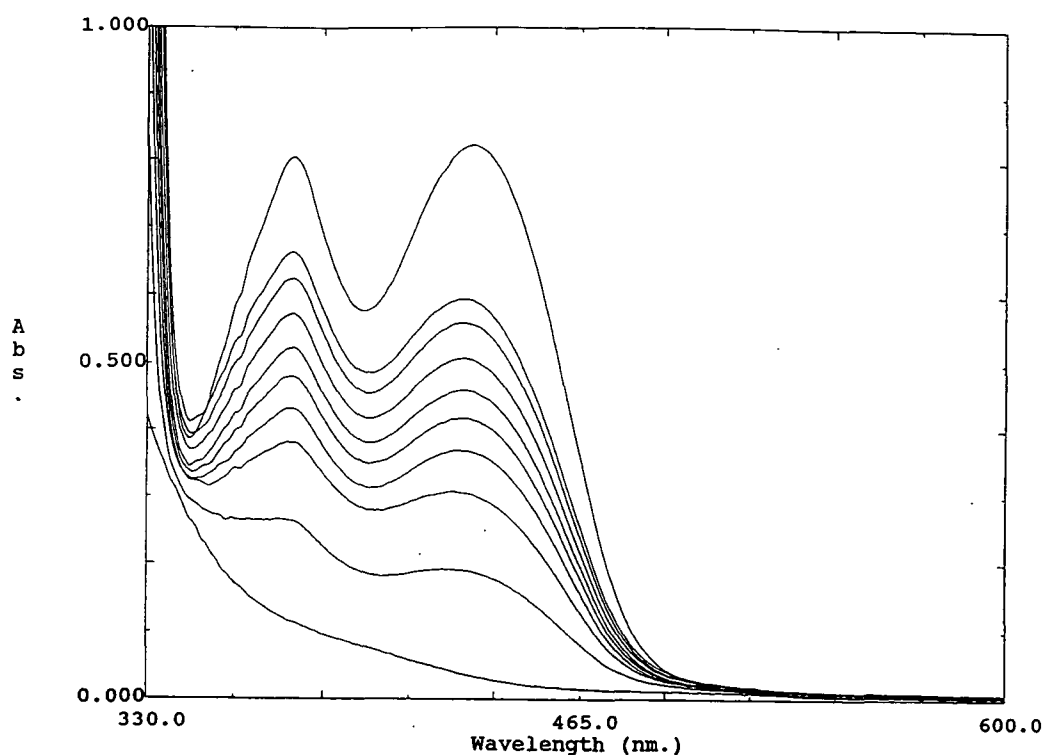


Table 3.4 Absorbance data for 2,4-dinitrophenol in DMSO containing various concentrations of aniline at 25°C. AnilineH⁺Cl⁻ = 0.01 mol dm⁻³.

Aniline / mol dm ⁻³	-	0.05	0.10	0.15	0.20	0.25	0.30	0.40	0.50	0.55
10 Abs. (λ_{\max} 430nm)	0.36°	1.90	3.05	3.68	4.18	4.61	5.08	5.59	5.94	8.23*

°A₀ & *A_∞ obtained without the presence of amine and amine salt respectively.

Figure 3.9 U.V./Vis. spectra of 4',2,4,6-tetranitrodiphenylamine, 4×10^{-5} mol dm^{-3} , in DMSO containing various concentrations of imidazole: Scans correspond to the conditions given in table 3.5.

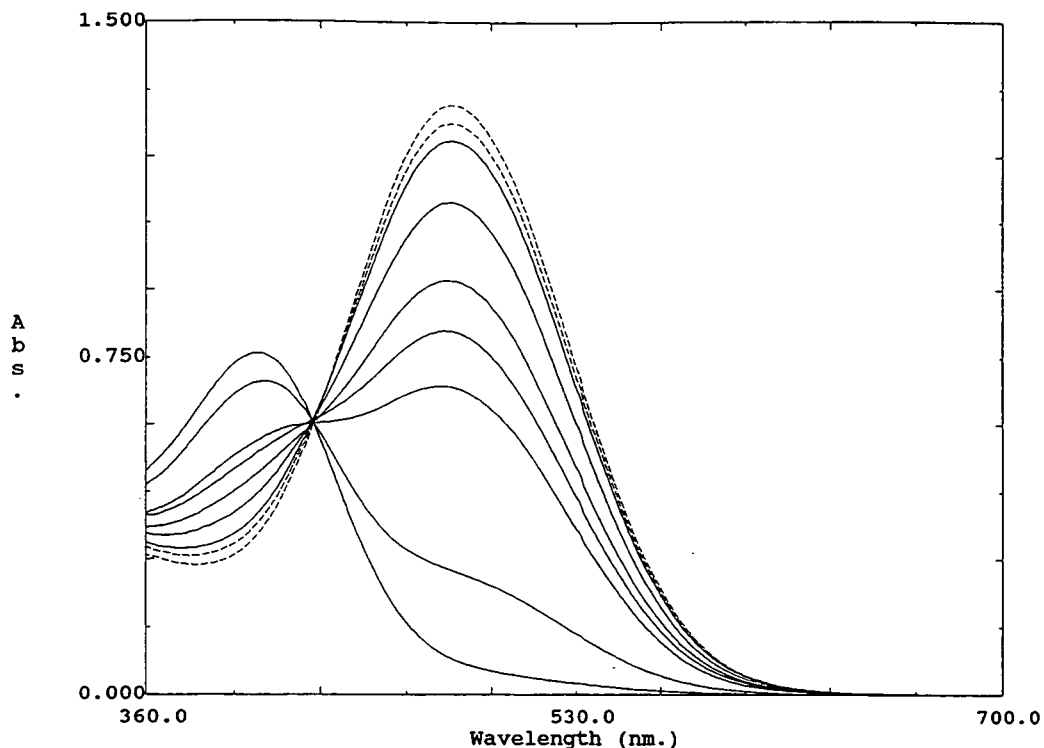


Table 3.5 Absorbance data for 4',2,4,6-tetranitrodiphenylamine in DMSO containing various concentrations of imidazole at 25°C.
Imidazole. $\text{H}^+\text{Cl}^- = 0.01 \text{ mol dm}^{-3}$.

Imidazole / mol dm^{-3}	-	0.001	0.005	0.007	0.01	0.02	0.05	0.10	0.10
10 Abs. (λ_{max} 480nm)	0.81°	2.75	6.85	8.08	9.19	11.0	12.4	12.8	13.4

$^{\circ}\text{A}_0$ & $^*\text{A}_{\infty}$ obtained without the presence of amine and amine salt respectively.

The following sections are a summary of various absorbance readings collected for the remaining indicators and amines.

3.5.1 Indicator: 4',2,4,6-Tetranitrodiphenylamine.

Table 3.6 Absorbance data for 4',2,4,6-tetranitrodiphenylamine in DMSO containing various concentrations of aniline at 25°C.

Aniline / mol dm ⁻³	-	0.10	0.10	0.20	0.40	0.40	0.40	0.70	0.70	0.7
An.H ⁺ Cl ⁻ / mol dm ⁻³	0.001	0.001	0.002	0.01	0.004	0.007	0.01	0.007	0.01	-
10 Abs. (λ _{max} 480nm)	0.47°	6.18	3.92	1.81	5.63	3.56	2.77	4.78	3.88	14.2*

The aniline salt concentration is varied here in an attempt to obtain a range of absorbance values close to the 50% conversion region of the indicator, which will provide a more accurate value of the equilibrium constant.

3.5.2 Indicator: 2,4,6-Trinitrodiphenylamine.

Table 3.7 Absorbance data for 2,4,6-trinitrodiphenylamine in DMSO containing various concentrations of imidazole at 25°C.

Imidazole.H⁺Cl⁻ = 0.001 mol dm⁻³.

Imidazole / mol dm ⁻³	-	0.01	0.03	0.05	0.07	0.10	0.12	0.15	0.20	0.20
10 Abs. (λ _{max} 448nm)	2.23°	3.64	5.29	6.23	6.65	7.27	7.42	7.84	8.10	9.45*

°A₀ & *A_∞ obtained without the presence of amine and amine salt respectively.

Table 3.8 Absorbance data for 2,4,6-trinitrodiphenylamine in DMSO containing various concentrations of Dabco at 25°C.
Dabco.H⁺Cl⁻ = 0.01 mol dm⁻³.

Dabco / mol dm ⁻³	-	0.001	0.002	0.003	0.004	0.005	0.10
10 Abs. (λ _{max} 450nm)	2.29°	6.08	7.43	8.01	8.45	8.56	9.70*

Table 3.9 Absorbance data for 2,4,6-trinitrodiphenylamine in DMSO containing various concentrations of triethylamine at 25°C.
Triethylamine.H⁺Cl⁻ = 0.01 mol dm⁻³.

Triethylamine / mol dm ⁻³	-	5×10 ⁻⁴	7×10 ⁻⁴	0.001	0.002	0.003	0.004	0.10
10 Abs. (λ _{max} 450nm)	2.12°	4.76	5.35	6.14	7.38	7.77	8.32	9.49*

3.5.3 Indicator: N-Phenyl-2,4-Dinitronaphthylamine.

Table 3.10 Absorbance data for N-phenyl-2,4-dinitronaphthylamine in DMSO containing various concentrations of triethylamine at 25°C.
Triethylamine.H⁺Cl⁻ = 0.001 mol dm⁻³.

Triethylamine / mol dm ⁻³	-	3×10 ⁻⁴	5×10 ⁻⁴	7×10 ⁻⁴	0.001	0.003	0.005	0.01	0.4
10 Abs. (λ _{max} 515nm)	0.49°	2.35	3.50	4.05	4.54	6.41	7.33	8.24	8.88*

°A₀ & *A_∞ obtained without the presence of amine and amine salt respectively.

Table 3.11 Absorbance data for N-phenyl-2,4-dinitronaphthylamine in DMSO containing various concentrations of Dabco at 25°C.
Dabco.H⁺Cl⁻ = 0.01 mol dm⁻³.

Dabco / mol dm ⁻³	-	0.005	0.007	0.01	0.02	0.03	0.05	0.10	0.15	0.10
10 Abs. (λ _{max} 515nm)	0.73°	3.39	4.20	5.09	6.22	7.14	7.80	8.15	8.55	8.94*

Table 3.12 Absorbance data for N-phenyl-2,4-dinitronaphthylamine in DMSO containing various concentrations of Morpholine at 25°C.
Morpholine.H⁺Cl⁻ = 0.001 mol dm⁻³.

Morpholine / mol dm ⁻³	-	3×10 ⁻⁴	4×10 ⁻⁴	7×10 ⁻⁴	0.001	0.002	0.003	0.005	0.10
10 Abs. (λ _{max} 515nm)	0.45°	4.20	5.09	6.22	7.14	7.80	8.15	8.55	8.59*

Table 3.13 Absorbance data for N-phenyl-2,4-dinitronaphthylamine in DMSO containing various concentrations of Benzylamine at 25°C.
Benzylamine.H⁺Cl⁻ = 0.01 mol dm⁻³.

Benzylamine / mol dm ⁻³	-	3×10 ⁻⁴	5×10 ⁻⁴	7×10 ⁻⁴	0.001	0.0015	0.003	0.40
10 Abs. (λ _{max} 515nm)	0.42°	2.61	3.50	4.28	4.97	5.89	6.87	8.57*

°A₀ & *A_∞ obtained without the presence of amine and amine salt respectively.

Table 3.14 Absorbance data for N-phenyl-2,4-dinitronaphthylamine in DMSO containing various concentrations of Piperidine at 25°C.
Piperidine.H⁺Cl⁻ = 0.01 mol dm⁻³.

Piperidine / mol dm ⁻³	-	1×10 ⁻⁴	2×10 ⁻⁴	3×10 ⁻⁴	4×10 ⁻⁴	5×10 ⁻⁴	0.001	0.40
10 Abs. (λ _{max} 515nm)	0.34°	3.42	4.88	5.79	6.43	6.62	7.79	8.78*

Table 3.15 Absorbance data for N-phenyl-2,4-dinitronaphthylamine in DMSO containing various concentrations of n-Butylamine at 25°C.
n-Butylamine.H⁺Cl⁻ = 0.01 mol dm⁻³.

n-Butylamine / mol dm ⁻³	-	8×10 ⁻⁵	1×10 ⁻⁴	2×10 ⁻⁴	3×10 ⁻⁴	4×10 ⁻⁴	5×10 ⁻⁴	0.40
10 Abs. (λ _{max} 515nm)	0.47°	3.49	3.92	5.92	6.85	7.05	7.48	8.67*

3.5.4 Indicator: 2,4-Dinitrodiphenylamine.

Table 3.16 Absorbance data for 2,4-dinitrodiphenylamine in DMSO containing various concentrations of n-butylamine at 25°C.
n-Butylamine.H⁺Cl⁻ = 0.01 mol dm⁻³.

n-Butylamine / mol dm ⁻³	-	0.1	0.3	0.5	0.7	1.0	1.2	1.4	1.6	1.2
10 Abs. (λ _{max} 490nm)	0.16°	1.36	2.77	3.84	4.16	4.97	5.14	5.24	5.44	6.80*

°A₀ & *A_∞ obtained without the presence of amine and amine salt respectively.

Table 3.17 Absorbance data for 2,4-dinitrodiphenylamine in DMSO containing various concentrations of pyrrolidine at 25°C.

pyrrolidine / mol dm ⁻³	-	0.1	0.1	0.1	0.1	0.1	0.4	1.0	1.3	0.8
pyrr.H ⁺ Cl ⁻ / mol dm ⁻³	0.01	0.001	0.003	0.005	0.007	0.01	0.01	0.01	0.01	-
10 Abs. (λ _{max} 490nm)	0.16°	4.76	2.90	2.18	1.62	1.21	2.94	4.56	4.76	6.62*

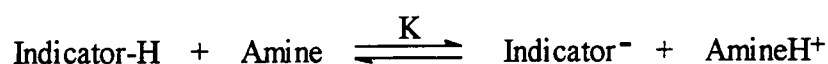
The pyrrolidine salt concentration is varied here in an attempt to obtain a range of absorbance values close to the 50% conversion region of the indicator, which will provide a more accurate value of the equilibrium constant.

°A₀ & *A_∞ obtained without the presence of amine and amine salt respectively.

3.6 Equilibrium Constants.

3.6.1 Determination of Equilibrium Constants.

Equation 3.1 defines an equilibrium constant K for the overall conversion of an indicator (Indicator-H) into its deprotonated form (Indicator⁻) by the respective amine. As shown previously all deprotonated species have a strong U.V./Vis. absorbance and measurements taken at a specific wavelength can yield the value of the equilibrium constant, K, on application of equation 3.3. Calculated values for K are collected in table 3.18.



equation 3.1

$$K = \frac{[\text{Indicator}^-][\text{AmH}^+]}{[\text{IndicatorH}][\text{Am}]} = \frac{(\text{Abs.} - A_0) [\text{AmH}^+]}{(A_\infty - \text{Abs.}) [\text{Am}]} \quad \text{equation 3.3}$$

A_0 = absorbance measurement for the indicator only, i.e. no amine present.

A_∞ = absorbance measurement for the fully deprotonated indicator, i.e. excess amine present.

$[\text{Am}]$ = amine concentration, mol dm⁻³.

$[\text{AmH}^+]$ = amine hydrochloride concentration, mol dm⁻³.

Table 3.18 Values of K defined in equation. 3.3, in DMSO at 25°C and with $I = 0.01$ mol dm⁻³.

Indicator	Amine	K
3.3	Aniline	0.050 ± 0.002
3.4	Aniline	0.0056 ± 0.0004
3.4	Imidazole	2.0 ± 0.2
3.5	Imidazole	0.023 ± 0.001
3.5	Dabco	11.3 ± 0.7
3.5	Triethylamine	11.5 ± 0.7
3.6	Triethylamine	1.0 ± 0.1
3.6	Dabco	1.0 ± 0.1
3.6	Morpholine	1.2 ± 0.1
3.6	Benzylamine	12.3 ± 0.9
3.6	Piperidine	60 ± 5
3.6	n-Butylamine	112 ± 10
3.7	n-Butylamine	0.024 ± 0.002
3.7	Pyrrolidine	0.021 ± 0.003

3.6.2 Determination of pK_a Values.

The use of equation 3.4 allows calculation of pK_a values for the substituted ammonium ions and also for the indicators 3.4 - 3.7, table 3.19. The reference point is the indicator 2,4-dinitrophenol, 3.3, whose pK_a is known to be 5.12 ± 0.04 in DMSO.¹⁴

$$\log_{10} K = \text{pK}_a(\text{AmH}^+) - \text{pK}_a(\text{IndicatorH}) \quad \text{equation 3.4}$$

Table 3.19 pK_a values of substituted ammonium ions and indicators.

Parent amine	pK _a (DMSO) ^a	pK _a (DMSO) ^b
Aniline	3.82 ± 0.03	3.6 ⁹
Imidazole	6.37 ± 0.06	
Dabco	9.06 ± 0.04	
Triethylamine	9.07 ± 0.05	9.0 ⁹
Morpholine	9.15 ± 0.05	
Benzylamine	10.16 ± 0.05	
Piperidine	10.85 ± 0.05	
Pyrrolidine	11.06 ± 0.07	
n-Butylamine	11.12 ± 0.05	11.1 ⁹ 10.7 ¹¹
Indicators		
3.3		5.12 ¹⁴
3.4	6.07 ± 0.04	
3.5	8.01 ± 0.03	
3.6	9.07 ± 0.07	
3.7	12.74 ± 0.06	12.4 ¹⁰

^a This work, ^b Literature values (with references).

3.7 Discussion.

3.7.1 Amines Basicities.

The results are important in that they allow the comparison of the basicities of the amines in DMSO. However it is useful also to make comparisons, table 3.20, with pK_a values in water and also with ΔG° values for proton transfer to ammonia in the gas phase, equation 3.5 below.



equation 3.5

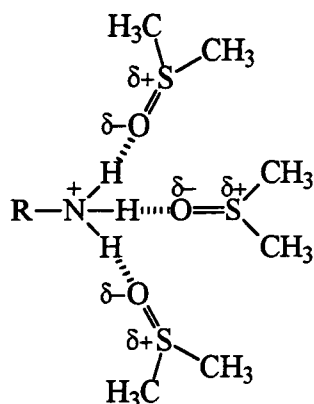
The latter results show that in the absence of solvent the basicities of aliphatic amines decrease from tertiary to secondary to primary. Nevertheless this order is inverted in DMSO where n-butylamine is the strongest base studied and piperidine and pyrrolidine are stronger bases than triethylamine and Dabco.

Table 3.20 Comparison of pK_a values for substituted ammonium ions.

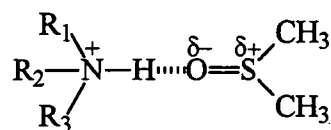
Parent amine	pK_a (DMSO) ^a	pK_a (water) ^b	ΔpK_a (DMSO-water)	$\Delta G^\circ / \text{kJmol}^{-1}$ (gas phase) ^c
Aniline	3.82	4.58	-0.76	28
Imidazole	6.37	7.00	-0.63	-
Dabco	9.06	8.82	0.24	98
Triethylamine	9.07	10.72	-1.65	115
Morpholine	9.15	8.49	0.66	63
Benzylamine	10.16	9.38	0.78	-
Piperidine	10.85	11.12	-0.27	89
Pyrrolidine	11.06	11.31	-0.25	84
n-Butylamine	11.12	10.64	0.48	58

^a This work, ^b ref. 23, ^c ref. 24, 25.

The results are consistent with the idea, expressed previously, that in solution solvation, involving hydrogen bonding of NH^+ protons, is important in stabilising the acid cations.²⁶⁻²⁸ It is known that DMSO is an extremely good hydrogen bond acceptor,²⁹ and in this solvent the stabilisation of cationic species will be expected to decrease as the number of NH^+ protons available for hydrogen bonding decreases. The results in table 3.20 show that the primary amines, n-butylamine and benzylamine are stronger bases in DMSO than in water. Here, as shown in 3.8, three acidic hydrogens are available for hydrogen bonding to DMSO. The tertiary amine, triethylamine, where the cation contains a single acidic proton, is a considerably weaker base in DMSO than in water. Here, as shown in 3.9, only a single acidic hydrogen is present.



3.8



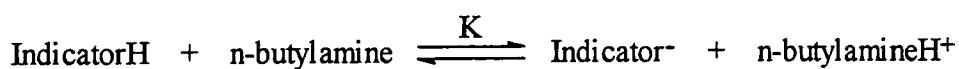
3.9

The number of acidic hydrogens in the cation available for hydrogen bonding is not the only factor affecting relative acidities in DMSO and water, dipole-dipole and dipole-ion interactions may also play an important role. Thus the bifunctional amines Dabco and morpholine, where the cations contain respectively one or two acidic protons, are slightly stronger bases in DMSO than in water. This may be due to good solvation of the cations by DMSO involving stabilisation by dipolar interactions. The higher basicity of aniline in water than in DMSO may reflect its poor solvation by water relative to DMSO.

3.7.2 Indicator Acidities.

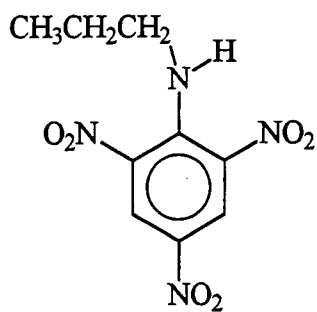
The results also allow the determination of the pK_a values for acid dissociation of the indicators, table 3.19. As expected,¹ increasing the number of nitro groups increases acidity. Comparison of the values of 3.6 and 3.5 indicates that annelation of a benzene ring in the naphthylamine derivative, 3.6, is almost as effective as addition of an extra nitro group.

It is of interest to compare the acidity of 3.5 with that of N-n-butyl-2,4,6-trinitroaniline, 3.10. Chamberlin and Crampton³⁰ showed that reaction of the latter compound with n-butylamine in DMSO resulted in competition between anion formation by proton loss and by base addition. They reported a value for K of 3.2, where K is defined in equation 3.6. Since the pK_a value of the n-butylammonium ion is 11.12 this allows the calculation of a pK_a value of 10.61 for 3.10 in DMSO.



equation 3.6

This result shows the strongly acidifying effect, by 2.6 pK units, of the N-phenyl group relative to the N-butyl group. This acidifying effect on the amino proton is sufficient to favour proton loss as the preferred mode of ionisation of the diphenylamines.



3.10

3.8 References.

1. F. Terrier, "Nucleophilic Aromatic Displacement : Influence of the Nitro Group", VCH, Weinheim, 1991.
2. E. Buncl and W. Eggimann, *J. Am. Chem. Soc.*, 1977, **99**, 5958.
3. J. Hirst, G. Hussain and I. Onyido, *J. Chem. Soc. Perkin Trans. 2*, 1986, 397.
4. T. A. Emokpae, P. U. Uwakwe and J. Hirst, *J. Chem. Soc. Perkin Trans. 2*, 1993, 125.
5. M. R. Crampton and B. Gibson, *J. Chem. Soc. Perkin Trans. 2*, 1981, 533.
6. M. R. Crampton and P. J. Routledge, *J. Chem. Soc. Perkin Trans. 2*, 1994, 443.
7. R. Chamberlin and M. R. Crampton, *J. Chem. Soc. Perkin Trans. 2*, 1995, 1831.
8. R. Chamberlin, M. R. Crampton and I. A. Robotham, *J. Phys. Org. Chem.*, 1996, **9**, 152.
9. I. M. Kolthoff, M. K. Chantooni and S. Bhowmik, *J. Am. Chem. Soc.*, 1968, **90**, 23.
10. C. D. Ritchie and R. E. Uschold, *J. Am. Chem. Soc.*, 1967, **89**, 1721; 1968, **90**, 2821.
11. C. D. Ritchie, *J. Am. Chem. Soc.*, 1969, **91**, 6749.
12. D. J. Cram, "Fundamentals of Carbanion Chemistry", Academic Press Inc., New York, 1965.
13. A. Streitwieser, *Progr. Phys. Org. Chem.*, 1965, **3**, 44.
14. F. G. Bordwell, J. C. Branca, D. L. Hughes and W. N. Olmstead, *J. Org. Chem.*, 1980, **45**, 3305.
15. F. G. Bordwell, *Acc. Chem. Res.*, 1988, **21**, 456.
16. J. F. Coetzee and C. D. Ritchie, "Solute-Solvent Interactions", Marcel Dekker, New York, 1969.
17. M. R. Crampton and V. Gold, *J. Chem. Soc. B*, 1966, 893.
18. "Dictionary of Organic Compounds", ed. J. Buckingham, Chapman and Hall, London, 1982.
19. C. F. van Duin, *Recl. Trav. Chim. Pays-Bas*, 1919, **38**, 359.
20. R. J. W. Le Fevre, *J. Chem. Soc.*, 1931, 813.
21. F. Ullmann and W. Bruck, *Ber. Dtsch. Chem. Ges.*, 1908, **41**, 3936
22. J. Blabak, *Liebigs. Ann. Chem.*, 1978, 1353.
23. D. D. Perrin, "Dissociation Constants of Organic Bases in Aqueous Solution", Butterworths, London, 1972.

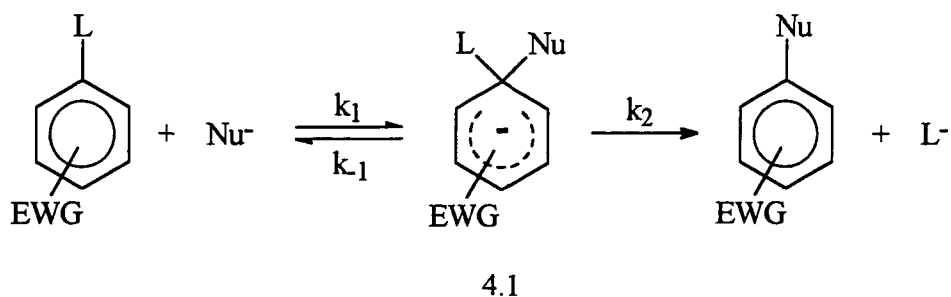
24. P. Kebarle, *Ann. Rev. Phys. Chem.*, 1977, **28**, 445.
25. D. H. Aue, H. M. Webb and M. T. Bowers, *J. Am. Chem. Soc.*, 1976, **98**, 311, 318.
26. E. M. Arnett, "Proton Transfer Reactions", ed. F. F. Caldin and V. Gold, Chapman and Hall, London, 1975, p. 79.
27. A. Mucci, R. Domain and R. L. Benoit, *Can. J. Chem.*, 1980, **58**, 953.
28. M. R. Crampton and S. D. Lord, *J. Chem. Soc. Perkin Trans. 2*, 1997, 369.
29. M. J. Kamlet and R. W. Taft, *J. Am. Chem. Soc.*, 1976, **98**, 377.
30. R. Chamberlin and M. R. Crampton, *J. Chem. Res.*, 1993, (S) 106; (M) 0811.

Chapter 4.

**Stepwise versus Concerted Mechanism in the Reactions
of Phenoxide Ions with Phenyl Picrates?**

4.1 Conflicting Evidence.

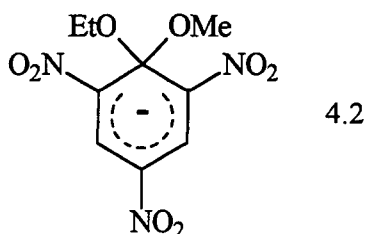
There is considerable evidence that most reactions proceeding via the S_NAr mechanism of nucleophilic aromatic substitution involve an intermediate sitting in a potential energy well. The two step Addition-Elimination mechanism, equation 4.1, postulated by Bunnett is well documented in the literature.^{1,2}



equation 4.1

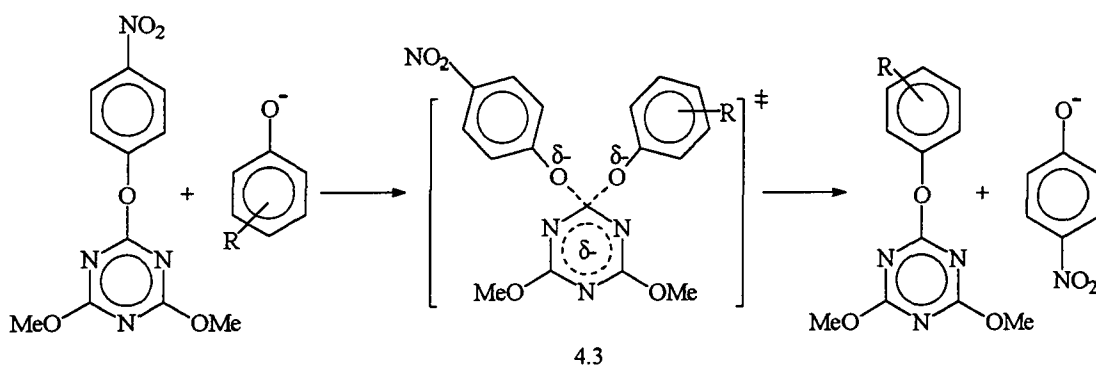
EWG - electron withdrawing groups

The observation and successful NMR identification of intermediates of the type 4.1, known as Meisenheimer complexes or σ -adducts, on the substitution pathways of some nitroaromatics offers significant support to the proposed mechanism.^{3,4} Such an example is that of complex 4.2 produced from the reaction of picryl ethers with alkoxides.⁵ Further, more detailed kinetic studies of leaving group effects and base catalysis in the reactions with amine nucleophiles can only be understood in terms of the presence of intermediates.⁶



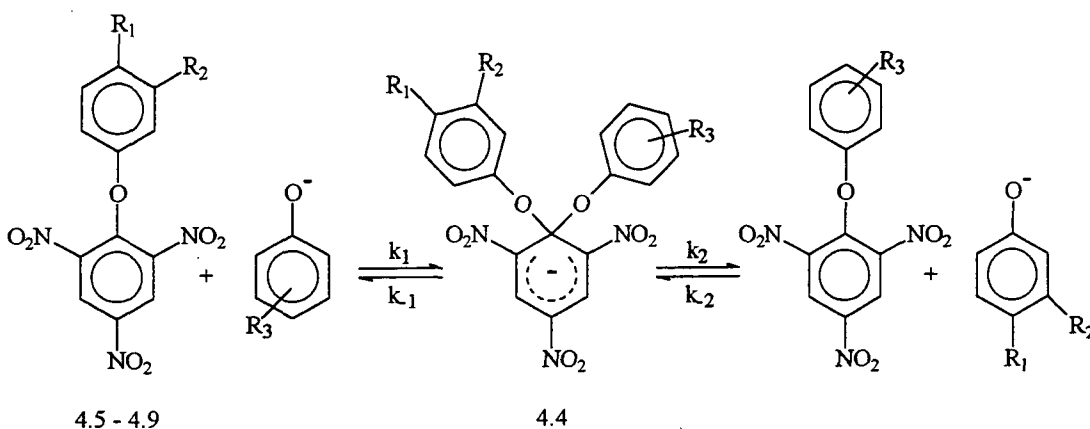
An alternative mechanism for nucleophilic aromatic substitution is one that involves a concerted pathway in which there is a single transition state, i.e. transformation from a two step to a one step process, without the presence of an intermediate. Evidence for the proposed route comes from the displacement of the 4-nitrophenolate ion from 2-(4-nitrophenoxy)-4,6-dimethoxy-1,3,5-triazine by substituted phenolate ions in aqueous solution,^{7,8} equation 4.2.

Here the reaction intermediate is regarded as being very unstable and replaced by a transition state, 4.3. A linear Brønsted plot of $\log k$, where k represents the second order rate constant for displacement, versus pK_a values was observed. The pK_a values are for the parent phenol from which the nucleophiles are derived. The linearity of the plot extended to pK_a values both above and below that of 4-nitrophenol and this linearity was thought to be evidence for a concerted mechanism.



equation 4.2

In order to test the generality of the proposed single step mechanism, second order rate constants for the reaction of various ring substituted phenyl 2,4,6-trinitrophenyl ethers have been measured with a series of substituted phenolate ions, equation 4.3. Whether 4.4 is an intermediate or a transition state is to be determined.



equation 4.3

Substrate	4.5	4.6	4.7	4.8	4.9
Substituent R_1	NO_2	NO_2	H	CHO	H
Substituent R_2	H	NO_2	NO_2	H	CHO

4.2 Linear Free Energy Relationships.

For many reactions of current interest a popular technique used for the investigation of transition state structure is that of linear free energy relationships (LFERs).⁹ Recently the direct calculation of charge densities of the transition states, from the information contained within the slopes of the LFERs, has been questioned.¹⁰ There is, however, agreement that important information is contained within the slopes of these correlations.

4.2.1 Brønsted Equation.

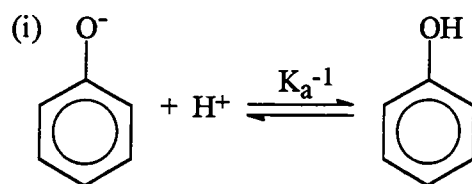
Among LFERs, one of the most important and regularly applied relationships is the Brønsted correlation, equation 4.4, in which k_n is the rate constant for any step 'n' in the reaction.

$$\log k_n = \beta_n \text{p}K_a + C_n \quad \text{equation 4.4}$$

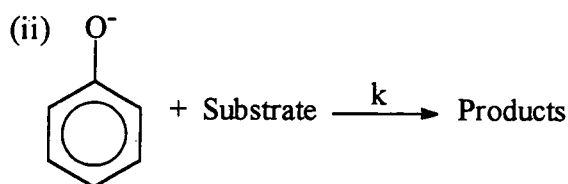
$$k = \text{constant} \left(\frac{1}{K_a} \right)^\beta \quad \text{equation 4.5}$$

Traditional Brønsted type diagrams are constructed in a manner where the $\text{p}K_a$ of the nucleophile is varied by changing substituents on the nucleophile at a position remote from the attacking atom. Originally this was the only method considered to vary $\text{p}K_a$. However, some studies recently have focused on the application of a novel method involving a single nucleophile whose $\text{p}K_a$ is altered using gradual changes in solvent composition.^{11,12} The Brønsted equation relates a rate constant to the equilibrium basicity of the nucleophile. It is derived from equation 4.5 which is obtained on comparison of the analogous reactions described in scheme 4.1, where 4.10 represents the nucleophile.

For a multistep reaction each β value refers to the Brønsted exponent for the individual rate constant in the reaction pathway and may be interpreted as the degree of bond formation in the transition state.^{13,14}



4.10



4.10

scheme 4.1

Linearity in a Brønsted plot, containing values above and below the $\text{p}K_a$ value of the leaving group, is consistent with a one-step process involving a single transition state. For a two step process occurring via a discrete intermediate, two distinct slopes are expected with a breakpoint in the diagram close to the $\text{p}K_a$ of the leaving group, if both entering and leaving groups are similar in structure.

As a consequence, e.g. for the reaction of phenyl 2,4,6-trinitrophenyl ether with substituted phenolates, each step will have its own Brønsted equation, and the second order rate constant, k_s , for the forward reaction will be governed theoretically by the global equation 4.6, where k_0 represents the identity constant, $\Delta\text{p}K_a = \text{p}K_{\text{nuc}} - \text{p}K_{\text{lg}}$ and $\Delta\beta = \beta_2 - \beta_{-1}$, (β_2 and β_{-1} correspond to the rate constants k_2 and k_{-1} in equation 4.3 shown previously). Similarly values of the second order rate constant for the reverse reaction, k_{-s} , can be theoretically calculated on application of the global equation 4.7 using identical expressions for $\Delta\text{p}K_a$ and $\Delta\beta$. A change in the rate determining step is predicted (where the two straight lines intersect) at $\Delta\text{p}K_a = 0$, i.e. when $k_{-1} = k_2$.

$$k_s = k_0 10^{\beta_{-1} \cdot \Delta\text{p}K_a} / (1 + 10^{-\Delta\beta \cdot \Delta\text{p}K_a}) \quad \text{equation 4.6}$$

$$k_{-s} = k_0 10^{\beta_2 \cdot \Delta\text{p}K_a} / (1 + 10^{\Delta\beta \cdot \Delta\text{p}K_a}) \quad \text{equation 4.7}$$

4.3 Experimental Procedure.

Reactions of various substituted phenol / phenolate buffers with five different phenyl 2,4,6-trinitrophenyl ether substrates, 4.5 - 4.9, have been examined in aqueous solution at 25°C. Addition of dioxane (between 5-15% v/v) was required in some cases due to the substrates poor solubility in water. Depending on the reactivity of the phenol either stopped-flow spectrophotometry or a conventional spectrophotometer was used to monitor the appearance of the appropriate leaving group. Table 4.1 lists the respective wavelengths for each deprotonated leaving groups. Figure 4.1 shows the appearance of the leaving group, 4-nitro-phenolate, from substrate 4.5 over time in the presence of a 4-cyano-phenol buffer, pH 7.9. A series of solutions were prepared of various phenolate concentrations at constant pH, solvent composition and ionic strength, 0.1 mol dm⁻³. Reactions were initiated by the addition of the substrate solution to a prepared sample solution contained within a thermostatted cuvette compartment.

Figure 4.1 U.V./Vis. spectra for the reaction of 4'-nitrophenyl 2,4,6-trinitrophenyl ether, 4×10^{-5} mol dm⁻³, with 4-cyano-phenolate buffer, 0.01 mol dm⁻³ at 25°C in 5% dioxane-water (v/v). Scans repeated every 25 seconds.

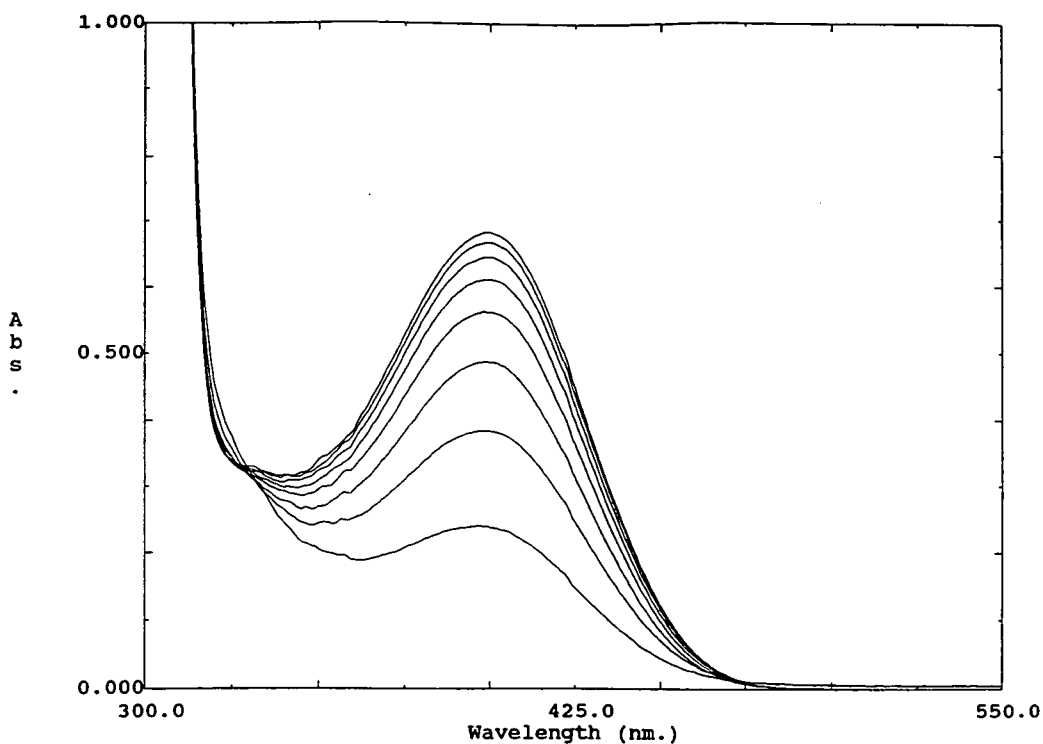


Table 4.1 Spectroscopic and pK_a details.

Substrate, substituent	4.5 4-NO ₂	4.6 3,4-NO ₂	4.7 3-NO ₂	4.8 4-CHO	4.9 3-CHO
λ /nm	400	400	400	365	360
log ε	4.32	4.18	3.40	3.48	3.40
pK _a	7.12	5.28	8.19	7.66	8.99

4.3.1 Buffer Solutions.

Stock solutions of each nucleophile were prepared with known concentrations of phenol (PhOH) and phenolate (PhO⁻) present. The latter was formed by the addition of a measured quantity of sodium hydroxide. The pH of the solution was calculated, using equation 4.8, and also measured using a pH meter. It is important to note that only the deprotonated form of the leaving group has a strong U.V./Vis. absorption. Consequently buffer solutions were prepared with a pH above the pK_a of the respective leaving group, table 4.1, by adjusting the ratio of PhOH / PhO⁻ accordingly. Although, solutions with very high pH could not be used due to the competing reaction of hydroxide occurring with the substrate, figure 4.2 and 4.3.

$$\text{pH} = \text{pK}_a + \log_{10} \frac{[\text{PhO}^-]}{[\text{PhOH}]} \quad \text{equation 4.8}$$

Addition of external buffers, e.g. tris(hydroxymethyl)aminomethane or borax was prevented because of an undetermined interaction with the substrates. In general buffer solutions were prepared with a pH value one unit higher than the pK_a of the leaving group. Solutions containing phenols with poor solubility were firstly converted fully to the phenolate, followed by gradual addition of dilute hydrochloric acid until the optimum pH value was obtained. A stock solution would then be diluted appropriately for each kinetic run, ensuring constant pH was maintained for all experimental solutions.

4.3.2 Sampling Technique.

This technique was used for phenols of very low reactivity, i.e. tetra and penta halogenated phenols, where a high pH buffer could not be employed as the reaction with hydroxide interferes. To overcome this, reactions were performed at a pH much lower than that of the pK_a of the leaving group, at high concentrations. Sampling involves the removal of 1ml of reaction solution to which is added 1ml of sodium carbonate buffer, in a cuvette. This restores the pH to a value above that of the leaving group allowing the absorbance measurement of the deprotonated phenol to be taken immediately. The reactions were followed over approximately 4-5 days, thermostatted at 25°C, with absorbance readings taken every hour initially increasing to longer intervals as the reaction proceeds.

Figure 4.2 Addition of U.V./Vis. spectrum (a) Picric acid, $4 \times 10^{-5} \text{ mol dm}^{-3}$, to (b) 4-nitro-phenol, $4 \times 10^{-5} \text{ mol dm}^{-3}$, both in the presence of phenol buffer, pH 10, and 5% dioxane-water, gives (c) spectrum expected for the formation of picric acid.

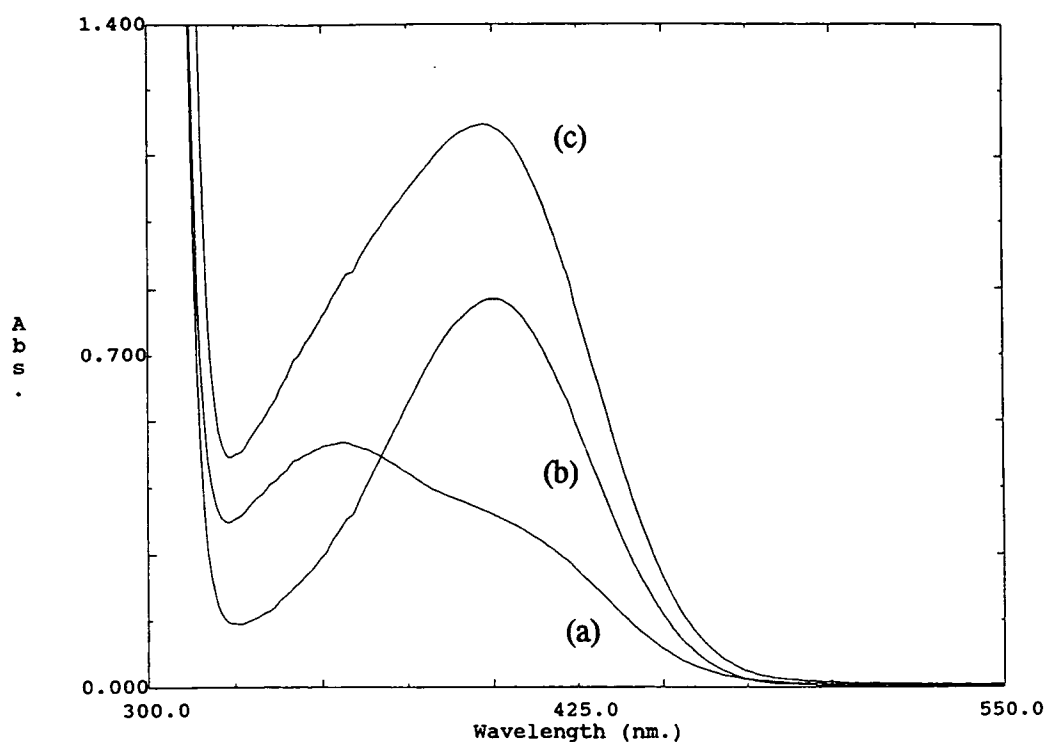
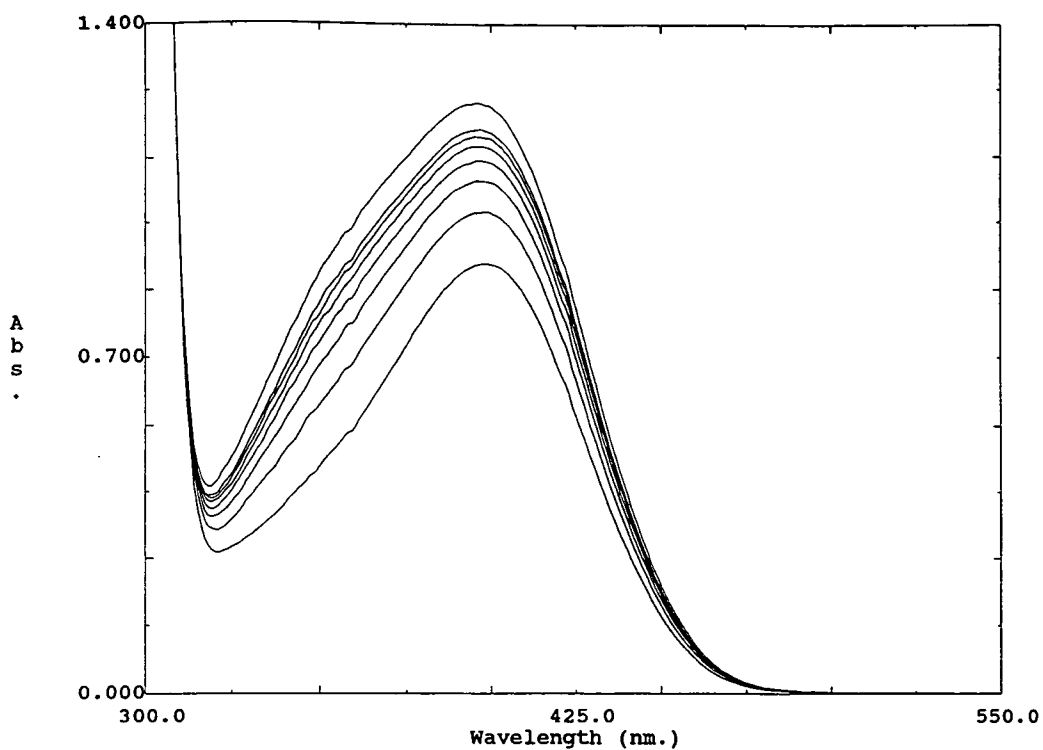


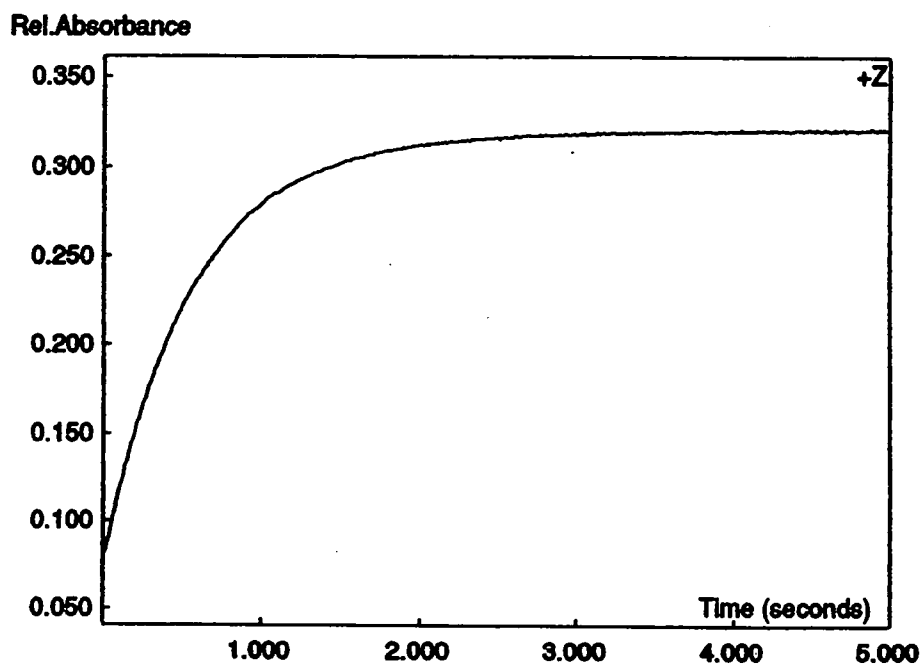
Figure 4.3 U.V./Vis. spectra showing the formation of picric acid after the completion of the initial reaction between 4'-nitrophenyl 2,4,6-trinitrophenyl ether, $4 \times 10^{-5} \text{ mol dm}^{-3}$, with 4-cyano-phenolate buffer, 0.01 mol dm^{-3} at 25°C in 5% dioxane-water (v/v). Scans taken every 4 minutes. Final scan after 3 hours.



4.4 The Forward Process: Reactions of Substituted Phenyl 2,4,6-Trinitrophenyl Ethers.

Kinetic measurements were conducted under pseudo first order conditions with the buffer concentration (PhOH / PhO⁻) in large excess of the substrate, 2×10^{-5} mol dm⁻³ unless otherwise stated. Figure 4.4 provides an example of the kinetic traces observed, from which values of the observed first order rate constant, k_{obs} , were calculated with correlation coefficients between 0.992 - 0.999. Ionic strength is maintained at 0.1 mol dm⁻³ using sodium chloride. In certain cases, kinetic traces showed a sloping infinity line due to the subsequent slow formation of picric acid. However this imposed no problem for obtaining a value of the observed rate constant, requiring only a slight change in the technique of calculation.

Figure 4.4 Kinetic trace produced for the reaction of 4.5 with 4-methoxy-phenol buffer, 0.005 mol dm⁻³, pH 10.19, $\lambda = 400\text{nm}$, in 5% dioxane-water at 25°C.



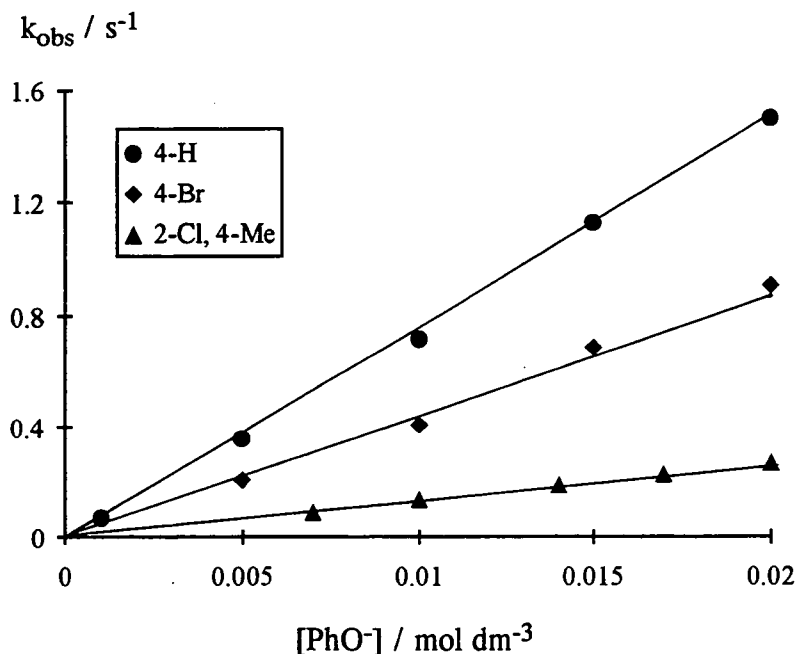
4.4.1 4'-Nitrophenyl 2,4,6-Trinitrophenyl Ether, 4.5.

Kinetic results obtained at a wavelength $\lambda = 400\text{nm}$, show a linear dependence on phenolate concentration at a constant pH, figure 4.5. Generally, buffer solution ratios, $\text{PhOH} / \text{PhO}^-$ are equal to 1:1 unless otherwise stated. On changing the pH, i.e. change the buffer ratio to 2:1, an almost identical dependence was observed, indicating no reaction with hydroxide ions. Table 4.2 displays the variation of the observed rate constant, k_{obs} , with phenolate concentration.

Table 4.2 Dependence of rate constants for reaction of 4'-nitro-phenyl 2,4,6-trinitrophenyl ether, 4.5, on phenolate concentration, pH 10, in 5% dioxane-water (v/v) at 25°C. $I = 0.1 \text{ mol dm}^{-3}$.

$[\text{PhO}^-] / \text{mol dm}^{-3}$	0.001	0.005	0.010	0.015	0.020
$k_{\text{obs}} / \text{s}^{-1}$	0.07	0.36	0.72	1.13	1.50

Figure 4.5 Rate dependency for different substituted phenols.



From the data above, values of the second order rate constant for the forward reaction, k_s , can be obtained by determining the gradients of the graphs for each substituted phenol, equation 4.9.

The values of the second order rate constants vary as the basicities of the phenolates are changed. For example, 4-bromo-phenolate is less nucleophilic than phenolate due to the presence of an electron withdrawing halogen. Values of k_s are summarised in table 4.3.

$$k_{\text{obs}} = k_s[\text{PhO}^-] \quad \text{equation 4.9}$$

Table 4.3 Kinetic data for the reactions of substituted phenolate ions with 4'-nitro-phenyl 2,4,6-trinitrophenyl ether, pK_a 7.12, $\lambda = 400\text{nm}$, in 5% dioxane-water (v/v) at 25°C. $I = 0.1 \text{ mol dm}^{-3}$.

Substituent, R_3	pK_a^a	$k_s / \text{dm}^3 \text{ mol}^{-1} \text{ s}^{-1}$	pH	$[\text{R}_3\text{-PhO}^-] / 10^{-2} \text{ mol dm}^{-3}$	$k_{\text{obs}} / \text{s}^{-1}$
4-MeO	10.3	370 ± 2	10.19	0.1 - 2.0	0.3 - 7.5
4-H	9.81	73 ± 1	10.0	0.05 - 1.5	0.07 - 1.5
4-H ^b	"	71 ± 1	9.59	0.5 - 3.0	0.17 - 1.1
4-Cl	9.26	52 ± 0.2	9.37	0.7 - 2.0	0.4 - 1.0
4-Br	9.21	44 ± 1	9.21	0.5 - 2.0	0.2 - 1.0
2-Cl, 4-Me	8.68	13.6 ± 0.2	9.40	0.7 - 2.0	0.1 - 0.3
2-Cl	8.32	4.5 ± 0.4	9.20	0.7 - 2.0	$3 - 9 \times 10^{-2}$
4-CN	7.80	1.28 ± 0.01	7.92	0.7 - 2.0	$1 - 3 \times 10^{-2}$
2-CN	7.22	$0.22 \pm 7 \times 10^{-3}$	7.15	0.7 - 2.0	$2 - 4 \times 10^{-3}$
2,3,5-trifluoro	6.93	$3.6 \times 10^{-2} \pm 5 \times 10^{-3}$	7.23	0.3 - 1.8	$2 - 7 \times 10^{-4}$
2,3,5-trichloro	6.58	$5.7 \times 10^{-2} \pm 8 \times 10^{-3}$	8.03	0.3 - 1.5	$5 - 12 \times 10^{-4}$
2,3,5,6-tetrafluoro ^c	5.41	$8.3 \times 10^{-5} \pm 2 \times 10^{-5}$	6.33	10 - 30	$1 - 3 \times 10^{-5}$
Penta-fluoro ^c	5.33	$< 4.0 \times 10^{-5}$	5.91	10 - 30	1.2×10^{-5}

^a Obtained from ref. 8 and 14.

^b Approximately 2:1 buffer ratio, $\text{PhOH}:\text{PhO}^-$.

^c Experiments completed using the sample method.

4.4.2 3',4'-Dinitrophenyl 2,4,6-Trinitrophenyl Ether, 4.6.

Experiments similar to those described previously have been repeated with substrate 4.6. Almost identical conditions have been applied, the only difference being the lowering of the buffer pH for the less reactive phenols to reduce the rate of unwanted picric acid formation caused by the increased reactivity of 4.6. Overall all reactions for substrate 4.6 occurred more rapidly than those for 4.5. Observed first order rate constants again showed a linear dependence on phenolate concentration, the results for various substituted phenols are summarised in table 4.4.

Table 4.4 Kinetic data for the reactions of substituted phenolate ions with 3',4'-dinitro phenyl 2,4,6-trinitrophenyl ether, 4.6, pK_a 5.28, $\lambda = 400\text{nm}$, in 10% dioxane-water (v/v) at 25°C. $I = 0.1 \text{ mol dm}^{-3}$.

Substituent, R_3	pK_a^a	$k_s / \text{dm}^3 \text{ mol}^{-1} \text{ s}^{-1}$	pH	$[\text{R}_3\text{-PhO}^-] / 10^{-2} \text{ mol dm}^{-3}$	$k_{\text{obs}} / \text{s}^{-1}$
4-MeO	10.3	1281 ± 14	10.04	0.1 - 1.5	1 - 20
4-H	9.81	260 ± 1	9.9	0.2 - 1.4	0.6 - 3.5
2-Cl, 4-Me	8.68	76 ± 0.6	9.26	0.7 - 2.0	0.5 - 1.5
2-Cl	8.32	23.5 ± 0.7	8.68	0.7 - 2.0	$2 - 5 \times 10^{-1}$
2-CN	7.22	$3.14 \pm 4 \times 10^{-2}$	6.92	0.7 - 1.7	$2 - 5 \times 10^{-2}$
2,3,5-trichloro	6.58	$1.19 \pm 8 \times 10^{-2}$	8.22	0.3 - 1.5	$2 - 19 \times 10^{-3}$
2,3,5,6-tetrafluoro	5.41	$1.5 \times 10^{-2} \pm 4 \times 10^{-4}$	6.33	0.5 - 2.5	$1 - 4 \times 10^{-4}$

^a Obtained from ref. 8 and 14.

4.4.3 3'-Nitrophenyl 2,4,6-Trinitrophenyl Ether, 4.7.

A similar experimental procedure was followed for the reactions of 4.7. It is required, for ease of measurement, that the pH of the phenolic buffers should be higher than that of the leaving group, pK_a 8.19. The use here of rather more alkaline media than previously, necessitated larger concentrations of phenolates to reduce interference from hydroxide ions. A first order dependence on phenolate ions was again observed and the results can be viewed in the table 4.5 below.

Table 4.5 Kinetic data for the reactions of substituted phenolate ions with 3'-nitro phenyl 2,4,6-trinitrophenyl ether, 4.7, pK_a 8.19, $\lambda = 400\text{nm}$, in 15% dioxane-water (v/v) at 25°C. $I = 0.1 \text{ mol dm}^{-3}$.

Substituent, R_3	pK_a^a	$k_s / \text{dm}^{-3} \text{ mol}^{-1} \text{ s}^{-1}$	pH	$[R_3\text{-PhO}^-] / 10^{-2} \text{ mol dm}^{-3}$	$k_{\text{obs}} / \text{s}^{-1}$
4-MeO	10.3	521 ± 2	10.35	0.7 - 1.5	3 - 8
4-H	9.81	124 ± 2	9.91	0.7 - 1.5	0.09 - 1.9
4-Cl	9.26	85 ± 2.0	9.30	0.7 - 1.5	0.5 - 1.3
2-Cl, 4-Me	8.68	23.4 ± 0.3	9.43	0.7 - 2.0	0.1 - 0.5
2-Cl	8.32	5.87 ± 0.04	9.23	1.4 - 2.5	$8 - 15 \times 10^{-2}$
4-CN	7.80	1.25 ± 0.01	8.72	1.4 - 2.5	$2 - 3 \times 10^{-2}$
2-CN	7.22	$0.063 \pm 5 \times 10^{-3}$	8.5	5 - 25	$4 - 16 \times 10^{-3}$
Penta-fluoro ^b	5.33	$1.4 \times 10^{-5} \pm 1 \times 10^{-6}$	7.58	5 - 15	$9 - 11 \times 10^{-6}$

^a Obtained from ref. 8 and 14.

^b Experiments completed using the sample method.

4.4.4 Forward Process: Brønsted Diagrams.

Values of the second order rate constant for displacement, k_s , and the corresponding pK_a value of the respective phenols can be utilised to form a Brønsted plot for each substrate, 4.5, 4.6 and 4.7. Table 4.6 provides values of $\log k_s$ and pK_a for substrates 4.5, 4.6 and 4.7 which can be viewed in the Brønsted diagrams, figure 4.6, 4.7 and 4.8.

Each diagram consists of two intersecting linear correlations consistent with a two step mechanism involving a Meisenheimer type intermediate. The break in linearity is predicted to occur at the pK_a of the leaving group, indicating a change in the rate limiting step for a stepwise process.⁷ Figures 4.6, 4.7 and 4.8 clearly show this shift in accordance with the pK_a of their respective leaving groups, 4-nitro-phenol, 7.12, 3,4-dinitro-phenol, 5.26 and 3-nitro-phenol 8.19. A precise break is not clearly visible in figure 4.7 because very few reactive phenol nucleophiles could be found with a pK_a lower than that of 5.26, although the plot still illustrates a shift in the break point.

Table 4.6 Brønsted correlation data.

pK_a^a	Substrate 4.5 ^b $\log k_2$	Substrate 4.6 ^c $\log k_2$	Substrate 4.7 ^d $\log k_2$
10.3	2.57	3.11	2.71
9.81	1.86	2.41	2.09
9.26	1.85	-	1.93
9.21	1.72	-	-
8.68	1.13	1.88	1.37
8.32	0.65	1.37	0.77
7.80	0.11	-	0.10
7.22	-0.66	0.50	-1.20
6.93	-1.44	-	-
6.58	-1.24	0.08	-
5.41	-4.08	-1.82	-
5.33	< -4.40 ^e	-	-4.85

^a Obtained from ref. 8 and 15.

^b 5% ^c 10% ^d 15% dioxane-water (v/v).

^e a limiting value.

Figure 4.6 Brønsted plot for the reaction of 4.5. Conditions are from table 4.3.

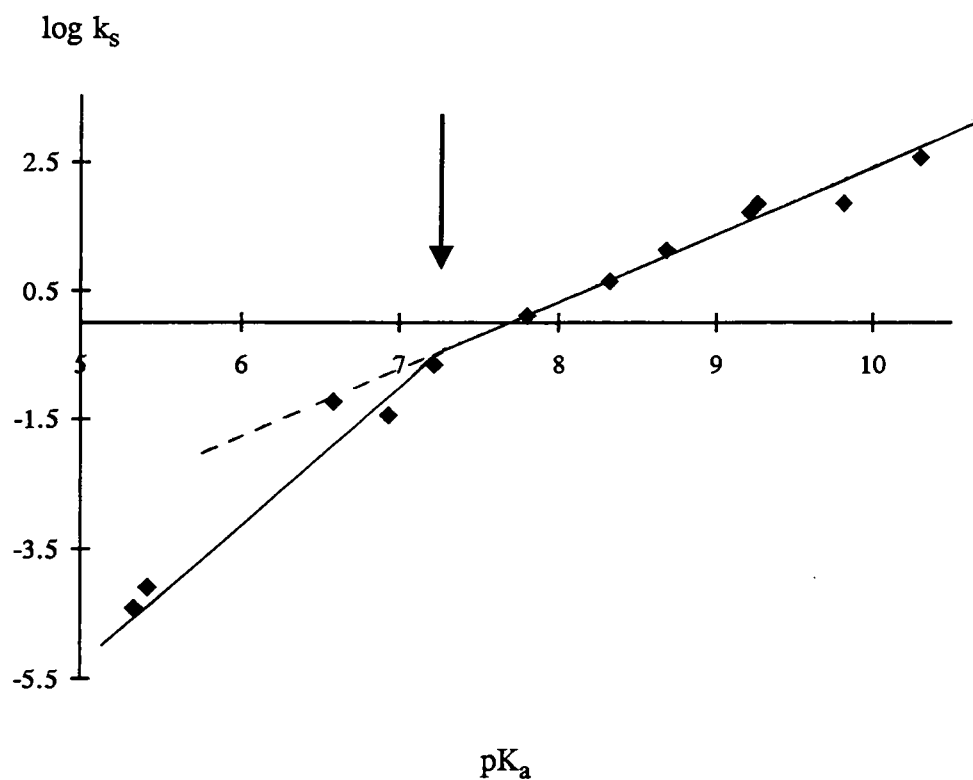


Figure 4.7 Brønsted plot for the reaction of 4.6. Conditions are from table 4.4.

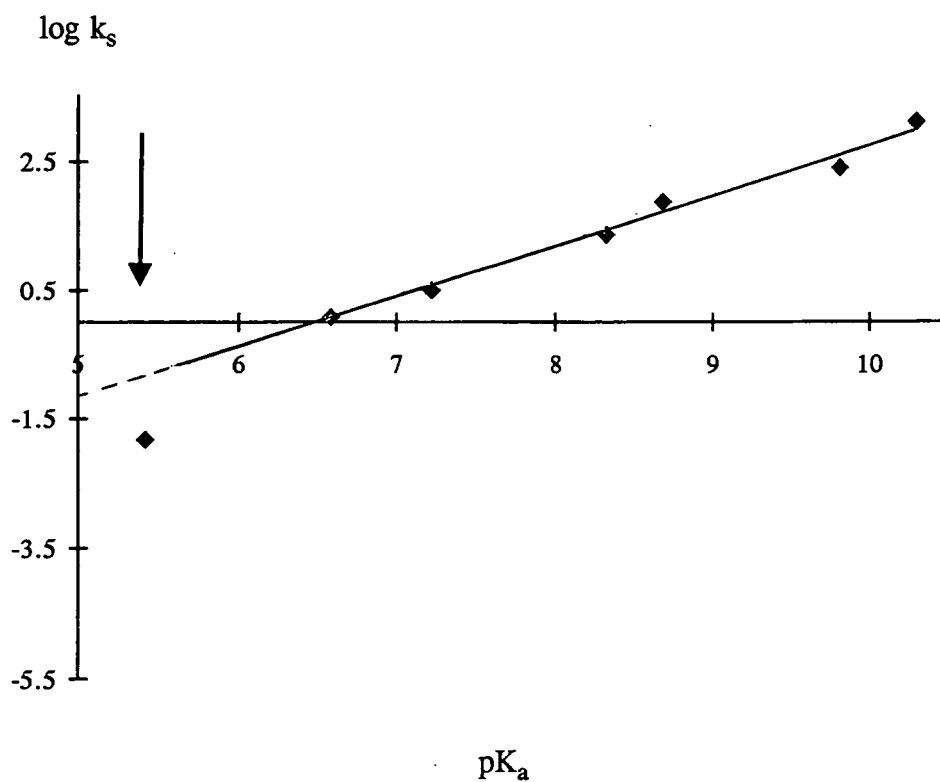
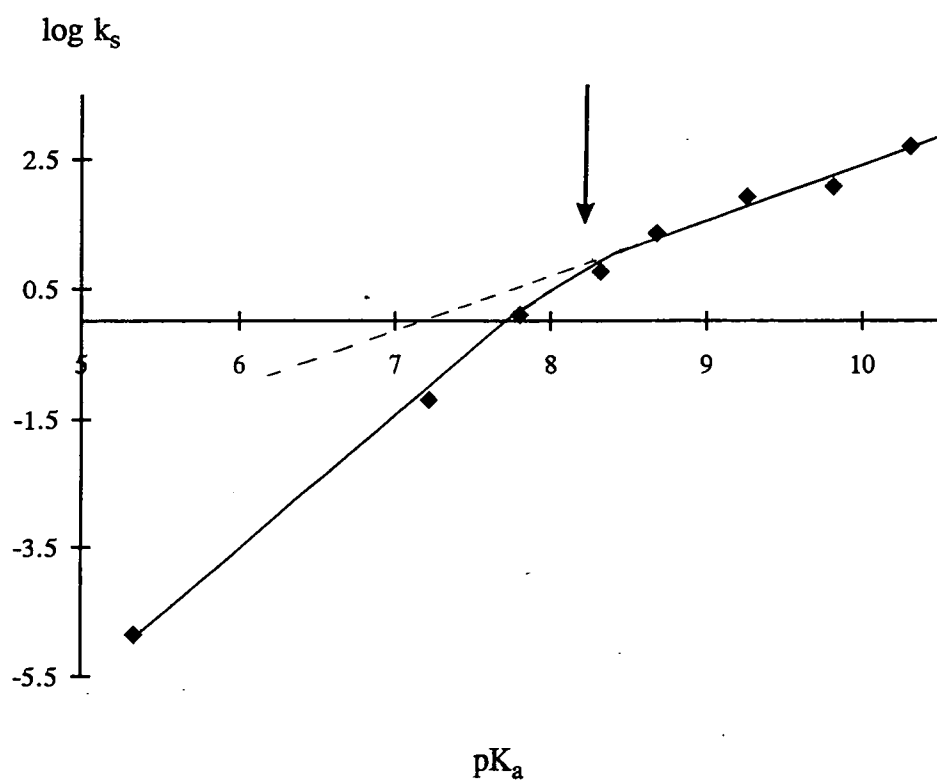


Figure 4.8 Brønsted plot for the reaction of 4.7. Conditions are from table 4.5.

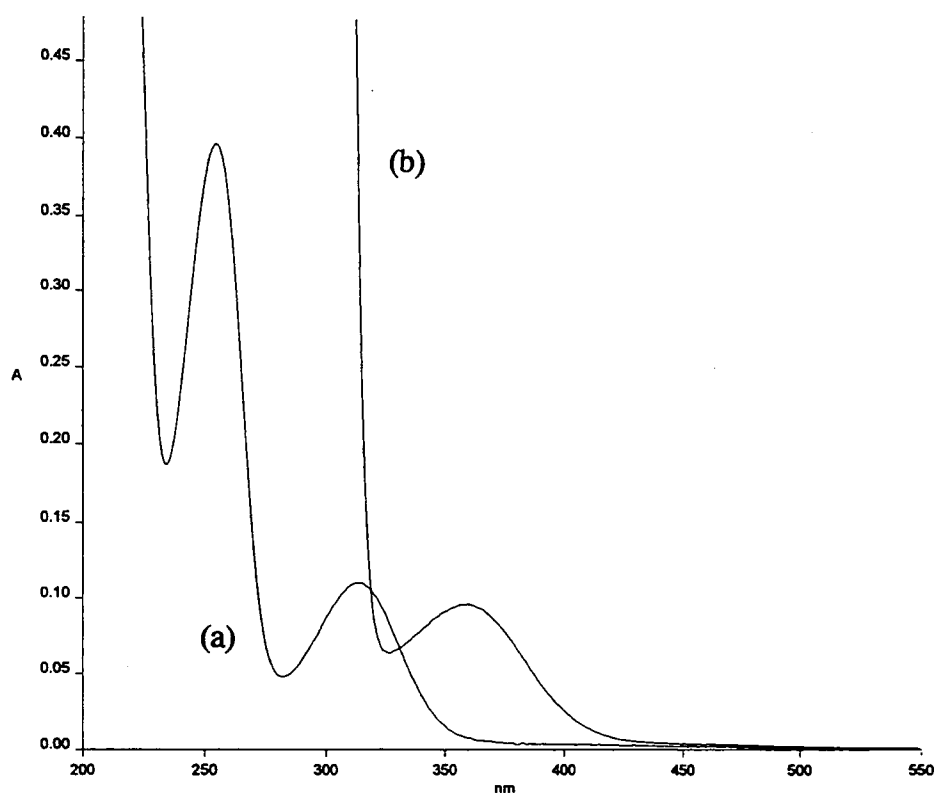


4.5 The Reverse Process: Dependence on Substrate Structure.

It is possible to construct an alternative type of Brønsted diagram by studying the variation of rate constants with various substrate structures while keeping the attacking nucleophile identity constant.

Five substrates were considered, compounds 4.5, 4.6, 4.7 mentioned previously and also 3'- and 4'-formyl-phenyl 2,4,6-trinitrophenyl ether, 4.8 and 4.9 respectively. Each substrate was added to various concentrations of a single substituted phenol buffer and monitored at the respective wavelength of the deprotonated leaving group, table 4.1. An example of the protonated and deprotonated U.V./Vis. spectrum of 3-formyl-phenol is shown in figure 4.9.

Figure 4.9 U.V./Vis. spectra of (a) 3-formyl-phenol, 4×10^{-5} mol dm⁻³.
(b) 3-formyl-phenol with pH 9.9 buffer in 15% dioxane-water (v/v).



With buffer concentrations in large excess of the substrate, first order kinetics were observed. All measurements were made in 15% dioxane-water (v/v) and in the presence of sodium chloride to maintain ionic strength at 0.1 mol dm⁻³. Depending on the reactivity of the phenol or substrate either a stopped-flow or a conventional spectrophotometer was used.

4.5.1 Phenol Nucleophile.

Results for the reaction of phenol buffer (PhOH:PhO⁻ 1:1) with each substrate are summarised in table 4.7. Note that data shown previously for the reaction of phenol were in different solvent compositions. Figure 4.10 shows the results graphically. The gradients of the lines are equal to a second order rate constant for the reverse reaction, k_s , and are summarised in table 4.8. It can be seen that values of k_s generally increase as the pK_a value of the leaving group decreases. This will be discussed in more detail later.

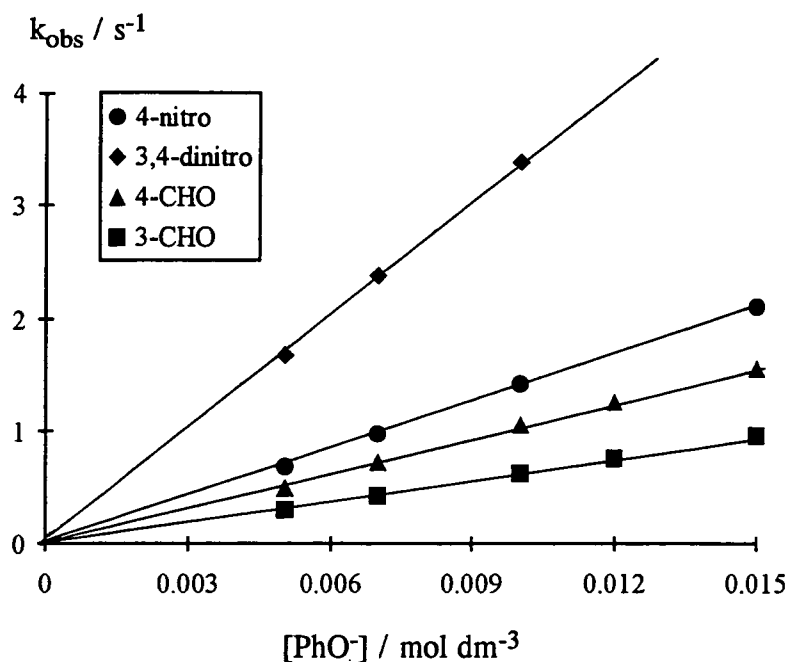
Table 4.7 Dependence of 4'-substituted-phenyl 2,4,6-trinitrophenyl ethers on phenolate concentration in 15% dioxane-water (v/v) at 25°C.
 $I = 0.1 \text{ mol dm}^{-3}$.

[PhO ⁻] / mol dm ⁻³	0.005	0.007	0.010	0.012	0.015	
$k_{\text{obs}} / \text{s}^{-1}$	4.5	0.69	0.98	1.42	-	2.12
	4.6	1.69	2.39	3.39	-	5.14
	4.7	-	0.87	1.17	1.55	1.85
	4.8	0.50	0.73	1.06	1.26	1.57
	4.9	0.31	0.43	0.64	0.76	0.96

Table 4.8 Summary of second order rate constants for the reaction of phenolate ion with substituted phenyl 2,4,6-trinitrophenyl ethers in 15% dioxane-water (v/v) at 25°C.

Substrate	4.9	4.7	4.8	4.5	4.6
$k_s /$ dm ³ mol ⁻¹ s ⁻¹	63.3 ± 0.7	123 ± 1	105 ± 0.3	142 ± 4	326 ± 20
pK_a	8.99	8.19	7.66	7.12	5.28

Figure 4.10 Rate dependency of different substrates reacting with phenol buffer.



4.5.2 4-Chloro-Phenol Nucleophile.

Kinetic data for the reaction of 4-chloro-phenol buffers (1:1) with each substrate are reported. Gradients calculated from the graphs of k_{obs} versus 4-chloro-phenolate are equal to second order rate constants for the reverse reaction, k_s , table 4.9.

Table 4.9 Summary of second order rate constants for the reaction of 4-chloro-phenolate ion with substituted phenyl 2,4,6-trinitrophenyl ethers in 15% dioxane-water (v/v) at 25°C. $I = 0.1 \text{ mol dm}^{-3}$.

Substrate	$k_s / \text{dm}^3 \text{ mol}^{-1} \text{ s}^{-1}$	pK _a	[4-Cl-PhO ⁻] / $10^{-3} \text{ mol dm}^{-3}$	$k_{\text{obs}} / 10^{-3} \text{ s}^{-1}$
4.9	30 ± 1	8.99	29 - 36	0.9 - 1.1
4.7	85 ± 1	8.19	7 - 15	0.5 - 1.3
4.8	63 ± 2	7.66	29 - 36	1.8 - 2.3
4.5	97 ± 1	7.12	5 - 15	0.5 - 1.5
4.6	231 ± 4	5.28	5 - 15	1.1 - 3.5

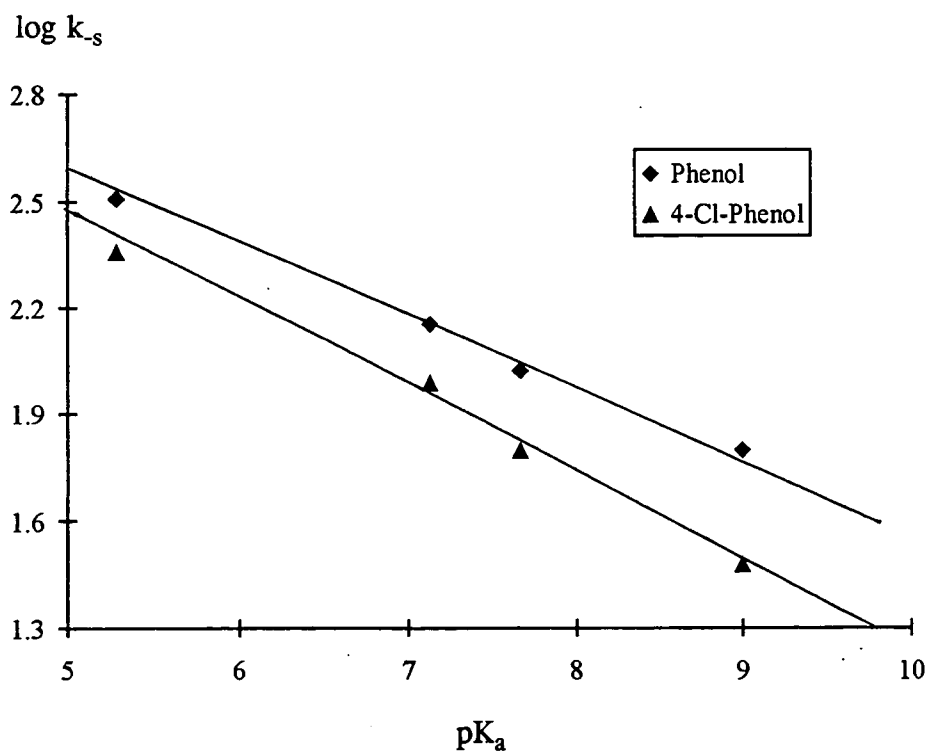
4.5.3 Reverse Process: Brønsted Diagrams.

Two Brønsted diagrams may be created upon plotting values of the second order rate constant for the reverse reaction, k_{-s} , obtained for each nucleophile, versus the pK_a of the various leaving groups examined. The required kinetic data are reported in table 4.10 and the Brønsted diagrams may be viewed in figure 4.11. Importantly, single linear correlations are produced due to the values of pK_a for the leaving groups all being below the pK_a value of the two nucleophiles, e.g. phenol pK_a 9.81 and 4-chloro-phenol pK_a 9.26. It is at these points where the break points are expected. Interestingly values approaching these break points show a slight deviation.

Table 4.10 Brønsted correlation data for phenol and 4-chloro-phenol.

pK_a	8.99	8.19	7.66	7.12	5.28
Phenol $\log k_{-s}$	1.80	2.09	2.02	2.15	2.51
4-Cl-Phenol $\log k_{-s}$	1.48	1.93	1.80	1.99	2.36

Figure 4.11 Brønsted plot for the reaction of phenol and 4-chloro-phenol. Conditions are from table 4.8 and 4.9 respectively.



4.6 Kinetic Analysis.

Kinetic and equilibrium results are interpreted in terms of equation 4.3, in which structure 4.4 is now proposed to be an intermediate in a two step process. Application of the steady-state approximation to the forward process gives equation 4.10. From this two limiting situations can apply; firstly nucleophilic attack may be rate limiting, i.e. $k_2 > k_{-1}$, which results in equation 4.11, followed secondly by the condition $k_{-1} > k_2$, where leaving group expulsion is rate limiting, equation 4.12. Each case can be recognised in the Brønsted diagrams pictured earlier.

$$k_s = \frac{k_1 k_2}{(k_{-1} + k_2)} \quad \text{equation 4.10}$$

$$k_s = k_1 \quad \text{equation 4.11}$$

$$k_s = K_1 k_2 \quad \text{equation 4.12}$$

4.6.1 Forward Process.

For the reactions of the 4'-substituted phenyl 2,4,6-trinitrophenyl ethers, 4.5, 4.6 and 4.7 with a range of nucleophiles with pK_a values both above and below that of the leaving group, two distinct lines may be observed from the Brønsted diagrams. In the case of substrate 4.7, the region comprising of nucleophiles with a pK_a value greater than that of the leaving group (pK_a 8.19) will correspond to equation 4.11 signifying that nucleophilic attack is rate limiting. An increase in pK_a , i.e. nucleophilicity, will produce an increase in k_s (now written k_1) and a subsequent increase in $\log k_s$. Appropriate use of equation 4.4 will therefore enable a value of β_1 to be determined from the gradient of the graph in this linear region, equation 4.13.

$$\log k_s = \log k_1 = \beta_1 pK_a + C_1 \quad \text{equation 4.13}$$

$$\log k_s = \log K_1 k_2 = (\beta_1 + \beta_2 - \beta_{-1}) pK_a + C_{12} \quad \text{equation 4.14}$$

The second linear section where pK_a values are below that of the leaving group corresponds to equation 4.12, signifying that expulsion of the leaving group is rate determining. In this region values of $\log k_s$ (now written $\log K_1 k_2$) decrease substantially with the lowering of pK_a , reflecting the slight decrease of k_1 observed in the first situation but now also an accompanying large increase in k_{-1} , due to the attacking nucleophile being a better leaving group.

Values of k_2 are expected to be affected little by the change in pK_a . Application of equation 4.4 and calculation of the gradient in the linear region allows the term $\beta_1 + \beta_2 - \beta_{-1}$ to be estimated, equation 4.14.

4.6.2 Reverse Process.

Ideally, it would be appropriate to study the reverse reaction shown in equation 4.3, that of the 4-nitro-phenolate ion (or the 3,4-dinitrophenolate ion or the 3-nitrophenolate ion) with different substrates. But, due to the poor reactivity of 4-nitro-phenolate this is not possible. An alternative is to conduct the reactions with a more reactive nucleophile, e.g. phenolate or 4-chloro-phenolate and extrapolate the β values determined to the pK_a of 4-nitro-phenol. On application of this method a similar kinetic analogy, as depicted previously in section 4.6, can be concluded for the reverse reactions involving a single nucleophile with various substrates. The appropriate changes to the kinetic expressions are shown below. Equation 4.16 and 4.17 relate to rate limiting nucleophilic attack and rate limiting leaving group departure respectively.

$$k_{-s} = \frac{k_{-2}k_{-1}}{(k_2 + k_{-1})} \quad \text{equation 4.15}$$

$$k_{-s} = k_{-2} \quad \text{equation 4.16}$$

$$k_{-s} = k_{-2}k_{-1} / k_2 \quad \text{equation 4.17}$$

Since all values of pK_a reported are below that of the nucleophile only one situation applies. The small increase in the values of $\log k_{-s}$ with decreasing pK_a , shown in figure 4.11, reflect the increased rate constants for nucleophilic attack when the substituents, R_3 in the diphenyl ether are made more electron withdrawing. Equation 4.15 now becomes equation 4.16 and applying equation 4.4, as previously, a value of β_{-2} may be determined from the gradient. The value of β_{-2} appears independent of the nucleophile used, i.e. a similar value is obtained for both phenol and 4-chloro-phenol and is therefore presumed to have an equivalent value in the case of 4-nitro-phenol. If kinetic data could be obtained above that of the pK_a of the nucleophile, values of $\log k_{-s}$ would be expected to decrease rapidly as the ratio k_{-1} / k_2 would decrease substantially due to the presence of poorer leaving groups.

4.6.3 Brønsted β Values.

Approximations for the various β values obtained from the Brønsted diagrams are summarised in table 4.11. It is important to recognise that the Brønsted diagrams are in fact curves and not simply two individual intersecting lines. Hence, application of the global equation 4.6 will enable optimum values of β_1 , $\Delta\beta$ and the identity rate constant k_0 to be determined, producing calculated values of k_s that best fit the experimental data. β Values acquired for substrate 4.7 and the average value of β_{-2} , all determined in 15% dioxane-water (v/v), will be used initially as estimates.

Table 4.11 Approximated β values.

Substrate	Nucleophile	β_1	$\beta_1 + \beta_2 - \beta_{-1}$	$\Delta\beta$	$-\beta_{-2}$
4.5	various	0.93 ± 0.08	1.88 ± 0.08	0.95	-
4.6	"	0.83 ± 0.06	-	-	-
4.7	"	0.89 ± 0.10	1.98 ± 0.06	1.09	-
various	phenol	-	-	-	0.18 ± 0.03
"	4-Cl-phenol	-	-	-	0.21 ± 0.04

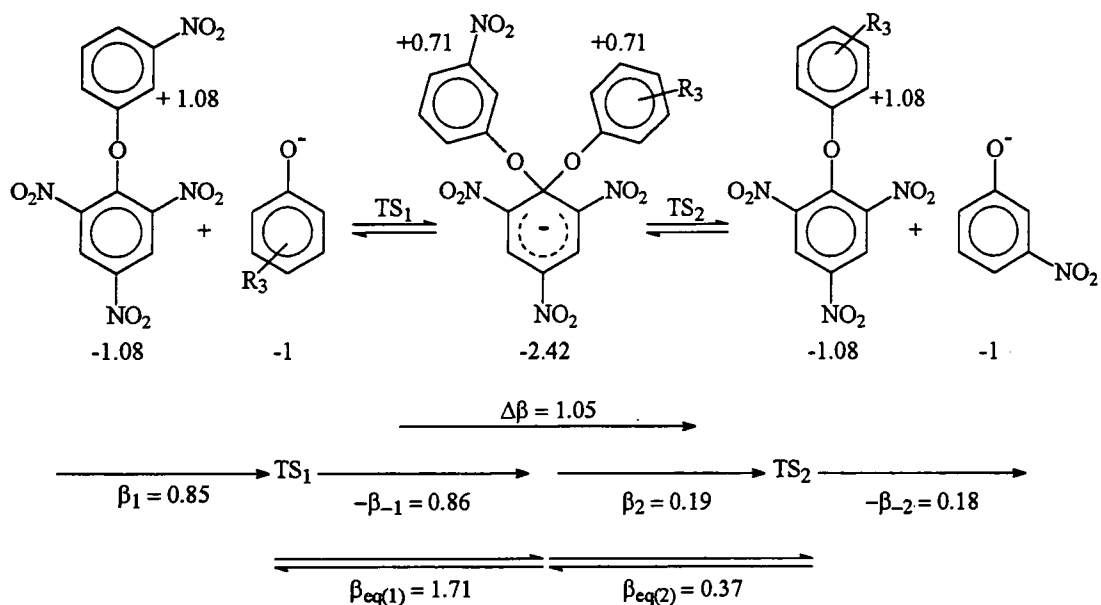
Excellent agreement is obtained between experimental and calculated data for substrate 4.7 with β_1 0.85 ± 0.05 , $\Delta\beta$ 1.05 ± 0.1 and the identity rate constant k_0 $7.8 \pm 0.4 \text{ dm}^3 \text{ mol}^{-1} \text{ s}^{-1}$, table 4.12. Experimental data acquired for the reverse process, k_{-s} , will not resemble the calculated rate constant values, as the latter is equivalent to the theoretical reaction of 3'-nitro-phenolate with various substrates.

Table 4.12 Comparison of experimental and kinetic data for the forward process involving reactions of substrate 4.7 with various phenols.

pK_a	$\log k_s$	$\log k_{\text{calc}}$
10.3	2.72	2.69 ± 0.03
9.81	2.09	2.26 ± 0.03
9.26	1.93	1.77 ± 0.02
8.68	1.37	1.20 ± 0.03
8.32	0.77	0.77 ± 0.04
7.8	0.10	0.01 ± 0.005
7.22	-1.20	-1.00 ± 0.004
5.33	-4.85	-4.54 ± 0.2

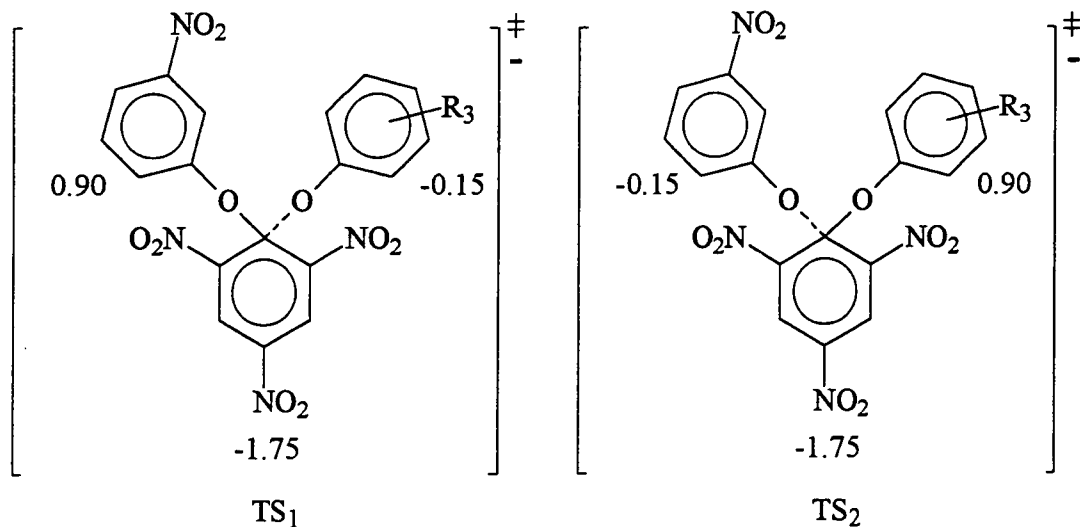
4.6.4 Effective Charge Map.

Scheme 4.2 shows diagrammatically the full effective charge map for the putative stepwise process for phenoxide ion attack on the parent phenyl 2,4,6-trinitrophenyl ether species. Detailed effective charge distribution for the transition states found in step 1 and 2 are represented by TS_1 and TS_2 , respectively.



scheme 4.2

It is important to note that the values of effective charge stated are calculated from data acquired for the 3'-nitro-phenyl 2,4,6-trinitrophenyl ether substrate. Changes in 3'-nitro or the R_3 substituent would alter the balance of effective charge values according to their electron withdrawing or donating ability.



Values of each subsequent β parameter were determined using β_1 0.85, $\Delta\beta$ ($= \beta_2 - \beta_{-1}$) 1.05 and the average value of $-\beta_{-2}$ 0.18, in conjunction with equations 4.18, 4.19 and 4.20. The value of Leffler's α -parameter, in this case 0.50 ± 0.06 , is identical for formation of an intermediate from reactant or product in a symmetrical reaction. Once the individual values have been obtained the effective charges throughout the reactive pathway may be worked through logically, starting from the attacking phenoxide ion having a charge of minus one. It should be noted that all total charges will be either neutral or minus one for the example shown and also the effective charges for the two phenyl groups on the intermediate will be equal since it is the study of a symmetrical reaction.

$$\alpha = \frac{\beta_1}{\beta_{eq1}} = \frac{-\beta_{-2}}{\beta_{eq2}} \quad \text{equation 4.18}$$

$$\beta_{(eq)n} = \beta_n - \beta_{-n} \quad \text{equation 4.19}$$

$$\beta_{eq} = \sum \beta_n \quad \text{where } n = 1 \text{ to } \infty \quad \text{equation 4.20}$$

Calculation of β_{-1} and β_2 .

$$\begin{aligned} \beta_{eq} &= \beta_{eq1} + \beta_{eq2} \\ &= \beta_1 + \beta_2 - \beta_{-1} - \beta_{-2} \\ &= \beta_1 + \Delta\beta - \beta_{-2} \\ &= 0.85 + 1.05 + 0.18 \\ &= 2.08 \pm 0.2 \end{aligned}$$

From equation 4.18

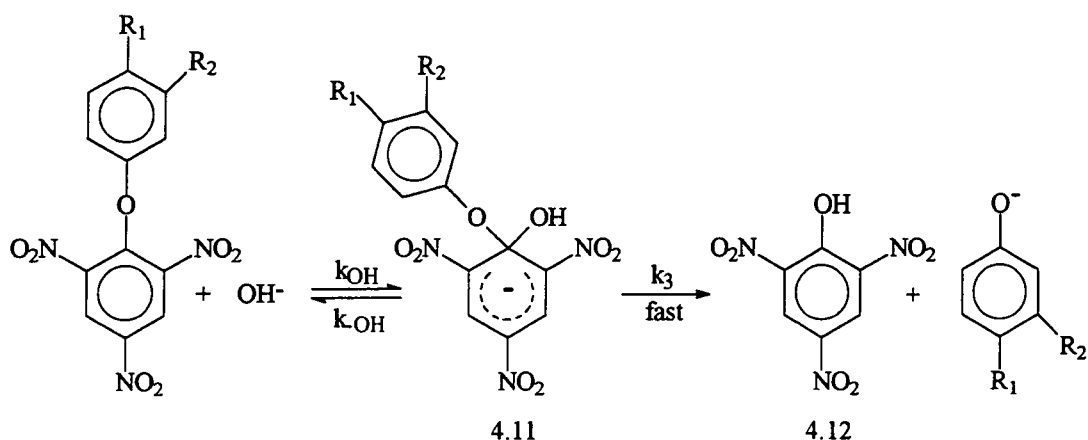
$$\begin{aligned} \alpha &= \frac{\beta_1}{\beta_{eq1}} = \frac{-\beta_{-2}}{\beta_{eq2}} \\ \Rightarrow \frac{\beta_1}{\beta_{eq1}} &= \frac{-\beta_{-2}}{\beta_{eq} - \beta_{eq1}} \\ \Rightarrow \frac{0.85}{\beta_{eq1}} &= \frac{0.18}{2.08 - \beta_{eq1}} \\ \therefore \beta_{eq1} &= 1.71 \pm 0.1 \end{aligned}$$

4.7 Reactions of Hydroxide with Substrates, 4.5 & 4.7.

U.V./Vis. spectra shown previously in figure 4.3 indicate the occurrence of a competing substitution involving the reaction of substrates with hydroxide ion, equation 4.21, to form picric acid, 4.12. Reactions with the less reactive phenols often have a sloping infinity on the kinetic trace, indicative of a slow reaction.

Experiments have been carried out to determine the rate constants for processes of this type and confirm that there is minimum interference with the primary process being studied. Initially buffer systems (e.g. Borax, TRIS (tris(hydroxymethyl) amino methane) and dihydrogen phosphate) were used at different pH values to vary the hydroxide concentration. Results obtained were inconsistent and non-linear, apparently caused by the interaction of the substrate with the buffer components themselves.

An alternative method was therefore found using sodium hydroxide in decarbonated water. In each case the reaction of the substrate with hydroxide resulted in a rapid colour forming reaction giving a spectrum with λ_{max} 396nm, consistent with the formation of the picrate ion and 4-nitrophenolate. There was no evidence for the formation in water in spectroscopically observable concentration of 4.11, the intermediate on the substitution pathway. Nor was there evidence for hydroxide attack at the 3-position. Hence the reaction is interpreted as rate determining nucleophilic attack of the hydroxide ion on the substrate.

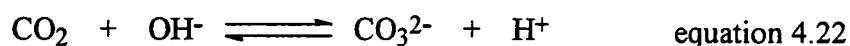


equation 4.21

4.7.1 Experimental Procedure.

Since the concentrations of hydroxide were required to be accurate, all distilled water required was boiled beforehand to eliminate the presence of any dissolved carbon dioxide and stop the possible side reaction shown in equation 4.22. Once the water had boiled a soda-lime tube was placed in the end of the flask to help stop any carbon dioxide re-entering.

Solutions of varying hydroxide concentration, $[\text{OH}^-]$, were prepared, maintaining 0.1 mol dm^{-3} ionic strength with sodium chloride, and placed accordingly in a stopped-flow spectrophotometer along with the required substrate solution. Owing to the insolubility of the substrates, 4.5 and 4.7, all measurements were completed with 5 or 15% dioxane-water (v/v) solvent composition respectively at 25°C



4.7.2 Results and Kinetic Analysis.

With hydroxide concentration in large excess over substrate, first order kinetics were observed and the appropriate rate expression is given in equation 4.23, where K_3 represents the equilibrium constant for attack at the 3-position. Values of the observed rate constant, k_{obs} , obtained for substrates 4.5 and 4.7 are shown in table 4.13 and graphically in figure 4.12. Since the graph plotted is linear with respect to $[\text{OH}^-]$, it can be presumed that the limit, $1 \gg K_3[\text{OH}^-]$ applies and equation 4.23 reduces to equation 4.24, enabling values of k_{OH} to be calculated.

$$k_{\text{obs}} = \frac{k_{\text{OH}}[\text{OH}^-]}{1 + K_3[\text{OH}^-]} \quad \text{equation 4.23}$$

$$k_{\text{obs}} = k_{\text{OH}}[\text{OH}^-] \quad \text{equation 4.24}$$

Data are collected in table 4.14, and appear to be in good agreement with a value of k_{OH} previously determined from measurements for the reaction of phenyl 2,4,6-trinitrophenyl ether with hydroxide in 20:80 DMSO-water (v/v) at 0.5 mol dm^{-3} ionic strength.⁹ Due to the very low concentrations of hydroxide present in the phenol buffers, the rates of reaction with hydroxide will not interfere significantly with the phenolate reactions wished to be studied.

Table 4.13 Kinetic data, $\lambda = 400\text{nm}$, for the reaction of hydroxide with substrates 4.5 and 4.7, at 25°C . $I = 0.1 \text{ mol dm}^{-3}$.

$[\text{OH}^-] / 10^{-3} \text{ mol dm}^{-3}$	1	2	3	4	5
Substrate 4.5 ^a , $k_{\text{obs}} / 10^{-2} \text{ s}^{-1}$	0.34	0.75	0.98	1.40	-
Substrate 4.7 ^b , $k_{\text{obs}} / 10^{-2} \text{ s}^{-1}$	1.29	1.66	2.18	2.46	2.76

a 5% b 15% dioxane-water (v/v) solvent composition.

Figure 4.12 Kinetic data, $\lambda = 400\text{nm}$, for the reaction of hydroxide with substrate 4.5, 5% dioxane-water (v/v), at 25°C . $I = 0.1 \text{ mol dm}^{-3}$.

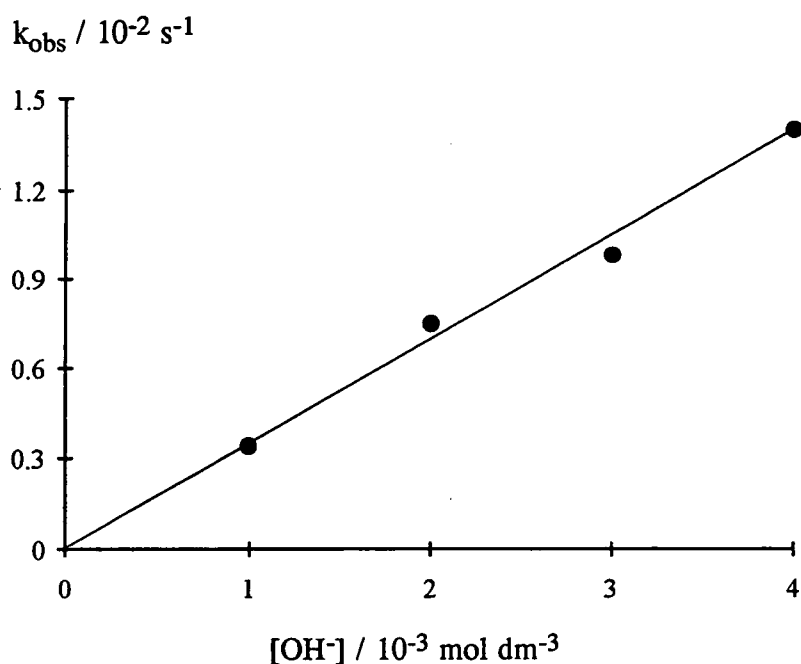


Table 4.14 Summary of kinetic data.

Substrate R_1, R_2	4.5 NO_2, H	4.7 H, NO_2	- H, H^a
$k_{\text{OH}} / \text{dm}^3 \text{ mol}^{-1} \text{ s}^{-1}$	3.5	3.9	2.4

^a Obtained from ref. 9.

4.8 Synthesis of Substrates.

The method applied for the preparation of the substituted phenyl 2,4,6-trinitrophenyl ethers 4.6 - 4.9 is discussed in chapter 2, section 2.7.1. In the case of 3',4'-dinitrophenyl 2,4,6-trinitrophenyl ether, 4.6, the reaction solution is stirred for 24 hours due to the poor nucleophilicity of the phenol.

4.8.1 NMR Data and Melting Points of Substrates Synthesised.

Analytical data for substrate 4.5 can be viewed in chapter 2, section 2.7.2. The melting points obtained for the remaining substrates are summarised in table 4.15 below. ^1H NMR data is summarised in table 4.16. The bands at δ_{H} /ppm 2.49 and 3 - 4.5 are due to the solvent and adventitious water respectively. Impurity signals occur at δ_{H} /ppm 9.25 (picryl chloride) and 8.6 (picric acid).

Table 4.15 Melting point data for substrates.

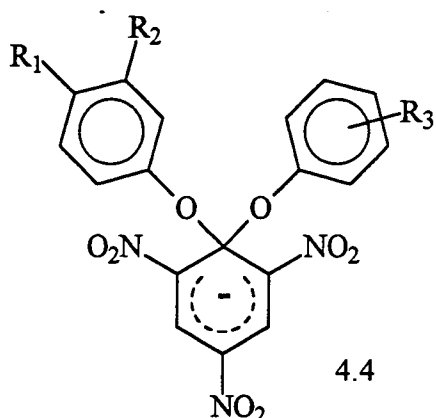
Reactant	m.p. (T/°C)	Literature m.p. (T/°C)
4.6	203	202 ¹⁰
4.7	172	174 ¹¹
4.8	127	128 ¹²
4.9	65	-

Table 4.16 ^1H NMR information for substrates 4.6 - 4.9 in d_6 -DMSO, 200MHz.

Substrate	^1H NMR signals δ_{H} / ppm in d_6 -DMSO.
4.6	7.70 (1H, d of d, $J = 9.1\text{Hz}$ & 2.9Hz), 8.07 (1H, d, $J = 2.9\text{Hz}$) and 8.40 (1H, d, $J = 9.1\text{Hz}$) phenyl ring. 9.37 (2H, s, trinitro phenyl ring)
4.7	7.62 (1H, d, $J = 8.3\text{Hz}$), 7.71 (1H, t, $J = 8.4\text{Hz}$), 7.90 (1H, t, $J = 3.0\text{Hz}$) and 8.05 (1H, d, $J = 8.4\text{Hz}$) phenyl ring. 9.29 (2H, s, trinitro phenyl ring)
4.8	7.30 (2H, d, $J = 8.8\text{Hz}$) and 7.94 (2H, d, $J = 8.7\text{Hz}$) phenyl ring. 9.29 (2H, s, trinitro phenyl ring) 9.94 (1H, s, aldehyde)
4.9	7.50 (2H, m), 7.64 (1H, t, $J = 7.9\text{Hz}$) and 7.74 (1H, d, $J = 7.8\text{Hz}$) phenyl ring. 9.28 (2H, s, trinitro phenyl ring) 9.95 (1H, s, aldehyde)

4.9 Discussion.

Each of the Brønsted diagrams for substrates 4.5 - 4.7 consists of two intersecting lines, possessing a break point as predicted at approximately the pK_a of the phenol nucleophile equal to that of the leaving group. For each substrate containing differing leaving groups the break point moves accordingly. These results are consistent with the intervention of a Meisenheimer / σ -adduct intermediate, 4.4.



It is expected that the kinetic data obtained for a Brønsted diagram are susceptible to varying degrees of scatter about a mean line.¹³ Due it is thought, excluding sources of discrepancies such as steric effects etc., to the small difference in energy induced by the substituent on the microscopic solvation in the standard reaction (usually ionisation) compared with the reaction under investigation.

4.9.1 Global Equation and Brønsted Diagram.

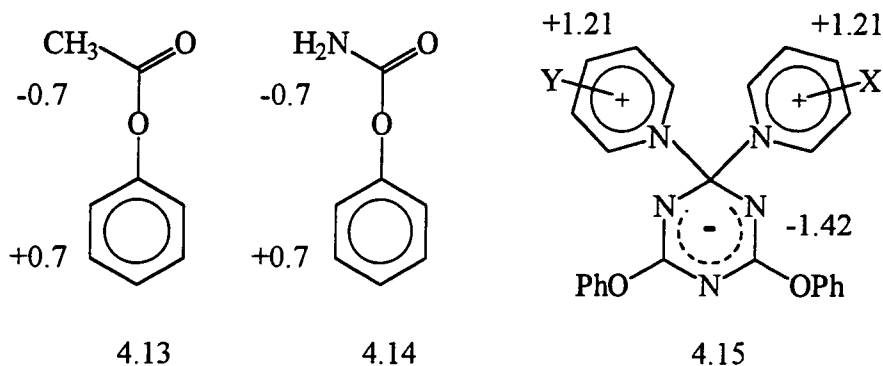
Calculated values, predicted by the global equation 4.6 are in good agreement with the experimental results acquired. Evidence for a stepwise process is confirmed in the value of $\Delta\beta$ 1.05 ± 0.05 which indicates conclusively that there is a substantial difference in effective charge on the reacting oxygen atom from the intermediate to one of the transition states corresponding to k_{-1} and k_2 in the proposed stepwise path. A $\Delta\beta$ value equal to zero is expected for a concerted process. Further, the absence of coupling between the respective changes in effective charge for the bond forming step, β_1 , and the bond undergoing fission, β_2 . implies a two step process. The value of 0.85 associated with β_1 indicates that the substituents present on the aromatic ring of the attacking phenolate ion see a significant change in effective charge and a considerable amount of bond formation in TS_1 .

Jencks and co-workers¹⁴ have reported decreases in the rate constants of reaction of substituted ortho-chlorophenolate anions with acetate and formate esters by 25-50%, believed to be attributed to steric hindrance encountered by the attacking nucleophile. Reactions of substrates 4.5-4.7 with both 2- and 6- substituted phenolate ions have been studied, which upon examination do not appear to deviate in any way from the Brønsted plots shown by other substituted nucleophiles.

4.9.2 Charge Distribution.

Values of charge distribution determined within the substrates and the proposed σ -adduct, 4.4, can be compared with similar reaction processes that have also been examined using Brønsted correlations.

Phenyl acetate¹⁵, 4.13, and phenyl carbamate¹⁶, 4.14, both exhibit an effective charge of +0.7 on the oxygen connected to the phenyl group, owing to the electron withdrawing properties of the the acetyl and carbamyl groups respectively. As expected, a higher value of +1.08 is found for phenyl 2,4,6-trinitrophenyl ether due to the greater electron withdrawing ability of the trinitroaromatic moiety.



The significant amount of effective charge, -2.42, distributed within the σ -adduct is also in good agreement with previous studies. Williams and co-workers¹⁷ have reported an effective charge of -1.42 within the triazine ring for the intermediate, 4.15, formed from reaction between substituted pyridines and 1'-(2,6-diphenoxy-1,3,5-triazin-2-yl)pyridinium ion in aqueous solution. It is the influence of the electron withdrawing nitro groups in delocalising the negative charge that may favour the formation of the intermediate 4.4. As opposed to the analogous reaction involving attack of substituted phenolates with 2-(4-nitrophenoxy)-4,6-dimethoxy-1,3,5-triazine in aqueous solution which appears to be a concerted process.^{7,8}

Bernasconi and Muller have published values of β_1 0.60 and β_{-1} -0.70 for the reaction of 2,4,6-trinitroanisole and various substituted phenoxide ions measured in 90% DMSO-10% water.¹⁸ A detailed effective charge map cannot be constructed to allow the comparison of effective charge distribution in a Meisenheimer type complex. However the values do imply that the extent of bond formation is approximately half complete in the first transition state, which is concordance with values of β_1 0.85 and β_{-1} -0.86 reported, here.

4.10 References.

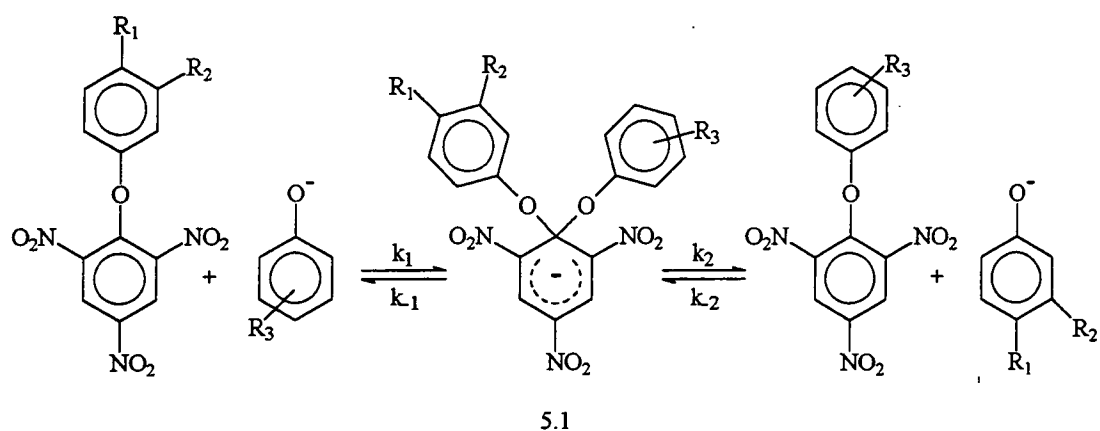
1. J. F. Bunnett and R. E. Zahler, *Chem. Rev.*, 1951, **49** 273.
2. J. F. Bunnett, *Q. Rev. Chem. Soc.*, 1958, **12**, 1.
3. C. A. Fyfe, A. Koll, S. W. H. Damji, C. D. Malkiewich and P. A. Forte., *J. Chem. Soc. Chem. Commun.*, 1977, 335.
4. C. A. Fyfe, S. W. H. Damji and A. Koll, *J. Am. Chem. Soc.*, 1979, **101**, 951.
5. M. J. Strauss, *Chem. Rev.*, 1970, **70**, 667.
6. F. Terrier, "Nucleophilic Aromatic Displacement : Influence of the Nitro Group", VCH, Weinheim, 1991.
7. A. H. M. Renfrew, J. A. Taylor, J. M. J. Whitmore and A. Williams, *J. Chem. Soc. Perkin Trans. 2*, 1993, 1703.
8. A. H. M. Renfrew, D. Rettura, J. A. Taylor, J. M. J. Whitmore and A. Williams, *J. Am. Chem. Soc.*, 1995, **117**, 5484.
9. R. Chamberlin, M. R. Crampton and R. L. Knight, *J. Chem. Research (S)*, 1993, 444.
10. O. Banjoko and C. Ezeani, *J. Chem. Soc. Perkin Trans. 2*, 1986, **4**, 531.
11. K. Okon, *Rocz. Chem.*, 1958, **32**, 213, 217.
12. K. H. Slotta and K. H. Soremba, *Chem. Ber.*, 1935, **68**, 2059, 2065.
13. T. C. Bruice and S. T. Benkovic, *Bio-organic Mechanisms*, Benjamin: New York, 1966, 153.
14. D. Stefanidis, S. Cho, S. Dhe-Paganon and W. P. Jencks, *J. Am. Chem. Soc.*, 1993, **115**, 1650.
15. S. Thea and A. Williams, *Chem. Soc. Rev.*, 1986, **15**, 125.
16. H. Al-Rawi and A. Williams, *J. Am. Chem. Soc.*, 1977, **99**, 2671.
17. N. R. Cullum, A. H. M. Renfrew, D. Rettura, J. A. Taylor, J. M. J. Whitmore and A. Williams, *J. Am. Chem. Soc.*, 1995, **117**, 9200.
18. C. F. Bernasconi and M. C. Muller, *J. Am. Chem. Soc.*, 1978, **100**, 5530.

Chapter 5.

**Kinetic Studies on the Reaction of Substituted
Aryl 2,4,6-Trinitrophenyl Ethers with Various Phenols in
DMSO / H₂O Mixtures. The Elusive Intermediate?**

5.1 Kinetic and Equilibrium Studies

The previous chapter indicated by use of Brønsted theory, that the process shown in equation 5.1 occurred in two steps via the reaction intermediate, 5.1. In this chapter an attempt is made to kinetically observe this reaction intermediate, proving conclusively that it may exist and enhancing further the results determined in chapter 4. From the reactions previously studied in chapter 4, the 4-methoxy substituted phenol is predicted to give the largest equilibrium constant for the possible formation of the desired σ -adduct, due to its high reactivity and poor leaving group ability.



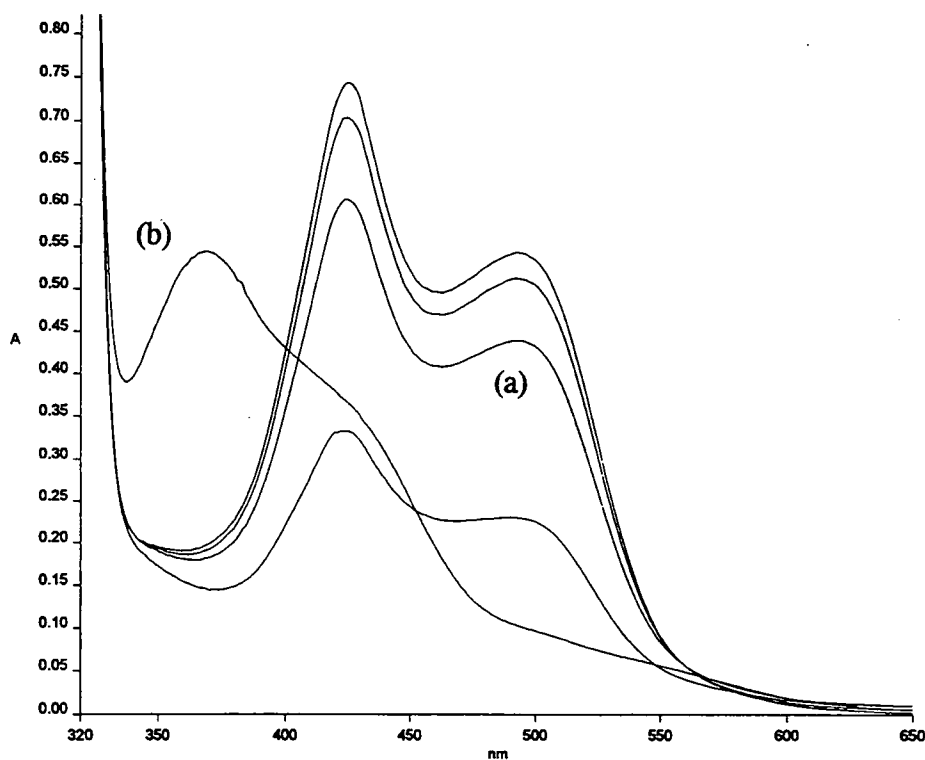
equation 5.1

Kinetic data are presented for the symmetrical reactions of 4-methoxy-phenolate with its corresponding substrate, 4'-methoxy-phenyl 2,4,6-trinitrophenyl ether, 5.2, and also phenol with phenyl 2,4,6-trinitrophenyl ether, 5.3, and 1,3,5-trinitrobenzene, 5.4. Substrates 5.3 and 5.4 allow the study of a similar reaction pathway, whose results may be compared to that of 5.2.

5.2 Experimental Procedure.

Reactions have been studied for substrates 5.2 - 5.4 with two different phenol / phenolate buffers in a DMSO-water co-solvent system at 25°C. The reason for the addition of DMSO will be discussed later. In general both a fast and a slow process could be studied. These were monitored respectively using a stopped-flow instrument or a standard U.V./Vis. spectrophotometer. Reactions were monitored by the appearance of the corresponding σ -adduct. Figure 5.1 shows the slow formation of the σ -adduct due to attack of the hydroxide ion at the 3-position of phenyl 2,4,6-trinitrophenyl ether, λ_{max} 425nm and 492nm (br.) followed by the final very slow formation of picric acid. Buffer solutions were prepared by the method discussed in chapter 4, section 4.3.1 with their pH being determined in water initially.

Figure 5.1 U.V./Vis. spectra for the slow formation process involving phenyl 2,4,6-trinitrophenyl ether, $4 \times 10^{-5} \text{ mol dm}^{-3}$, with phenolate, 0.01 mol dm^{-3} , $\text{pH}(\text{water}) = 9.10$ in 74% DMSO-water (v/v) at 25°C. Scans repeated every minute.
(a) Initial spectrum. (b) Final spectrum after 20 hours.



Generally kinetic experiments consisted of reacting the substrate with a series of solutions firstly containing a constant buffer ratio, PhOH : PhO⁻ (i.e. constant pH), with the buffer concentration varied, and secondly by solutions of differing pH obtained by keeping [PhO⁻] constant while varying [PhOH]. Reported observed rate constants, calculated with correlation coefficients between 0.992 - 0.999 are the means of several determinations and are precise to ± 5%. Solvent composition, 74% DMSO-water (v/v), and ionic strength 0.1 mol dm⁻³ maintained by sodium chloride, were kept constant through out all experiments. It should be noted that addition of water and DMSO results in a decrease in their combined volume, due to this solutions were always prepared with known volumes of water and DMSO. Reactions were initiated by the addition of the substrate solution to the required buffer solution within a thermostatted cell compartment.

5.2.1 Determination of pH.

Addition of a solvent, e.g. DMSO, to an aqueous solution of known pH will cause the value to change. In the case of DMSO it will cause the value of pH determined in water to rise by approximately seven pH units, for 70% DMSO-water (v/v), due to DMSO being "more acidic" than water. In a paper published by R. Schaal *et al.* in 1969, each different solvent composition has had its own acidity constant, pK_s, established.¹ Using this value and the measured pH, equation 5.2 may be used to calculate the concentration of hydroxide ions in the new solvent system. As the standard pH meter did not measure pH above fourteen, the combination of equation 5.2 and kinetic analysis allowed the new values of pH for each different buffer system in 74% DMSO-water (v/v) to be calculated.

$$\log[\text{OH}^-] = \text{pH} - \text{pK}_s \qquad \text{equation 5.2}$$

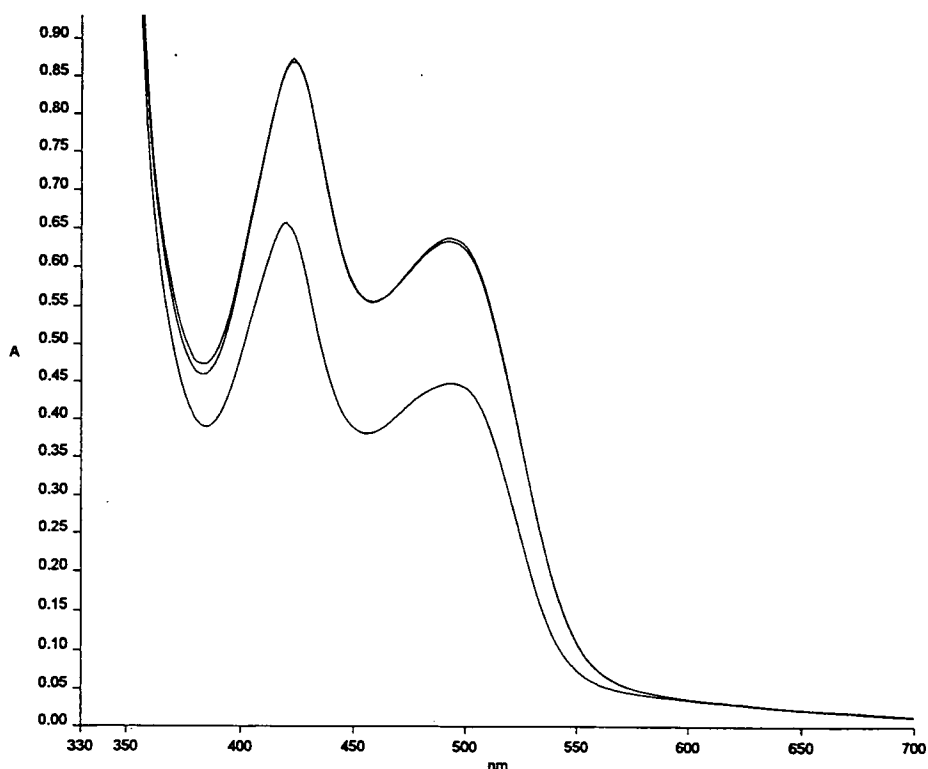
5.3 Solvent Studies.

Initial U.V./Vis. experiments were carried out on the reaction of 5.2 with 4-methoxy-phenol buffer, PhOH:PhO⁻ 5:1, to observe the formation of any possible reaction intermediates.

5.3.1 Observation of a Slow Reaction.

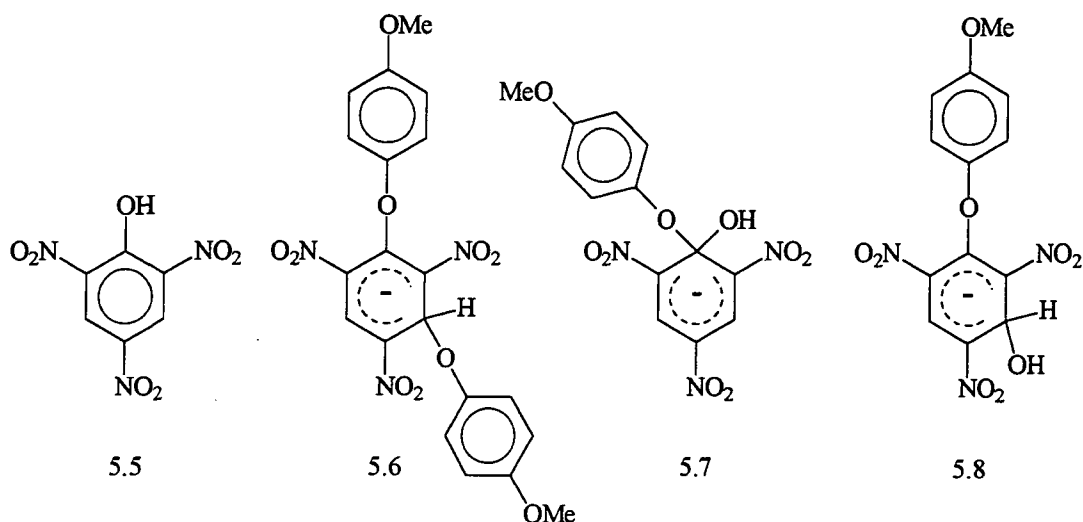
Scans were recorded on a standard U.V./Vis. spectrophotometer every five minutes and the reaction spectrum monitored. Investigations using only water as the solvent showed the gradual formation of picric acid, 5.5, over approximately nineteen hours, and there was no trace of the characteristic U.V./Vis. spectrum expected for the formation of a σ -adduct. From previous studies², it is known that the dipolar aprotic solvent DMSO can greatly stabilise the delocalised negative charge found in σ -adducts.

Figure 5.2 U.V./Vis. spectra of the intermediate observed on reaction of 4'-methoxy-phenyl 2,4,6-trinitrophenyl ether, $4 \times 10^{-5} \text{ mol dm}^{-3}$, with 4-methoxy-phenolate, 0.01 mol dm^{-3} , pH(water) = 9.53 in 74% DMSO-water (v/v) at 25°C. Scans repeated every two minutes.



Consequently reactions were repeated with various compositions of DMSO and water present. At 60% DMSO-water (v/v) two absorption maxima in the region λ 420nm and 490nm started to become prominent. A further increase in DMSO to 74% enabled the gradual formation of a complex to be observed clearly with λ_{max} 423nm and 494nm (br.) over a time period of 10 minutes, figure 5.2.

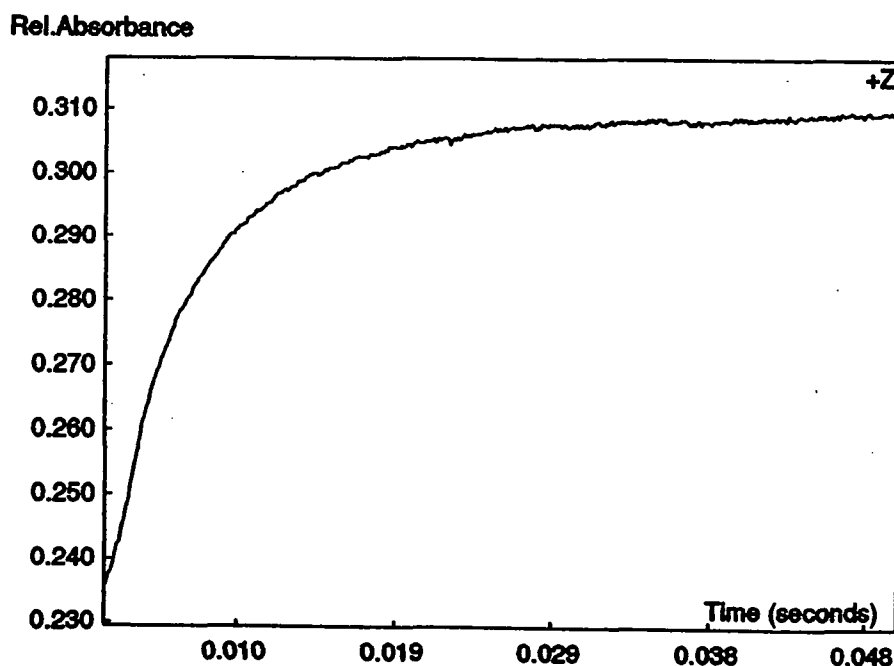
The shape is characteristic of a σ -adduct (Meisenheimer complexes) encountered before, although initially it was not possible to distinguish its exact structure. Within the reaction medium there were two possible nucleophiles, 4-methoxyphenolate and hydroxide, which may attack the substrate at either the 1- or 3- position, e.g. 5.1 and 5.6 - 5.8. Addition of substrate 5.2 to a buffer, pH(water) = 9.43, obtained by the use of known quantities of Borax / sodium hydroxide containing no phenol, should allow the nature of the complex to be determined. Under the same experimental conditions, the U.V./Vis. spectrum contained a similar curve shape with values of λ_{max} 423nm and 494nm implying that the reaction complex observed was in fact either 5.7 or 5.8.



5.3.2 Observation of a Fast Reaction.

Results discussed in section 5.2 lead to the belief that the reaction intermediate, 5.1, may in fact be produced rapidly before the production of the σ -complex involving hydroxide and go undetected by the standard spectrophotometer. Initial investigations were completed using a stopped-flow spectrophotometer at various wavelengths in an attempt to observe any possible increase in absorbance due to the formation of complex 5.1.

Figure 5.3 Kinetic trace acquired, $\lambda = 425\text{nm}$, for the fast reaction of 4'-methoxy-phenyl 2,4,6-trinitrophenyl ether, $4 \times 10^{-5} \text{ mol dm}^{-3}$, with 4-methoxy-phenolate, $0.001 \text{ mol dm}^{-3}$, pH = 9.53 in 74% DMSO-water (v/v) at 25°C .

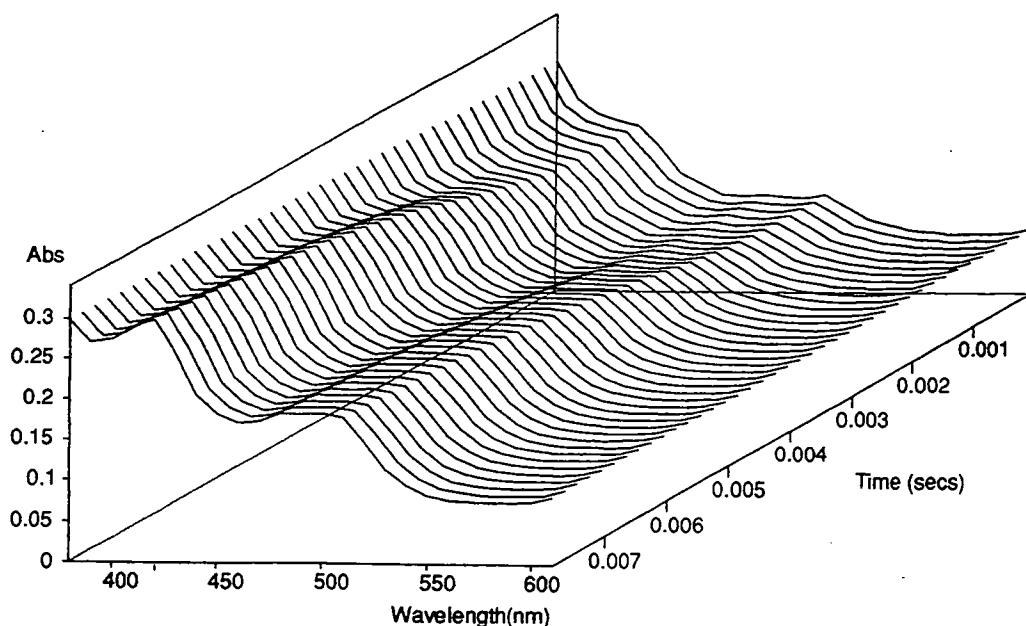


A point of concern was that not only would a high proportion of DMSO help to stabilise the production of σ -adducts involving phenolate but would also enhance the reactivity of the hydroxide ions present owing to their poor solvation. However this did not pose a problem as the reaction of 5.2 with 4-methoxy-phenol showed an increase in absorbance of approximately 0.05 over 0.05 seconds at a wavelength λ 420nm, figure 5.3.

This was undoubtedly a separate process to the reaction with hydroxide studied previously. A slow reaction was monitored over a much longer time period, e.g. 200 seconds, whose absorbance change corresponded to earlier data. Importantly, reaction of Borax buffer solutions with all substrates occurs without observation of the fast process. Mixing effects were also discounted as no absorbance change was observed over a one second time period when the phenol concentration was reduced to zero.

To obtain the approximate shape of the spectrum corresponding to the product of the initial reaction several reactions of length 0.1 seconds and of equivalent concentrations were completed using a wavelength range 300 - 600nm making measurement at 10nm intervals. These were then compiled in a global analysis software package and are illustrated in figure 5.4. The spectrum after 0.01 seconds was again consistent with those expected for the formation of σ -complexes, giving λ_{\max} 420nm and 490nm (br.). Further kinetic studies now follow relating to the adducts formed in both the slow and fast processes observed.

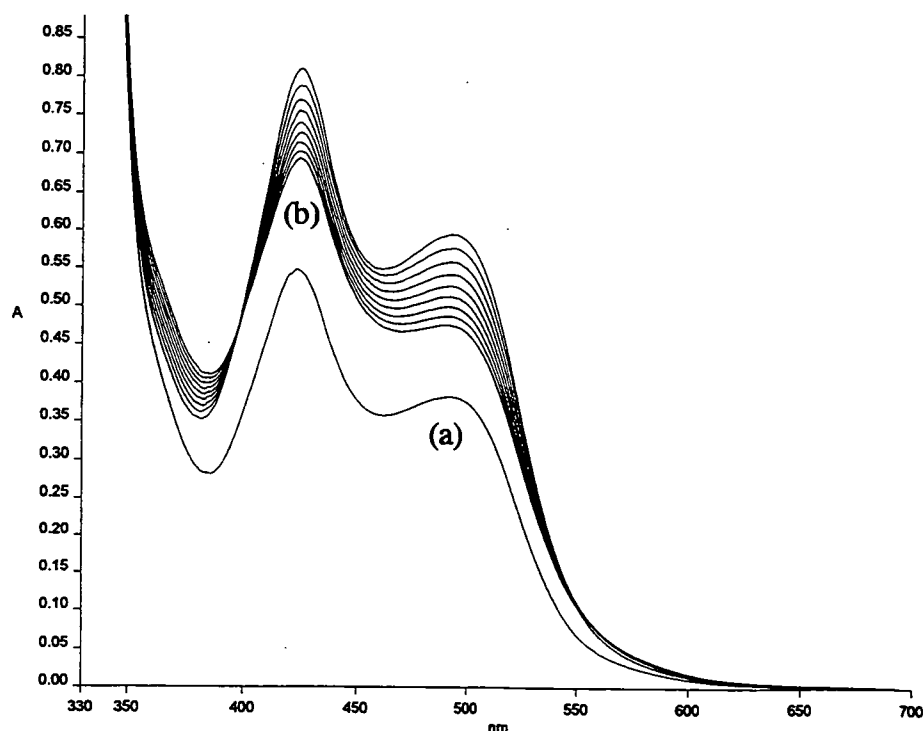
Figure 5.4 3-D view of the fast process, produced by the reaction of 4'-methoxyphenyl 2,4,6-trinitrophenyl ether, $4 \times 10^{-5} \text{ mol dm}^{-3}$, with 4-methoxyphenolate, $0.007 \text{ mol dm}^{-3}$, $\text{pH}(\text{water}) = 9.53$ in 74% DMSO-water (v/v) at 25°C .

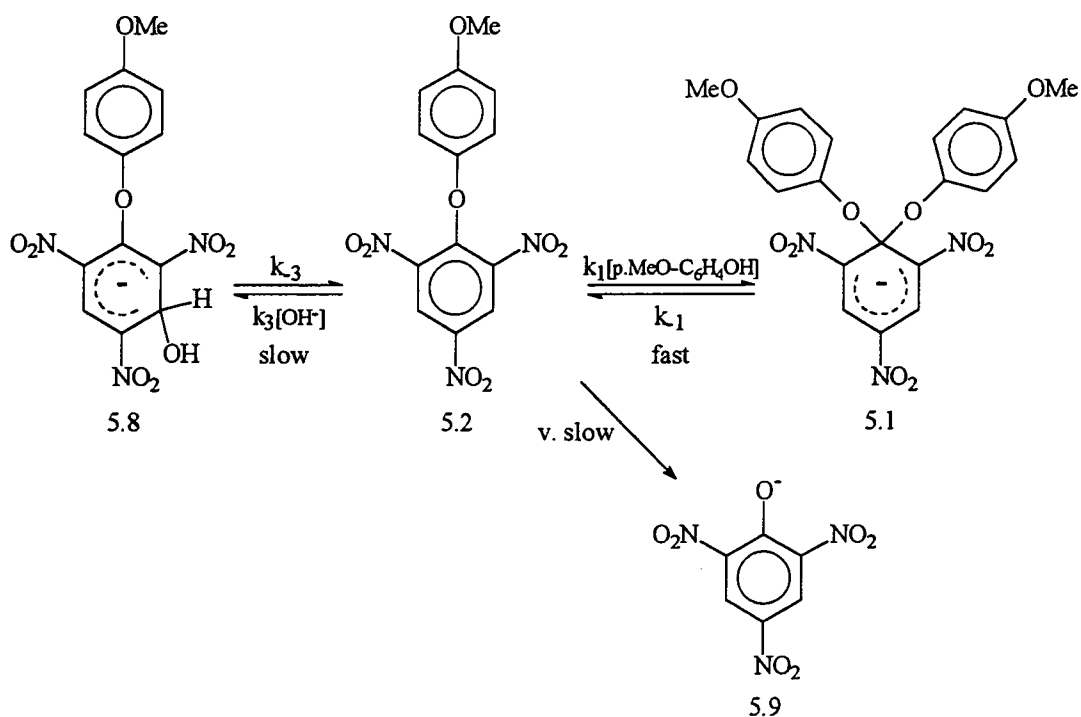


5.4 Reactions of 4'-Methoxy-Phenyl 2,4,6-Trinitrophenyl Ether, with 4-Methoxy-Phenol.

Both the slow and fast processes have been observed with substrate 5.2 and 4-methoxy-phenol buffers. Figure 5.5 provides an example of the spectra observed for the slow formation of the proposed σ -adduct, 5.8, λ_{\max} 423nm and 494nm (br.), and also the decomposition to eventually produce the picrate ion, 5.9. The postulated reaction process can be viewed in scheme 5.1. All reactions were conducted in 74% DMSO-water (v/v) under pseudo first order conditions with the buffer component concentrations in large excess of that of the substrate, 4×10^{-5} mol dm^{-3} unless otherwise stated.

Figure 5.5 U.V./Vis. spectra for the slow formation process involving 4'-methoxy-phenyl 2,4,6-trinitrophenyl ether, 4×10^{-5} mol dm^{-3} , with 4-methoxy-phenolate, 0.002 mol dm^{-3} , pH(water) = 9.56 in 74% DMSO-water (v/v) at 25°C. Spectra repeated every 2 minutes. (a) Initial spectrum. (b) Spectrum after 20 minutes.





scheme 5.1

5.4.1 Reactions of 5.2 with Sodium Hydroxide.

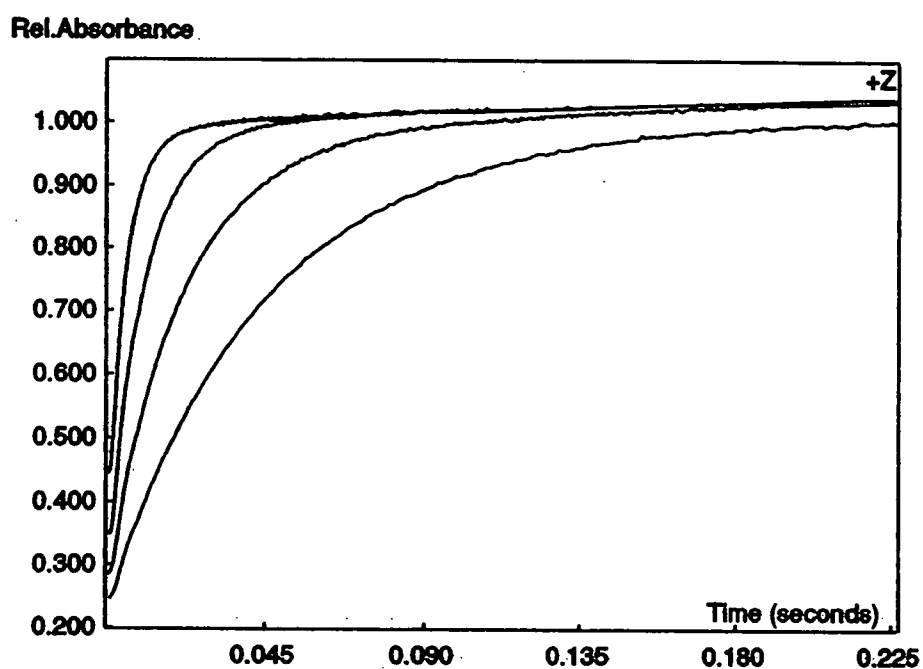
Firstly reactions were conducted with sodium hydroxide to enable a value of the rate constant for hydroxide ion attack on the substrate, k_3 , to be determined, scheme 5.1. For reasons discussed later it is presumed that attack occurs at the 3-position of the substrate and it is the formation of σ -adduct 5.8 that is monitored. Since very low concentrations of hydroxide, $[\text{OH}^-]$, were used, a similar method to that mentioned in section 4.7.1, chapter 4 was followed.

Kinetic measurements were made by stopped-flow spectrophotometry with hydroxide in large excess of the substrate. Figure 5.6 provides examples of the first order kinetic traces observed relating to the formation of the σ -adduct, 5.8, for various concentrations of hydroxide. Values of the observed rate constant, k_{obs} , can be viewed in table 5.1.

Table 5.1 Kinetic data for the reaction of 5.2 and hydroxide in 74% DMSO-water (v/v), $\lambda = 425\text{nm}$, at 25°C . $I = 0.1\text{mol dm}^{-3}$.

$[\text{OH}^-] / 10^{-2} \text{ mol dm}^{-3}$	0.25	0.50	1.0	2.0
$k_{\text{obs}} / \text{s}^{-1}$	20.7	42.6	92.1	198

Figure 5.6 Kinetic traces for the formation of 5.8 upon reaction of 5.2, $4 \times 10^{-5} \text{ mol dm}^{-3}$ with differing hydroxide concentrations, 74% DMSO-water (v/v), $\lambda = 425\text{nm}$, at 25°C . $I = 0.1 \text{ mol dm}^{-3}$.



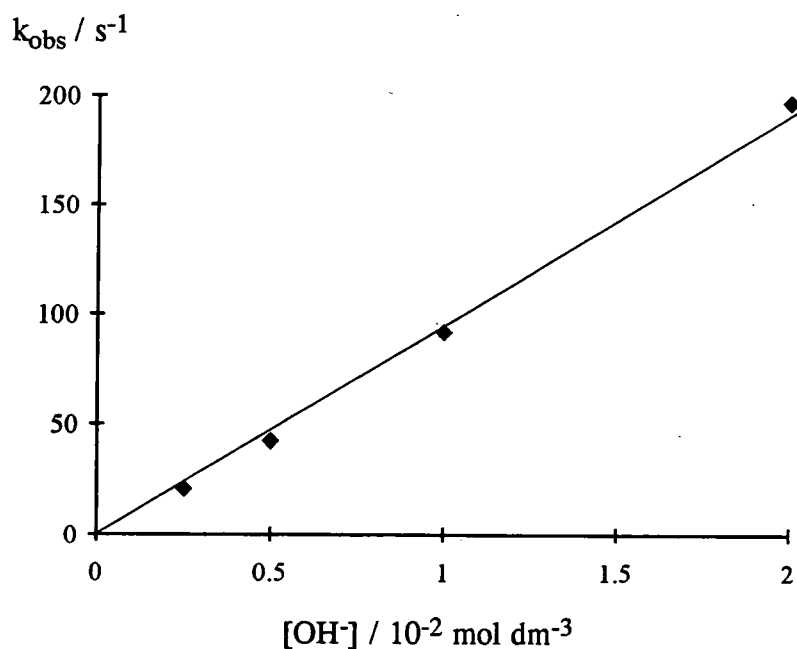
5.4.1.1 Kinetic Analysis.

The kinetic expression for the observed rate constant, k_{obs} , is equation 5.3. This implies that the graph formed when plotting k_{obs} versus $[\text{OH}^-]$ will be linear and the gradient of the graph will be equal to k_3 with k_3 being determined from the intercept, figure 5.7.

A value of $k_3 = 9.7 \pm 0.2 \times 10^3 \text{ dm}^3 \text{ mol}^{-1} \text{ s}^{-1}$ is calculated and k_3 is very small, estimated to be in the range of $0\text{--}5 \text{ s}^{-1}$ for the reaction of hydroxide with substrate 5.2 in 74% DMSO-water (v/v).

$$k_{\text{obs}} = k_3[\text{OH}^-] + k_{-3} \quad \text{equation 5.3}$$

Figure 5.7 Rate dependency of k_{obs} on hydroxide concentration, $[\text{OH}^-]$.



5.4.2 The Fast Process: Reaction of 5.2 with 4-Methoxy-Phenolate.

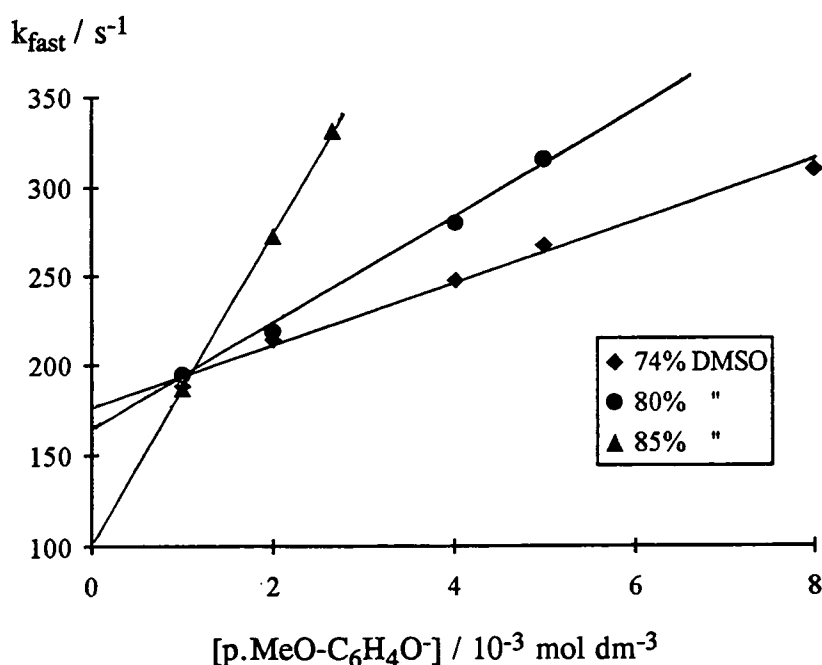
Kinetic data were obtained for the fast reaction discussed previously in section 5.3.2. Investigations were conducted for a series of buffer solutions with a single buffer ratio, (PhOH:PhO⁻ 3:1 pH(water) = 9.75), but varying the buffer concentration, [p.MeO-C₆H₄O⁻]. The reactions were also repeated with different solvent compositions. With buffer concentrations in excess of the substrate concentration, first order reactions were obtained, illustrated in figure 5.3 shown previously. Values of the observed first order rate constant, k_{fast} , are in table 5.2 and figure 5.8.

Table 5.2 Kinetic data for the reaction of 5.2 with 4-methoxy-phenolate, 74% DMSO-water (v/v), $\lambda = 425\text{nm}$, at 25°C. $I = 0.1 \text{ mol dm}^{-3}$.

[p.MeO-C ₆ H ₄ O ⁻] / 10 ⁻³ mol dm ⁻³	1.00	2.00	2.65	4.00	5.00	8.00
74% DMSO $k_{\text{fast}} / \text{s}^{-1}$	188	214	-	247	267	310
74% ^a " "	185	213	-	250	267	302
80% " "	194	219	-	280	316	-
84% " "	187	273	332	-	-	-

^a Buffer ratio 5:1, PhOH:PhO⁻.

Figure 5.8 Rate dependency of k_{fast} on buffer concentration, [p.MeO-C₆H₄O⁻].



5.4.2.1 Kinetic Analysis: Fast Process

A kinetic expression for k_{fast} is defined below in equation 5.4. Plotting k_{fast} versus 4-methoxy-phenolate concentration as viewed in figure 5.8 enables a value of k_1 , the gradient and k_{-1} , the intercept, to be determined for each solvent composition, table 5.3. Knowing a value of k_1 and k_{-1} , the equilibrium constant K_1 for the formation of the proposed σ -adduct 5.1 may be deduced using equation 5.5. The results given for the reaction in 74% DMSO-water (v/v) using different buffer ratios provides good evidence for the interpretation that the fast reaction is due to the addition of 4-methoxy-phenolate and does not involve the attack of hydroxide ions.

$$k_{\text{fast}} = k_1[\text{p.MeO-C}_6\text{H}_4\text{O}^-] + k_{-1} \quad \text{equation 5.4}$$

$$K_1 = k_1 / k_{-1} \quad \text{equation 5.5}$$

Table 5.3 Summary of results for the fast process involving 5.2 and 4-methoxy-phenolate buffers at differing solvent compositions.

% DMSO-water (v/v)	$k_1 /$ $10^4 \text{ dm}^3 \text{ mol}^{-1} \text{ s}^{-1}$	$k_{-1} /$ 10^2 s^{-1}	$K_1 /$ $\text{dm}^3 \text{ mol}^{-1}$
74	1.72 ± 0.09	1.77 ± 0.04	97 ± 7
80	3.10 ± 0.10	1.61 ± 0.04	190 ± 10
85	8.10 ± 0.40	1.14 ± 0.08	710 ± 90

5.4.3 The Slow Process: Reaction of 5.2 with 4-Methoxy-Phenolate.

Kinetic data were obtained for the slow reaction discussed previously in section 5.3.2. Investigations were conducted in two parts. Firstly for a series of buffer solutions with a single buffer ratio, (PhOH:PhO⁻ 3:1 pH_(water) = 9.81), varying the buffer concentration, [p.MeO-C₆H₄O⁻] only, and secondly using a constant concentration of [p.MeO-C₆H₄O⁻] with different buffer ratios. With buffer concentrations in excess of the substrate concentration, first order reactions were observed.

5.4.3.1 Constant Buffer Ratio.

Table 5.4 provides a summary of the results for the observed first order rate constant, k_{slow} . As expected the change in k_{slow} with [p.MeO-C₆H₄O⁻] is very small which agrees with the interpretation that the process is due to the slow formation of the σ -adduct 5.8.

Table 5.4 Kinetic data for the slow reaction of 5.2 with 4-methoxy-phenolate, 74% DMSO-water (v/v), $\lambda = 425\text{nm}$, at 25°C. $I = 0.1 \text{ mol dm}^{-3}$.

[p.MeO-C ₆ H ₄ O ⁻] / 10 ⁻³ mol dm ⁻³	1.0	2.0	4.0	5.0	8.0
[p.MeO-C ₆ H ₄ OH] / 10 ⁻³ mol dm ⁻³	3.0	6.0	12.0	15.0	24.0
k_{slow} / 10 ⁻² s ⁻¹	2.9	3.2	3.2	3.1	3.0

5.4.3.2 Variation in Buffer Ratio, [p.MeO-C₆H₄OH : p.MeO-C₆H₄O⁻].

Examples of the kinetic traces obtained for various buffer ratios can be viewed in figure 5.9. Table 5.5 provides a summary of the results for the observed first order rate constant, k_{slow} and the corresponding absorbance values, $\lambda = 425\text{nm}$, at completion of the reaction. The results are in accord with the formation of the hydroxide-adduct, 5.8, since values of k_{slow} exhibit a clear dependence on pH, i.e. the buffer ratio.

Figure 5.9 Kinetic traces for the formation of 5.8 upon reaction of 5.2, 4×10^{-5} mol dm⁻³ with differing buffer ratios, $\lambda = 425$ nm, at 25°C.

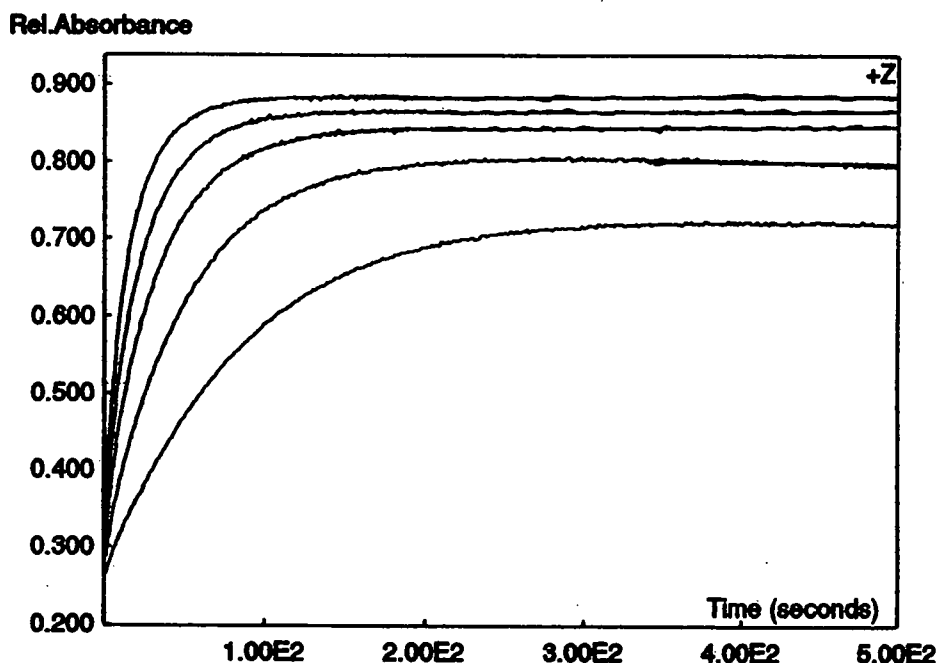
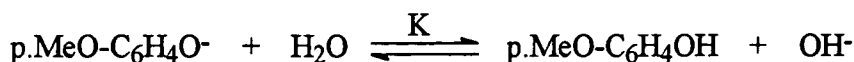


Table 5.5 Kinetic and absorbance data for the slow reaction of 5.2, 4×10^{-5} mol dm⁻³, with different buffer solutions, [p.MeO-C₆H₄O⁻] = 0.001 mol dm⁻³, 74% DMSO-water (v/v), $\lambda = 425$ nm, at 25°C. $I = 0.1$ mol dm⁻³.

[p.MeO-C ₆ H ₄ OH] / 10 ⁻³ mol dm ⁻³	1	2	3	5	10
$k_{\text{slow}} /$ 10 ⁻² s ⁻¹	6.4	4.5	3.2	2.1	1.3
Abs. (425nm)	0.878	0.859	0.844	0.803	0.724

5.4.4 Kinetic Analysis: Slow Process.

Firstly it is important to establish a value of the equilibrium constant, K , defined by the protonation of 4-methoxy-phenolate, equation 5.6, in 74% DMSO-water (v/v), since it was not possible to use a standard pH meter.



equation 5.6

Once a value for K is established it may be used to calculate values of $[\text{OH}^-]$ in buffer solutions made up from known concentrations of 4-methoxy-phenolate and 4-methoxy-phenol.

The method of calculation of K relies on the knowledge that the value of k_3 for reaction of hydroxide with 5.2 has a value of $9700 \text{ dm}^3 \text{ mol}^{-1} \text{ s}^{-1}$ (section 5.4.1). The general kinetic expression for the process shown in scheme 5.1 is equation 5.7. The value of K_1 is known to be *ca.* $100 \text{ dm}^3 \text{ mol}^{-1}$. Hence at low concentrations of 4-methoxy-phenolate ($[\text{p.MeO-C}_6\text{H}_4\text{O}^-] \approx 10^{-3}$) the condition $1 \gg K_1[\text{p.MeO-C}_6\text{H}_4\text{O}^-]$ will apply. Hence under this condition equation 5.7 reduces to equation 5.8. Further, absorbance measurements indicate that under the experimental conditions used $K_3[\text{OH}^-] \gg 1$. Hence the value of k_{-3} will be relatively small compared to the value of $k_3[\text{OH}^-]$. Thus to a good approximation the hydroxide concentrations may be calculated from equation 5.9.

$$k_{\text{slow}} = \frac{k_3[\text{OH}^-]}{1 + K_1[\text{p.MeO-C}_6\text{H}_4\text{O}^-]} + k_{-3} \quad \text{equation 5.7}$$

$$k_{\text{slow}} = k_3[\text{OH}^-] + k_{-3} \quad \text{equation 5.8}$$

$$[\text{OH}^-] = \frac{k_{\text{slow}}}{9700} \quad \text{equation 5.9}$$

Application of equation 5.9 to the data in table 5.5 allows the calculation of a value for K of $1.0 \pm 0.1 \times 10^{-5} \text{ mol dm}^{-3}$. K is defined in equation 5.10.

$$K = \frac{[\text{OH}^-][\text{p.MeO-C}_6\text{H}_4\text{OH}]}{[\text{p.MeO-C}_6\text{H}_4\text{O}^-]} \quad \text{equation 5.10}$$

Using the now known value of K , hydroxide concentrations, $[\text{OH}^-]_{\text{calc}}$, corresponding to the buffers reported in table 5.5 were calculated. These values in conjunction with the measured absorbance values and equation 5.11 allowed the calculation of values for K_3 , the equilibrium constant for attack of hydroxide at the 3-position of 5.2. Data are in table 5.6. An absorbance value for the total conversion to the σ -adduct was not recorded, consequently a value of 0.90 was estimated.

$$K_3 = \frac{[\text{5.8}]}{[\text{5.2}][\text{OH}^-]_{\text{calc}}} = \frac{(\text{Abs.})}{(A_\infty - \text{Abs.})[\text{OH}^-]_{\text{calc}}} \quad \text{equation 5.11}$$

Table 5.6 Absorbance and equilibrium data for the formation of 5.8 in 74% DMSO-water (v/v) containing various concentrations of hydroxide at 25°C. $I = 0.1 \text{ mol dm}^{-3}$.

$[\text{OH}^-]_{\text{calc}}^*/$ $10^{-6} \text{ mol dm}^{-3}$	10	5.0	3.3	2.0	1.0
Abs. (425nm)	0.878	0.859	0.844	0.803	0.724
$K_3 /$ $10^6 \text{ dm}^3 \text{ mol}^{-1}$	4.0	4.2	4.6	4.1	4.1

A_∞ absorbance measurement for total conversion to 5.8, estimate 0.9.

* value of hydroxide concentration calculated for each buffer ratio, table 5.5.

An average value of $K_3 = 4.2 \pm 0.2 \times 10^6 \text{ dm}^3 \text{ mol}^{-1}$ is found.

A value of $k_3 (= k_3 / K_3)$ of $2 \times 10^{-3} \text{ s}^{-1}$ may now be calculated. All the parameters in equation 5.7 have now been evaluated. Nevertheless these did not give a good fit with the data in table 5.4, where the concentrations of $[\text{p.MeO-C}_6\text{H}_4\text{O}^-]$ are varied. Application of equation 5.12, which is similar to equation 5.7 but includes the extra term $k_{\text{PhO}}[\text{p.MeO-C}_6\text{H}_4\text{O}^-]$ enables excellent agreement between the calculated and the observed values of k_{slow} to be obtained, with $K_1 100 \pm 5 \text{ dm}^3 \text{ mol}^{-1}$, $k_3 9.3 \pm 0.4 \times 10^3 \text{ dm}^3 \text{ mol}^{-1} \text{ s}^{-1}$, $k_3 2 \pm 0.2 \times 10^{-3} \text{ s}^{-1}$ and $k_{\text{PhO}} 2.7 \pm 0.3 \text{ dm}^3 \text{ mol}^{-1} \text{ s}^{-1}$, table 5.7.

$$k_{\text{slow}} = \frac{k_3[\text{OH}^-] + k_{\text{PhO}}[\text{p.MeO-C}_6\text{H}_4\text{O}^-]}{1 + K_1[\text{p.MeO-C}_6\text{H}_4\text{O}^-]} + k_{-3} \quad \text{equation 5.12}$$

The rate constant k_{PhO^-} represents the catalysed addition of hydroxide by 4-methoxy phenolate, equation 5.13, and improves significantly the correlation between the observed and calculated kinetic data. Initial values were estimated using a rearranged form of equation 5.12 and the kinetic data reported in table 5.4, to give the gradient equal to k_{PhO^-} and the intercept equal to the hydroxide concentration for the 3:1 buffer ratio used. Division of the values k_3 by k_3 leads to a value of K_3 $4.7 \pm 0.7 \times 10^6 \text{ dm}^3 \text{ mol}^{-1}$ which is in acceptable agreement with that obtained independently from absorbance measurements at equilibrium. A computer correlation program was applied to a rearranged form of equation 5.12 to determine these final kinetic parameters.

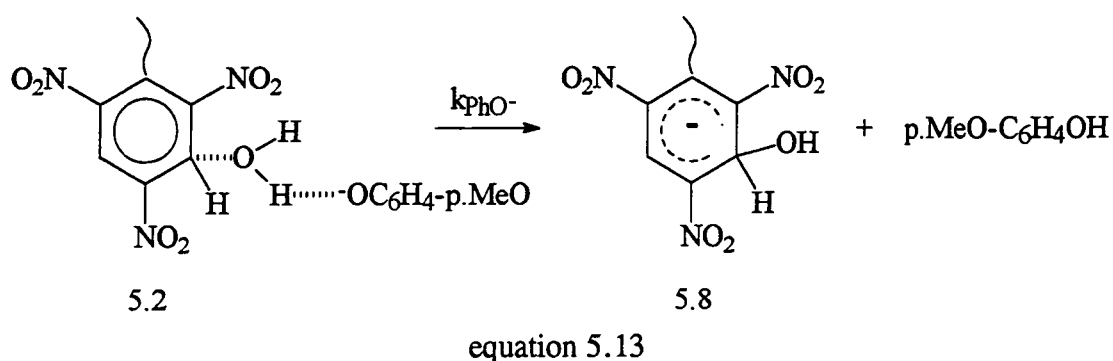


Table 5.7 Kinetic data for the equilibration of 5.2 and 5.8 in 74% DMSO-water (v/v) at 25°C.

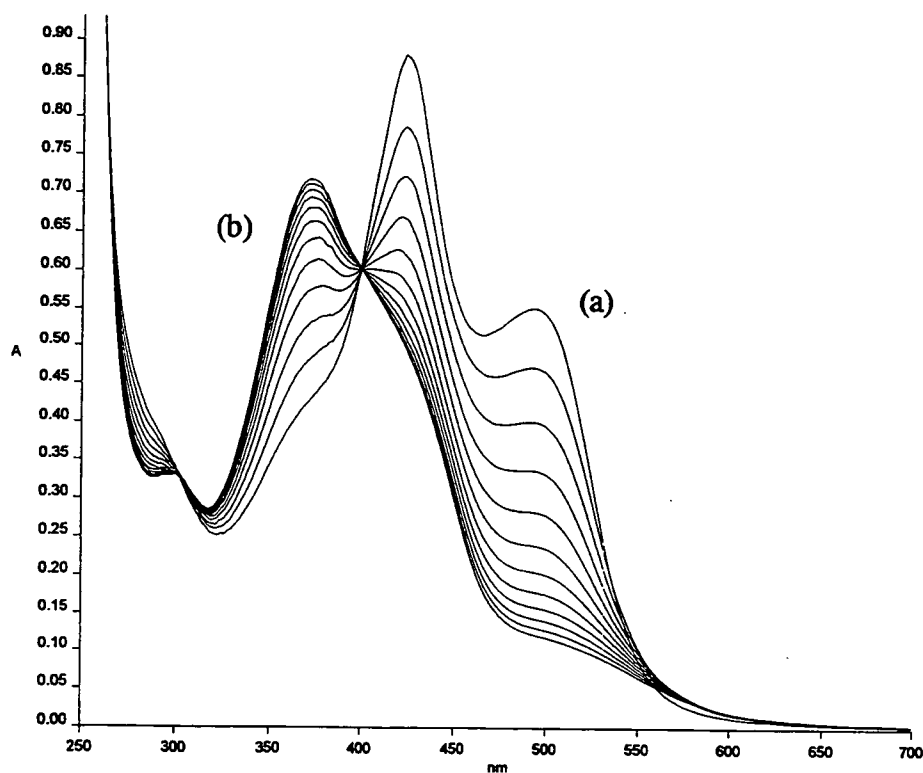
$[\text{p.MeO-C}_6\text{H}_4\text{O}^-] / \text{mol dm}^{-3}$	$[\text{p.MeO-C}_6\text{H}_4\text{OH}] / \text{mol dm}^{-3}$	$[\text{OH}^-]_{\text{calc}} / 10^{-6} \text{ mol dm}^{-3}$	$k_{\text{slow}} / \text{s}^{-1}$	$k_{\text{calc}}^a / \text{s}^{-1}$
0.001	0.003	3.3	0.029	0.032
0.002	0.006	"	0.032	0.032
0.004	0.012	"	0.032	0.032
0.005	0.015	"	0.031	0.031
0.008	0.024	"	0.030	0.031
0.001	0.001	10.0	0.064	0.089
0.001	0.002	5.0	0.045	0.047
0.001	0.003	3.3	0.032	0.030
0.001	0.005	2.0	0.021	0.021
0.001	0.010	1.0	0.013	0.013

^a Calculated from equation 5.12 with K_1 $100 \text{ dm}^3 \text{ mol}^{-1}$, k_3 $9.3 \times 10^3 \text{ dm}^3 \text{ mol}^{-1} \text{ s}^{-1}$, k_3 $2 \times 10^{-3} \text{ s}^{-1}$ and k_{PhO^-} $2.7 \text{ dm}^3 \text{ mol}^{-1} \text{ s}^{-1}$.

5.5 Reactions of Phenyl 2,4,6-Trinitrophenyl Ether with Phenol.

A similar reaction sequence is observed as for that of substrate 5.2, consisting of three discrete processes all separated significantly in time. All three processes for the reaction of substrate 5.3 with phenol buffer solutions have been observed spectrophotometrically. Spectra for attack of hydroxide ions to form a σ -complex similar to that of 5.8, λ_{max} 425nm and 492nm (br.) have previously been presented in figure 5.1, section 5.2. Figure 5.10 shows the following process involving its decomposition, presumably via a short lived σ -adduct similar to that of 5.7, to give finally the picrate ion, λ_{max} 371nm. Evidence for the fast process occurring over an initial time interval of 0.05 seconds is provided.

Figure 5.10 U.V./Vis. spectra for the slow formation of the picrate ion involving phenyl 2,4,6-trinitrophenyl ether, 4×10^{-5} mol dm⁻³ with phenolate, 0.005 mol dm⁻³, pH(water) 9.20 in 74% DMSO-water (v/v) at 25°C. Scans repeated every hour.
(a) Initial spectrum. (b) Final spectrum after 11 hours.



Kinetic measurements are presented for the first two processes and a reaction scheme identical to that shown in scheme 5.1 is postulated. Rate constants, conducted in 74% DMSO-water (v/v), were measured under first order conditions, hence for reactions in buffers, the buffer components were in large excess of the substrate concentration, $4 \times 10^{-5} \text{ mol dm}^{-3}$.

5.5.1 Reaction of 5.3 with Sodium Hydroxide.

An identical experimental procedure was followed to that discussed earlier in section 5.4.1. Examples of the first order kinetic traces observed relating to the formation of a σ -complex similar to that of 5.8 from addition of hydroxide ions is presented in figure 5.11. Table 5.8 provides a summary of the results.

Figure 5.11 Kinetic traces for the reaction of 5.3, $4 \times 10^{-5} \text{ mol dm}^{-3}$ with various hydroxide ion concentrations in 74% DMSO-water (v/v), λ 425nm, at 25°C . $I = 0.1 \text{ mol dm}^{-3}$.

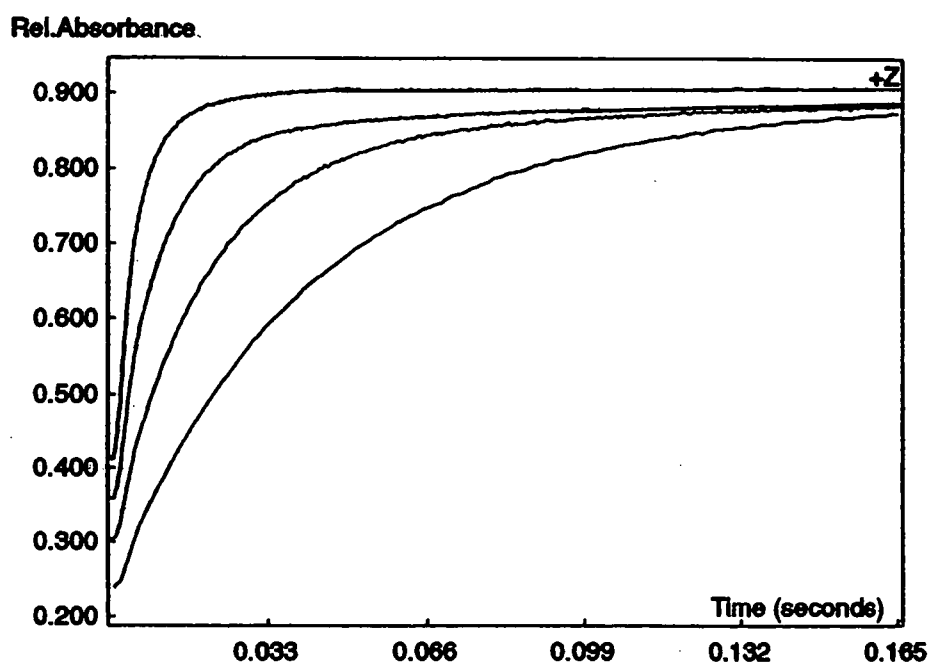


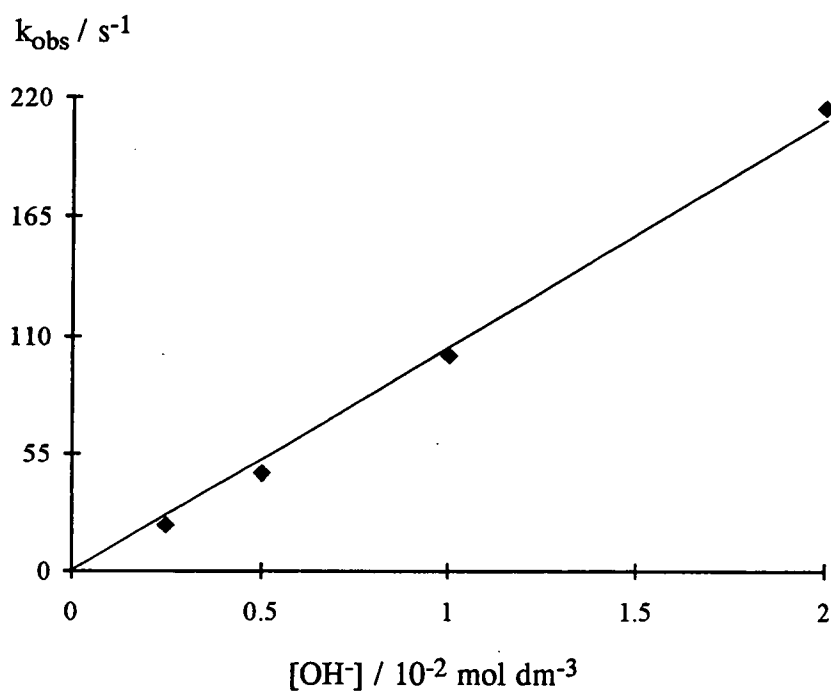
Table 5.8 Kinetic data for the reaction of 5.3 and hydroxide ions in 74% DMSO-water (v/v), λ 425nm, at 25°C. $I = 0.1 \text{ mol dm}^{-3}$.

$[\text{OH}^-] / 10^{-2} \text{ mol dm}^{-3}$	0.25	0.50	1.0	2.0
$k_{\text{obs}} / \text{s}^{-1}$	21.8	46.2	101	215

5.5.1.1 Kinetic Analysis.

Under the conditions mentioned in section 5.4.1.1 combined with equation 5.4, figure 5.12 leads to the calculation of $k_3 = 1.05 \pm 0.03 \times 10^4 \text{ dm}^3 \text{ mol}^{-1} \text{ s}^{-1}$ for the reaction of hydroxide ions with substrate 5.3 in 74% DMSO-water (v/v) and k_{-3} estimated in the range of 0-5 s^{-1} .

Figure 5.12 Rate dependency of k_{obs} on hydroxide concentration, $[\text{OH}^-]$.



5.5.2 The Fast Process: Reaction of 5.3 with Phenolate.

Investigations were conducted for a series of buffer solutions with a single buffer ratio, (PhOH:PhO⁻ 5:1 pH(water) = 9.25), but with various buffer concentrations. Figure 5.13 shows the kinetic trace obtained for the formation of the proposed intermediate 5.1. Table 5.9 reports a summary of the first order rate constants, k_{fast} , which may also be seen graphically in figure 5.14.

Figure 5.13 Kinetic trace acquired, $\lambda = 420\text{nm}$, for the fast reaction of 5.3, $2 \times 10^{-5} \text{ mol dm}^{-3}$, with phenolate, $0.001 \text{ mol dm}^{-3}$, pH(water) 9.25, 74% DMSO-water (v/v), at 25°C.

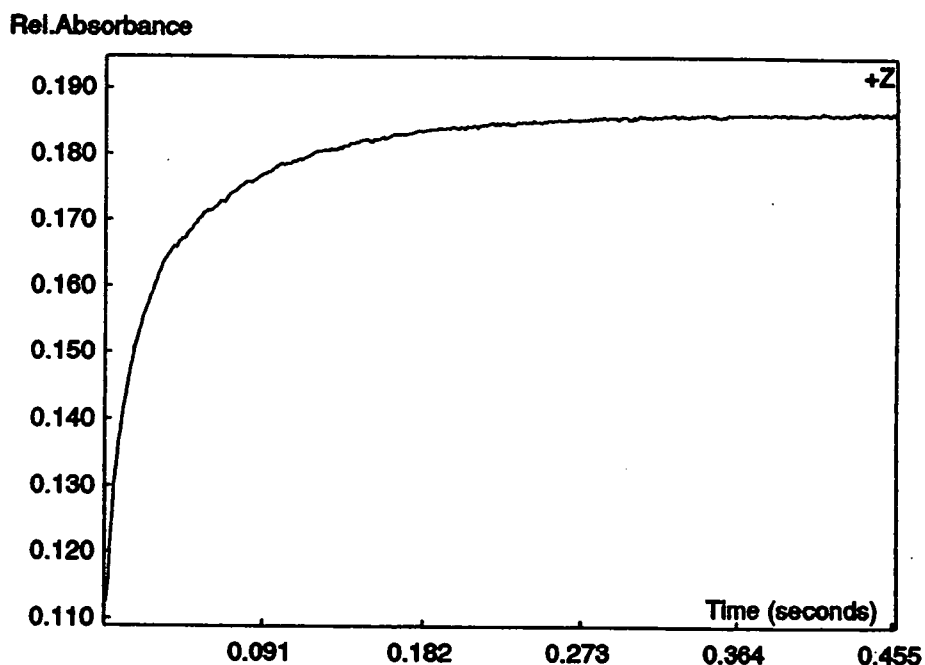
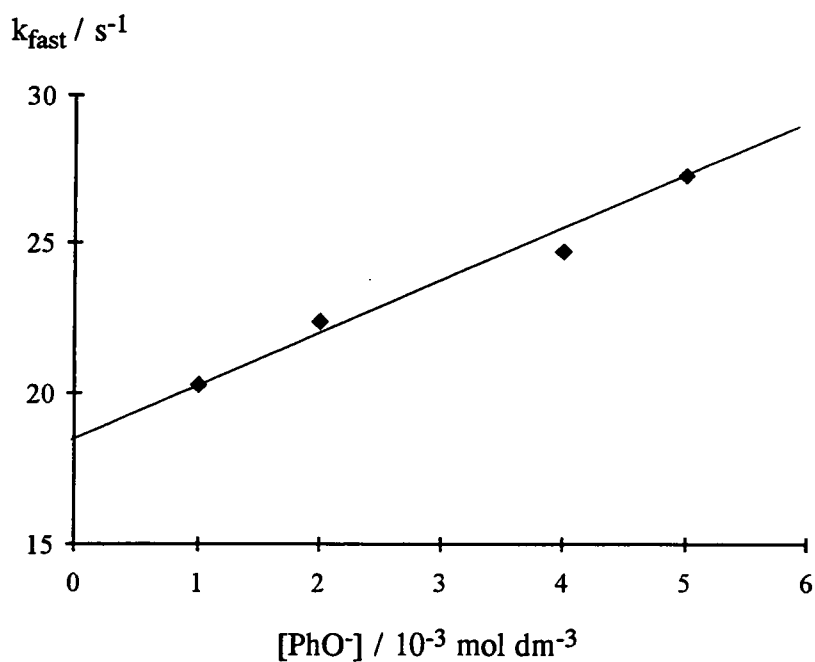


Table 5.9 Kinetic data for the reaction of 5.3 with phenolate, 74% DMSO-water (v/v), pH(water) 9.25, $\lambda = 420\text{nm}$, at 25°C. $I = 0.1 \text{ mol dm}^{-3}$.

[PhO ⁻] / $10^{-3} \text{ mol dm}^{-3}$	1.00	2.00	4.00	5.00
$k_{\text{fast}} / \text{s}^{-1}$	20.3	22.4	24.7	27.3

Figure 5.14 Rate dependency of k_{fast} on buffer concentration, $[\text{PhO}^-]$.



5.5.2.1 Kinetic Analysis: Fast Process

Application of equation 5.4 allows values of k_1 $1.6 \pm 0.2 \times 10^3 \text{ dm}^3 \text{ mol}^{-1} \text{ s}^{-1}$ and k_{-1} $18.7 \pm 0.6 \text{ s}^{-1}$ to be deduced from the graph in figure 5.14. Knowing values of k_1 and k_{-1} , the equilibrium constant K_1 for the formation of the proposed σ -adduct 5.10 may be calculated, K_1 $86 \pm 10 \text{ dm}^3 \text{ mol}^{-1}$.

5.5.3 The Slow Process: Reaction of 5.3 with Phenolate.

Results are reported for the slow reaction involving the formation of a σ -adduct similar to that of 5.8. As described previously investigations were conducted under two sets of conditions.

5.5.3.1 Constant Buffer Ratio.

Kinetic data for the observed first order rate constant, k_{slow} , are summarised in table 5.10. Again the relative change in k_{slow} with $[\text{PhO}^-]$ is small. Any increase is believed to result from the catalytic effect of the phenolate ions, k_{PhO^-} , discussed in section 5.4.4. Consequently an increase in phenolate ions implies an increase in k_{slow} . Figure 5.15 shows clearly the effect of the k_{PhO^-} term which is roughly equivalent for both 5:1 and 12:1 buffer ratio results plotted.

Figure 5.15 Rate dependency of k_{slow} on buffer concentration, $[\text{PhO}^-]$.

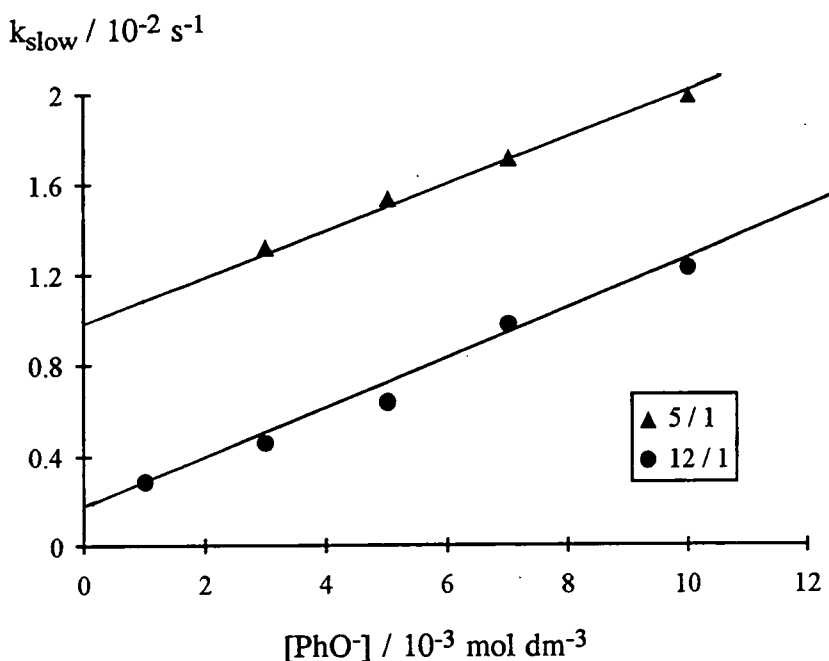


Table 5.10 Kinetic data for the slow reaction of 5.3 with phenolate ions in 74% DMSO-water (v/v), $\lambda = 425\text{nm}$, at 25°C . $I = 0.1 \text{ mol dm}^{-3}$.

$[\text{PhO}^-] / 10^{-3} \text{ mol dm}^{-3}$	1.0	3.0	5.0	7.0	10.0
$k_{\text{slow}}^{\text{a}} / 10^{-2} \text{ s}^{-1}$	-	1.32	1.54	1.72	2.00
$k_{\text{slow}}^{\text{b}} / 10^{-2} \text{ s}^{-1}$	0.29	0.46	0.64	0.98	1.23

^a PhOH:PhO⁻ 5:1, pH(water) 9.25 ^b PhOH:PhO⁻ 12:1, pH(water) 8.79

5.5.3.2 Variation in Buffer Ratio, [PhOH : PhO⁻].

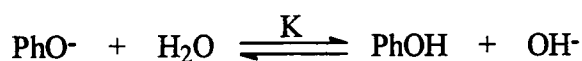
Results for the reaction of 5.3 with various buffer ratios of PhOH:PhO⁻ are summarised in table 5.11. Absorbance values, λ 425nm, at completion of the reaction are also reported. Values of k_{slow} exhibit a clear dependence on pH, i.e. the buffer ratio, which complies with the postulate that formation of σ -adduct involves attack of hydroxide ions at the 3-position of substrate 5.3.

Table 5.11 Kinetic and absorbance data for the slow reaction of 5.3, $4 \times 10^{-5} \text{ mol dm}^{-3}$, with different buffer solutions, $[\text{PhOH}] = 0.01 \text{ mol dm}^{-3}$ 74% DMSO-water (v/v), $\lambda = 425\text{nm}$, at 25°C . $I = 0.1 \text{ mol dm}^{-3}$.

$[\text{PhO}^-] / 10^{-3} \text{ mol dm}^{-3}$	1.6	1.0	0.83	0.5
$k_{\text{slow}} / 10^{-3} \text{ s}^{-1}$	9.60	7.34	7.04	6.01
Abs. (425nm)	0.600	0.565	0.522	0.471

5.5.4 Kinetic Analysis: Slow Process.

Equation 5.14 defines the equilibrium constant, K , for the protonation of phenolate ions in 74% DMSO-water (v/v). Applying the method described previously in section 5.4.3 corresponding to reactions of 4-methoxy-phenolate, with data from table 5.11 enables an average value of $K = 6.0 \pm 1 \times 10^{-6} \text{ mol dm}^{-3}$ to be determined. Although it is in good agreement with the value of $K = 5.7 \pm 0.7 \times 10^{-6} \text{ mol dm}^{-3}$ established for the reaction of 1,3,5-trinitrobenzene with phenol buffer solutions (section 5.6.4), the range of values associated with the phenolate concentration were very low. Thus the latter value of K will be used throughout the following calculations.



equation 5.14

Absorbance data reported in table 5.11 can yield values of K_3 , the equilibrium constant for attack of hydroxide at the 3-position of substrate 5.3, along with equation 5.11 and the recalculated values of hydroxide, $[\text{OH}^-]_{\text{calc}}$, table 5.12. An absorbance value for the total conversion to the σ -adduct was not recorded, consequently a value of 0.73 was estimated.

Table 5.12 Absorbance and equilibrium data for the formation of the phenol equivalent of σ -adduct 5.8 in 74% DMSO-water (v/v) containing various concentrations of hydroxide at 25°C. $I = 0.1 \text{ mol dm}^{-3}$.

$[\text{OH}^-]_{\text{calc}}^*/$ $10^{-6} \text{ mol dm}^{-3}$	0.91	0.57	0.47	0.29
Abs. (425nm)	0.600	0.565	0.522	0.471
$K_3 /$ $10^6 \text{ dm}^3 \text{ mol}^{-1}$	5.1	6.0	5.3	6.2

A_∞ absorbance measurement for total conversion to σ -adduct, estimate 0.73.

* value of hydroxide concentration determined for each buffer ratio, table 5.11.

An average value of $K_3 = 5.6 \pm 0.5 \times 10^6 \text{ dm}^3 \text{ mol}^{-1}$ is found.

Equation 5.12 is applicable and a good fit is achieved with values of K_1 $90 \pm 10 \text{ dm}^3 \text{ mol}^{-1}$, k_3 $1.00 \pm 0.03 \times 10^4 \text{ dm}^3 \text{ mol}^{-1} \text{ s}^{-1}$, k_{-3} $2.0 \pm 0.2 \times 10^{-3} \text{ s}^{-1}$ and k_{PhO^-} $1.5 \pm 1 \text{ dm}^3 \text{ mol}^{-1} \text{ s}^{-1}$, table 5.13. Introduction of the rate constant k_{PhO^-} again improves significantly the correlation between the observed and calculated kinetic data. Division of the values k_3 by k_{-3} leads to a value of K_3 $5.0 \pm 0.7 \times 10^6 \text{ dm}^3 \text{ mol}^{-1}$ which is in acceptable agreement with that obtained independently from absorbance measurements at equilibrium. A computer correlation program was applied to a rearranged form of equation 5.12 to determine these final kinetic parameters.

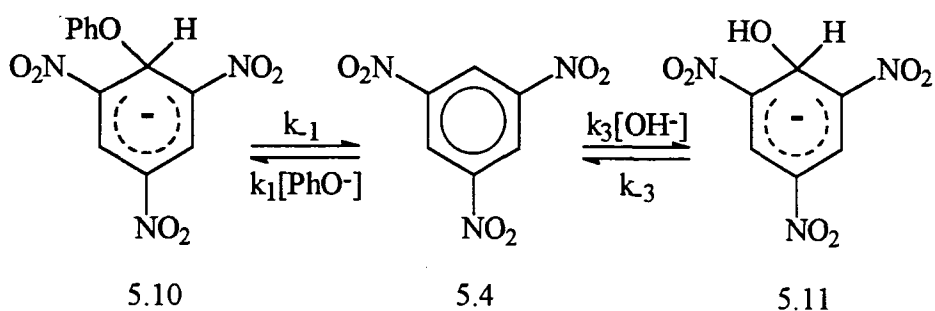
Table 5.13 Kinetic data for the equilibration of 5.3 with hydroxide in 74% DMSO-water (v/v) at 25°C.

[PhO ⁻] / 10 ⁻² mol dm ⁻³	[PhOH] / mol dm ⁻³	[OH ⁻] _{calc} / 10 ⁻⁶ mol dm ⁻³	k_{slow} / 10 ⁻² s ⁻¹	k_{calc}^a / 10 ⁻² s ⁻¹
0.1	0.005	1.14	0.9	1.4
0.3	0.015	"	1.3	1.5
0.5	0.025	"	1.5	1.5
0.7	0.035	"	1.7	1.5
1.0	0.050	"	2.0	1.6
0.1	0.012	0.475	0.3	0.8
0.3	0.036	"	0.5	0.9
0.5	0.060	"	0.6	1.0
0.7	0.084	"	1.0	1.1
1.0	0.120	"	1.2	1.2
0.160	0.010	0.91	0.96	1.2
0.100	"	0.57	0.73	0.9
0.083	"	0.47	0.70	0.8
0.050	"	0.29	0.60	0.5

^a Calculated from equation 5.12 with K_1 $90 \text{ dm}^3 \text{ mol}^{-1}$, k_3 $1.0 \times 10^4 \text{ dm}^3 \text{ mol}^{-1} \text{ s}^{-1}$, k_{-3} $2.0 \times 10^{-3} \text{ s}^{-1}$ and k_{PhO^-} $1.5 \text{ dm}^3 \text{ mol}^{-1} \text{ s}^{-1}$.

5.6 Reactions of 1,3,5-Trinitrobenzene with Phenol.

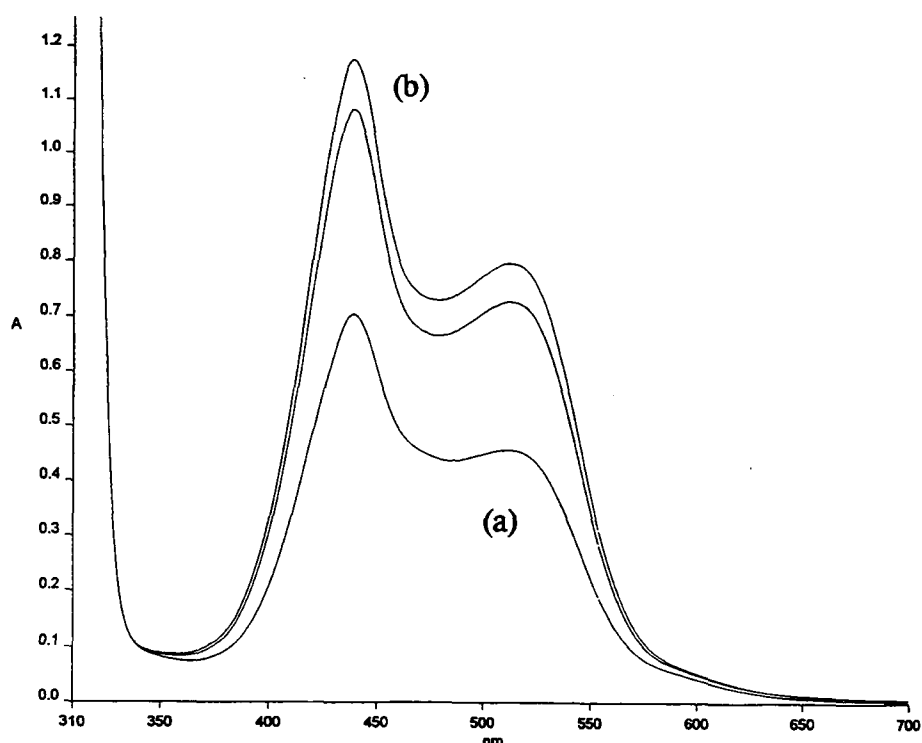
Equation 5.15 is proposed for the reaction of phenol buffer solutions with 1,3,5-trinitrobenzene, 5.4. The appearance of the σ -adduct 5.10, resulting from rapid attack of the phenolate ion, is followed by formation of the hydroxide adduct 5.11, λ_{max} 440nm and 514nm (br.). The absorption maxima found for 5.11 are in accordance with previous studies, λ_{max} 440nm and 510nm (br.).³ The formation of this adduct is shown in figure 5.16.



equation 5.15

Figure 5.16 U.V./Vis. spectra for the slow formation of σ -adduct 5.11 involving 1,3,5-trinitrobenzene, 4×10^{-5} mol dm⁻³, with phenolate, 0.005 mol dm⁻³ and phenol, 0.025 mol dm⁻³, pH(water) = 9.25 in 74% DMSO-water (v/v) at 25°C. Spectra repeated every 2 minutes.

(a) Initial spectrum. (b) Final spectrum after 10 minutes.



5.6.1 Reactions with Sodium Hydroxide and Methoxide.

Reaction of 5.4 with hydroxide in a DMSO-water mixture resulted in the rapid formation of a species having absorption maxima at 440nm and 515nm (br.), characteristic of σ -adduct 5.11. There is a wide range of literature referring to the reaction of hydroxide ions to substrate 5.4. Although many solvents systems have been investigated²⁻⁵ an accurate comparison with the former reactions is necessary, therefore experiments have been conducted in 74% DMSO-water (v/v) and 0.1 mol dm⁻³ ionic strength. A method corresponding to section 4.7.1 chapter 4 was employed. Results are also reported for the reaction in 50% DMSO-water (v/v) and addition to 5.4 of sodium methoxide in methanol, table 5.14 and 5.15, which will be discussed later. Kinetic measurements were made by stopped-flow spectrophotometry, figure 5.17, with either hydroxide / methoxide in large excess of the substrate.

Table 5.14 Kinetic data for the reaction of 5.4 and hydroxide in 74% DMSO-water (v/v), $\lambda = 425\text{nm}$, at 25°C. $I = 0.1 \text{ mol dm}^{-3}$.

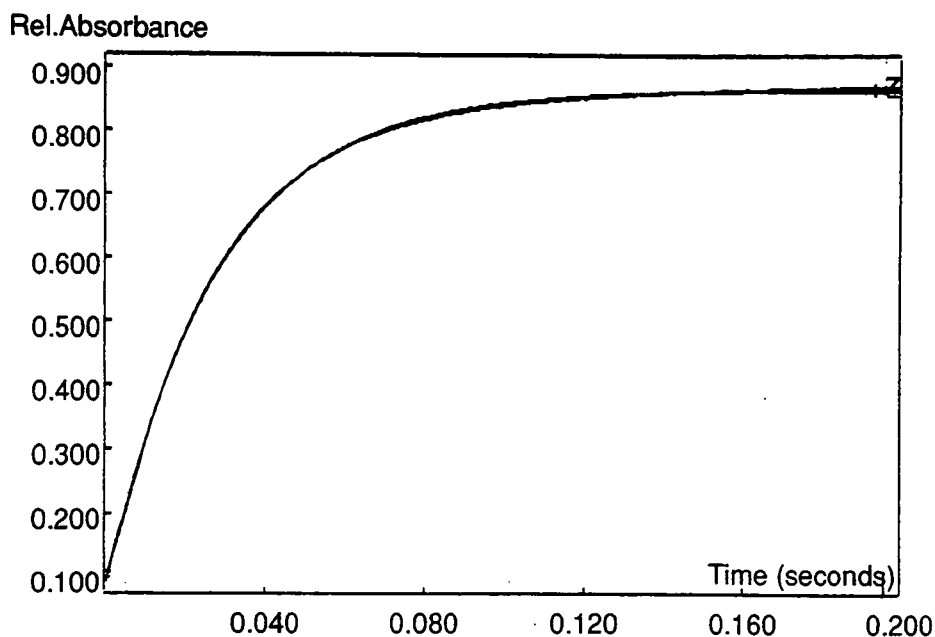
$[\text{OH}^-] / 10^{-2} \text{ mol dm}^{-3}$	0.50	1.0	1.5	2.0	10.0	20.0
$k_{\text{obs}} / \text{s}^{-1}$	117	244	392	540	-	-
$k_{\text{obs}}^{\text{a}} / \text{s}^{-1}$	-	-	-	-	35.5	73.1

^a 50% DMSO-water (v/v), $\lambda = 500\text{nm}$ and 258nm, varying ionic strength.

Table 5.15 Kinetic data for the reaction of 5.4 and methoxide in methanol, $\lambda = 500\text{nm}$, at 25°C.

$[\text{MeO}^-] / \text{mol dm}^{-3}$	0.04	0.10
$k_{\text{obs}}^{\text{a}} / \text{s}^{-1}$	470	750

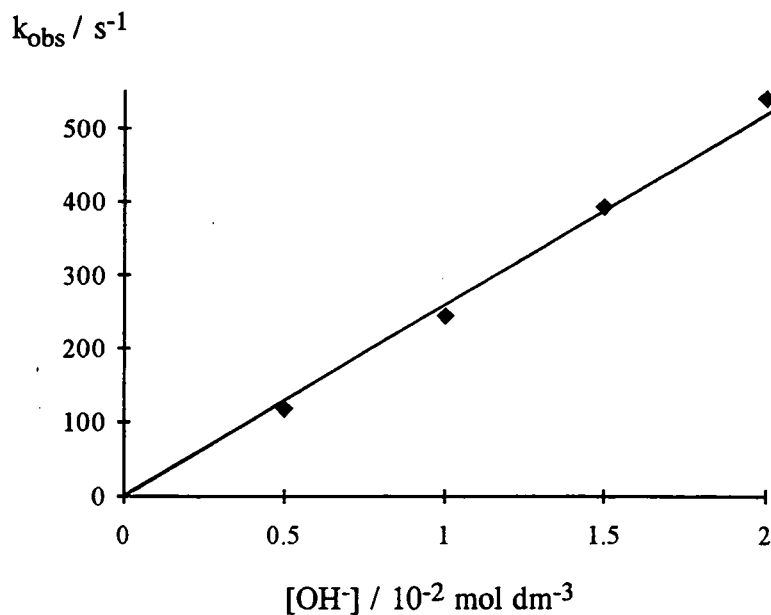
Figure 5.17 Kinetic traces involving 5.4, 1×10^{-4} mol dm⁻³ with [OH⁻] 0.1 mol dm⁻³ in 50% DMSO-water (v/v), $\lambda = 500$ nm at 25°C.



5.6.1.1 Kinetic Analysis.

Kinetic data for the reaction of hydroxide with substrate 5.4 in 74% DMSO-water (v/v) produced a linear plot according to equation 5.3 giving values of $k_3 = 2.63 \pm 0.06 \times 10^4$ dm³ mol⁻¹ s⁻¹ and k_{-3} estimated in the range of 0-5 s⁻¹, figure 5.18.

Figure 5.18 Rate dependency of k_{obs} on hydroxide concentration, [OH⁻].



5.6.2 The Fast Process: Reaction of 5.4 with Phenolate.

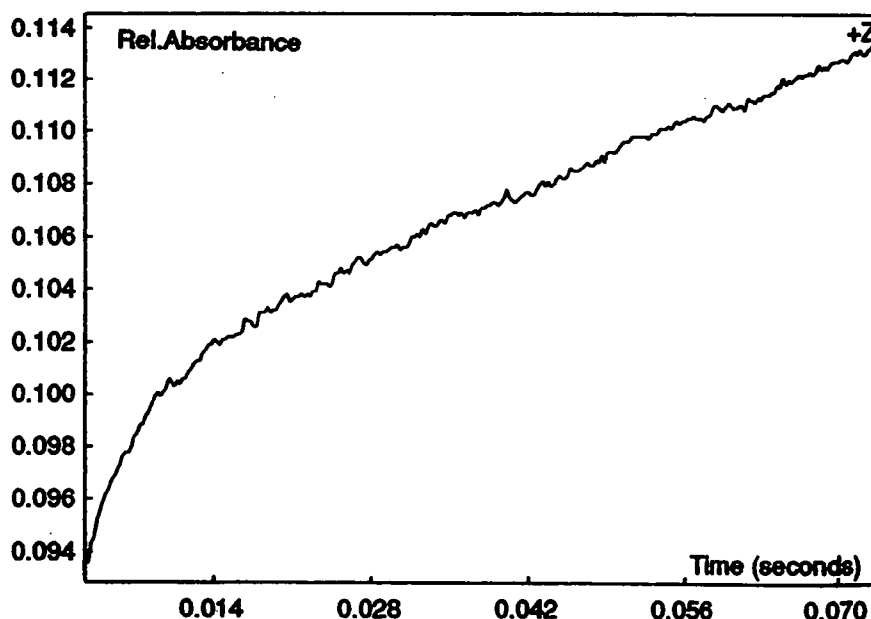
Kinetic measurements were made for the rapid reaction of 5.4, 4×10^{-5} mol dm^{-3} , with a series of buffer solutions of different concentration at a constant buffer ratio, PhOH:PhO⁻ 5:1 pH(water) 9.26 in 74% DMSO-water (v/v) at 25°C. Data collected initially showed very little change in the rate constant, k_{fast} over the range of phenolate concentrations, $1 - 7 \times 10^{-3}$ mol dm^{-3} . Experiments were repeated over a greater concentration range, $2.0 - 5.5 \times 10^{-2}$ mol dm^{-3} , still indicating no significant change with values of k_{fast} in the region of 170 ± 20 s⁻¹.

5.6.2.1 Kinetic Analysis: Fast Process.

Since values of k_{fast} remained almost constant even under a substantial change in phenolate concentration, it is concluded from equation 5.4 that $k_{\text{fast}} \approx k_{-1}$. Evidence for this is also provided by the kinetic traces obtained, figure 5.19, which denote a very low absorbance change (i.e. little adduct formation) with respect to those observed already in substrates 5.2 and 5.3. The implication is that the value of K_1 , the equilibrium constant for formation of 5.10, is small. The results indicate that the value of k_{fast} has risen to no more than 190 s⁻¹ in a solution where [PhO⁻] = 0.05 mol dm^{-3} . Use of equation 5.4 with a value of k_{-1} 170 s⁻¹, allows an estimate for k_1 of ≤ 400 $\text{dm}^3 \text{ mol}^{-1} \text{ s}^{-1}$. This value combined with the value of k_{-1} 170 s⁻¹ leads to a maximum value for K_1 ($= k_1 / k_{-1}$) of 2 $\text{dm}^3 \text{ mol}^{-1}$.

$$k_{\text{fast}} = k_1[\text{PhO}^-] + k_{-1} \quad \text{equation 5.4}$$

Figure 5.19 Kinetic trace for the formation of 5.10.



5.6.3 The Slow Process: Reaction of 5.4 with Phenolate.

Investigations involving the formation of the σ -adduct 5.11 are reported in the two following sections.

5.6.3.1 Constant Buffer Ratio.

A summary of the kinetic data, k_{slow} monitored at 425nm, may be viewed in table 5.16. Reactions involving the 1:1 buffer at high concentrations of phenolate were conducted to dispel any doubts concerning the ability of the 5:1 and 12:1 ratios to maintain their buffer properties. Results presented here are compatible with those already analysed for the related systems which incorporate the catalytic term of k_{PhO^-} .

Table 5.16 Kinetic data for the slow reaction of 5.4 with phenolate ions in 74% DMSO-water (v/v), $\lambda = 425\text{nm}$, at 25°C . $I = 0.1 \text{ mol dm}^{-3}$.

[PhO ⁻] / 10 ⁻² mol dm ⁻³	0.1	0.3	0.5	0.7	1.0	2.0	3.0	4.0
$k_{\text{slow}}^{\text{a}}$ / 10 ⁻² s ⁻¹	2.44	3.33	3.58	-	3.90	-	-	-
$k_{\text{slow}}^{\text{b}}$ / 10 ⁻² s ⁻¹	1.83	2.68	3.29	3.92	4.60	-	-	-
$k_{\text{slow}}^{\text{c}}$ / 10 ⁻² s ⁻¹	-	-	-	-	16.7	19.0	21.2	23.6

^a PhOH:PhO⁻ 5:1, pH_(water) 9.21 ^b PhOH:PhO⁻ 12:1, pH_(water) 8.80

^c PhOH:PhO⁻ 1:1, pH_(water) 9.79

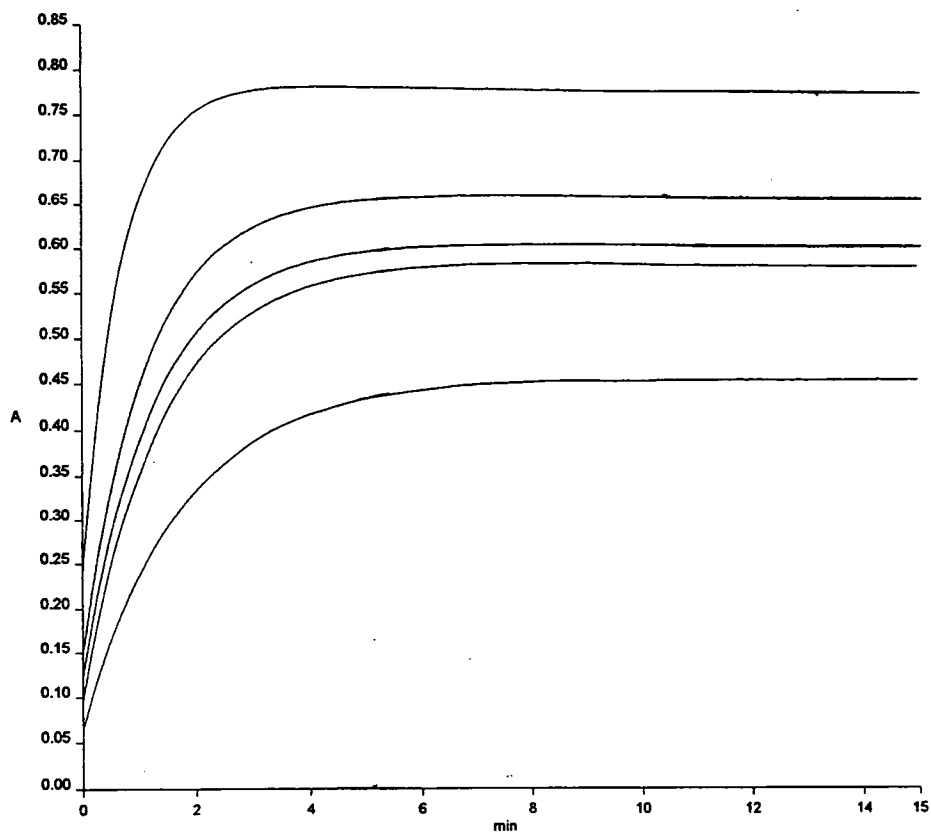
5.6.3.2 Variation in Buffer Ratio, [PhOH : PhO⁻].

Results for the reaction of 5.4 at various buffer ratios of PhOH:PhO⁻ are summarised in table 5.17. Absorbance values, $\lambda = 425\text{nm}$, at completion of the reaction are also reported. Values of k_{slow} exhibit a clear dependence on pH, i.e. the buffer ratio, which complies with the postulate that formation of 5.11 involves attack of hydroxide ions. Figure 5.20 provides examples of the first order kinetic traces observed.

Table 5.17 Kinetic and absorbance data for the slow reaction of 5.4, 4×10^{-5} mol dm^{-3} , with different buffer ratios in 74% DMSO-water (v/v), $\lambda = 425\text{nm}$, at 25°C . $I = 0.1$ mol dm^{-3} .

[PhOH] / 10^{-2} mol dm^{-3}	1.0	1.0	1.0	1.0	1.0	2.0	3.0	4.0	5.0
[PhO ⁻] / 10^{-3} mol dm^{-3}	1.6	1.0	0.83	0.66	0.50	10	10	10	10
$k_{\text{slow}} / 10^{-3} \text{ s}^{-1}$	23.9	14.6	13.3	12.3	9.78	100	74	64	54
Abs.(425nm)	0.78	0.66	0.60	0.58	0.45	-	-	-	-

Figure 5.20 Kinetic traces for the formation of 5.11 for reaction of 5.4, 4×10^{-5} mol dm^{-3} with differing buffer ratios, $\lambda = 425\text{nm}$, at 25°C .



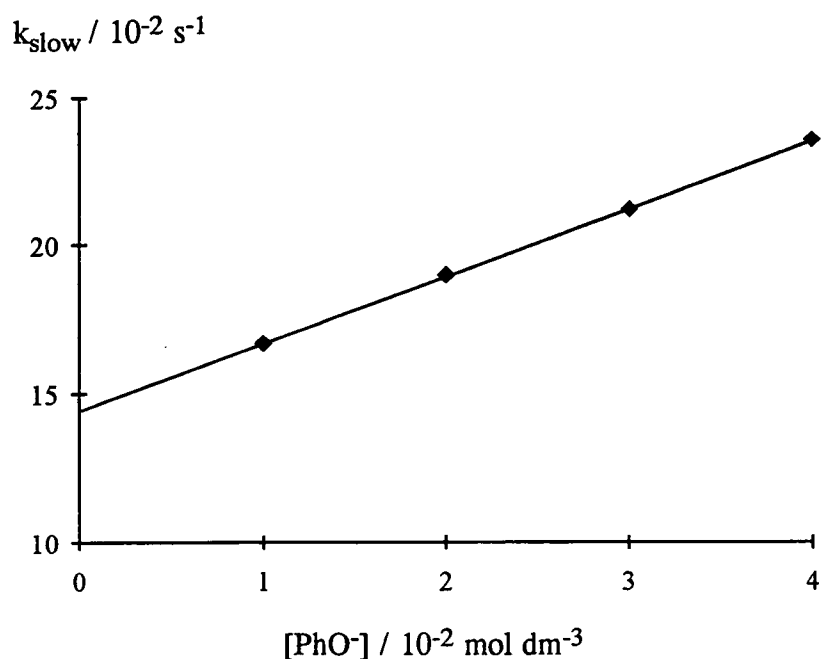
5.6.4 Kinetic Analysis: Slow Process.

Due to the low concentrations of phenolate present in the group of reactions involving various buffer ratios it is not possible to obtain a reliable value of the equilibrium constant K for the protonation of phenolate in 74% DMSO-water (v/v), equation 5.14 defined previously. A value of K can be established by an alternative method using the data provided for the reactions with a 1:1 buffer ratio, table 5.16. Evidence acquired in section 5.6.2 shows the condition $1 \gg K_1[\text{PhO}^-]$ applies, hence reducing equation 5.12 to equation 5.16 below.

$$k_{\text{slow}} = k_3[\text{OH}^-] + k_{\text{PhO}^-}[\text{PhO}^-] + k_{-3} \quad \text{equation 5.16}$$

A graph of k_{slow} versus $[\text{PhO}^-]$ will now enable the rate constant k_{PhO^-} and $[\text{OH}^-]$ to be determined from the gradient and intercept respectively, figure 5.21. Estimations of k_{PhO^-} $2.3 \pm 0.03 \text{ dm}^3 \text{ mol}^{-1} \text{ s}^{-1}$ and $[\text{OH}^-]$ $5.5 \pm 0.1 \times 10^{-6} \text{ mol dm}^{-3}$ are calculated where $k_3 = 2.63 \times 10^4 \text{ dm}^3 \text{ mol}^{-1} \text{ s}^{-1}$ and k_{-3} is approximated to zero. An equation similar to that of 5.10 yields a value of $K = 5.5 \pm 0.1 \times 10^{-6} \text{ mol dm}^{-3}$.

Figure 5.21 Rate dependency of k_{slow} with $[\text{PhO}^-]$ for a 1:1 buffer ratio.



Values of hydroxide concentration can now be calculated for each buffer ratio in table 5.17 and combination with the corresponding absorbance values will enable a value of the equilibrium constant K_3 to be determined, table 5.18. An absorbance value for the total conversion to the σ -adduct is estimated to be 1.1.

Table 5.18 Absorbance and equilibrium data for the formation of 5.11 in 74% DMSO-water (v/v) containing various concentrations of hydroxide at 25°C. $I = 0.1 \text{ mol dm}^{-3}$.

$[\text{OH}^-]_{\text{calc}}^*/$ $10^{-6} \text{ mol dm}^{-3}$	0.88	0.55	0.46	0.36	0.28
Abs. (λ 425nm)	0.78	0.66	0.60	0.58	0.45
$K_3 /$ $10^6 \text{ dm}^3 \text{ mol}^{-1}$	2.8	2.7	2.6	3.1	2.5

A_∞ absorbance measurement for total conversion to σ -adduct, estimate 1.1.

* value of hydroxide concentration determined for each buffer ratio, table 5.17.

An average value of $K_3 = 2.7 \pm 0.2 \times 10^6 \text{ dm}^3 \text{ mol}^{-1}$ is found.

Values calculated from equation 5.16 with $k_3 2.55 \pm 0.03 \times 10^4 \text{ dm}^3 \text{ mol}^{-1} \text{ s}^{-1}$, $k_{-3} 6.0 \pm 1 \times 10^{-3} \text{ s}^{-1}$, $k_{\text{pH}O^-} 2.8 \pm 0.5 \text{ dm}^3 \text{ mol}^{-1} \text{ s}^{-1}$ and $K 5.5 \pm 0.2 \times 10^{-6} \text{ mol dm}^{-3}$ give excellent agreement with the experimental data, table 5.19. Introduction of the rate constant $k_{\text{pH}O^-}$ again improves significantly the correlation between the observed and calculated kinetic data. Combination of the values k_3 and k_{-3} yields a value of $K_3 4.3 \pm 0.7 \times 10^6 \text{ dm}^3 \text{ mol}^{-1}$ which is in acceptable agreement with that obtained independently from absorbance measurements at equilibrium. A computer correlation program was applied to equation 5.16 to determine these final kinetic parameters.

Table 5.19 Kinetic data for the equilibration of 5.4 with hydroxide in 74% DMSO-water (v/v) at 25°C.

[PhO ⁻] / mol dm ⁻³	[PhOH] / mol dm ⁻³	[OH ⁻] _{calc} / 10 ⁻⁶ mol dm ⁻³	k _{slow} / 10 ⁻² s ⁻¹	k _{calc} ^a / 10 ⁻² s ⁻¹
0.001	0.012	0.46	1.8	2.0
0.003	0.036	"	2.7	2.6
0.005	0.060	"	3.3	3.2
0.007	0.084	"	3.9	3.7
0.01	0.12	"	4.6	4.6
0.01	0.010	5.5	17	17
0.02	0.02	"	19	20
0.03	0.03	"	21	23
0.04	0.04	"	24	26
0.01	0.02	2.75	10	10
0.01	0.03	1.83	7.4	8.1
0.01	0.04	1.38	6.4	7.0
0.01	0.05	1.10	5.4	6.2

^a Calculated from equation 5.16 with $k_3 2.55 \pm 0.03 \times 10^4 \text{ dm}^3 \text{ mol}^{-1} \text{ s}^{-1}$, $k_{-3} 6.0 \pm 1.0 \times 10^{-3} \text{ s}^{-1}$, $k_{\text{PhO}^-} 2.8 \pm 0.5 \text{ dm}^3 \text{ mol}^{-1} \text{ s}^{-1}$ and $K 5.5 \pm 0.1 \times 10^{-6} \text{ mol dm}^{-3}$.

5.7 Reactions of Substrates 5.2, 5.3 & 5.4 with Borax Buffers.

Kinetic studies have been completed for the reactions of substrates 5.2, 5.3 and 5.4 with Borax buffers in 74% DMSO-water (v/v). The slow formation of the 1,3 σ -adduct was monitored at a wavelength of 425nm at 25°C. With the substrate concentration equal to 4×10^{-5} mol dm³ and the buffer concentration in excess, first order rate constants were observed, figure 5.22. Results are presented in table 5.20 along with the corresponding values of pH(water). Analysis of the results is not possible due to the difficulty in determining the pH(DMSO) values.

Figure 5.22 Kinetic traces obtained for the reaction of 5.2 and Borax Buffer.

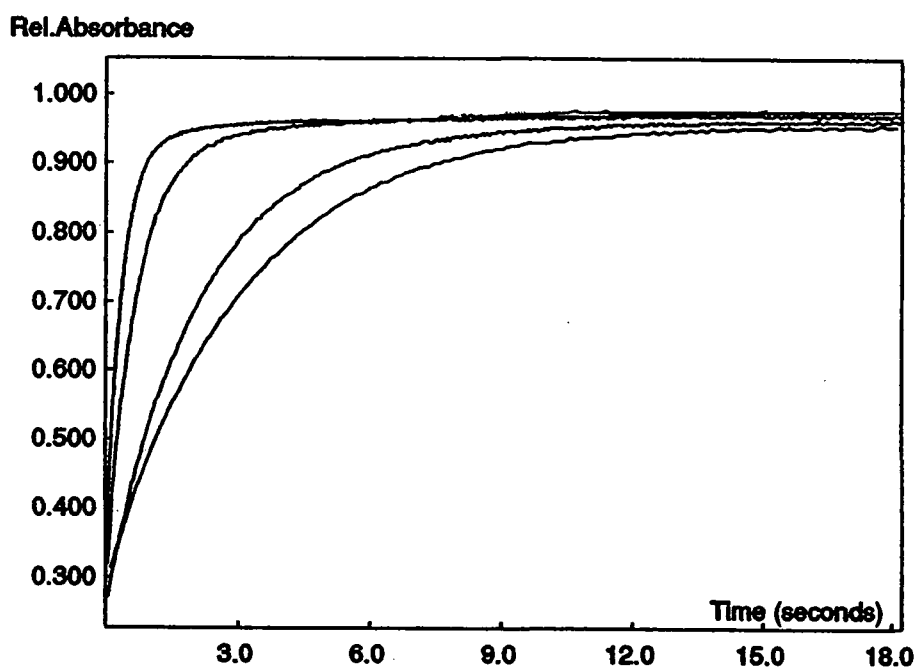


Table 5.20 Kinetic data for the reaction of substrates 5.2, 5.3 and 5.4 with different buffer systems of Borax in 74% DMSO-water (v/v), $\lambda = 425\text{nm}$, at 25°C.

pH(water)	8.73	8.92	9.17	9.36	9.55
5.2 $k_{\text{obs}} / \text{s}^{-1}$	0.32	0.47	1.45	2.76	6.19
5.3 "	0.67	0.69	1.64	3.01	6.11
5.4 "	1.95	1.95	3.98	7.84	16.5

5.8 Discussion and Summary

Measurements were made in 74% DMSO-water (v/v). The choice of this solvent system was made to optimise the possibility of observing the intermediates 5.1. It is known^{6,7} that σ -adducts are stabilised in DMSO relative to water, due both to their favourable solvation and also by the desolvation of the anionic nucleophiles.

Since the systems under study will contain two nucleophiles, phenolate and hydroxide, the relative solvation of these is important. It is to be expected that phenolate ions, where the negative charge may be partially delocalised, will be solvated relatively well by DMSO compared to hydroxide. Hence increasing the proportion of DMSO will tend to favour hydroxide attack on the substrate relative to phenolate attack. The proportion of 74% chosen is a compromise between having enough DMSO to enable observation of the σ -adducts and having too much, when only hydroxide addition will be observed. The choice was also guided by previous work by Bernasconi and Muller⁸ who examined the reactions of phenolates with 2,4,6-trinitroanisole in DMSO-water mixtures in the range 50-90% DMSO (v/v).

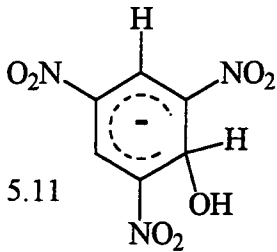
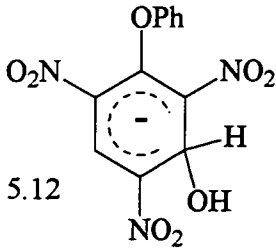
5.8.1 The Slow Process: Attack by Hydroxide Ions.

The results are summarised in table 5.21. With each of the three substrates, measurements are made with hydroxide alone in the chosen solvent system. With 1,3,5-trinitrobenzene, 5.4, the data yield a value of $4.3 \times 10^6 \text{ dm}^3 \text{ mol}^{-1}$ for the equilibrium constant K_3 . This value is *ca.* 10^5 times higher than the value of $29 \text{ dm}^3 \text{ mol}^{-1}$ reported previously⁹ in 20% DMSO - 80% water (v/v). The value of k_3 is *ca.* one hundred times higher in the DMSO rich solvent, and the value of k_{-3} is *ca.* a thousand times smaller. Similarly the values of K_3 for hydroxide attack at the three position of 5.3 is *ca.* 10^5 higher than that reported⁹ in 20% DMSO - 80% water (v/v).

The rather small effect on values of K_3 resulting from the introduction of the phenoxy substituent in the trinitrobenzene ring is likely to be a compromise between electronic and steric effects. The Hammett σ_{meta} value for the phenoxy group is 0.25,¹⁰ indicating that it is electron withdrawing relative to hydrogen, thus encouraging nucleophilic attack. However the steric effect of the phenoxy group will disrupt the planarity of the ortho-nitro groups so that their electron withdrawing ability is decreased.

The effect on values of k_3 , k_{-3} and K_3 of the 4-methoxy substituent in the phenyl ring of 5.2 is small. This is to be expected given the remoteness of the substituent from the reaction site. Values for hydroxide attack on substrates 5.3 and 5.4 are summarised below in table 5.21.

Table 5.21 Kinetic values for the attack of hydroxide on substrates 5.3 and 5.4.

σ -adducts	 5.11	 5.12
$k_3 / 10^4 \text{ dm}^3 \text{ mol}^{-1} \text{ s}^{-1}$	2.55	1.0
$k_{-3} / 10^{-3} \text{ s}^{-1}$	6	2
$K_3 / 10^6 \text{ dm}^3 \text{ mol}^{-1}$	4.3	5.0

5.8.2 Base Catalysis, k_{PhO^-} .

It is also of interest that the results obtained in phenol / phenolate buffers require a base catalysed pathway for hydroxide addition. As shown in equation 5.13 this results from catalysis of attack of water by the phenolate ions. The values of k_{PhO^-} quoted in table 5.22 do not, as expected, show large variations either on the nature of the phenolate or the nature of the substrate. The values obtained for k_{PhO^-} are *ca.* 10^4 times smaller than the corresponding value of k_3 , for direct hydroxide attack. Nevertheless as a result of the large excess of phenolate ions over hydroxide ions in the buffer systems used a considerable part of the reaction flux may involve the base catalysed pathway.

Table 5.22 Comparison of Data in 74% DMSO-water (v/v) at 25°C.

Substrate	$k_3 /$ $10^4 \text{ dm}^3 \text{ mol}^{-1} \text{ s}^{-1}$	$k_{-3} /$ 10^{-3} s^{-1}	$K_3 /$ $10^6 \text{ dm}^3 \text{ mol}^{-1}$	$k_{\text{phO}^-} /$ $\text{dm}^3 \text{ mol}^{-1} \text{ s}^{-1}$	$k_1 /$ $10^4 \text{ dm}^3 \text{ mol}^{-1} \text{ s}^{-1}$	$k_{-1} /$ s^{-1}	$K_1 /$ $\text{dm}^3 \text{ mol}^{-1}$	$K /$ $10^{-5} \text{ mol dm}^{-3}$
5.2 ^a	0.93 ± 0.04	2 ± 0.2	4.7 ± 0.7 4.2 ± 0.2^e	2.7 ± 0.3	1.72 ± 0.09 3.10 ± 0.10^c 8.10 ± 0.40^d	177 ± 4 161 ± 4^c 114 ± 8^d	100 ± 5 190 ± 10^c 710 ± 90^d	1.0 ± 0.1
5.3 ^b	1.00 ± 0.03	2 ± 0.2	5.0 ± 0.7 5.6 ± 0.5^e	1.5 ± 1.0	0.16 ± 0.02	18.7 ± 0.6	90 ± 10	0.6 ± 0.1
5.4 ^b	2.55 ± 0.03	6 ± 1.0	4.3 ± 0.7 2.7 ± 0.2^e	2.8 ± 0.5	≤ 0.04	170 ± 20	≤ 2	0.55 ± 0.1

^a Reactions with 4-methoxy-phenolate.

^b Reactions with phenolate.

^c 80%, ^d 84% DMSO-water (v/v).

^e Value calculated using absorbance data.

5.8.3 π -Complexes?

In media containing hydroxide as the only anionic nucleophile 1,3,5-trinitrobenzene, 5.4, shows a single rate process corresponding to equilibration with the hydroxide adduct, 5.11. This system and also the system containing 5.4 and methoxide in methanol, table 5.15, were carefully examined in view of literature reports³ that σ -adduct formation involves several rate processes. These reportedly involve π -complexes and radical-ion pairs preceding the formation of σ -adducts. No evidence was found, in the present work, for these additional processes.

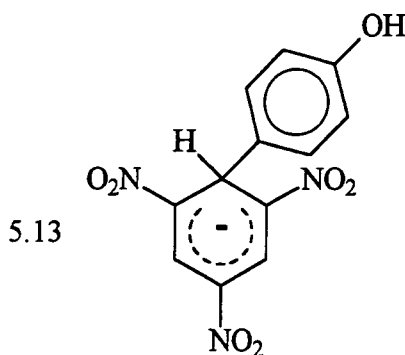
Reactions of the phenyl ethers, 5.2 and 5.3, with hydroxide showed two rate processes. The faster gave rise to the 3-hydroxy adducts, 5.8, while the second, much slower process, resulted in the formation of the picrate ion, 5.9. This second slower process was not investigated kinetically but is likely to involve rate determining hydroxide attack at the 1-position of the substrate to give intermediates such as 5.7 which rapidly expel phenolate ions.

5.8.4 The Fast Process: Addition of Phenolate.

In the presence of phenol / phenolate buffers all three substrates investigated show a very rapid rate process, much faster than that expected for hydroxide attack. In the case of trinitrobenzene, 5.4, this is likely to indicate formation of the phenoxy adduct 5.10.

5.8.4.1 Carbon Bound σ -Adduct?

There is NMR evidence for the formation of adduct 5.10 in d_6 -DMSO and in CD_3CN -glyme.¹¹ It is known that the isomeric carbon-bound adduct¹² may also be formed, 5.13, but this is a very slow reaction and is unlikely to be observed on the time-scale of the present measurements.

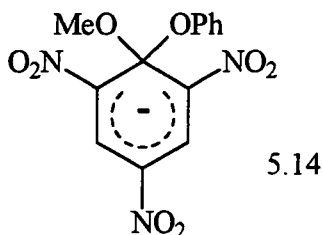


5.8.4.2 Formation of the 1,1 σ -Adduct.

It is interesting that the equilibrium constant for formation of 5.10 has a maximum value of $2 \text{ dm}^3 \text{ mol}^{-1}$. From the previous discussion of the electronic and steric effects of the phenoxy group it may be estimated that the values of the equilibrium constant for formation of 3-phenoxy adducts from substrates 5.2 and 5.3 should also have values *ca.* $2 \text{ dm}^3 \text{ mol}^{-1}$. The observed values, given as K_1 values in table 5.14, for reaction of 5.2 with 4-methoxy-phenolate, and 5.3 with phenolate are *ca.* $100 \text{ dm}^3 \text{ mol}^{-1}$. This is strong evidence that the observed reactions of these substrates with phenolate ions form the 1-adducts with structure 5.1.

In fact there are two additional pieces of evidence supporting the conclusion that the 1-phenolate adducts, 5.1, are likely to be thermodynamically more stable than the isomeric 3-phenolate adducts, 5.6. These relate to the study of the reactions of 2,4,6-trinitroanisole with phenoxide ions.

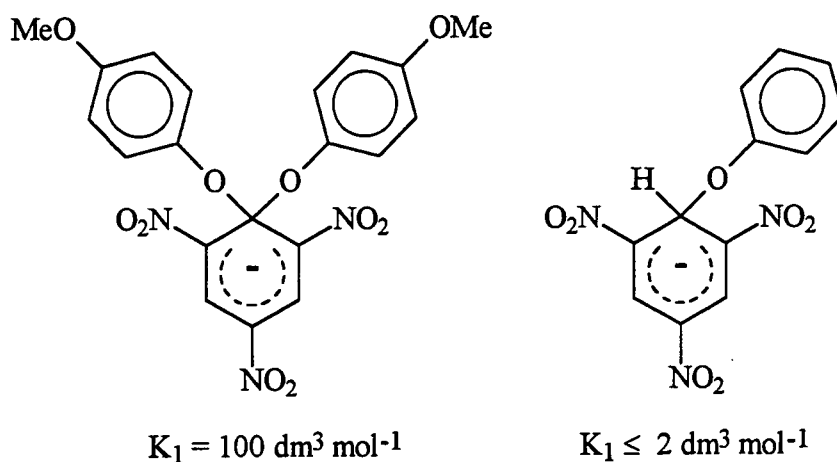
Buncel and co-workers¹³ reported an NMR study of the reactions of phenoxide with 2,4,6-trinitroanisole. They found that in d_6 -DMSO and in CD_3CN -glyme the 1-adduct, 5.14, was the kinetically and thermodynamically favoured product. There was no evidence for phenolate attack at the 3-position.



Bernasconi and Muller⁸ reported a kinetic study by the stopped-flow temperature-jump method of the reaction of 2,4,6-trinitroanisole with substituted phenolate ions in DMSO-water mixtures. They observed two processes, the faster representing phenolate attack at the 1-position give 5.14, and the slower hydroxide attack at the three position. They showed that the ratio of extinction coefficients at the absorption maxima of the initially favoured adduct was that expected for a 1,1-adduct. Values for k_1 of $3000 \text{ dm}^3 \text{ mol}^{-1} \text{ s}^{-1}$ and for k_{-1} of 350 s^{-1} were reported for reaction with phenolate in a solvent system similar to that used in the present work.

The evidence favours the conclusion that the fast reactions observed in the present work gives rise to the 1-adducts 5.1 rather than their isomers, the 3-adducts 5.6. Values of k_1 , k_{-1} and K_1 thus refer to formation of the 1-adduct.

Most data are available for the reaction of 4-methoxy-phenolate with 5.2. The data in table 5.22 show that values of k_1 increase with increasing DMSO content, while values of k_{-1} decrease. Thus values of K_1 increase with increasing DMSO. The value of K_1 obtained in 74% DMSO is >50 times larger than that for formation of the phenoxide adduct from 5.4. This can be attributed to i) the electronic effect of the phenoxy group at the 1-position which will encourage nucleophilic attack and ii) the release in steric strain present in the parent as the phenoxy group is rotated from the ring-plane on adduct formation.



The values of K_1 are similar for reaction of phenolate with 5.3, and for reaction of 4-methoxy phenolate with 5.2. Perhaps, surprisingly, values both of k_1 and k_{-1} are somewhat lower for the former reaction than for the latter. The reason for this is unclear.

These results supplement those in the previous chapter in that they show that adduct 5.1 may have a definite existence, at least in DMSO-water mixtures.

5.9 References.

1. J. C. Halle, R. Gaboriaud and R. Schaal, *Bull. Soc. Chim. Fr.*, 1969, **6**, 1851.
2. F. Terrier, *Chem. Rev.*, 1982, **82**, 77.
3. R. Bacaloglu, C. A. Bunton and F. Ortega, *J. Am. Chem. Soc.*, 1988, **110**, 3503.
4. C. F. Bernasconi, *J. Am. Chem. Soc.*, 1970, **92**, 4682.
5. C. F. Bernasconi and R. G. Bergstrom, *J. Org. Chem.*, 1971, **36**, 1325.
6. E. Buncel, M. R. Crampton, M. J. Strauss and F. Terrier, "Electron-Deficient Aromatic & Heteroaromatic - Base Interactions", Elsevier, New York, 1984.
7. F. Terrier, "Nucleophilic Aromatic Displacement : Influence of the Nitro Group", VCH, Weinheim, 1991.
8. C. F. Bernasconi and M. C. Müller, *J. Am. Chem. Soc.*, 1978, **100**, 5530.
9. R. Chamberlin, M. R. Crampton and R. L. Knight, *J. Chem. Research (S)*, 1993, 444.
10. D. H. McDaniel and R. H. C. Brown, *J. Org. Chem.*, 1958, **23**, 420.
11. E. Buncel and R. A. Manderville, *J. Phys. Org. Chem.*, 1993, **6**, 71.
12. E. Buncel, A. Jonczyk and J. G. K. Webb, *Can. J. Chem.*, 1975, **53**, 3761.
13. E. Buncel, J. M. Dust, A. Jonezyk, R. A. Manderville and I. Onyido, *J. Am. Chem. Soc.*, 1992, **114**, 5610.

Chapter 6.

Experimental Details.

6.1 Measurement Techniques.

6.1.1 U.V./Vis. Spectrophotometry.

U.V./Vis. spectra were recorded using freshly prepared solutions in thermostatted 1cm path length quartz cuvettes on either a Shimadzu UV-2101PC or Perkin Elmer Lambda 2 / 12 instruments. Kinetics of slow reactions ($t_{1/2} > 20\text{s}$) were also monitored using these instruments. For kinetic reactions occurring at a much faster rate ($2\text{ms} \leq t_{1/2} \leq 20\text{s}$) a stopped-flow spectrophotometer was used to obtain measurements (section 6.1.2). At a temperature of 298K, to which all solutions / cuvettes (containing the required solvent composition) were thermostatted beforehand, reactions were investigated under pseudo first order conditions. Absorbance / time data were analysed using either a computer correlation program "Enzfitter" or a data fitting program "P.E.C.S.S." (Perkin Elmer Computerised Spectroscopy Software) depending on the spectrophotometer used. Both pieces of software provided consistent results for a standard reaction. Each program determined the observed rate constant, k_{obs} , using a calculation based on the following derivation.

For a first order process $A \rightarrow B$, the rate of formation of product, B, or removal of reactant, A, can be represented by equation 6.1.

$$\frac{d[B]}{dt} = -\frac{d[A]}{dt} = k_{\text{obs}}[A] \quad \text{equation 6.1}$$

Integration of equation 6.1 gives an expression for the observed first order rate constant, k_{obs} , equation 6.2.

$$-\int_{[A]_0}^{[A]_t} \frac{1}{[A]} d[A] = \int_0^t k_{\text{obs}} dt$$

$$\ln[A]_t - \ln[A]_0 = -k_{\text{obs}}t$$

$$k_{\text{obs}} = -\frac{1}{t} \ln \frac{[A]_t}{[A]_0} \quad \text{equation 6.2}$$

Where $[A]_0$ and $[A]_t$ are concentrations of A at times $t = 0$ and $t = t$ respectively.

Applying the Beer-Lambert law ($A = \epsilon.c.l$, where A is the absorbance, ϵ is the molar extinction coefficient and l is the path length) and assuming the path length to be 1 cm, expressions for the absorbance at times $t = 0$ and $t = t$ can be derived, equations 6.3 and 6.4.

$$A_0 = \epsilon_A [A]_0 \quad \text{equation 6.3}$$

$$A_t = \epsilon_A [A]_t + \epsilon_B [B]_t \quad \text{equation 6.4}$$

Ideally a suitable wavelength is one in which the absorbance of the product B is strong and that of the reactant A is negligible.

However, since $[B]_t = [A]_0 - [A]_t$, then substituting for $[B]_t$ into equation 6.4 gives:

$$A_t = \epsilon_A [A]_t + \epsilon_B [A]_0 - \epsilon_B [A]_t \quad \text{equation 6.5}$$

Now $A_\infty = \epsilon_B [B]_\infty = \epsilon_B [A]_0$ since $[B]_\infty = [A]_0$

Thus $(A_\infty - A_t) = \epsilon_B [A]_t - \epsilon_A [A]_t$

$$[A]_t = \frac{(A_\infty - A_t)}{(\epsilon_B - \epsilon_A)} \quad \text{equation 6.6}$$

Similarly

$$A_0 = \epsilon_A [A]_0$$

and $A_\infty = \epsilon_B [B]_\infty = \epsilon_B [A]_0$

Hence $(A_\infty - A_0) = \epsilon_B [A]_0 - \epsilon_A [A]_0$

$$[A]_0 = \frac{(A_\infty - A_0)}{(\epsilon_B - \epsilon_A)} \quad \text{equation 6.7}$$

Substituting equations 6.6 and 6.7 into equation 6.2 gives:

$$k_{\text{obs}} = -\frac{1}{t} \ln \frac{(A_{\infty} - A_t)}{(A_{\infty} - A_0)} \quad \text{equation 6.8}$$

Rearrangement of equation 6.8 gives the form:

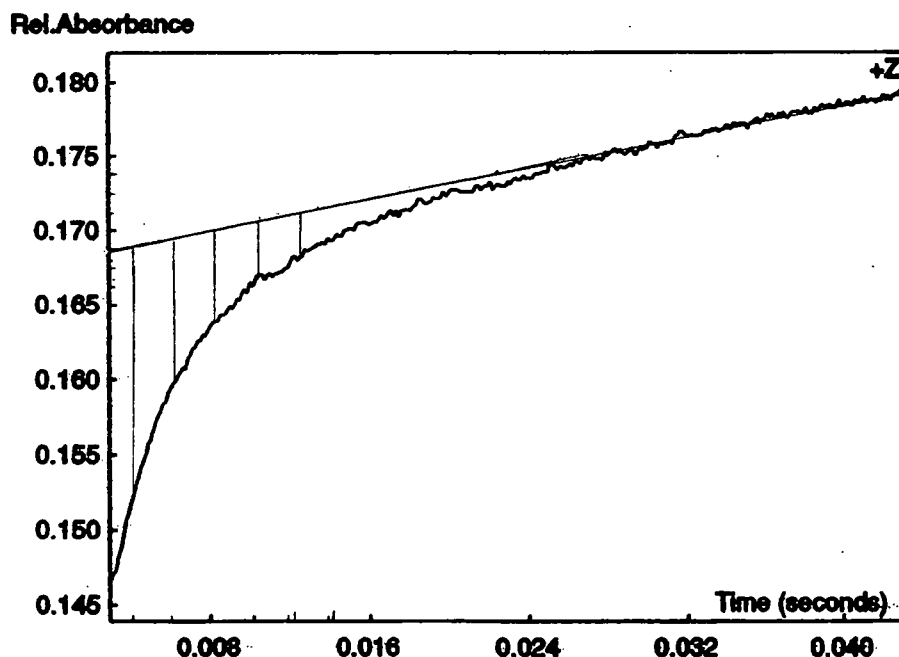
$$\ln(A_{\infty} - A_t) = -k_{\text{obs}}t + \ln(A_{\infty} - A_0)$$

Where a plot of $\ln(A_{\infty} - A_t)$ against t will give a linear line with a slope of $-k_{\text{obs}}$. The infinity values, A_{∞} , were determined after a period of ten half lives and the change in absorbance followed for at least two half lives.

For kinetic traces consisting of two processes, figure 6.1, the differences in absorbance, $\Delta\text{Abs.}$, were calculated between the experimental absorbance measurement and that of the absorbance value at an equivalent time acquired from an extrapolated sloping line. Approximately twenty values of $\Delta\text{Abs.}$ were determined, from the region of greatest change, after which a graph of $\ln(\Delta\text{Abs.})$ versus time, t , resulted in a gradient equivalent to the observed rate constant, k_{obs} .

The computer correlation software used to optimise specific values of rate and equilibrium constants is the "solver" utility found within Microsoft Excel version 4.0

Figure 6.1 Example of a kinetic trace acquired consisting of two processes.



6.1.2 Stopped-Flow Spectrophotometry.

Often reactions in solution can be too fast to study by conventional methods. Flow techniques overcome this and measurements were made using either an Applied Photophysics SX-17MV or a Hi-Tech SF-3 Series stopped-flow spectrophotometer, shown schematically in figure 6.2.

The two solutions to be reacted, A and B, are stored in reservoirs and are filled into two identical syringes so that equal volumes are mixed. Both syringes are compressed simultaneously either pneumatically or by hand and mixing occurs at point M very quickly. The dead time of the instruments is estimated to be *ca.* 2ms so reactions with half lives smaller than this cannot be measured by stopped-flow techniques. Reacting solution flows into a thermostatted 2mm path length quartz cell at point O. The plunger of the third syringe will knock a trigger switch and the flow of solution will terminate. Pressing the trigger initiates the acquisition of absorbance and time data for the reaction. By passing a beam of monochromatic light at the appropriate wavelength through the cell by fibre optic cable the reaction is monitored. Light passes through a photomultiplier and a change in absorbance of the solution causes a subsequent change in the measured voltage. Software used to run the stopped-flow instruments also transforms voltage/time data into absorbance/time data upon application of equation 6.9. Additionally the software interprets these results, calculating the observed rate constants, the infinity value and the associated errors.

$$\text{Absorbance} = \log_{10} \left(\frac{V_0}{V_0 - \Delta V} \right) \quad \text{equation 6.9}$$

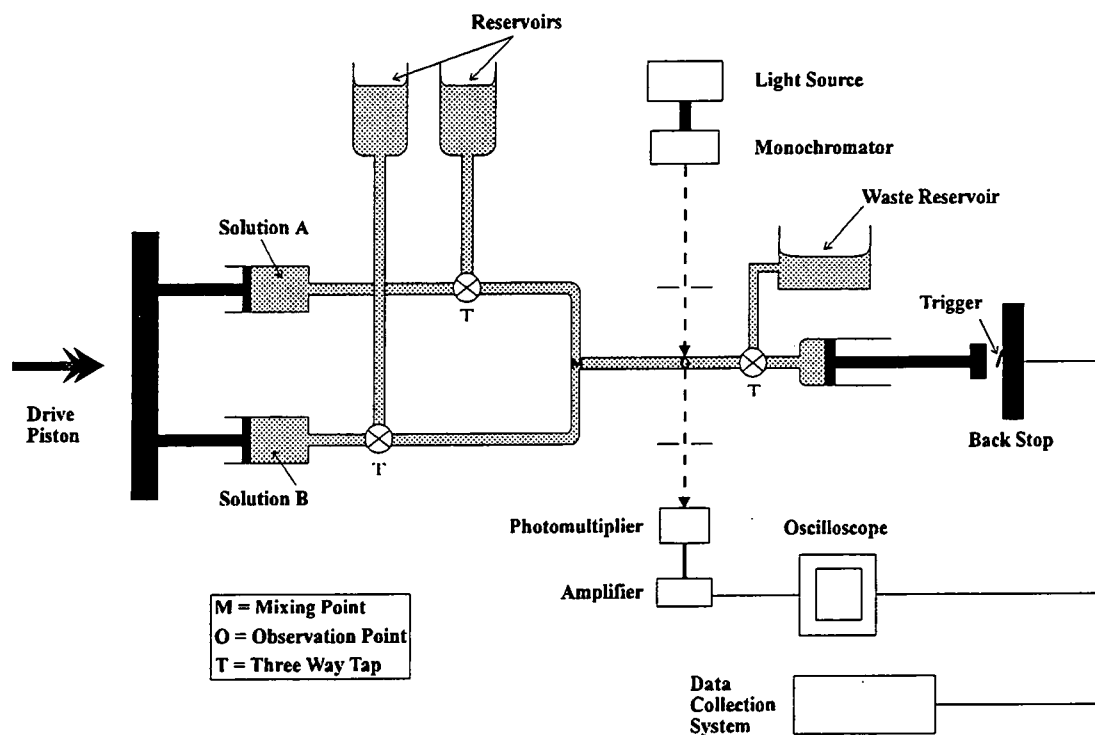
6.1.3 NMR Spectroscopy.

All NMR spectra were recorded on the following Varian machines XL 200, VXR 200, Gemini 200 (all 200MHz) and Gemini 400 (400MHz).

6.1.4 pH Measurements.

All pH measurements were performed using a Jenway 3020 pH meter (accurate to 0.02 pH units). The pH meter was calibrated over the range pH 4.0 to 7.0 or pH 7.0 to 10.0 depending on the solution to be measured.

Figure 6.2. Schematic of a stopped-flow spectrometer.



6.2 Materials.

6.2.1 Solvents.

For all kinetic work it was found that 99+% dimethyl sulfoxide and 99.9+% HPLC grade 1,4-dioxane from Aldrich were adequate. High purity water was departmentally produced. For N.M.R. experiments d_6 -dimethyl sulfoxide, 99.9 atom % D was used. General purpose acetone and methanol were used for washing all apparatus. Solvents for synthetic work were of the highest grades. Specially dried diethyl ether for extractions was stored over sodium wire.

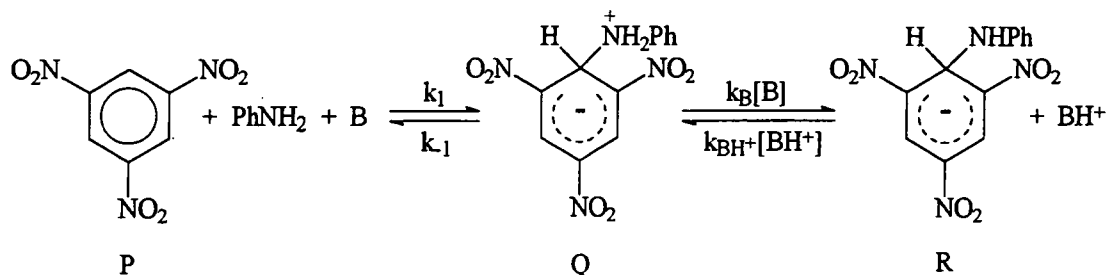
6.2.2 Reagents

All reagents purchased commercially were of the highest grades. Those needed to be synthesised were produced as instructed in the text previously. Borax, TRIS (tris(hydroxymethyl)aminomethane) and potassium dihydrogen orthophosphate used for preparing standard buffer solutions were purchased commercially.

6.3 Derivation of Rate Equations.

6.3.1 Attack at an Unsubstituted Ring Position.

For attack at an unsubstituted position on an aromatic ring equation 6.10 applies. Where B and BH⁺ represent both aniline, (An), or/and Dabco, and anilineH⁺, (AnH⁺), or/and DabcoH⁺ respectively.



equation 6.10

$$\frac{d[R]}{dt} = k_B[B][Q] - k_{BH^+}[BH^+][Q] \quad \text{equation 6.11}$$

$$\frac{d[Q]}{dt} = k_1[An][P] + k_{BH^+}[BH^+][R] - (k_{-1} + k_B[B])[Q] \quad \text{equation 6.12}$$

If the zwitterion, Q, is treated as a steady-state intermediate then $\frac{d[Q]}{dt} = 0$ and

$$[Q] = \frac{k_1[An][P] + k_{BH^+}[BH^+][R]}{k_{-1} + k_B[B]}$$

Substituting for [Q] into equation 6.11 and multiplying the $k_{BH^+}[BH^+][R]$ term by

$$\frac{k_{-1} + k_B[B]}{k_{-1} + k_B[B]} \text{ gives}$$

$$\frac{d[R]}{dt} = \frac{k_1 k_B [An][B][P] - k_{-1} k_{BH^+} [BH^+][R]}{k_{-1} + k_B[B]} \quad \text{equation 6.13}$$

In the reaction solution the sum of the concentrations of the species P, Q and R is equal to the initial stoichiometric concentration of P. Therefore

$$[P]_0 = [P] + [Q] + [R]$$

Since Q has been regarded as a steady-state intermediate, $[Q] \approx 0$

Hence $[P] = [P]_0 - [R]$, substituting $[P]$ in equation 6.13 yields

$$\frac{d[R]}{dt} = \frac{k_1 k_B [An][B][P]_0 - k_1 k_B [An][B][R] - k_{-1} k_{BH^+} [BH^+][R]}{k_{-1} + k_B [B]} \quad \text{equation 6.14}$$

At equilibrium $\frac{d[R]}{dt} = 0$ and $[R] = [R]_{eq}$, resulting in

$$0 = \frac{k_1 k_B [An][B][P]_0 - k_1 k_B [An][B][R]_{eq} - k_{-1} k_{BH^+} [BH^+][R]_{eq}}{k_{-1} + k_B [B]} \quad \text{equation 6.15}$$

Subtracting equation 6.15 from 6.14 gives

$$\frac{d[C]}{dt} = \left(\frac{k_1 k_B [An][B] + k_{-1} k_{BH^+} [BH^+]}{k_{-1} + k_B [B]} \right) ([R]_{eq} - [R]) \quad \text{equation 6.16}$$

This can be rewritten in the form

$$\frac{d[C]}{dt} \cdot \frac{1}{([R]_{eq} - [R])} = \left(\frac{k_1 k_B [An][B] + k_{-1} k_{BH^+} [BH^+]}{k_{-1} + k_B [B]} \right) \quad \text{equation 6.17}$$

The parent, P, does not absorb at the wavelength where the reaction is being investigated. Since the concentration of Q, the steady-state intermediate is presumed to be negligible, it too does not contribute to the absorbance at that wavelength.

Hence the only absorbing species is the product, R. Application of the Beer-Lambert law, absorbance = $\epsilon \cdot c \cdot l$ results in

$$\text{Abs.} = \epsilon_R \cdot [\text{R}] \cdot l \quad \text{equation 6.18}$$

$$\text{At equilibrium, } \text{Abs}_{\text{eq}} = \epsilon_R \cdot [\text{R}]_{\text{eq}} \cdot l \quad \text{equation 6.19}$$

Subtracting equation 6.18 from equation 6.19 gives

$$\text{Abs}_{\text{eq}} - \text{Abs} = \epsilon_R ([\text{R}]_{\text{eq}} - [\text{R}]) \cdot l \quad \text{equation 6.20}$$

Differentiating equation 6.18 yields

$$\frac{d\text{Abs}}{dt} = \epsilon_R \cdot l \cdot \frac{d[\text{R}]}{dt} \quad \text{equation 6.21}$$

Division of this by equation 6.20 leads to equation 6.22.

$$\frac{d\text{Abs}}{dt} \cdot \frac{1}{\text{Abs}_{\text{eq}} - \text{Abs}} = \frac{d[\text{R}]}{dt} \cdot \frac{1}{[\text{R}]_{\text{eq}} - [\text{R}]} \quad \text{equation 6.22}$$

The observed rate constant, k_{obs} , is defined thus

$$k_{\text{obs}} = \frac{d\text{Abs}}{dt} \cdot \frac{1}{\text{Abs}_{\text{eq}} - \text{Abs}} \quad \text{equation 6.23}$$

Hence, combining equations 6.17, 6.22 and 6.23 yields the overall rate expression for attack at an unsubstituted ring position is

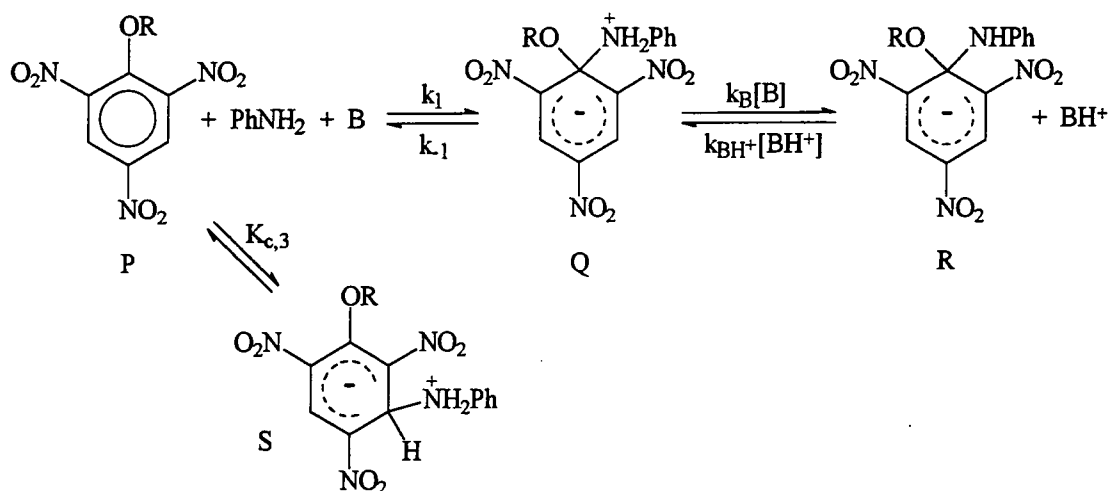
$$k_{\text{obs}} = \left(\frac{k_1 k_B [\text{An}] [\text{B}] + k_{-1} k_{\text{BH}^+} [\text{BH}^+]}{k_{-1} + k_B [\text{B}]} \right) \quad \text{equation 6.24}$$

In the case where aniline and Dabco both act as bases, the term $k_B [\text{B}]$ is replaced by $(k_{\text{An}} [\text{An}] + k_{\text{Dabco}} [\text{Dabco}])$.

Similarly $k_{\text{BH}^+} [\text{BH}^+]$ is replaced by $(k_{\text{AnH}^+} [\text{AnH}^+] + k_{\text{DabcoH}^+} [\text{DabcoH}^+])$.

6.3.2 Attack at a Substituted Ring Position.

Scheme 6.1 is a general example for attack at a substituted position on the aromatic ring. Formation of the 3-adduct is a rapid process in comparison.



Equation 6.25 is the rate expression for the formation of the R. It is derived in an analogous way to the corresponding equation shown previously.

$$\frac{d[\text{R}]}{dt} = \frac{k_1 k_{\text{B}} [\text{An}] [\text{B}] [\text{P}] - k_{-1} k_{\text{BH}^+} [\text{BH}^+] [\text{R}]}{k_{-1} + k_{\text{B}} [\text{B}]} \quad \text{equation 6.25}$$

$$\text{Now, } [\text{P}]_0 = [\text{P}] + [\text{S}] + [\text{R}] \quad \text{equation 6.26}$$

and the overall equilibrium constant for formation of S is

$$K_{c,3} = \frac{[\text{S}] [\text{BH}^+]}{[\text{P}] [\text{An}] [\text{B}]}$$

This can be rewritten as

$$[\text{S}] = \frac{K_{c,3} [\text{P}] [\text{An}] [\text{B}]}{[\text{BH}^+]} \quad \text{equation 6.27}$$

Substituting for [S] in equation 6.26 and rearranging to get a term for [P] gives

$$[P] = \frac{[A]_0 - [R]}{1 + \frac{K_{c,3}[An][B]}{[BH^+]}} \quad \text{equation 6.28}$$

Substituting this term for [P] in equation 6.25 yields

$$\frac{d[R]}{dt} = \frac{k_1 k_B [An][B] ([P]_0 - [R])}{(k_{-1} + k_B [B]) \left(1 + \frac{K_{c,3}[An][B]}{[BH^+]} \right)} - \frac{k_{-1} k_{BH^+} [BH^+] [R]}{(k_{-1} + k_B [B])} \quad \text{equation 6.29}$$

At equilibrium $\frac{d[R]}{dt} = 0$ and $[R] = [R]_{eq}$. Therefore

$$0 = \frac{k_1 k_B [An][B] ([P]_0 - [R]_{eq})}{(k_{-1} + k_B [B]) \left(1 + \frac{K_{c,3}[An][B]}{[BH^+]} \right)} - \frac{k_{-1} k_{BH^+} [BH^+] [R]_{eq}}{(k_{-1} + k_B [B])} \quad \text{equation 6.30}$$

Subtracting equation 6.30 from 6.29 gives,

$$\frac{d[R]}{dt} = \left(\frac{k_1 k_B [An][B]}{(k_{-1} + k_B [B]) \left(1 + \frac{K_{c,3}[An][B]}{[BH^+]} \right)} + \frac{k_{-1} k_{BH^+} [BH^+]}{(k_{-1} + k_B [B])} \right) ([R]_{eq} - [R]) \quad \text{equation 6.31}$$

This can be rewritten in the form

$$\frac{d[R]}{dt} \cdot \frac{1}{([R]_{eq} - [R])} = \left(\frac{k_1 k_B [An][B]}{(k_{-1} + k_B [B]) \left(1 + \frac{K_{c,3}[An][B]}{[BH^+]} \right)} + \frac{k_{-1} k_{BH^+} [BH^+]}{(k_{-1} + k_B [B])} \right) \quad \text{equation 6.32}$$

Both S and R are absorbing species at the wavelength used in the reaction. Applying the Beer-Lambert law, absorbance = $\epsilon \cdot c \cdot l$.

$$\frac{\text{Abs}}{l} = \epsilon_R [R] + \epsilon_S [S] \quad \text{equation 6.33}$$

From equation 6.26 it can be followed that $[S] = [P]_0 - [P] - [R]$

Substituting this term for [S] and the term for [P] from equation 6.28 into equation 6.33, after rearrangement gives

$$\frac{\text{Abs}}{l} = [R] \left(\epsilon_R - \frac{\epsilon_S K_{c,3} [An][B][BH^+]}{[BH^+] + K_{c,3} [An][B]} \right) + \frac{\epsilon_S [P]_0 K_{c,3} [An][B][BH^+]}{[BH^+] + K_{c,3} [An][B]} \quad \text{equation 6.34}$$

This can be simplified to the form

$$\frac{\text{Abs}}{l} = [R]Y + Z \quad \text{equation 6.35}$$

$$\text{where } Y = \epsilon_R - \frac{\epsilon_S K_{c,3} [An][B][BH^+]}{[BH^+] + K_{c,3} [An][B]} \quad \text{and} \quad Z = \frac{\epsilon_S [P]_0 K_{c,3} [An][B][BH^+]}{[BH^+] + K_{c,3} [An][B]}$$

At equilibrium

$$\frac{\text{Abs}_{\text{eq}}}{l} = [R]_{\text{eq}} Y + Z \quad \text{equation 6.36}$$

Subtracting equation 6.35 from 6.36 and multiplying both sides by l gives

$$\text{Abs}_{\text{eq}} - \text{Abs} = l([R]_{\text{eq}} - [R])Y \quad \text{equation 6.37}$$

Differentiating equation 6.35 and multiplying both sides by l yields

$$\frac{d\text{Abs}}{dt} = l \cdot Y \cdot \frac{d[R]}{dt} \quad \text{equation 6.38}$$

Division of this by equation 6.37 leads to equation 6.39.

$$\frac{dAbs}{dt} \cdot \frac{1}{Abs_{eq} - Abs} = \frac{d[R]}{dt} \cdot \frac{1}{[R]_{eq} - [R]} \quad \text{equation 6.39}$$

The definition of the observed rate constant k_{obs} is

$$k_{obs} = \frac{dAbs}{dt} \cdot \frac{1}{Abs_{eq} - Abs} \quad \text{equation 6.23}$$

Combination of equations 6.32, 6.39 and 6.23 gives the term for k_{obs}

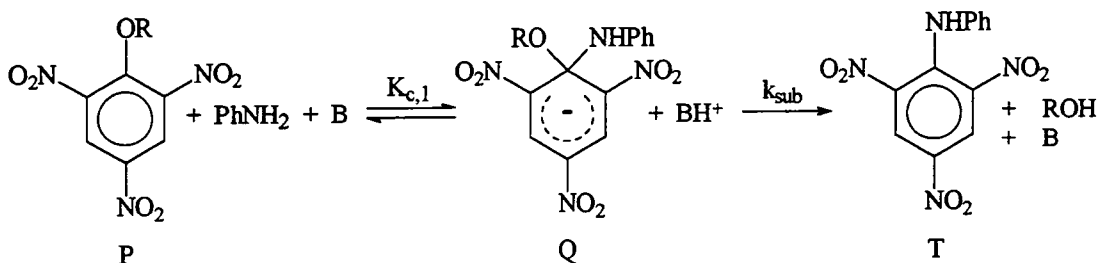
$$k_{obs} = \frac{k_1 k_B [An][B]}{(k_{-1} + k_B [B]) \left(1 + \frac{K_{c,3} [An][B]}{[BH^+]} \right)} + \frac{k_{-1} k_{BH^+} [BH^+]}{(k_{-1} + k_B [B])} \quad \text{equation 6.40}$$

In the case where aniline and Dabco both act as bases, the term $k_B [B]$ is replaced by $(k_{An} [An] + k_{Dabco} [Dabco])$.

Similarly $k_{BH^+} [BH^+]$ is replaced by $(k_{AnH^+} [AnH^+] + k_{DabcoH^+} [DabcoH^+])$.

6.3.3 Formation of the Substituted Product.

Equation 6.41 applies to the formation of the substituted product, T. It involves acid catalysed expulsion of the alkoxy group.



equation 6.41

The reaction is followed by monitoring the formation of the substituted product, T.

$$\frac{d[T]}{dt} = k_{\text{sub}} [\text{BH}^+] [Q] \quad \text{equation 6.42}$$

$$\text{Now, } [P]_0 = [P] + [Q] + [T] \quad \text{equation 6.43}$$

and the overall equilibrium constant for formation of Q is

$$K_{c,1} = \frac{[Q][\text{BH}^+]}{[P][\text{An}][B]}$$

Which can be rewritten in the form

$$[P] = \frac{[Q][\text{BH}^+]}{K_{c,1}[\text{An}][B]} \quad \text{equation 6.44}$$

Substituting for [P] in equation 6.43 and rearranging to get a term for [Q] gives

$$[Q] = \frac{K_{c,1}[\text{An}][B]}{K_{c,1}[\text{An}][B] + [\text{BH}^+]} ([P]_0 - [T]) \quad \text{equation 6.45}$$

Substituting this term for [Q] in equation 6.42 yields

$$\frac{d[T]}{dt} = \frac{k_{\text{sub}}K_{c,1}[An][B][BH^+]}{K_{c,1}[An][B]+[BH^+]}([P]_0 - [T]) \quad \text{equation 6.46}$$

At equilibrium $\frac{d[T]}{dt} = 0$ and $[T] = [T]_{\text{eq}}$. Implying

$$0 = \frac{k_{\text{sub}}K_{c,1}[An][B][BH^+]}{K_{c,1}[An][B]+[BH^+]}([P]_0 - [T]_{\text{eq}}) \quad \text{equation 6.47}$$

Subtracting equation 6.47 from 6.46 yields,

$$\frac{d[T]}{dt} = \frac{k_{\text{sub}}K_{c,1}[An][B][BH^+]}{K_{c,1}[An][B]+[BH^+]}([T]_{\text{eq}} - [T]) \quad \text{equation 6.48}$$

This can be rewritten in the form

$$\frac{d[T]}{dt} \cdot \frac{1}{([T]_{\text{eq}} - [T])} = \frac{k_{\text{sub}}K_{c,1}[An][B][BH^+]}{K_{c,1}[An][B]+[BH^+]} \quad \text{equation 6.49}$$

T is the only absorbing species at the wavelength from which the reaction is followed. Applying the Beer-Lambert law, absorbance = $\epsilon \cdot c \cdot l$.

$$\text{Abs} = \epsilon_T [T] \cdot l \quad \text{equation 6.50}$$

At equilibrium

$$\text{Abs}_{\text{eq}} = \epsilon_T [T]_{\text{eq}} \cdot l \quad \text{equation 6.51}$$

Subtracting equation 6.50 from 6.51 gives

$$\text{Abs}_{\text{eq}} - \text{Abs} = \epsilon_T ([T]_{\text{eq}} - [T]) \cdot l \quad \text{equation 6.52}$$

Differentiating equation 6.50 yields

$$\frac{dAbs}{dt} = 1 \cdot \epsilon_T \cdot \frac{d[T]}{dt} \quad \text{equation 6.53}$$

Division of this by equation 6.52 leads to

$$\frac{dAbs}{dt} \cdot \frac{1}{Abs_{eq} - Abs} = \frac{d[T]}{dt} \cdot \frac{1}{[T]_{eq} - [T]} \quad \text{equation 6.54}$$

The definition of the observed rate constant k_{obs} is

$$k_{obs} = \frac{dAbs}{dt} \cdot \frac{1}{Abs_{eq} - Abs} \quad \text{equation 6.23}$$

Hence, combination of equations 6.49, 6.54 and 6.23 gives the term for k_{obs}

$$k_{obs} = \frac{k_{sub} K_{c,1} [An][B][BH^+]}{K_{c,1} [An][B] + [BH^+]} \quad \text{equation 6.55}$$

In some cases $k_{sub}[BH^+]$ may be a single / summation of the terms k_{sub,AnH^+} and $k_{subDabcoH^+}$, which represent the rate constants for the substitution reactions involving protonated aniline and Dabco respectively.

$$\text{Also } K_{c,1} = \frac{k_1}{k_{-1}} \cdot \frac{k_B}{k_{BH^+}} = K_1 K_B \quad \text{equation 6.56}$$

Where k_B represents the rate constant for proton catalysis involving possibly Dabco and/or aniline, k_{Dabco} and k_{An} , and k_{BH^+} is the rate constant for the opposite step consisting of k_{DabcoH^+} and k_{AnH^+} .

Appendix

**Research Colloquia, Seminars, Lectures
and Conferences Attended.**

A.1 First Year Induction Course (October 1994).

The course consists of a series of one hour lectures on the services available in the department.

1. Introduction, research resources and practicalities.
2. Safety matters.
3. Electrical appliances and hands on spectroscopic services.
4. Departmental computing.
5. Chromatography and high pressure operations.
6. Elemental analysis.
7. Mass spectrometry.
8. Nuclear magnetic resonance spectroscopy.
9. Glassblowing techniques.

A.2 Research Colloquia, Seminars and Lectures arranged by Durham University Chemistry Department 1994 - 1997.

* Denotes lectures attended.

1994

- October 5 Prof. N. L. Owen, Brigham Young University, Utah, USA *
Determining Molecular Structure - the INADEQUATE NMR way.
- October 19 Prof. N. Bartlett, University of California *
Some Aspects of Ag(II) and Ag(III) Chemistry.
- November 2 Dr P. G. Edwards, University of Wales, Cardiff
The Manipulation of Electronic and Structural Diversity in Metal
Complexes- New Ligands.
- November 3 Prof. B. F. G. Johnson, Edinburgh University
Arene-metal Clusters.
- November 9 Dr G. Hogarth, University College, London *
New Vistas in Metal-imido Chemistry.
- November 10 Dr M. Block, Zeneca Pharmaceuticals, Macclesfield *
Large-scale Manufacture of ZD 1542, a Thromboxane Antagonist
Synthase Inhibitor.
- November 16 Prof. M. Page, University of Huddersfield *
Four-membered Rings and β -Lactamase.
- November 23 Dr J. M. J. Williams, University of Loughborough *
New Approaches to Asymmetric Catalysis.
- December 7 Prof. D. Briggs, ICI and University of Durham
Surface Mass Spectrometry.

1995

- January 11 Prof. P. Parsons, University of Reading *
Applications of Tandem Reactions in Organic Synthesis.
- January 18 Dr G. Rumbles, Imperial College, London
Real or Imaginary Third Order Non-linear Optical Materials.
- January 25 Dr D. A. Roberts, Zeneca Pharmaceuticals *
The Design and Synthesis of Inhibitors of the Renin-angiotensin System.
- February 1 Dr T. Cosgrove, Bristol University
Polymers do it at Interfaces.
- February 8 Dr D. O'Hare, Oxford University
Synthesis and Solid-state Properties of Poly-, Oligo- and Multidecker Metallocenes.
- February 22 Prof. E. Schaumann, University of Clausthal
Silicon- and Sulphur-mediated Ring-opening Reactions of Epoxide.
- March 1 Dr M. Rosseinsky, Oxford University *
Fullerene Intercalation Chemistry.
- March 22 Dr M. Taylor, University of Auckland, New Zealand
Structural Methods in Main-group Chemistry.
- April 26 Dr M. Schroder, University of Edinburgh *
Redox-active Macrocyclic Complexes : Rings, Stacks and Liquid Crystals.
- May 4 Prof. A. J. Kresge, University of Toronto *
The Ingold Lecture Reactive Intermediates : Carboxylic-acid Enols and Other Unstable Species.
- October 11 Prof. P. Lugar, Frei Univ Berlin, FRG
Low Temperature Crystallography.

- October 13 Prof. R. Schmutzler, Univ Braunschweig, FRG.
Calixarene-Phosphorus Chemistry: A New Dimension in Phosphorus Chemistry.
- October 18 Prof. A. Alexakis, Univ. Pierre et Marie Curie, Paris, *
Synthetic and Analytical Uses of Chiral Diamines.
- October 25 Dr.D.Martin Davies, University of Northumbria *
Chemical reactions in organised systems.
- November 1 Prof. W. Motherwell, UCL London *
New Reactions for Organic Synthesis.
- November 3 Dr B. Langlois, University Claude Bernard-Lyon
Radical Anionic and Psuedo Cationic Trifluoromethylation.
- November 8 Dr. D. Craig, Imperial College, London *
New Stategies for the Assembly of Heterocyclic Systems.
- November 15 Dr Andrea Sella, UCL, London
Chemistry of Lanthanides with Polypyrazoylborate Ligands.
- November 17 Prof. David Bergbreiter, Texas A&M, USA
Design of Smart Catalysts, Substrates and Surfaces from Simple Polymers.
- November 22 Prof. I Soutar, Lancaster University *
A Water of Glass? Luminescence Studies of Water-Soluble Polymers.
- November 29 Prof. Dennis Tuck, University of Windsor, Ontario, Canada *
New Indium Coordination Chemistry.
- December 8 Professor M.T. Reetz, Max Planck Institut, Mulheim
Perkin Regional Meeting

1996

- January 10 Dr Bill Henderson, Waikato University, NZ *
Electrospray Mass Spectrometry - a new sporting technique.
- January 17 Prof. J. W. Emsley, Southampton University
Liquid Crystals: More than Meets the Eye.
- January 24 Dr Alan Armstrong, Nottingham University *
Alkene Oxidation and Natural Product Synthesis.
- January 31 Dr J. Penfold, Rutherford Appleton Laboratory,
Soft Soap and Surfaces.
- February 7 Dr R.B. Moody, Exeter University *
Nitrosations, Nitrations and Oxidations with Nitrous Acid.
- February 12 Dr Paul Pringle, University of Bristol
Catalytic Self-Replication of Phosphines on Platinum(O).
- February 14 Dr J. Rohr, Univ Gottingen, FRG
Goals and Aspects of Biosynthetic Studies on Low Molecular Weight
Natural Products.
- February 21 Dr C R Pulham, Univ. Edinburgh
Heavy Metal Hydrides - an exploration of the chemistry of stannanes
and plumbanes.
- February 28 Prof. E. W. Randall, Queen Mary & Westfield College *
New Perspectives in NMR Imaging.
- March 6 Dr Richard Whitby, Univ of Southampton *
New approaches to chiral catalysts: Induction of planar and metal
centred asymmetry.
- March 7 Dr D.S. Wright, University of Cambridge
Synthetic Applications of Me₂N-p-Block Metal Reagents.

- March 12 RSC Endowed Lecture - Prof. V. Balzani, Univ of Bologna *
Supramolecular Photochemistry.
- March 13 Prof. Dave Garner, Manchester University *
Mushrooming in Chemistry.
- April 30 Dr L.D.Pettit, Chairman, IUPAC Commission of Equilibrium Data.
pH-metric studies using very small quantities of uncertain purity. *
- October 9 Professor G. Bowmaker, University Auckland, NZ
Coordination and Materials Chemistry of the Group 11 and Group 12
Metals : Some Recent Vibrational and Solid State NMR Studies.
- October 14 Professor A. R. Katritzky, University of Gainesville, University of
Florida, USA
Recent Advances in Benzotriazole Mediated Synthetic Methodology.
- October 16 Professor Ojima, Guggenheim Fellow, State University of New York
at Stony Brook
Silylformylation and Silylcarbocyclisations in Organic Synthesis.
- October 22 Professor Lutz Gade, Univ. Wurzburg, Germany *
Organic transformations with Early-Late Heterobimetallics: Synergism
and Selectivity.
- October 22 Professor B. J. Tighe, Department of Molecular Sciences and *
Chemistry, University of Aston
Making Polymers for Biomedical Application - can we meet Nature's
Challenge?
Joint lecture with the Institute of Materials
- October 23 Professor H. Ringsdorf (Perkin Centenary Lecture), Johannes *
Gutenberg-Universitat, Mainz, Germany
Function Based on Organisation.
- October 29 Professor D. M. Knight, Department of Philosophy, University of
Durham.
The Purpose of Experiment - A Look at Davy and Faraday. *

- October 30 Dr Phillip Mountford, Nottingham University *
Recent Developments in Group IV Imido Chemistry.
- November 6 Dr Melinda Duer, Chemistry Department, Cambridge
Solid-state NMR Studies of Organic Solid to Liquid-crystalline Phase
Transitions.
- November 12 Professor R. J. Young, Manchester Materials Centre, UMIST *
New Materials - Fact or Fantasy?
Joint Lecture with Zeneca & RSC
- November 13 Dr G. Resnati, Milan
Perfluorinated Oxaziridines: Mild Yet Powerful Oxidising Agents.
- November 18 Professor G. A. Olah, University of Southern California, USA *
Crossing Conventional Lines in my Chemistry of the Elements.
- November 19 Professor R. E. Grigg, University of Leeds
Assembly of Complex Molecules by Palladium-Catalysed Queuing
Processes.
- November 20 Professor J. Earnshaw, Department of Physics, Belfast
Surface Light Scattering: Ripples and Relaxation.
- November 27 Dr Richard Templer, Imperial College, London *
Molecular Tubes and Sponges.
- December 3 Professor D. Phillips, Imperial College, London
"A Little Light Relief."
- December 4 Professor K. Muller-Dethlefs, York University
Chemical Applications of Very High Resolution ZEKE Photoelectron
Spectroscopy.
- December 11 Dr Chris Richards, Cardiff University *
Sterochemical Games with Metallocenes.

1997

- January 15 Dr V. K. Aggarwal, University of Sheffield
Sulfur Mediated Asymmetric Synthesis.
- January 16 Dr Sally Brooker, University of Otago, NZ
Macrocycles: Exciting yet Controlled Thiolate Coordination
Chemistry.
- January 21 Mr D. Rudge, Zeneca Pharmaceuticals *
High Speed Automation of Chemical Reactions.
- January 22 Dr Neil Cooley, BP Chemicals, Sunbury *
Synthesis and Properties of Alternating Polyketones.
- January 29 Dr Julian Clarke, UMIST
What can we learn about polymers and biopolymers from computer-
generated nanosecond movie-clips?
- February 4 Dr A. J. Banister, University of Durham *
From Runways to Non-metallic Metals - A New Chemistry Based on
Sulphur.
- February 5 Dr A. Haynes, University of Sheffield
Mechanism in Homogeneous Catalytic Carbonylation.
- February 12 Dr Geert-Jan Boons, University of Birmingham *
New Developments in Carbohydrate Chemistry.
- February 18 Professor Sir James Black, Foundation/King's College London *
My Dialogues with Medicinal Chemists.
- February 19 Professor Brian Hayden, University of Southampton
The Dynamics of Dissociation at Surfaces and Fuel Cell Catalysts.
- February 25 Professor A. G. Sykes, University of Newcastle *
The Synthesis, Structures and Properties of Blue Copper Proteins.

- February 26 Dr Tony Ryan, UMIST *
- Making Hairpins from Rings and Chains.
- March 4 Professor C. W. Rees, Imperial College
- Some Very Heterocyclic Chemistry.
- March 5 Dr J. Staunton FRS, Cambridge University
- Tinkering with biosynthesis: towards a new generation of antibiotics.
- March 11 Dr A. D. Taylor, ISIS Facility, Rutherford Appleton Laboratory
- Expanding the Frontiers of Neutron Scattering.
- March 19 Dr Katharine Reid, University of Nottingham *
- Probing Dynamical Processes with Photoelectrons.

A.3 Conferences Attended.

1. 5th European Symposium on Organic Reactivity,
Santiago de Compostela, Spain, 16-21st July 1995.
Poster presented- "Base Catalysis in the Reactions of Aromatic Nitro-
Compounds with Amine Nucleophiles in Dimethyl Sulfoxide."
2. Royal Society of Chemistry 6th International Meeting on Reaction
Mechanisms,
University of Kent at Canterbury, England, 9-12th July 1996.
Poster presented- "Stepwise or Concerted Mechanism in the Reactions of
Phenoxide Ions with Phenyl Picrates?"
3. Postgraduate Winter School on Organic Reactivity - WISOR VI,
Bressanone, Italy, 10-17th January 1997.
Poster presented- "Stepwise or Concerted Mechanism in the Reactions of
Phenoxide Ions with Phenyl Picrates?"
4. Royal Society of Chemistry Organic Reaction Mechanisms Group
Annual seminars attended:
 - a. Merck, Sharp and Dohme, Harlow, poster presented, September 1995.
 - b. Astra Charnwood, Loughborough, talk given, September 1996.

